Molecular and physiological characterisation of the two *Arabidopsis thaliana* mutants *atpd* and *petc*

Inaugural – Dissertation
zur
Erlangung des Doktorgrades der
Mathematisch-Naturwissenschaftlichen Fakultät
der Heinrich-Heine-Universität Düsseldorf

vorgelegt von Daniela Sabine Maiwald
aus Hilden

Kopier Center Süd, Düsseldorf
2003

Gedruckt mit der Genehmigung der Mathematisch-Naturwissenschaftlichen Fakultät der Heinrich-Heine-Universität Düsseldorf.

Refernt: Prof. Dr. P. Westhoff

1. Koreferent: Prof. Dr. W. Martin
2. Koreferent: Prof. Dr. F. Salamini

Tag der mündlichen Prüfung: 02.07.2003

CONTENTS

ABBREVIATIONS

_as	anti-sense
_s	sense
°C	degree Celsius
1-D	one-dimensional
2-D	two-dimensional
A. th.	*Arabidopsis thaliana*
aa	amino acid
Amp	ampicillin
ATP	adenosine triphosphate
bp	base pairs
Bq	Becquerel
BSA	bovine serum albumin
Carb	carbenicillin
Chl	chlorophyll
Col-0	*Arabidopsis thaliana*, ecotype Colmbia 0
cpTP	chloroplast transit peptide
cyt	cytochrome
cyt b_6/f	cytochrome b_6/f complex
DCMU	3-(3-4-di-chlorophenyl)-1,1-dimethylurea
DEPS	de-epoxidation state = (violaxanthin + 0.5 antheraxanthin)/ (violaxanthin + antheraxanthin + zeaxanthin)
DNA	deoxyribonucleic acid
E. coli	*Escherichia coli*
EDTA	ethylenediaminetetraacetic acid
F_0	minimal fluorescence
F_{0S}	initial fluorescence in the steady-state
Fd	soluble ferredoxin
F_M	maximal fluorescence
F_M’	maximal fluorescence in light adapted leaves
F_{MS}	stationary (quenched) level of maximum fluorescence
FNR	ferredoxin-NADP$^+$ oxidoreductase
F_T	transient fluorescence
F_V/F_M	maximal fluorescence yield of PSII
g	gram
GST	gene sequence tags
hcf	high-chlorophyll-fluorescence
HPLC	high pressure liquid chromatography
Kan	kanamycin
l	litre
LDS	lithium dodecyl sulphate
L*er*	*Arabidopsis thaliana*, ecotype Landsberg *erecta*
LHC	light harvesting complex
M	molar
mol	mole
mRNA	messenger RNA
mV	milliVolt
NADP$^+$	oxidized nicotinamide adenine dinucleotide phosphate
NPQ	non-photochemical quenching

o/n	over night
OD	optical density
OEC	oxygen evolving complex
Φ_{II}	effective quantum yield of PSII
P680	reaction centre of PSII
P700	reaction centre of PSI
PA	polyacrylamide
PAGE	polyacrylamide gel electrophoresis
PAM	pulse amplitude modulation
PBQ	1-4 benzochinone
Pc	plastocyanin
PCR	polymerase chain reaction
Pet	photosynthetic electron transport
PFD	photon flux density
Phe	pheophytin
PQ	plastoquinone
PQH_2	plastoquinol
PSI	photosystem I
PSII	photosystem II
Q_A	bound plastoquinone
Q_B	plastoquinone able to exchange with plastoquinone (PQ) pool
qE	energy-dependent quenching
qI	photoinhibition
Q_o	plastoquinol binding pocket
qP	photochemical quenching
RNA	ribonucleic acid
rpm	revolutions per minute
RT	room temperature
rv	relative values
s	second
SD	standard deviation
SDS	sodium dodecyl sulphate
T-DNA	transfer DNA
TMPD	2,3,5,6-tetramethyl-p-phenylen-diamine
Tris	Tris(hydroxymethane)aminomethane
U	unit of enzyme activity given by supplier
v/v	volume per volume
VAZ	sum of xanthophyll cycle pigments (violaxanthin + antheraxanthin + zeaxanthin)
w/v	weight per volume
WT	wild-type

.

1 INTRODUCTION

1.1 The chloroplast and photosynthesis

By the process of photosynthesis solar light energy is converted into chemical energy, thereby enabling most life on earth. The photosynthetic reactions are performed in a specialized organelle, the chloroplast, which is enclosed by three systems of membranes (Figure 1.1). It is believed that chloroplasts derive from an ancestral cyanobacterial endosymbiont (Douglas, 1998). Chloroplasts have their own genome (plastome) and a transcription and translation apparatus which closely resembles that of the prokaryotes. The chloroplast is not only involved in photosynthesis, but also in the synthesis of compounds such as amino acids, nucleotides, fatty acids and lipids, vitamins, plant hormones and secondary metabolites and it also plays a central role in the assimilation of sulphur and nitrogen.

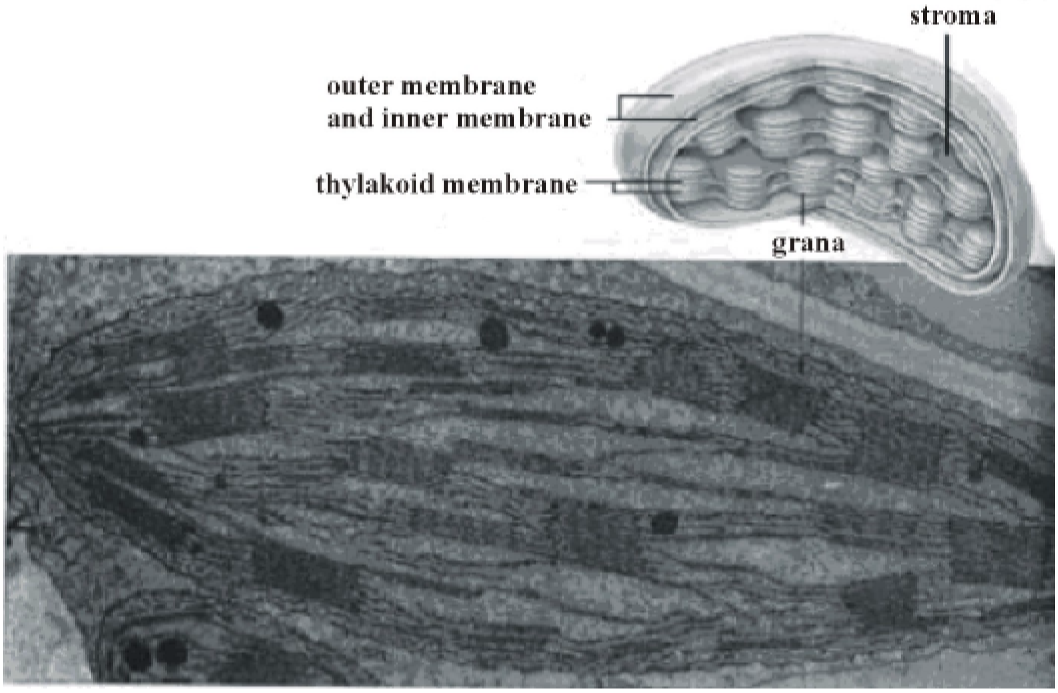

Figure 1.1 Structure of the chloroplast shown as a diagrammatical representation and an electron microscope micrograph.

Photosynthesis in higher plants consists of a series of light-driven reactions which in turn lead to the generation of ATP and NADPH used for the fixation of atmospheric CO_2 into organic compounds. The protein complexes involved in photosynthesis are photosystem II (PSII), the cytochrome (cyt) b_6/f complex, photosystem I (PSI) and the ATP synthase, all located in the thylakoid membranes of the chloroplast (Figure 1.2). Photons are absorbed mainly by the light-harvesting complexes (LHCs) of PSI and PSII.

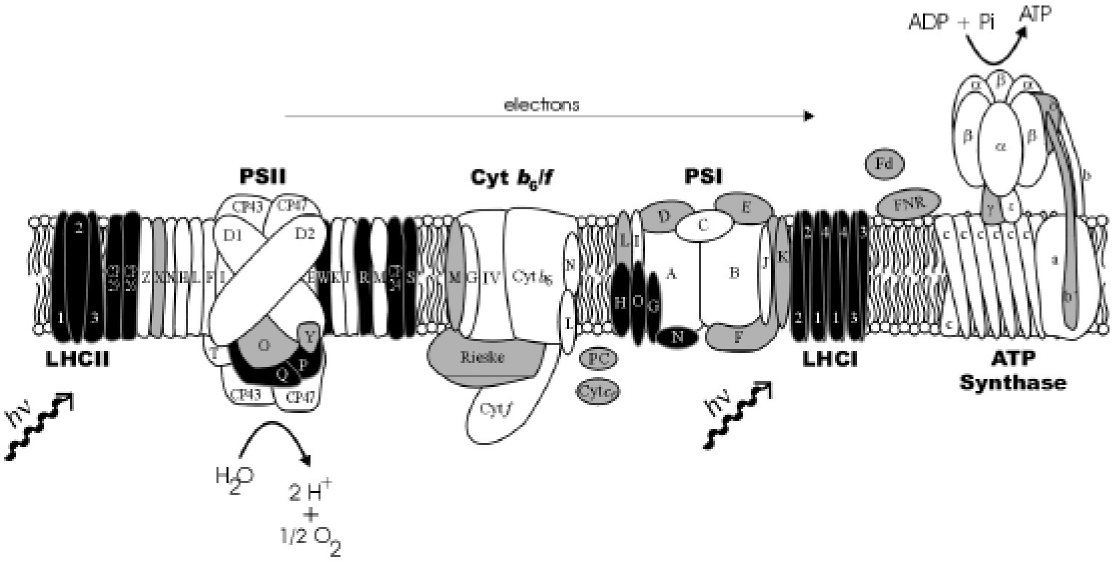

Figure 1.2 Schematic view of the photosynthetic apparatus.

Membrane-located multi-protein complexes: LHCII, light harvesting complex of PSII; PSII, photosystem II; Cyt b_6/*f* complex, cytochrome b_6/*f* complex; PSI, photosystem I; LHCI, light harvesting complex of PSI. The soluble electron carriers: PC, plastocyanin; Fd, ferredoxin; Cyt c_6, cytochrome c_6 and the membrane-bound electron carrier FNR, ferredoxin-NADPH-reductase. Nuclear-encoded subunits are indicated in grey, or black if they are plant specific. Chloroplast encoded subunits are drawn in white.

1.2 The photosynthetic electron transport chain

The first complex in the photosynthetic electron transport chain, accepting electrons from H_2O, is PSII which acts as a water-plastoquinone oxireductase (Renger and Govindjee, 1985). When the reaction centre of PSII (P680) becomes photoexcited it reduces the quinone Q_A via a rapid oxidoreduction of a pheophytin molecule (Phe) (Figure 1.3). Q_A then reduces the two-electron carrier plastoquinone (Q_B). When Q_B is fully reduced, it binds two protons and is thereby converted to plastoquinol (PQH_2) which is not any longer bound to PSII. PQH_2 moves freely in the thylakoid membrane and connects PSII and the cyt b_6/*f* complex to which it transfers the electrons. The cyt b_6/*f* complex acts as a plastoquinol-plastocyanin oxidoreductase. It catalyses the oxidation of the lipophilic two-electron carrier donor PQH_2 and the reduction of the hydrophilic one-electron acceptor protein plastocyanin (Pc).

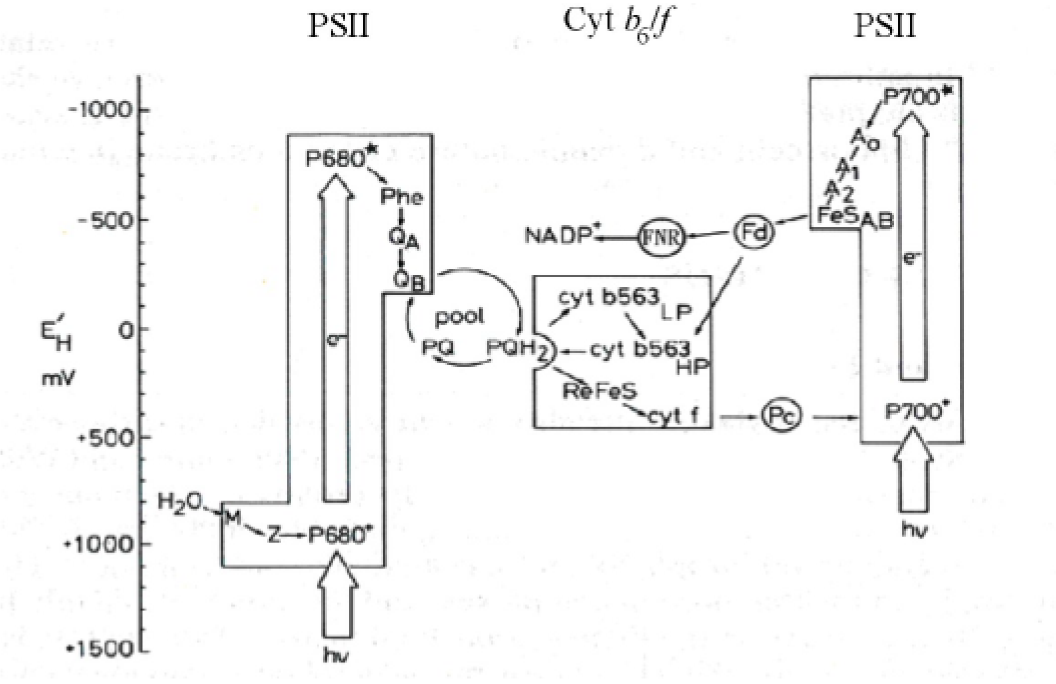

Figure 1.3 A scheme of the electron transport in oxygen evolving photosynthetic organisms (Hill and Bendall, 1960).

M, components of the oxygen evolving complex; Z, primary electron donor to P680; P680, the reaction centre of PSII; Phe, pheophytin; Q_A, bound plastoquinone; Q_B, plastoquinone able to exchange with the plastoquinone (PQ) pool; ReFeS, Rieske iron-sulphur centre; cyt, cytochrome; Pc, plastocyanin; P700, reaction centre of PSI; A_0, A_1, A_2, primary and secondary electron acceptors of PSI; $FeS_{A,B}$, bound iron-sulphur centres A and B; Fd, soluble ferredoxin; FNR, ferredoxin-$NADP^+$ oxidoreductase; $NADP^+$, oxidized nicotinamide adenine dinucleotide phosphate.

Three subunits of the cyt b_6/f complex bear prosthetic groups necessary for the electron transport: cyt b_6 bearing two *b*-type heme moieties (E_m = -84 mV and – 158 mV) (Pierre et al., 1995); cyt *f* bearing a covalently bound *c*-type heme moiety (E_m = + 330 mV), (Pierre et al., 1995); and the Rieske protein bearing a [Fe_2S_2] cluster (E_m = + 290 mV), (Nitschke et al., 1992). According to the Q-cycle model the transfer of the two electrons is branched in the complex between the low-potential chain (composed of the two b_6 type hemes, b_l and b_h) and the high-potential chain (formed by the Rieske protein and cyt *f*) (Mitchell, 1975; Crofts et al., 1983). This mechanism postulates both an oxidation and a reduction of plastoquinol at two distinct sites of the protein, the Q_o and the Q_i sites, on opposite sites of the membrane. The oxidation of plastoquinol at the Q_o site is associated with the reduction of cyt *f* and cyt b_1 (Hope, 1993; Hauska et al., 1996) and the release of two protons into the lumen. Two in-series turnovers of the complex are required to reduce both b_l- and b_h-hemes and trigger the generation of a PQH_2 molecule at the Q_i site. The cyt *f* then finally reduces the plastocyanin which can (re-) reduce PSI. PSI acts as a plastocyanin-ferredoxin oxidoreductase. Within PSI, light induces charge separation between the reaction centre chlorophyll dimer P700 and the primary chlorophyll A acceptor (A_0) (Rutherford and Heathcope, 1985). The electrons flow then to the phylloquinone molecule A_1, 4Fe-4S, A_2, the FeS_A and then to FeS_B. This terminal electron acceptor reduces ferredoxin, which in turn reduces the membrane-bound ferredoxin-$NADP^+$ oxidoreductase (FNR) that transfers the electrons to $NADP^+$.

As a net result of this process two molecules of water are split and two molecules of NADPH are synthesised. The linear electron transfer is coupled to proton translocation across the thylakoid membrane and contributes to the formation of the proton gradient, which can be utilised by the ATP-synthase to generate ATP (Cramer et al., 1991).

1.3 The cytochrome b_6/f complex (cyt b_6/f)

As already mentioned, the cyt b_6/f complex plays a central role in the photosynthetic electron transfer chain and it was shown for Chlamydomonas that it is active as a dimer (Breyton et al., 1997). It is similar to the mitochondrial ubiquinol-cytochrome c reductase complex (the bc_1 complex) in its transmembrane domains, however the extra-membrane domains are markedly different (Breyton, 2000) and the cytochromes *f* and c_1 of cyt b_6/f and cyt bc_1 are completely dissimilar. Another major difference between the two complexes is that the cyt b_6/f complex contains a chlorophyll *a* and a β-carotene molecule. The postulated role of the β-carotene is to prevent generation of singlet O_2 from the photoexcited complex, whereas the role of the chlorophyll *a* molecule is still unclear (Pierre et al., 1997; Zhang et al., 1999).

The cyt b_6/f complex consists of at least eight subunits, which are encoded by the *Pet* genes (photosynthetic electron transport genes). The cyt b_6/f monomer contains one copy of each subunit (Pierre et al., 1995). In flowering plants, the nuclear genes *PetC* and *PetM* code for the Rieske iron-sulphur protein and a small peptide (subunit VII), respectively, whereas the chloroplast genes *petA*, *petB* and *petD* code for the cytochrome *f* (cyt *f*), cytochrome b_6 (cyt b_6) and the subunit IV (suIV), respectively. Two additional small subunits are encoded by chloroplast genes: PetG (*petG*) and subunit VI (*petL*); however, subunit VI is absent in cyanobacteria (Boronowsky et al., 2001). A third small subunit (subunit VIII) proposed to be encoded by the gene *ycf6* (*petN*) was identified in tobacco by Hager et al., (1999).

Recently, another subunit was identified in *C. reinhardtii*: a 15.2 kDa polypeptide, encoded for by the nuclear *PetO* gene which is reversibly phosphorylated during state transitions. This points to a possible role in signal transduction during redox-controlled adaptation of the photosynthetic apparatus. However, a sequence homologous to the *PetO* gene has only been found in the green alga Volvox and it remains to be shown whether this subunit also exists in higher plants (Hamel et al., 2000).

The Rieske protein is encoded by the single-copy nuclear gene *PetC* in Arabidopsis, spinach and pea (Salter et al., 1992) and by two nuclear genes in tobacco (Palomares et al., 1991; Madueno et al., 1992) The Rieske protein is synthesised as a 27-28 kDa precursor protein consisting of the mature protein and 49-68 N-terminal amino acid residues responsible for targeting the protein to the chloroplast (Madueno et al., 1992; Salter et al., 1992). A high degree of sequence similarity exists among the Rieske proteins which have been investigated to date (de Vitry, 1994). In Arabidopsis, the *PetC* gene contains five exons.

1.4 Mutational analysis of the cyt b_6/f complex

To date mutated alleles for several proteins of the cyt b_6/f complex have been analysed in Chlamydomonas, Lemna, tobacco and Arabidopsis: deletion strains for the three major chloroplast *Pet* genes *petA*, *petB* and *petD* have been constructed in *C. reinhardtii* (Kuras and Wollman, 1994). These deletion strains can be only grown heterotrophically and were unable to synthesize cyt *f*, cyt b_6 or suIV, respectively. It was shown that mature cyt *f* is stable in the absence of cyt b_6 or suIV, but that its rate of synthesis was severely decreased. In contrast, the presence of the other subunits of the complex is independent of the rate of synthesis of cyt b_6 and suIV. Moreover, suIV accumulation is dependent on cyt b_6 accumulation. Kuras and Wollman, (1994) concluded that the stoichiometric accumulation of the chloroplast-encoded subunits of the cyt b_6/f complex results from two regulatory processes: a post-translational regulation leading to the proteolytic disposal of unassembled cyt b_6 and suIV and a co-translational regulation, which ensures the production of cyt *f* next to its site of assembly.

Similar work has been carried out on tobacco chloroplast mutants having interrupted *petA*, *petB* and *petD* genes. These mutants were non-photosynthetic and had about three times less chlorophyll than the wild-type, leading to a pale-green leaf phenotype. In contrast, the corresponding *C. reinhardtii* mutants showed no reduction in chlorophyll. Also the chloroplast ultra structure was altered in all three tobacco mutants: 2-3 times less thylakoid membranes per unit chloroplast area were observed and the grana were comprised of many fewer thylakoid layers than in the wild-type. Another effect of the disrupted genes in the tobacco mutants was a high chlorophyll fluorescence phenotype and the loss of a functional cyt b_6/f complex. Unlike the Chlamydomonas mutant, the cyt *f* was barely detectable in Δ*petB* or Δ*petD* tobacco mutants. The amounts of *petB* and *petD* mRNA were reduced in the mutants, but the mRNAs were normally associated with polysomes. In contrast, there was a decrease in polysome accumulation of *petA* mRNA in Δ*petB* or Δ*petD*, suggesting that the synthesis of cyt *f* may be decreased in the absence of cyt b_6 or suIV. This demonstrates that vascular plants and the green algae *C. reinhardtii* share certain chloroplast gene regulatory mechanisms. For the afore mentioned cyt *f* protein it was concluded that there may be an autoregulatory effector in tobacco chloroplast, as the protein was virtually undetectable in the Δ*petB* or Δ*petD* tobacco mutants in contrast to the observations in *C. reinhardtii* (Monde et al., 2000). Moreover, the deletion of the *petG* gene in *Chlamydomonas reinhardtii* results in markedly decreased levels of cyt b_6, cyt *f*, the Rieske protein and suIV and the mutants are unable to grow photosynthetically. This suggests that the absence of the PetG protein affects the assembly or stability of the cyt b_6/f complex (Berthold et al., 1995).

In a stable deletion mutant of the *C. reinhardtii* nuclear *PetC* gene (a TG deletion resulting in a 52 residue truncated version of the protein) lacking the Rieske protein, the other subunits of the cyt b_6/f complex still accumulate (de Vitry et al., 1999). However, without a functional Rieske protein photosynthetic electron flow was completely suppressed. Contradictory results were obtained with the photosynthetic mutant no. 1073 of *Lemna perpusilla*, in which accumulation of the Rieske protein was reduced by a factor 100. In this mutant less than 1% of the four proteins cyt *f*, cyt b_6, suIV and the Rieske protein are detectable (Bruce and Malkin, 1991). However, the chloroplast genes for the cyt *f*, cyt b_6 and suIV proteins are normally transcribed and processed in the mutant. Interestingly, the cyt *f* and suIV proteins are synthesised at rates similar to the wild-type, indicating that the Rieske protein may function as a key assembly protein in an “all-or-none” assembly process. Thus, Bruce and Malkin, (1991) proposed that all cyt b_6/f components must be present for the stabilization of the complex.

In an Arabidopsis mutant having a point mutation in the *PetC* gene (Munekage et al., 2001) the electron transport rate was not affected at low light intensity. However, electron flow was significantly restricted at high light intensity. This indicates that the luminal acidification was not sufficient to induce thermal dissipation in this mutant. Furthermore the electron transfer from cyt b_6/f to PSI is not generally reduced in the mutant, but the pH dependence of this reaction is altered (Jahns et al., 2002).

Targeted inactivation of open-reading frames of the plastid genome has led to the discovery of the *petL* and *petN* gene in tobacco. The plants with a disruption in the *petL* gene display photoautotrophic growth, the amount of cyt b_6/f complex is reduced to 25-50% of wild-type level and the rate of transmembrane electron transfer by the cyt b_6/f complex *in vivo*; under saturating light, is three to four times slower than in wild-type. The remaining cyt b_6/f complex appeared more fragile than wild-type complexes, selectively loosing the Rieske iron-sulphur protein during purification. These observations indicate that PetL is an authentic subunit of the cyt b_6/f complex, which is required for its stability, accumulation and optimal efficiency (Takahashi et al., 1996). Tobacco plants having a targeted knock-out of the *PetN* gene display a photosynthetically incompetent phenotype (Hager et al., 1999). The photosystems are intact and physiologically active, but the electron transfer from PSII to PSI is interrupted as a result of the complete absence of the cyt b_6/f complex. These data indicate that the PetN protein plays a crucial role in complex assembly and/or stability.

In summary it has been shown by mutational analysis that the absence or mutation of one or more of the proteins of the cyt b_6/f complex may lead to a variety of phenotypes: to photosynthetically incompetent phenotypes, to a markedly reduced stability of the cyt b_6/f complex, or to the absence of the entire cyt b_6/f complex, but may also lead to markedly mild phenotypes with the phenotype observable only under stress conditions such as high light. These different phenotypes are thought to be caused by the effects of the mutation on transcription, translation, complex stability and/or function. However, although many such mutants have been studied, to date no stable null allele for the Rieske protein of flowering plants has been investigated.

1.5 The chloroplast ATP synthase

Photosynthetic electron flow is coupled with proton translocation across the thylakoid membrane. This produces a transmembrane electrochemical proton potential difference, which is used to form ATP out of ADP and P_i. One ATP is formed when four protons (Van Walraven et al., 1996) flow down the gradient through the membrane-bound proton translocating ATP synthase (also called CF_0CF_1 super-complex). This coupled process found in chloroplasts and cyanobacteria is called “photophosphorylation”.

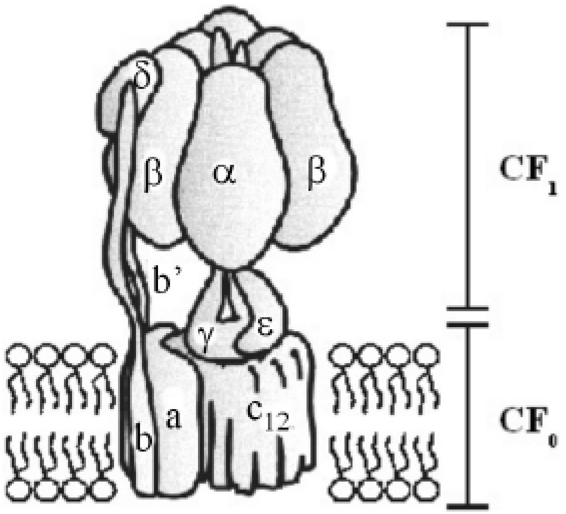

Figure 1.4 A model of the chloroplast ATP synthase (Groth and Strotmann, 1999)

For more information on the individual subunits see Table 1.1.

The structure of the chloroplast ATP synthase most closely resembles the bacterial ATP synthase in its subunit composition (Hatefi, 1985). The chloroplast ATP synthase is localized in the thylakoid membrane and consists of nine subunits. These are organized into two separate sectors: the membrane-embedded proton-conducting CF_0-complex and the water-soluble CF_1-complex containing the nucleotide binding site (Engelbrecht and Junge, 1990). The CF_0 consists of four different polypeptides in a stoichiometry of $a_1b_1b'_1c_{12}$ (Fromme et al., 1987) encoded by the chloroplast genes *atpI* (a) *atpF* (b) and *atpH* (c) and the nuclear *AtpG* (b’) gene. The extrinsic catalytic CF_1 complex contains five different subunits in the stoichiometry of $\alpha_3\beta_3\delta\gamma\varepsilon$ encoded by the nuclear genes *AtpC* (γ) and *AtpD* (δ) and the chloroplast genes *atpA* (α), *atpB* (β) and *atpE* (ε) (Groth and Strotmann, 1999). In Arabidopsis, the γ–subunit is encoded by the two nuclear genes *AtpC1* and *AtpC2* (Inohara et al., 1991).

Table 1.1 Nomenclature and characteristics of the subunits of the chloroplast ATP synthase in spinach.

*In Arabidopsis the γ subunit is encoded by the *AtpC1* and *AtpC2* genes.

Symbol	Old symbol	Molecular weight (kDa)	Gene name	Gene location	Main function
a	IV	25.1	*atpI*	chloroplast	H^+ translocation
b	I	20.9	*atpF*	chloroplast	binding of CF_1
b’	II	16.4	*AtpG*	nucleus	binding of CF_1 (?)
c	III	7.9	*atpH*	chloroplast	H^+ translocation
α	α	55.4	*atpA*	chloroplast	non catalytic nucleotide binding site
β	β	53.8	*atpB*	chloroplast	catalytic site
γ	γ	35.8	*AtpC*	nucleus	energy coupling, thiol modulation
δ	δ	20.4	*AtpD*	nucleus	binding to CF_0 anchor
ε	ε	14.7	*atpE*	chloroplast	activation / deactivation
γ*	γ	35,7	*AtpC1*	nucleus	energy coupling, thiol modulation
γ*	γ	36,1	*AtpC2*	nucleus	energy coupling, thiol modulation

In the CF_1 complex, the a- and ß-subunits are arranged alternatingly as a hexamer around a central ?-subunit (Figure 1.4). The α- and β-subunits show high homology, but the catalytic nucleotide binding sites are mainly located on the ß-subunits (Boyer, 1999). The central stalk of the complex is composed of the γ– and ε–subunits, which connects a central part of CF_1 with a slightly peripheral part of CF_0. This central stalk builds, together with 12 copies of c-subunits, the rotating portion (“rotor”) (Engelbrecht and Junge, 1997). The static part (“stator”) is formed by a second stalk, which is composed of the subunits b, b’ and d of the CF_1 complex (Boettcher et al., 1998). That means that the CF_0 complex is connected to the CF_1 complex by at least two stalks building the rotor-stator machinery, the so-called tentative model (Engelbrecht and Junge, 1997).

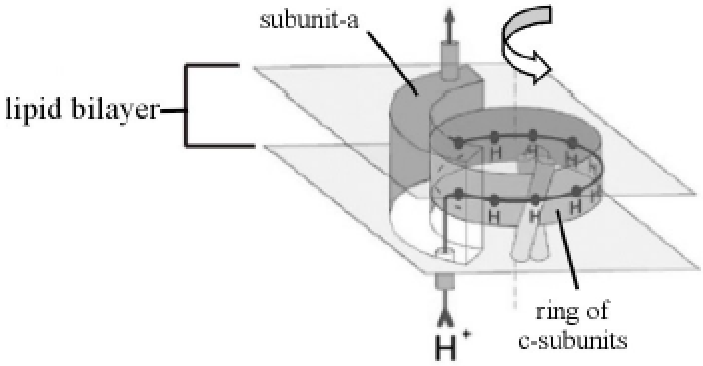

Figure 1.5 Model of the generation of torque in CF_0 driven by proton-motive force.

A ring of proteolipid molecules (composed of c-subunits) and subunit-a carry two access channels for protons from either side of the membrane (Junge et al., 1997).

Synthesis of ATP takes place in the following sequence: ion flow → intersubunit rotation → extrusion of spontaneously formed ATP. The ion channel is formed by the a-subunit, which contacts the ring of c-subunits and provides groups that probably participate in proton transfer through the CF_0 complex (ion flow) (Figure 1.5). Such proton transfer is thought to cause the ring of c-subunits to move in a step-wise fashion relative to the a-subunit (Junge et al., 1997) and so in turn causes rotation of the ε- and γ-subunits (intersubunit rotation) (Boyer, 1999).

The chloroplast ATP synthase is unique among chloroplast, prokaryotic and mitochondrial ATP synthases in that it is a latent enzyme. Without preceding activation its activity is zero. The activity of the chloroplast enzyme is controlled by the proton gradient between the stroma and the thylakoid lumen, by thiol modulation of the γ subunit and by nucleotide binding (Richter et al., 2000). As soon as the transmembrane proton gradient exceeds a critical threshold upon energization of the thylakoid membrane, the CF_1CF_0 super-complex undergoes a conformational change. This causes the disulfide bond of the γ-subunit to become significantly more exposed (Ketcham et al., 1984; Nalin and McCarty, 1984) and the disulfide bridge can be reduced by thioredoxin. Thioredoxin is, in turn, reduced by ferredoxin during active photosynthetic electron transport (Ort and Oxborough, 1992; Mills, 1995). Reduction of the γ-subunit disulfide bridge enhances the rate of activation of the CF_1 complex both for ATP hydrolysis and synthesis. Cyanobacteria lack this regulatory sequence in their γ-subunit and thus having no thiol modulation (Figure 1.6). Therefore this disulfide group is characteristic for higher plants and green algae (Hisabori et al., 2002).

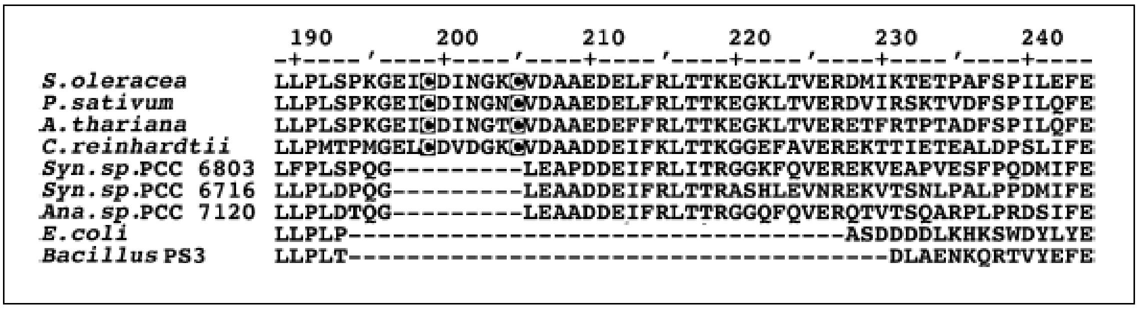

```
                  190       200       210       220       230       240
                 -+----'----+----'----+----'----+----'----+----'----+----
S.oleracea       LLPLSPKGEI●DINGK●VDAAEDELFRLTTKEGKLTVERDMIKTETPAFSPILEFE
P.sativum        LLPLSPKGEI●DINGN●VDAAEDELFRLTTKEGKLTVERDVIRSKTVDFSPILQFE
A.thariana       LLPLSPKGEI●DINGT●VDAAEDEFFRLTTKEGKLTVERETFRTPTADFSPILQFE
C.reinhardtii    LLPMTPMGEL●DVDGK●VDAADDEIFKLTTKGGEFAVEREKTTIETEALDPSLIFE
Syn.sp.PCC 6803  LFPLSPQG---------LEAPDDEIFRLITRGGKFQVEREKVEAPVESFPQDMIFE
Syn.sp.PCC 6716  LLPLDPQG---------LEAADDEIFRLTTRASHLEVNREKVTSNLPALPPDMIFE
Ana.sp.PCC 7120  LLPLDTQG---------LEAADDEIFRLTTRGGQFQVERQTVTSQARPLPRDSIFE
E.coli           LLPLP----------------------------------ASDDDDLKHKSWDYLYE
Bacillus PS3     LLPLT-------------------------------------DLAENKQRTVYEFE
```

Figure 1.6 Comparison of the amino acid sequences of the g-subunit from different species at and around the regulatory region.

Residue numbers are those from spinach CF_1-γ subunit. The regulatory cysteines are indicated by black shading (Hisabori et al., 2002).

1.6 The d-subunit of the ATP synthase

The role of the δ-subunit (in chloroplasts and *E. coli*), being a subunit of the second stalk, has been extensively studied. The δ-subunit can be cross-linked to the (aß)$_3$ portion of the CF$_1$ (Lill et al., 1996). The main feature of the δ-subunit is a six alpha-helix bundle, composed of the N-terminal domain. This domain interacts with the CF$_1$ core via the N-terminal part of the a-subunit (Wilkens et al., 1997; Rodgers et al., 1997). It was shown by Beckers et al., (1992) that the δ-subunit crosslinks also with the b-subunit, forming a connection between the second stalk and the CF$_0$ complex. In chloroplasts and bacteria it could be shown that the δ-subunit plays a role in modulating proton conductance through the complex (Monticello and Brusilow, 1994; Engelbrecht and Junge, 1988).

The mitochondrial counterpart of the *E. coli* and chloroplast δ-subunit is the OSCP-subunit (Devenish et al., 2000). The δ-subunit of spinach and the porcine OSCP-subunit are composed of approximately 85% alpha helices, with practically no beta sheets and a very low sequence homology (~23% identity). But they are indistinguishable with respect to their secondary structure indicating a high degree of structural similarity between chloroplast δ- and mitochondrial OSCP-subunits (Engelbrecht et al., 1991). It has been shown for isolated spinach thylakoids that the removal of the δ-subunit of CF$_1$ has no effect on its catalytic properties but does weaken the binding between CF$_1$ and CF$_0$ (Patrie and McCarty, 1984). However an *S. cerevisiae* OSCP-subunit depletion mutant exhibits a significant reduction in subunit d accumulation (which does not have a chloroplast homologue) and this subunit failed to assemble or to be associated with the CF$_1$ complex. Furthermore a disruption of the gene coding for the OSCP-subunit lead to *S. cerevisiae* strains exhibiting a high level of genetic instability (petite formation). Taken together, these results indicate that the yeast OSCP-subunit plays a role in the assembly and function of the enzyme complex (Prescott et al., 1994; Straffon et al., 1998).

A δ-subunit deletion strain in *E. coli* shows no ATP synthase activity in membrane vesicle preparation. In the absence of the CF$_1$ complex the membranes were impermeable to protons (Stack and Cain, 1994). In membrane preparations of the deletion strain lacking CF$_1$, the ATP synthase could be reconstituted by adding partially purified CF$_1$ from wild-type cells. Interestingly the amount of the b-subunit in the deletion strain was 3% that of the wild-type. These data indicate either that the absence of the δ-subunit, and thus the CF_1 complex, renders the b-subunit subject to proteolysis or that the incorporation of the b-subunit into CF_0 may be facilitated by the δ-subunit.

These analysis have shown that the δ-subunit plays a role in the modulation of the proton conductance, and in the assembly of CF_1 and its association with CF_0. It may also play a role in the stabilization of certain subunits of the CF_1 complex.

1.7 Mutational analysis of the ATP synthase

Several mutants in the chloroplast ATP synthase have been characterised: the Δ*atpA* and the Δ*atpB* deletion mutants of *C. reinhardtii* cannot grow photoautotrophically and none of the subunits of CF_1 and of CF_0 were detectable (Fiedler et al., 1997). The PSII and PSI activities were not affected and thylakoids from the deletion mutants were able to maintain a light-induced proton gradient significantly higher than wild-type thylakoids. This shows that the absence of the α- or β-subunit leads to the loss of a functional proton channel in the deletion mutants.

Lemaire and Wollman, (1989) carried out an analysis of *C. reinhardtii* mutants defective in photophosphorylation focusing on the biogenesis of the ATP synthase. Results of this analysis are listed in Table 1.2.

Table 1.2 List of *C. reinhardtii* mutants defective in photophosphorylation analysed by Lemaire and Wollman (1989).

Strain	Main characteristics	Putative mutation
FUD50	No synthesis of the β-subunit	Deletion in the *atpB* gene
FUD16	Overproduction of the α- and β-subunits	Altered in chloroplast gene regulating the expression of the *atpA* and *atpB* genes
FUD17	No synthesis of subunit ε	Altered in the *atpE* gene
FUD18	No synthesis of subunit I (b)	Altered in the *atpF* gene
FUD23	No synthesis of subunit IV (a)	Altered in the *atpI* gene
thm24	No synthesis of the α- and β-subunits	Altered in nuclear gene regulating either transcription or translation of the *atpA* and *atpB* chloroplast genes
F54	No synthesis of subunit α	Altered in nuclear gene regulating either transcription or translation of the *atpA* gene
ac46	No synthesis of subunit III (c) and IV (a)	Altered in nuclear gene regulating either transcription or translation of the *atpH* and *atpI* chloroplast genes

Of the mutants listed in Table 1.2, only the FUD16 mutant showed ATP synthase activity, whereas no activity was detectable in any of the other mutants. Further analyses gave evidence for a control of the rate of synthesis of the β-subunit by the α-subunit in the absence of ATP synthase assembly and for an interaction between α- and β-subunits in the stroma of the chloroplast. It was proposed that the β-subunit protects the α-subunit from proteolytic degradation. The role of several chloroplast-encoded subunits of the CF_1 and CF_0 complexes in the stabilization of the partially assembled super-complex has also suggested that: subunit IV further stabilizes the complex and is required for ATP synthase activity; subunit III plays a major role in the formation of the CF_0 complex and is required for membrane binding of the CF_1 complex and subunit I is responsible for binding of α- and β-subunits. These results show that the assembly of the ATP synthase super-complex is dependent on the intricate cooperation of many factors. Further analyses of the mutant ac46 (lacking the *atpH* transcript; Table 1.2) revealed an increased sensitivity to light (Majeran et al., 2001). Exposure of ac46 to moderate light intensities, for a few minutes, leads to an inhibition of the electron transfer downstream of the primary quinone acceptor of PSII, accompanied by a thylakoid swelling. Longer exposure leads to a progressive loss of PSII core and the thylakoids deflate. The block in the electron transport is likely to result from the light induced acidification of the lumen. This acidification is caused by the release of protons, coupled to photosynthetic electron transfer, that cannot be translocated back to the stroma in the absence of the ATP synthase. Taken together, the analysed chloroplast ATP synthase mutants demonstrate that the ATP synthase assembly is dependent on the presence of particular subunits and a lack of ATP synthase activity leads to a lack of photoautotrophy and an increased transthylakoid pH-gradient.

In summary, it has been shown by mutational analysis that the absence or overproduction (Lemaire and Wollman; 1989) of one or more of the proteins of the ATP synthase super-complex may lead to a variety of phenotypes: from a mild phenotype where the ATP synthase is functional and the plants appear normal, to photosynthetically incompetent phenotypes with no functional ATP synthase activity and a high transthylakoid pH-gradient. These different phenotypes are thought to be caused by mutation-induced alteration of transcription, translation, complex stability and/or function. However, although many such mutants have been studied, to date no stable null allele for the δ-subunit of the ATP synthase of flowering plants has been reported.

1.8 Chlorophyll fluorescence, photochemical and non-photochemical quenching and the role of the xanthophyll cycle

Chlorophyll is the main antenna pigment, funnelling the absorbed light energy into the reaction centres. By the absorption of light, electrons of the chlorophyll molecule become excited. The de-excitation of the electrons can take place by three different mechanisms (Sauer, 1975) as depicted in Figure 1.7: dissipation into heat, photochemistry or reemission as fluorescence, which comes mainly from PSII.

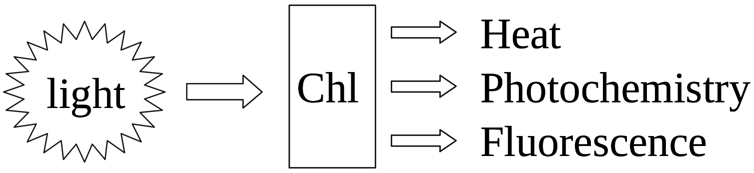

Figure 1.7 Mechanisms for de-excitation of chlorophyll (Chl) molecules.

Dissipation of excitation energy can occur by an increased molecular vibration of the chlorophyll molecule (resulting in heat) or by the transfer of the energy to a chemical acceptor (photochemistry), which is the central event in photosynthesis. Under normal conditions, fluorescence emission can be regarded as being the only process competing with photochemistry. Therefore, there is a direct relationship between photochemistry and fluorescence: the higher the fluorescence yield, the lower the yield of photochemistry. As a result, chlorophyll fluorescence can be used as a tool to determine both the maximal and the effective efficiency of photon usage in photochemistry (Clayton, 1980). For quantifying chlorophyll fluorescence the Pulse Amplitude Modulation (PAM) fluorometer system has been developed (Schreiber et al., 1986). This system can be used to measure the parameters summarized in Figure 1.8. The minimal fluorescence of dark-adapted plants (F_0) is measured by illuminating the leaf with a light intensity, which is low enough that is does not drive photosynthesis. The maximal fluorescence (F_M) is determined after illumination with a light saturating pulse (Krause and Weis, 1991). This saturating light pulse is so short that it does not allow photosynthetic electron transport (photochemical quenching) or heat dissipation (non-photochemical quenching) and hence the fluorescence is maximal. Therefore the ratio $F_V/F_M = (F_M-F_0)/F_M$ is called the maximal fluorescence yield of PSII and indicates the maximal fraction of absorbed photons, that can theoretically be used to drive photosynthesis.

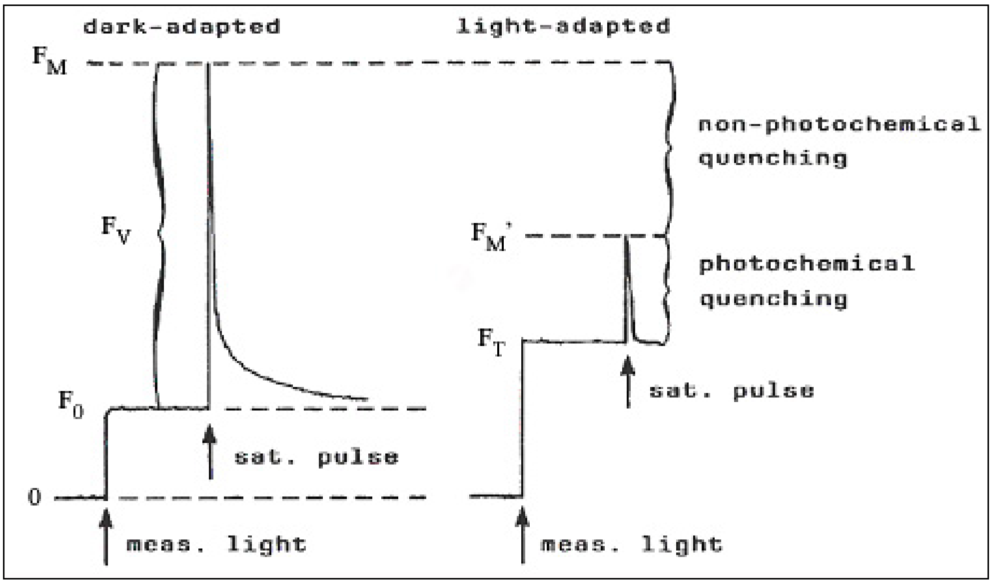

Figure 1.8 Fluorescence parameters measured by the Pulse Amplitude Modulation fluorometer system (PAM).

Meas. light, measuring light; F_0, minimal fluorescence of a dark-adapted leaf; F_M, maximal fluorescence of a dark-adapted leaf; F_V, variable fluorescence; sat. pulse, saturating light pulse; F_T, transient fluorescence of a light-adapted leaf; F_M’, maximal fluorescence of a light-adapted leaf.

These parameters can also be measured for light-adapted plants. F_0 corresponds to F_t for light-adapted plants and F_M to F_M’. The effective fluorescence yield of PSII (Φ_{II}) is given by $F_{II} = (F_M’-F_T)/F_M’$ (Genty et al., 1989). This parameter indicates the fraction of photons that is actually used to drive photosynthesis under illumination and is an indicator of the efficiency of photosynthesis in the plant. In addition, Φ_{II} and the fluorescence quenching parameters: qP (photochemical quenching) = $(F_M’-F_S)/(F_M’-F_0’)$ and NPQ (non-photochemical quenching) = $1 - (F_M’-F_0’)/(F_M-F_0)$ (Schreiber et al., 1986) were recorded.

The dissipation of excess absorbed light energy is believed to play a central role in regulating light harvesting and electron transport and appears to be critical for the prevention of photo-oxidative damage to the photosynthetic apparatus. The dissipation of excess absorbed light energy proceeds through non-photochemical quenching (NPQ). The major component of the NPQ is the pH-dependent energy dissipation (qE). But decreases in PSII fluorescence due to state transition (qT) and photoinhibition (qI) also contribute to the measured NPQ (Krause and Weis, 1991).

Xanthophyll pigments in the LHCs appear to have a critical role in NPQ as the extent of qE in plants strongly correlates with the levels of zeaxanthin and antheraxanthin (Demmig-

Adams et al., 1990). Also the ΔpH is absolutely necessary for the NPQ (Noctor et al., 1993) as in excessive light, when the ΔpH reaches a critical threshold, violaxanthin is converted to zeaxanthin by the violaxanthin deepoxidase (Figure 1.9).

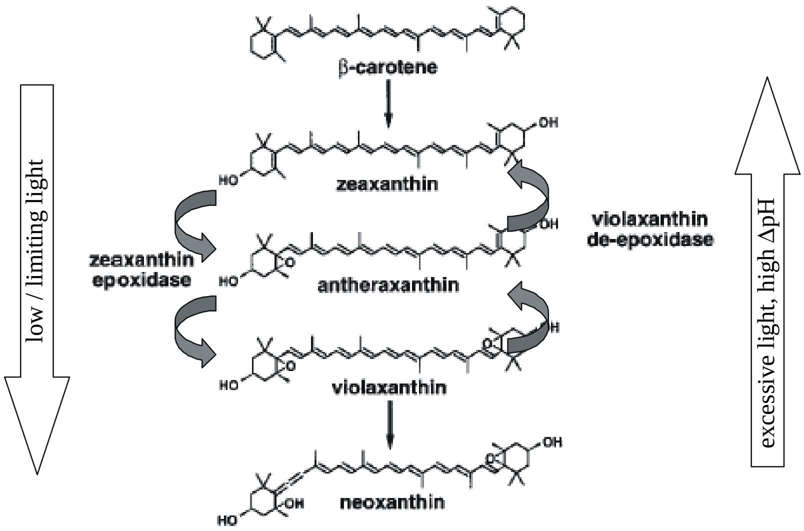

Figure 1.9 The xanthophyll cycle in the β-carotene branch of the carotenoid biosynthetic pathway in plants.

These non-photochemical quenching processes occur in almost all photosynthetic eukaryotes and they contribute to the regulation and protection of photosynthesis in environments in which light energy absorption exceeds the capacity for light utilization.

1.9 Aim of the thesis

The aim of this thesis was to analyse the two Arabidopsis mutants *petc-2* and *atpd-1* in terms of the assembly of the corresponding complexes (cyt b_6/f and ATP synthase, respectively). Furthermore, the overall effects of the mutations on the plants with specific attention to the photosynthetic parameters were analysed. Effects on photosynthesis, the thylakoid pigments and protein composition were characterised and interpreted. In addition, effects of the two photosynthetic lesion on nuclear gene expression were quantified and discussed in terms of plastid-to-nucleus signalling.

2 MATERIAL & METHODS

2.1 Chemicals and enzymes

The chemicals and kits used in this thesis were purchased from the following companies: Acros Organics (New Jersey, USA), Amersham International plc (Buckinghamshire, England), Baker (Deventer, Netherlands), BIOMOL (Hamburg, Germany), Biozym (Hess. Oldendorf, Germany), Difco-Laboratories (Detroit, USA), Fluka AG (Basel, Switzerland), Invitrogen (Karlsruhe, Germany), Merck (Darmstadt, Germany), Millipore (Eschborn, Germany), Pharmacia (Freiburg, Germany), Promega (Mannheim, Germany), Riedel-de-Haen (Seelze, Germany), Roth (Karlsruhe, Germany), Serva (Heidelberg, Germany), Sigma (St. Louis, USA), Qiagen (Hilden, Germany).

Enzymes were purchased from the following companies: Roche (Mannheim, Germany), Invitrogen (Karlsruhe, Germany) and New England Biolabs (Frankfurt, Germany).

2.2 Strains

E. coli: JM202 (Promega; Invitrogen, Karlsruhe, Germany).

Agrobacterium tumefaciens: Arabidopsis plants were transformed with the *A. tumefaciens* strain GV3101. This strain has a C58C1 chromosomal background with a rifampicin resistance mutation marker and carries the Ti helper plasmid pMP90RK, which encodes virulence functions for the T-DNA transfer from *A. tumefaciens* to the plant cells (Koncz et al., 1990).

2.3 Media and cultivation

2.3.1 *E. coli:* Luria Broth (LB) Medium

E. coli cells were grown o/n at 37°C in LB medium [10 g/l casein-hydrolysate (Peptone No. 140, Gibco), 5 g/l yeast extract, 5 g/l NaCl] with shaking (150 rpm) for liquid cultures. LB medium was supplemented with 1.6% (w/v) agar-agar before autoclaving to produce solid LB medium. For the selection of transformants the medium was supplemented with 500 µg/ml ampicillin (LB/amp).

2.3.2 *A. tumefaciens*: YEB medium

YEB medium: 0.5% (w/v) beef extract, 0.1% (w/v) bacto yeast extract, 0.5% (w/v) bacto peptone, 0.5% (w/v) sucrose. For the selection of transformants 100 mg/l carbenicillin, 25 mg/l kanamycin and 100 mg/l rifampicin were added.

Solid YEB medium: YEB medium with 1.6% (w/v) agar-agar. The cells were incubated for 2-5 days at 28°C, in addition liquid cultures were shaken at 150 rpm.

2.3.3 *A. thaliana* axenic culture: Murashige & Skoog (MS) medium

1x MS medium: 4.33 g/l Murashige & Skoog Basal Salt Mixture (Sigma, St. Louis, USA), 1 ml/l 1000x Murashige & Skoog Vitamin Solution (Sigma, St. Louis, USA), pH 5.7-5.8.

1x MS1 medium: 1x MS medium with 1% (w/v) sucrose.

1x MS2 medium: 1x MS medium with 2% (w/v) sucrose.

For making solid MS medium 1% (w/v) agar-agar was added to the medium before autoclaving.

2.4 Plant propagation

2.4.1 On soil

Arabidopsis thaliana seeds were incubated for 1-2 days in the dark at 4°C to break the seed dormancy and then sown out in plastic trays with *Minitray* soil (Gebr. Patzer GmbH & CoKG, Sinntal-Jossa, Germany). Plants were grown in a greenhouse under long day conditions (day period of 16 h at 20°C with a photon flux density (PFD) of 80 µmol photons m^{-2} s^{-1}, night period of 8 h at 15°C). Fertiliser was applied according to manufacturer’s instructions with “Osmocote Plus” (15% N, 11% P_2O_5, 13% K_2O, 2% MgO; Scotts Deutschland GmbH, Nordhorn, Germany).

2.4.2 Sterile culture

Mutants that were lethal on soil were grown on MS medium supplemented with 2% sucrose. Seeds were surface sterilised with 10% (w/v) NaOCl and sown out on petri dishes containing 1x MS2 medium, 1% (w/v) agar-agar, pH 5.7-5.8. The plates were incubated for 1-2 days at 4°C in the dark and then transferred to the culture room under low light conditions (day period of 16 h with PFD of 15 µmol photons m^{-2} s^{-1} at 22°C, night period 8 h at 22°C).

Transformed plants were grown on 1x MS medium with 100 mg/l kanamycin in a culture room (day period of 16 h with PFD of 60 µmol photons m^{-2} s^{-1} at 22°C, night period 8 h at 22°C) for 3-4 weeks and then transferred to soil and grown in the greenhouse as described in section 5.1.

2.5 Oligonucleotide sequences

Primer name	**Sequence (5’-3’)**
AtpD_118180_s	CACAGATATCACACCAATCA
AtpD_118720_as	TTCTTCTCGACGGTGATTGTT
AtpD_Northern_as	TCAAGTAGCTAATTGAATCTCAC
AtpD_Northern_s	ATGGCGTCTCTTCAA CAAACT
Compl_AtpD_as	ACTTGGATCCTCAAGTAGCTAATTGAATCTCAC
Compl_AtpD_s	ACTTGGATCCATGGCGTCTCTTCAACAAACT
DsLb	ATCGGGATGATCCCGTTTCG
DsRb	TTCCCGTCCGATTTCGACTT
EnRb	GTCGGCTTATTTCAGTAAGAGTGTGGG
petc-1_as	TACGGTATCAACGCAGTGTG
petc-1_s	TGGAGCATCACCTGACCTGA
petc-2_as	GACCCGATTGTTTCGATTCG
petc-2_s	CAGCCCAATAAGGCCCACT
petc-3_as	ATTCATCTTCGTTGGCTTC AC
petc-3_s	ACGCCATGCACATTTCATCAT
PetC_Northern_as	ACCACCATGGAGCATCACCAGTC
PetC_Northern_s	CGTCGAGTATTCCAGCAGAC
pROK2	GCGTGGACCGCTTGCTGCAACT
SKI015_lb	CATGTAGATTTCCCG GACATG
SKI015_rb3	AGACGTTCCAACCACGTCTT

2.6 Gel electrophoresis

2.6.1 Agarose gel electrophoresis

Agarose gels for the electrophoresis of DNA or RNA contained 1-2% (w/v) agarose melted in 1x TAE (40 mM Tris-acetate, 20 mM sodium acetate, 2 mM EDTA. pH 8.2) buffer. Electrophoresis was performed in 1x TAE buffer at 80 V. After electrophoresis the gel was incubated for 15 minutes in 0.5µg/ml ethidium bromide before being photographed.

2.6.2 Polyacrylamide gel electrophoresis

Footprint analysis was performed on 6% polyacrylamide gels. Electrophoresis was performed in 1x TBE (90 mM Tris-HCl, pH 8.3, 90 mM sodium borate, 2 mM EDTA) buffer at 62 V for 4-6 hours. For visualizing the DNA fragments the gel was silver stained according to Sanguinetti et al., (1994)

2.7 Enzymatic reactions

2.7.1 PCR

PCR reactions were performed according to the supplier's instructions with the PCR Expand Kit (Roche, Mannheim, Germany) or by using the Taq DNA polymerase (Roche, Mannheim, Germany). Standard conditions were: 93°C for 3 minutes followed by 35-40 cycles of: 95°C for 15 s; 55°C for 45 s; 72°C for 90 s. This was followed by 72°C for 5 minutes. Samples were used immediately or stored at –20°C.

2.7.2 Ligation of DNA fragments

For the ligation of DNA fragments a ratio of insert to vector of 3:1 was used. To the ligation assay 1U of T4-ligase (Roche, Mannheim, Germany) and $^{1}/_{10}$ of the 10x ligation buffer were added and then incubated at 16°C o/n. 1-5 µl of the ligation assay were used for transformation (see material and methods, section 2.12).

2.7.3 Restriction analysis

Restriction of DNA was performed according to manufacturer's instructions and in the recommended buffer at the appropriate temperature for 1-2 h. For each µg of DNA 1-10U of restriction enzyme were used.

2.7.4 Radioactive labelling of DNA

Labelling of probes for Northern analysis was performed as described in Sambrook et al., (1989).

2.7.5 cDNA single strand synthesis

cDNA single strand synthesis was performed with oligo(dT)$_{12\text{-}18}$ according to the „Superscript^{TM} First-Strand Synthesis System for RT-PCR“ (Invitrogen, Karlsruhe, Germany).

2.8 Sequence analyses

Sequence data were analysed with the Wisconsin Package Version 10.0, Genetics Computer Group, Madison, Wisconsin (GCG) (Devereux et al., 1984) and amino acid sequences were aligned using the CLUSTAL-W program, (version 1.7) (Thompson et al., 1994). Chloroplast import sequence predictions were carried out using the TargetP program (version 1.0; *http://www.cbs.dtu.dk/services/TargetP/#submission*; Emanuelsson et al., 2000). For the protein and nucleotide sequence comparison, the databases at the NCBI (http://www.ncbi.nlm.nih.gov*)* and MIPS (http://mips.gsf.de) were employed.

2.9 Plasmids

2.9.1 pGEM-Teasy

PCR products were cloned in the pGEM-Teasy vector according to manufacturer’s instructions (Promega, Mannheim, Germany).

2.9.2 pPVC702

pPVC702 was the binary expression vector used for complementation analysis with cDNA. The vector contains the cauliflower mosaic virus 35S promotor, a β-lactamase gene (amp^R) und a carbenicillin resistance gene for the selection in *E. coli* and *A. tumefaciens* and a kanamycin resistance gene for the selection in Arabidopsis (Koncz et al., 1990).

2.9.3 pPVC702-*AtpD*

The cDNA of the *AtpD* gene was amplified with the primers Compl_AtpD_s and Compl_AtpD_as. The primers each contain an additional 5’ sequence containing a *BamHI* site. The PCR product was subsequently digested with *BamHI* and then cloned into the *BamHI* linearised vector pPVC702.

2.10 Nucleic acid preparation

2.10.1 DNA preparation

A. thaliana

The isolation of DNA from *A. thaliana* was performed according to Liu et al., (1995).

E. coli

The isolation of plasmid DNA from *E. coli* for restriction analysis was performed according to Sambrook et al. (1989). For sequencing reactions the preparation was performed with the Plasmid Mini Kit from Qiagen (Hilden, Germany) according to the manufacturer's instructions.

Isolation of DNA-fragments from agarose gels

The isolation of DNA fragments from agarose gels was performed with the PCR-Purification Kit (Roche, Mannheim, Germany) according to the supplied protocol.

2.10.2 RNA preparation

RNA for Northern analysis or microarray analysis was isolated according to Chomczynski and Sacchi, (1987). RNA for cDNA synthesis was isolated with the "Total RNA Isolation Reagent" from BIOMOL (Hamburg, Germany) according to the supplied protocol.

2.11 Northern analysis

Northern analyses were performed with 30 µg of total RNA under stringent conditions according to Sambrook et al., (1989). For the hybridisation, probes complementary to the gene of interest were used.

2.12 Transformation of *E. coli*

Chemically competent *E. coli* cells, strain JM202, were purchased from Promega (Mannheim, Germany) and transformed according to the protocol of Hanahan, (1983).

2.13 Complementation analysis of Arabidopsis plants via *A. tumefaciens* transformation

2.13.1 Transformation of Arabidopsis using *A. tumefaciens*

Heterozygous Arabidopsis plants were transformed as described by Clough and Bent, (1998). Plants for transformation were grown under short day conditions and then in order to induce flowering, transferred to long day conditions. Flowering plants were then dipped in an *A. tumefaciens* suspension containing 5% (w/v) sucrose and 0.0005 % Silwet L-77 as surfactant. After dipping, plants were sealed in plastic bags for 2 days and transferred to the greenhouse. The plastic bags were removed after two days and plants were kept in the greenhouse until seeds were harvested.

2.13.2 Selection of transformed plants

Seeds of transformed plants were surface sterilized in 10% (w/v) NaOCl and sown out on 1x MS1 medium containing 50 mg/ml kanamycin. Transformants were transferred after 3-4 weeks to soil to generate seeds.

2.14 Thylakoid preparation from Arabidopsis leaves

2.14.1 For 2-D gel electrophoresis and Western analysis

Leaves of 4-6 weeks old plants were harvested at 4°C and the isolation of the thylakoids was performed as described by Bassi et al., (1985). The amount of thylakoid membranes in the preparation was calculated according to Porra et al., (1989).

2.14.2 For electron transport measurements

Leaves from 4-6 weeks old plants were homogenised in a medium containing 330 mM sorbitol; 20 mM Tricine/NaOH, pH 7.6; 5 mM EGTA; 5 mM $NaCO_3$; 0.1% (w/v) BSA and 330 mg/l ascorbate, centrifuged for 5 minutes at 3000 rpm and the pellet was resuspended in 300 mM sorbitol; 20 mM HEPES/KOH, pH 7.6; 5 mM $MgCl_2$ and 2.5 mM EDTA according to Jahns et al., (2002).

2.15 Western blot analysis

Thylakoid membranes corresponding to 5 µg of chlorophyll were separated on a denaturing SDS-PAGE gradient gel (10-16%) as described by Schagger and von Jagow, (1987).

For Western blot analysis the proteins were transferred to Immobilon-P membrane (Millipore, Eschborn, Germany) by wet-blot in 10% methanol containing 15 g/l Tris and 70 g/l glycine at 300 V for 16 hours. The membranes were blocked with 5% (w/v) milk powder in 1x TTBS buffer (10 mM Tris, pH 8.0; 150 mM NaCl; 1 ml/l Tween 20) for 16 hours at 4°C, before being incubated with antibodies specific for individual subunits of PSII (PSII-D1), PSI (PSI-F), cyt b_6/f (Cyt b_6, Rieske), ATPase (α-/β-, δ-, a- and b-subunits) in blocking solution. After the incubation with the 1st antibody the membranes were washed three times for 10 minutes at room temperature with 1x TTBS buffer, before incubating with the appropriate 2nd antibody, which had horseradish peroxidase attached. Signals were detected using the Enhanced Chemiluminescence Western-Blotting Kit (Amersham, Buckinghamshire, England).

2.16 2-D gel electrophoresis

In the first dimension, thylakoid membranes corresponding to 30 µg of total chlorophyll were fractionated on a native polyacrylamide gradient gel (4-12% acrylamide) as described by Peter and Thornber, (1991) with the modification of using lithium dodecyl sulphate (LDS) instead of lauryl β-D imminopropionidate in the upper electrophoresis buffer. Lanes from the first dimension were cut, denatured (by incubating in 2% (w/v) SDS, 6 M urea for 45 minutes at RT) and overlayered on the second dimension which was run according to the method described by Schagger and von Jagow, (1987). The 2nd dimension gel was stained with Comassie Brillant Blue R 250 as described by Sambrook et al., (1989). Densitometric analyses of protein gels after staining were performed by using the Lumi Analyst 3.0 (Roche, Mannheim, Germany).

2.17 Pigment analysis

For pigment extraction, leaves were harvested in liquid nitrogen, ground using metal beads and pigments were extracted with 80% (v/v) acetone. Pigment analyses were performed according to Farber et al., (1997) by reverse phase HPLC.

2.18 Chlorophyll fluorescence measurements and redox state of P700

In vivo Chl fluorescence of single leaves was excited and detected by a pulse amplitude modulated fluorometer (PAM 101/103, Walz, Effeltrich, Germany) as described by Meurer et al., (1996). 800 ms white light pulses of 6000 µmol m^{-2} s^{-1} were used to determine the maximum fluorescence (F_M) and the ratio $(F_M\text{-}F_0)/F_M = F_V/F_M$. Actinic light of 12 µmol m^{-2} s^{-1} intensity was used to drive photosynthesis. In addition, fluorescence quenching parameters: qP (photochemical quenching) = $(F_M'\text{-}F_S)/(F_M'\text{-}F_0')$, NPQ (non-photochemical quenching) = $1 - (F_M'\text{-}F_0')/(F_M\text{-}F_0)$ (Schreiber et al., 1986) and Φ_{II} were recorded.

For measuring qE (Thiele et al., 1997), leaves were stored in low light and placed in the thermostated (25°C) chamber of an electrode setup (Hansatech, Kings Lynn, Norfolk, UK) connected with a PAM 101 (WALZ, Effeltrich, Germany). A moist air stream of 20 l h^{-1} was passed over the leaf section. After 5 minutes dark adaptation, the initial fluorescence yield emitted during a saturating light pulse (1s), F_M, were determined. The leaf was then illuminated with continuous actinic red light (λ_{max}, 660 nm) of 12, 130, 450 and 900 µmol m^{-2} s^{-1} provided by photodiodes (Hansatech, Kings Lynn, Norfolk, UK). The decline in F_M was monitored by means of further saturating pulses applied every 100 seconds. After 20 minutes in actinic light, a stationary (quenched) level of maximum fluorescence, F_{MS}, was reached; the actinic light was switched off and weak far-red light was applied to record the initial fluorescence in the steady-state, F_{0S}. Relaxation of quenching of maximum and initial fluorescence were followed in the dark until a new steady-state was reached (after 10 minutes darkness) and the fluorescence parameters F_0' and F_M' were recorded. The energy-dependent quenching related to the transthylakoid proton gradient was calculated using the formula: $qE = (F_M'/F_{MS} - 1)F_M/F_M' = F_M/F_{MS} - F_M/F_M'$.

The redox-state of P700 under continuous white actinic light was calculated from measurements of changes in P700 absorption at 820 nm with the PAM 101 fluorometer connected to a dual-wavelength emitter-detector unit ED-P700/DW (Walz, Effeltrich, Germany) according to Barth et al., (2001).

For measuring fluorescence induction kinetics, plants were dark adapted o/n. The actinic beam (green light-emitting diodes HLMP-CM15) was concentrated on ~20 mm^2 of leaf fragment, and the fluorescence was detected from the opposite face of the sample. The time resolution of this method was 30 µs. The saturating red light pulse (max. 680 nm, 400 ms) fully reduced Q_A (Joliot and Joliot, 2002). The kinetics of the fluorescence induction curve was monitored within the first 20 s.

2.19 Membrane potential measurements

Spectroscopic measurements were performed with an apparatus similar to that described in Joliot et al., (1980). The variation of the delocalized membrane potential was measured by the electrochromic shift of membrane pigments as the difference in absorption (518-548 nm), which was assumed to be a reliable indicator of the membrane potential changes (Joliot and Joliot, 2001). For the measurements plants were kept in the dark o/n. Membrane potential changes were induced by a saturating light pulse (~690 nm) of 15ms (wild-type) or 25ms (*atpd-1* mutant). The membrane potential reached at the end of the pulse is ~equal for WT and mutant, and has been normalized to 10000 (at time=0 of the analyzed dark period following the illumination). The membrane potential is analyzed using 520 nm short light pulses, weak enough to have no actinic effect.

2.20 Electron transport measurements

Electron transport rates under illumination with saturating actinic light (150 µmol photons m^{-2} s^{-1}) were derived from measurements of photosynthetic oxygen evolution using a Clark-type oxygen electrode (Hansatech Instruments Ltd., Laborbedarf Helmut Sauer, Reutlingen, Germany) at 20°C. Thylakoid concentrations equivalent to 10 µg of chlorophyll ml^{-1} were used for all measurements. Linear electron transport ($H_2O \rightarrow K_3[Fe(CN)_6]$) was measured in a medium containing 330 mM sorbitol, 40 mM HEPES/NaOH (pH 7.6), 10 mM NaCl, 5 mM $MgCl_2$, 2 µM gramicidin D and 5 mM NH_4Cl; using 0.5 mM $K_3[Fe(CN)_6]$ as terminal electron acceptor. PSII activity ($H_2O \rightarrow$ 1,4-benzoquinone) was measured in the same medium using 1 mM 1,4-benzoquinone instead of $K_3[Fe(CN)_6]$ as terminal electron acceptor. PSI activity was measured in 40 mM Tricine/NaOH (pH 8.0), 60 mM KCl, 5 mM $MgCl_2$, 1 mM NaN_3, 1 mM sodium-ascorbate, 100U superoxide dismutase, 1 µM 3-(3-4-di-chlorophenyl)-1,1-dimethylurea (DCMU); using 0.5 mM 2,3,5,6-tetramethyl-p-phenylene-diamine (TMPD) as electron donor and 25 µM methyl viologen as electron acceptor.

2.21 Expression profiling

2.21.1 Probe synthesis

A mixture of oligonucleotides (2.5 pmol each) matching the spotted genes in antisense orientation (‘antisense primer mix’) and 25–30 µg total RNA were denatured for 10 minutes at 70°C and then annealed by cooling to room temperature. 6 µl of 5x Superscript buffer (Invitrogen, Karlsruhe, Germany), 3 µl of 0.1 M DTT, 3 µl of 10 mM dNTP-mix (except for 50 µM dCTP), and 3 µl of $^{33}P\alpha dCTP$ ($3.7x10^5$ Bq/µl) were added. After transfer of the mixture to 43°C, 1 µl of Superscript Reverse Transcriptase (200 U/µl, Invitrogen, Karlsruhe, Germany) was added and reverse transcription was performed for 1 hours. RNA was hydrolysed by adding 1 µl of 1% (w/v) SDS, 1 µl of 0.5 M EDTA, and 3 µl of 3 M NaOH, and incubating at 65°C for 30 minutes, followed by 15 minutes at room temperature. The mixture was neutralised by adding 1 µl of 1 M Tris-HCl (pH 5.3) and 3 µl of 2 M HCl. cDNAs were precipitated after addition of 5 µl of 3 M sodium acetate (pH 5.3), 5 µl of tRNA (10 mg/µl) and 60 µl of isopropanol at -20°C for 30 minutes. After centrifugation the labelled cDNA was dried and resuspended in 100 µl of sterile water.

2.21.2 Hybridisation procedure

The 3292-GST array, representing genes known or predicted to code for proteins featuring a chloroplast transit peptide (cTP), has been described previously (Kurth et al., 2002; Richly et al., 2002). Filters were pre-hybridised for at least 30 minutes at 65°C in 30 ml of

Church buffer (0.5 M Na_2HPO_4, pH 7.2; 7% (w/v) SDS; 1 mM EDTA) including 300 µl of denatured salmon sperm DNA (10 mg/ml). Hybridisation was carried out at 65°C o/n after adding the labelled cDNA probe. Filters were washed at 65°C successively for 15 minutes and 30 minutes in 2x SSPE (300 mM NaCl, 20 mM NaH_2PO_4, 2 mM EDTA, pH 7.4), 0.1% (w/v) SDS, followed by a final washing step at room temperature in 50 mM NaH_2PO_4 (pH 7.0), 1.2 mM EDTA, 0.2% (w/v) SDS for 30 minutes. Filters were finally wrapped in plastic foil and exposed to phosphoimager plates (Molecular Dynamics). At least three experiments with different filters and independent cDNA probes derived from plant material corresponding to pools of at least 50 individuals were performed for each condition or genotype, thus minimising variation between individual plants, filters or probes.

2.21.3 Data analysis

Images were read using the Storm phosphoimager (Molecular Dynamics, Sunnyvale, CA, USA). Hybridization images were imported into the *ArrayVision* program (version 6; Imaging Research Inc., Ontario, Canada) and statistically evaluated using the *ArrayStat* program (version 1.0 Rev. 2.0; Imaging Research Inc., Ontario, Canada). Normalization of data was performed with reference to all spots on the array as described by Kurth et al., (2002) and Richly et al., (2002). Clustering of expression ratios was performed using *Genesis* Software (version 1.1.3) (Sturn et al., 2002).

3 RESULTS

3.1 Characterisation of the *petc-2* mutant

3.1.1 Identification of the Rieske protein mutant lines

The mutant *petc-1* (*PetC*::*En1*, ecotype Col-0) was identified by a reverse genetic screening approach as described (Wisman et al., 1998). This line has an *En* transposon inserted in the fourth intron of the *PetC* gene - coding for the Rieske protein - at position +1233 bp relative to the ATG codon. The insertion of the *En* transposon caused a duplication of three bps (Figure 3.1).

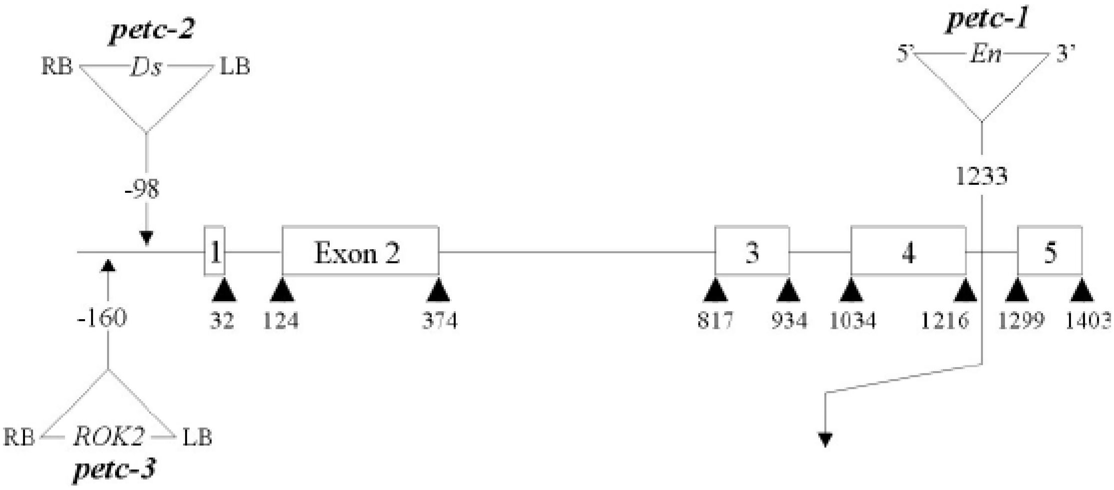

wild-type	CAAATAC**ATT** GCATTCTT
petc-1	CAAATAC**ATT**-*En*-**att**GCATTCTT
REV1	CAAATAC**ATT** **aatatt**GCATTCTT
REV2	CAAAT..... .**tt**GCATTCTT
REV3	CAAATAC**ATT** **att**GCATTCTT

Figure 3.1 Mutations of the *PetC* locus.

In *petc-1*, the *PetC* gene (At4g03180) is disrupted by an insertion of the autonomous *En* transposon (Wisman et al., 1998). Progenies of *petc-1* resulted in three independent somatic revertants, exhibiting a wild-type phenotype. The sequences of the empty donor sites of DNA from three independent somatically revertant leaves (*REV1* to *3*) were obtained by PCR; upper case letters indicate plant DNA sequences flanking the *En*, deletions are indicated by dots, insertion footprints left at each locus after *En* transposition are indicated by bold lowercase letters, and bold uppercase letters indicate the target site in the wild-type. In the other two mutant alleles, a copy of the non-autonomous *Ds* transposon (*petc-2*) and the *ROK2* T-DNA (*petc-3*), respectively, are inserted 5' of the start codon of the *PetC* gene. The *En*, *Ds* and T-DNA insertions are not drawn to scale.

Two additional independent mutations of the *PetC* locus have been identified: the second *petc* allele in the course of a phenotypic screen of *Ds* transposon mutagenized *Arabidopsis thaliana* lines (ecotype L*er*). This is a seedling-lethal line with an insertion in the *PetC* locus and was described by Budziszewski et al., (2001). This line, designated *petc-2*, contains an insertion of the non-autonomous *Ds* element 98 bp 5' of the start codon ATG of the *PetC* gene (Figure 3.1). This insertion caused a duplication of eight bps. The third *petc* allele was identified when the insertion flanking database, SIGnAL (http://signal.salk.edu/cgi-bin/tdnaexpress) was searched for insertions at the *PetC* locus. This line (ecotype Col-0) had a copy of the 5.2 kb p*ROK2* T-DNA inserted 160 bp 5' of the start codon ATG of the *PetC* gene (Figure 3.1) and was designated *petc-3*.

3.1.2 Phenotype of the *petc* mutant lines

All three *petc* mutants were seedling-lethal when grown on soil. In addition, they exhibit a yellowish pigmentation of the cotyledons. All three *petc* mutant alleles could, however, be propagated in sterile culture on 1x MS medium supplemented with 2% sucrose. However, heterotrophically-grown *petc* plants had light-green leaf coloration and exhibited a substantially reduced growth rate compared to wild-type plants (Figure 3.2a). The pigment deficiency was less severe under low light conditions (15 µmol photons s^{-1} m^{-2}) than under higher light conditions (70 µmol photons s^{-1} m^{-2}) (Figure 3.2b) indicating that the mutants are photosensitive.

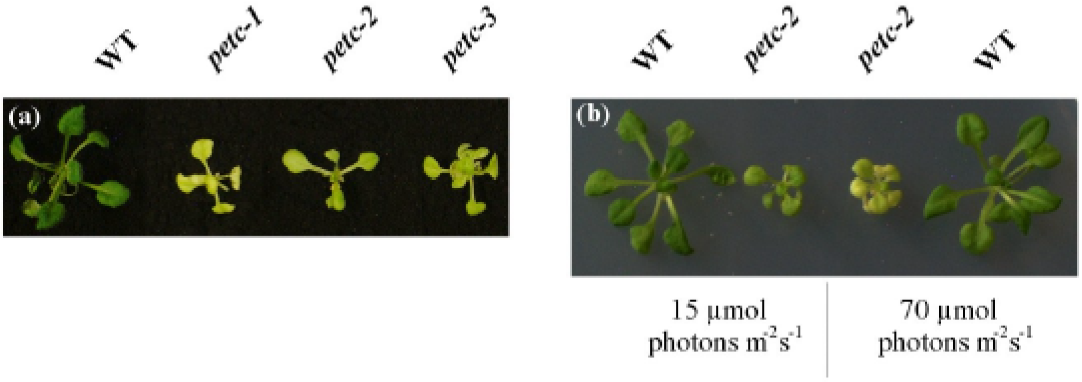

Figure 3.2 Phenotypes of wild-type and *petc* plants grown on 1x MS medium supplemented with 2% sucrose.

(a) Wild-type (WT) and *petc-1*, *-2* and *–3* plants, respectively.

(b) Wild-type (WT) and *petc-2* mutant plants grown under low light conditions (15 µmol photons s^{-1} m^{-2}) and under higher light conditions (70 µmol photons s^{-1} m^{-2}).

The *En*-tagged *petc-1* mutant displayed somatic wild-type reversions due to the excision of the *En* transposon (Figure 3.1). In each such wild-type sector, empty donor sites could be amplified by PCR and sequenced (Figure 3.1), confirming the tagging of the *PetC* locus. Upon illumination with UV-light, the *petc* mutants showed a high-chlorophyll-fluorescence (hcf) phenotype (Figure 3.3), indicating that a block in the photosynthetic electron flow exists in the absence of the Rieske protein. Crosses between heterozygous *petc-1*, *-2*, and *–3* plants resulted in progenies that segregated with a 1 to 3 ratio for the mutant phenotype, demonstrating that the three mutations are allelic (data not shown). Of the three *petc* alleles, *petc-2* was chosen for all further analyses.

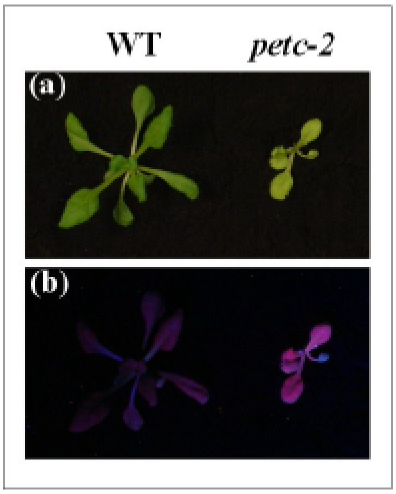

Figure 3.3 Plants grown on 1x MS medium supplemented with 2% sucrose were illuminated with white light (a) or UV light (B-100AP/R, UVP Inc., CA, USA) (b).

3.1.3 Expression analysis of the *PetC* gene

Northern analysis of *petc-2* plants using a *PetC* specific probe revealed that the *Ds* insertion drastically destabilises the *PetC* transcript. As a loading control the blot was re-probed with a cDNA fragment derived from the *ACTIN1* gene (Figure 3.4a). Western analyses of thylakoid membranes demonstrated the absence of detectable amounts of the Rieske protein in the *petc-2* mutants (Figure 3.4b).

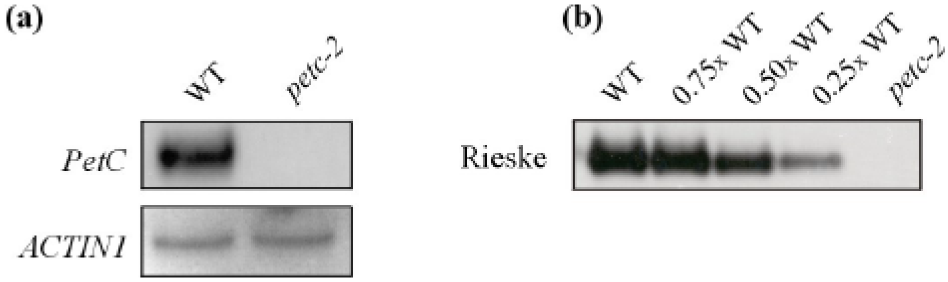

Figure 3.4 mRNA and protein expression of the *PetC* gene.

(a) Northern analysis of the *PetC* transcript in wild-type (WT) and *petc-2* plants. Thirty-microgram samples of total RNA were analysed using a fragment of the *PetC* transcript as a probe. As a loading control the blot was re-probed with a cDNA fragment derived from the *ACTIN1* gene.

(b) Western analysis of thylakoid membranes equivalent to 5 µg chlorophyll of wild-type (WT) and *petc-2* plants. Decreasing amounts of wild-type thylakoid membranes (3.75 µg; 2.5 µg; 1.25 µg chlorophyll) were loaded in the lanes marked 0.75x, 0.5x and 0.25x WT and fractionated by denaturing SDS-PAGE. Filters were probed with an antibody specific for the Rieske protein.

3.1.4 The pigment composition in the *petc-2* mutants

Pigments of wild-type and *petc-2* plants were extracted and analysed by HPLC analysis (Table 3.1). Absolute levels of pigments are provided (relative to the total amount of chlorophyll) and relative levels indicate the alteration of pigment concentrations based on the fresh weight of the plants.

Table 3.1 Abundance of leaf pigments in wild-type and *petc-2* plants.

The pigment content of WT (n = 5) and mutant (n = 5) plants was determined by HPLC. Total chlorophyll content is given in nmol Chl (*a* + *b*) g^{-1} fresh weight. The carotenoid content is expressed as mmol per mol Chl (*a* + *b*). Mean values (+/- SD) are shown. Nx, neoxanthin; β-Car, β-carotene; VAZ, sum of xanthophyll cycle pigments (violaxanthin + antheraxanthin + zeaxanthin); DEPS, de-epoxidation state = (violaxanthin + 0.5 antheraxanthin) / (violaxanthin + antheraxanthin + zeaxanthin).

	Absolute amounts (mmol per mol Chl (*a* + *b*))		**Relative level in**
Pigment	**WT**	***petc-2***	***petc-2* (%)**
Chl *a*/*b* ratio	3.04 ± 0.03	2.72 ± 0.07	-
Chl *a* + *b*	1900 ± 33	845 ± 24	44
Lutein	123 ± 3	164 ± 7	59
Nx	36 ± 2	44 ± 3	54
VAZ	27 ± 1	65 ± 5	106
β-Car	70 ± 2	59 ± 3	37
DEPS	0.03 ± 0.01	0.08 ± 0.01	-

As indicated by the pigment deficient phenotype the total chlorophyll concentration (Chl *a* + *b*) is decreased in the *petc-2* mutant to 44% of that of the wild-type (Table 3.1). Also the Chl *a*/*b* ratio is decreased in the mutant (WT: 3.04 ± 0.03; *petc-2*: 2.72 ± 0.07) which indicates a change in the photosystem composition and/or stoichiometry in the mutant. The mutant also shows a significant increase in the xanthophyll content and a reduction in β-carotene level in comparison to the wild-type. This implies the accumulation of antenna proteins relative to reaction centre core proteins. The disproportionate increase in the size of the xanthophyll cycle pigments (VAZ-pool) can be interpreted as a consequence of the higher photosensitivity in the mutant.

3.1.5 The composition of the photosynthetic apparatus in the *petc-2* plants

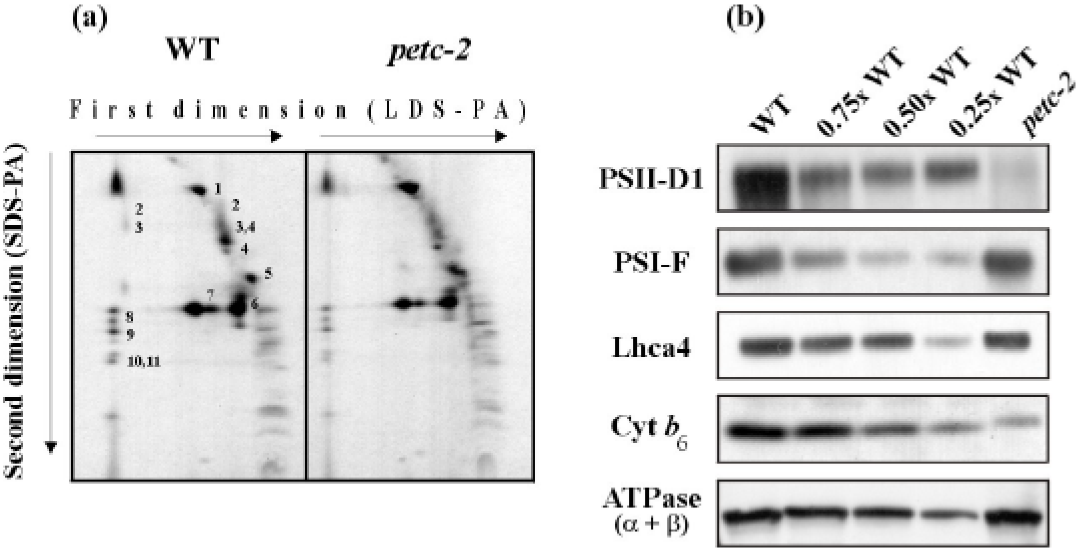

Figure 3.5 Protein composition of the thylakoid membranes in wild-type and *petc-2* mutant plants.

(a) Thylakoid membranes equivalent to 30 µg of chlorophyll from wild-type (WT) and *petc-2* mutant plants were fractionated firstly by electrophoresis on a non-denaturing LDS-PA gel and secondly on a denaturing SDS-PA gel (Schagger and von Jagow, 1987). Positions of wild-type thylakoid proteins which were previously identified by Western analyses with appropriate antibodies (Pesaresi et al., 2001) are indicated by numbers to the right of the corresponding spots: 1, α- and β-subunits of the ATPase complex; 2, D1-D2 dimers; 3, CP47; 4, CP43; 5, oxygen-evolving complex (OEC); 6, LHCII monomer; 7, LHCII trimer; 8, PSI-D; 9, PSI-F; 10, PSI-C; 11, PSI-H.

(b) Samples of thylakoid membranes equivalent to 5 µg chlorophyll of WT and *petc-2* were fractionated by 1–D SDS-PAGE. Decreasing amounts of wild-type thylakoid membranes (3.75µg; 2.5 µg; 1.25 µg chlorophyll) were loaded in the lanes marked 0.75x, 0.5x and 0.25x WT. Replicate filters were probed with the corresponding antibodies. The alterations observed in the *petc-2* mutant compared to the wild-type are quantified in Table 3.2.

To analyse the effect of the absence of the Rieske protein on the thylakoid protein composition, thylakoid membranes of sterile-culture-grown wild-type and *petc-2* plants were isolated and analysed by 2-D PAGE (Figure 3.5a) and Western blot analyses (Figure 3.5b). Densitometric determination of 2-D PAGE and Western analyses were performed and are listed in Table 3.2.

Table 3.2 Analyses of thylakoid protein levels and chlorophyll content (nmol Chl (*a* + *b*) g^{-1} fresh weight) in wild-type (WT) and *petc-2* mutant plants.

Values for proteins are average optical densities (± SD) measured from three independent 2-D protein gel analyses (PSII core (spots 2, 3 and 4), PSI (spots 8, 9, 10 and 11), ATPase (α+β) and LHCII (spots 6 and 7); see also Figure 3.5a) or from three independent Western analyses* (PSII-D1*, PSI-F*, ATPase (α+β)* and Cyt b_6*; see also Figure 3.5b). In column 4, relative values for the mutants are expressed as percentages based on g fresh leaf weight.

Pigment/protein	Absolute optical density		Relative level in *petc-2* (%)
	WT	***petc-2***	
Chl *a* + *b*	1900 ± 33	845 ± 24	44
PSII core	4.93 ± 0.32	1.52 ± 0.30	14
PSII-D1*	1.76 ± 0.13	0.18 ± 0.02	5
OEC	0.97 ± 0.01	0.36 ± 0.02	16
PSI	2.77 ± 0.17	2.11 ± 0.35	34
PSI-F*	1.10 ± 0.12	1.15 ± 0.06	46
ATPase (α + β)	2.92 ± 0.25	3.87 ± 0.27	58
ATPase (α + β)*	0.71 ± 0.05	1.02 ± 0.02	63
Rieske	1.38 ± 0.15	0	0
cyt b_6*	1.34 ± 0.46	0.12 ± 0,01	4
LHCII	8.07 ± 0.30	6.88 ± 0.13	38
Lhca4*	2.10 ± 0.08	1.66 ± 0.11	35

The abundance of the antenna proteins of both photosystems (LHCII and Lhca4) were decreased to 38% and 35% of wild-type levels, respectively. This change in the stoichiometry and composition of the photosystems was already indicated by the decreased Chl *a*/*b* ratio in the mutants. Also the accumulation of antenna proteins in relation to reaction core centre proteins, in particular PSI, was indicated by the reduced β-carotene levels in the mutant as well as by the increased xanthophyll content. Western analysis using the cyt b_6-specific antibody revealed no detectable amount of the cyt b_6 protein, indicating that the absence of the Rieske protein destabilised the entire complex.

Interestingly, the α- and β-subunit of the ATPase are reduced to 58% and 63% of wild-type levels (2-D SDS-PAGE and Western analyses), respectively. This is a relative increase with respect to the photosystems.

3.1.6 Photosystems are functional in *petc-2*, but there is no linear electron transport

The *petc-2* mutants are non photosynthetic, as they fail to grow on soil, and display a hcf phenotype. Photosynthetic electron flow was measured in wild-type and mutant plants by monitoring parameters of chlorophyll fluorescence and steady-state levels of the oxidized reaction centre chlorophyll in PSI ($P700^+$) (Table 3.3, Figure 3.7).

Table 3.3 Spectroscopic analysis of wild-type (WT, n = 5) and *petc-2* (n = 5) plants.

Mean values (± SD) are shown. F_V/F_M, maximum quantum yield of PSII; Φ_{II}, effective quantum yield of PSII; 1-qP, fraction of Q_A (the primary electron acceptor of PSII) present in the reduced state; NPQ, non-photochemical quenching.

Parameter	**WT**	***petc-2***
F_V/F_M	0.81 ± 0.01	0.42 ± 0.01
Φ_{II}	0.77 ± 0.01	0.16 ± 0.02
1-qP	0.03 ± 0.01	0.81 ± 0.02
NPQ	0.08 ± 0.01	0.01 ± 0.00

The maximal quantum efficiency of PSII (F_V/F_M) was substantially reduced in the mutants ($F_V/F_M = 0.42 \pm 0.01$) compared to wild-type ($F_V/F_M = 0.81 \pm 0.01$), indicating the presence of inactive PSII centres. Moreover, the effective quantum yield of PSII (Φ_{II}) showed a strong decrease in the mutant ($\Phi_{II} = 0.16 \pm 0.02$) compared to wild-type ($\Phi_{II} = 0.77 \pm 0.01$), indicating a severe pertubation in electron flow. For increased light intensities Φ_{II} decreases dramatically, suggesting a substantially increased photosensitivity of the mutants (Figure 3.6).

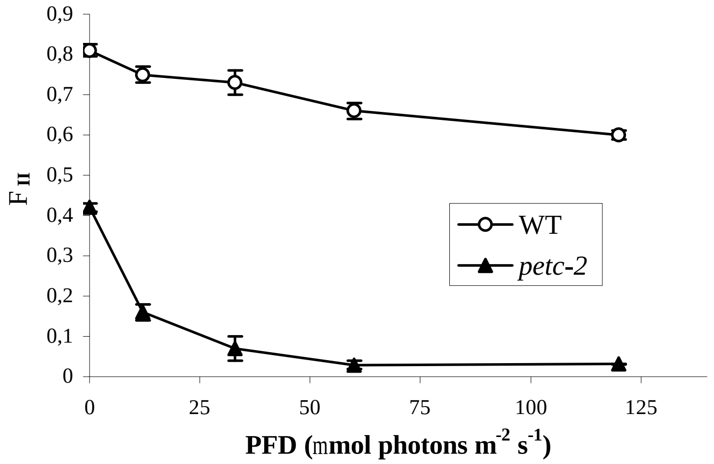

Figure 3.6 Effective quantum yield of PSII in the *petc-2* and WT plants illuminated at increasing light intensities.

Five wild-type (WT) and five mutant plants were incubated for 30 minutes in the dark prior to each measurement. Mean values are shown, bars indicate standard deviations.

In addition, the fraction of Q_A (the primary electron acceptor of PSII) present in the reduced state was, in *petc-2*, dramatically increased (1-qP = 0.81 ± 0.02) compared to the wild-type (1-qP = 0.03 ± 0.01), implying a block in subsequent electron transfer steps. In *petc-2* mutant plants no NPQ was detectable (Table 3.3). The oxidation state of P700 in intact leaves was determined by measuring the absorbance changes at 820 nm at four different light intensities (Figure 3.7).

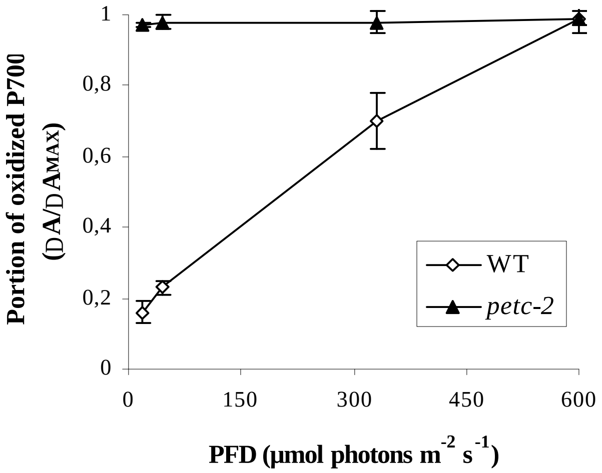

Figure 3.7 Steady-state levels of oxidized reaction centre chlorophyll in PSI ($P700^+$) for wild-type (WT) and *petc-2* mutant plants.

After five minutes of illumination with actinic light the steady-state level of P700 absorption changes at 820 nm ($\Delta A/\Delta A_{MAX}$) were measured for wild-type (WT) and *petc-2* mutant plants (n = 3 each). Mean values are shown, bars indicate standard deviations.

In *petc-2* plants, P700 was fully oxidised even at the lowest light intensities, implying that the absence of the Rieske protein completely suppresses electron transport from PSII to PSI through the cyt b_6/f complex.

To analyse the intersystem electron transfer (PSII → PSI), thylakoids from WT and *petc-2* mutant plants were isolated and the rate of uncoupled electron transport, the PSI activity and the PSII activity were analysed by measuring the photosynthetic oxygen evolution using a Clark type oxygen electrode. Using artificial electron acceptors and donors, the activity of both photosystems was recorded (Table 3.4). The PSII activity of the *petc-2* mutant is reduced to 4% compared to that of the wild-type. The reduction in activity is in line with the level of reduction of PSII core proteins. Surprisingly, the PSI activity is only slightly reduced (to 73% of wild-typ levels) even though the protein level of PSI is reduced to 34% (2-D PAGE) or 45% (Western analysis). These results indicate that the residual levels of PSI and PSII that accumulate in the mutant are functional. No linear electron transport could be recorded, supporting the conclusion derived from the P700 absorbance measurements (see above) that in the *petc-2* mutant the absence of the Rieske protein completely suppresses the electron transport via the cyt b_6/f complex.

Table 3.4 Activity of PSII and PSI, and the rate of uncoupled linear electron transport in WT and *petc-2* thylakoids.

Values of average oxygen evolution (PSII activity and linear electron transport) or consumption (PSI activity) (± SD) in µmol O_2 (mg Chl^{-1}) h^{-1} were derived from three independent measurements of thylakoids equivalent to 10 µg chlorophyll ml^{-1}. Relative levels provided in column 4 are calculated by the given formula ([absolute value$_{petc\text{-}2}$/absolute value$_{WT}$] x chlorophyll correction factor (0.44)). These are relative values for the mutants in percentage based on g fresh weight.

	Absolute values (µmol O_2 (mg Chl^{-1}) h^{-1})		**Relative level in**
Parameter	**WT**	***petc-2***	***petc-2* (%)**
PSII activity	134 ± 7	12 ± 0	4.0
PSI activity	151 ± 7	251 ± 8	73
Linear electron transport (uncoupled)	84 ± 7	0	0

Similar results were obtained analysing the linear electron transport in intact leaves by fluorescence induction kinetics (Figure 3.8). In the wild-type there is an initial rapid increase in fluorescence to a relative value (rv) of approx. 0.3 after 0.05 s and then a slower increase in fluorescence, before reaching a maximum. This second, slower increase in fluorescence is caused by electron flow to PSI acceptors. After reaching the maximum fluorescence in the wild-type the fluorescence decreases. This is caused by NPQ and the Calvin cycle (=photochemistry). In the *petc-2* mutant only a rapid increase after 0.05 seconds in fluorescence to approx. 0.7 is observed. The absense of the second slower increase in fluorosecence in the mutant indicates that there is no electron transfer to PSI acceptors. After reaching the maximum fluorescence in the *petc-2* mutant no decay in the curve is visible, indicating the absence of an NPQ and the lack of an active Calvin cycle in this mutant. These results are consistent with a block in linear and cyclic electron flow and the existence of an over-reduced plastoquinol pool.

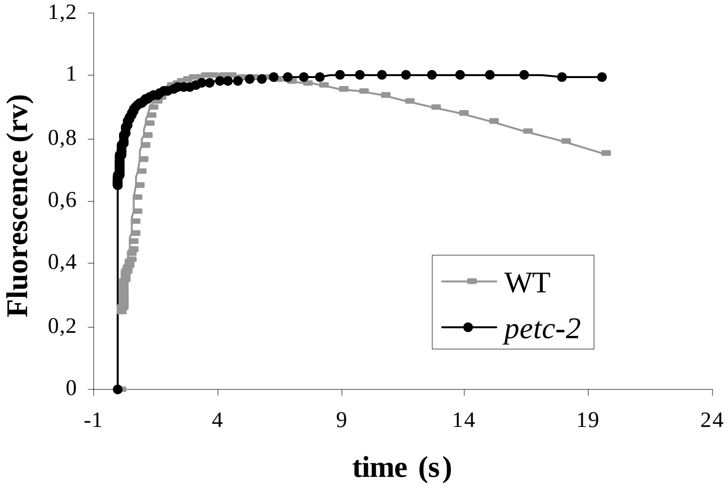

Figure 3.8 Induction kinetics of the fluorescence in intact leaves.

Plants were dark adapted o/n before being exposed to a saturating red-light pulse (max. 680 nm) for 400 ms that fully reduces Q_A.Values are the averages of three repetitions with a standard deviation less than 5%.

3.2 Characterisation of the *atpd-1* mutant

3.2.1 Phenotype of the *atpd-1* mutant line

In the course of a phenotypic screen of T-DNA mutagenized *Arabidopsis thaliana* lines (ecotype Col-0) (Budziszewski et al., 2001), a seedling-lethal line having a T-DNA insertion in the promoter region of the *AtpD* gene was described. This line, designated *atpd-1*, contains an insertion of the *SKI015* T-DNA 49 bps before the ATG codon of the *AtpD* gene (Figure 3.9c). The T-DNA insertion caused a deletion of 7 bps adjacent to the right border of the T-DNA.

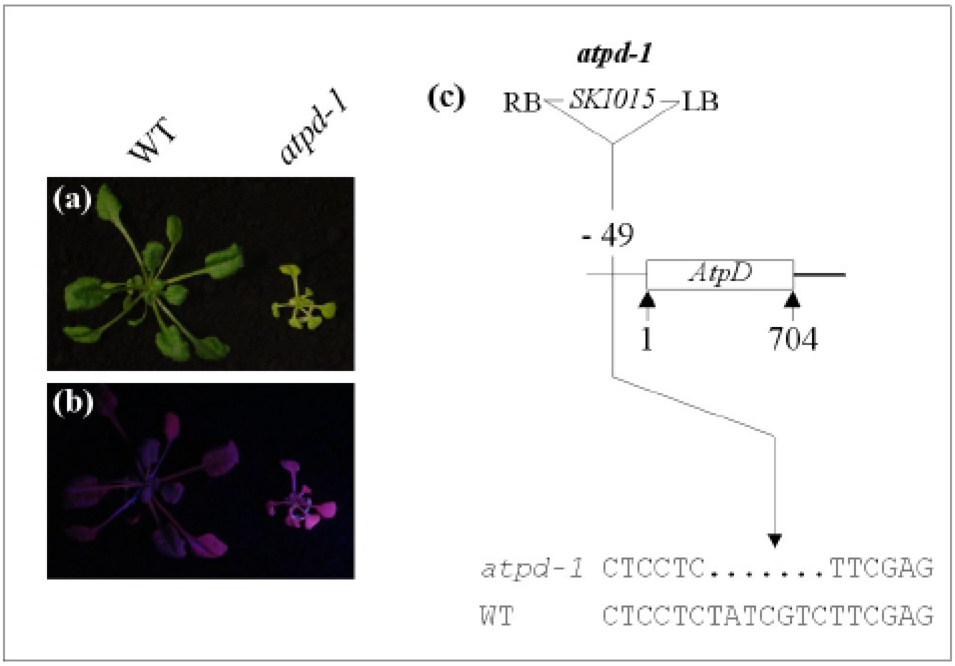

Figure 3.9 Mutation in the *AtpD* locus and phenotype of mutant plants.

(a) + (b) Phenotypes of WT and *atpd-1* plants. Plants grown on 1x MS medium supplemented with 2 % sucrose were illuminated with white light (a) or UV light (b) (B-100AP/R, UVP Inc., CA, USA).

(c) In the *atpd-1* mutant, a copy of the 5.2 kb *SKI015* is inserted in the promoter region of *AtpD* gene (At4g09650). PCR analysis indicated a small deletion of 7 bps adjacent to the right border of the *SKI015* insertion. The T-DNA insertion is not drawn to scale.

Greenhouse-grown *atpd-1* plants displayed pale-green leaf coloration and were seedling-lethal. When grown heterotrophically, the *atpd-1* mutants were not lethal but grew slower than the wild-type. Furthermore, the mutant plants displayed a light-green leaf coloration

(Figure 3.9a) and an hcf phenotype upon illumination with UV light (Figure 3.9b), indicating an impaired electron transport.

3.2.2 Expression analysis of the *AtpD* gene and complementation analysis of the *atpd-1* mutation

Northern analysis using the full-length cDNA *AtpD* as a probe, revealed that the T-DNA insertion drastically destabilises the *AtpD* transcript (Figure 3.10a). Western analysis of thylakoid membranes of wild-type and *atpd-1* plants using an ATPase-δ-subunit specific antibody demonstrated the absence of detectable amounts of the ATPase-δ-subunit (Figure 3.10b).

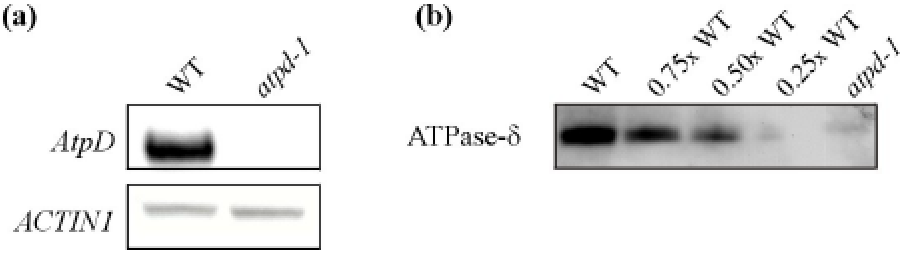

Figure 3.10 mRNA and protein expression of the *AtpD* gene.

(a) Northern analysis of the *AtpD* transcript in *atpd-1* and wild-type (WT) plants. Thirty-microgram samples of total RNA were analysed using the *AtpD* transcript as a probe. As a loading control the blot was re-probed with a cDNA fragment derived from the *ACTIN1* gene.

(b) Samples of thylakoid membranes equivalent to 5 µg chlorophyll of wild-type (WT) and *atpd-1* plants were fractionated by denaturing PAGE. Decreasing amounts of wild-type thylakoid membranes (3.75 µg; 2.5 µg; 1.25 µg chlorophyll) were loaded in the lanes marked 0.75x, 0.5x and 0.25x WT. Filters were probed with an antibody specific for the δ-subunit of the chloroplast ATPase.

To confirm that the *atpd-1* phenotype was due to the T-DNA insertion in the *AtpD* locus a complementation analysis was carried out. The *AtpD* cDNA was fused to the 35S promoter of the cauliflower mosaic virus and introduced into heterozygous plants by *A. tumefaciens* transformation. All obtained transformants were analysed by PCR for their genotypes and transformed homozygous mutant plants were transferred to soil to generate seeds. Ten independent transformants displaying the wild-type phenotype were obtained. In particular the growth, fluorescence yield (Φ_{II}) and leaf pigmentation of these transformants did not differ from wild-type plants (Figure 3.11a). Northern analysis of wild-type plants and the T1 generation of mutant plants using a full-length *AtpD*-specific probe showed the presence of *AtpD* mRNA in the T1 plants (Figure 3.11b). These results demonstrate that the *atpd-1* phenotype was due to lack of *AtpD* function.

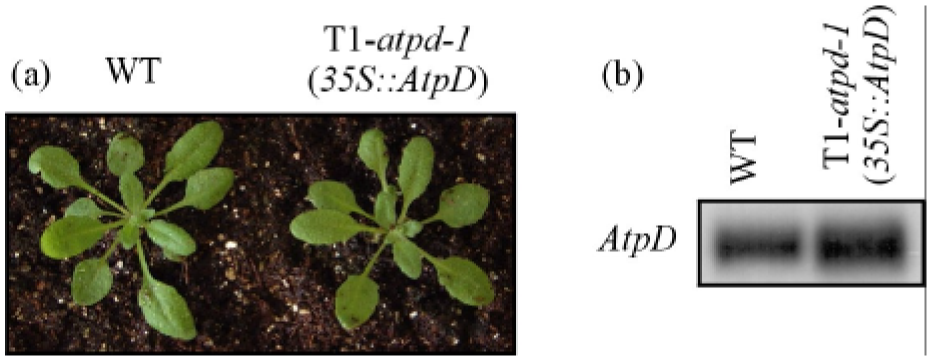

Figure 3.11 Complementation of the *atpd-1* mutation.

(a) 4 week-old wild-type (WT) plants and T1 transformants (*atpd-1* plants) transformed with the *AtpD* cDNA under the control of the 35S promotor (35S::*AtpD*).

(b) Northern analysis of the *AtpD* transcript in WT and T1 plants (35S::*AtpD*). Thirty-microgram samples of total RNA were analysed using the *AtpD* transcript as a probe.

3.2.3 ATP synthase activity in *atpd-1* mutant plants

To analyse ATP synthase activity, membrane potential changes (518-548 nm) were measured.

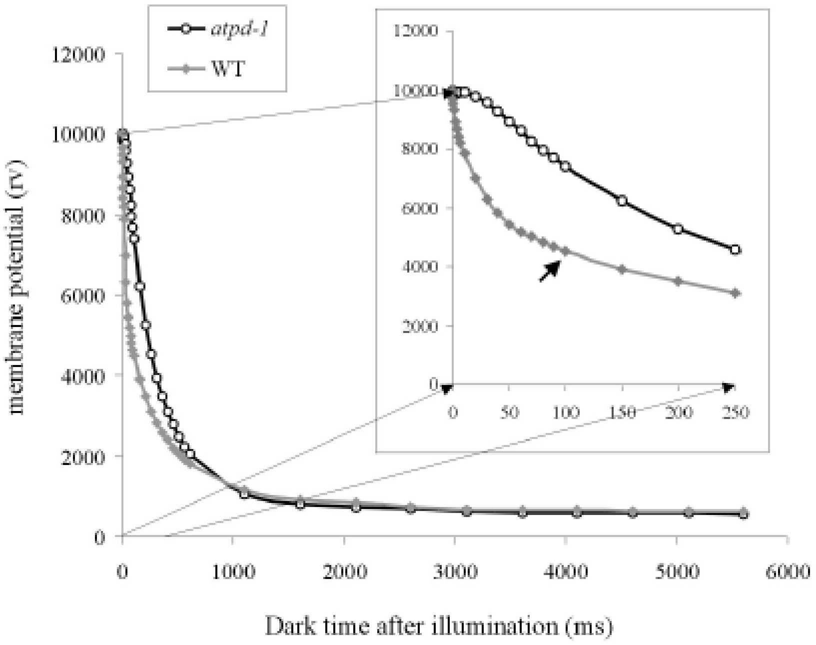

Figure 3.12 Membrane potential changes measured in intact leaves using a saturating light pulse.

The variation of the delocalized membrane potential has been measured by the electrochromic shift of membrane pigments as the difference in absorption (518-548 nm) which was assumed to be a reliable indicator of the membrane potential changes (Joliot and Joliot, 2001).

As shown in Figure 3.12 wild-type and mutant plants exhibit a significant difference. In the wild-type the membrane potential decay is biphasic. A fast phase, completed in ~100 ms (the end of which is indicated in the insert by the black arrow in Figure 3.12), is ascribed to ATP synthase activity (Junge et al., 1992). After ~100 ms the threshold membrane potential is reached and ATPase synthase activity most likely ceases. After ~100 ms a slower membrane potential decay is observable (completed in ~3 s). This slower decay may be ascribed to ion leakage through the membrane. This biphasic decay has been already described and interpreted by Junge et al., (1992) for isolated thylakoids. In contrast, in the *atpd-1* mutant the fast decaying phase is specifically inhibited, indicating the absence of ATP synthase activity and only the slow decay remains and this may be ascribed to ion leakage through the membrane.

3.2.4 Leaf pigment composition in the *atpd-1* mutants

Sterile culture-grown wild-type and *atpd-1* mutant plants were analysed for their leaf pigments (Table 3.5).

Table 3.5 Abundance of leaf pigments in wild-type and *atpd-1* mutant plants.

The pigment content of WT (n = 5) and mutant (n = 5) plants was determined by HPLC. Total Chl content is given in nmol chlorophyll (*a* + *b*) g^{-1} fresh weight. The carotenoid content is expressed as mmol per mol Chl (*a* + *b*). Mean values (+/- SD) are shown. Nx, neoxanthin; β-Car, β-carotene; VAZ, sum of xanthophyll cycle pigments (violaxanthin + antheraxanthin + zeaxanthin) and DEPS, de-epoxidation state = (violaxanthin + 0.5 antheraxanthin) / (violaxanthin + antheraxanthin + zeaxanthin).

	Absolute amounts (mmol per mol Chl (*a* + *b*))		**Relative level in**
Pigment	**WT**	***atpd-1***	***atpd-1* (%)**
Chl *a*/*b*	3.02 ± 0.07	2.24 ± 0.06	-
Chl *a* + *b*	1999 ± 40	894 ± 11	45
Lutein	129 ± 4	144 ± 1	50
Nx	35 ± 1	46 ± 3	59
VAZ	25 ± 3	95 ± 6	171
β-Car	71 ± 7	32 ± 5	20
DEPS	0	0.30 ± 0.02	-

Consistent with the light-green coloration of *atpd-1* mutant plants a decrease in the total chlorophyll concentration (Chl *a* + *b*) to 45% of that of the wild-type was observed. The Chl *a/b* ratio was also decreased in mutant plants (WT: 3.02 ± 0.07; *atpd-1*: 2.24 ± 0.06), indicating dramatic changes in the photosystem composition and/or stoichiometry. An accumulation of antenna proteins in relation to reaction centre core proteins is indicated by the reduced β-carotene level and a significantly increased xanthophyll content in comparison to wild-type plants. It should be noted that there is an over-proportional increase of the VAZ-pool size compared to the other leaf pigments, which could be due to higher photosensitivity and/or an increased transmembrane proton gradient in the mutant. Moreover, the high de-epoxidation state (DEPS) of the VAZ-pool for *atpd-1* plants (0.30 ± 0.02) indicates a permanently high transmembrane proton gradient in this mutant, as violaxanthin de-epoxidase activity is activated even at low light intensities such as 15 µmol photons m^{-2} s^{-1}.

3.2.5 The composition of the photosynthetic apparatus in the *atpd-1* plants

To study the effect of the absence of the ATPase-δ-subunit on the thylakoid protein composition, thylakoid membranes of sterile-culture-grown wild-type and *atpd-1* plants were isolated and analysed by 2-D PAGE (Figure 3.13a) and Western analyses (Figure 3.13b). Densitometric analyses of 2-D PAGE and Western analyses were performed and are shown in Table 3.6. The abundance of the cores of PSII and PSI were substantially reduced in the *atpd-1* mutant (to 29% and 17% of wild-type levels, respectively), while the abundance of the antenna proteins of both photosystems (LHCII and Lhca4) were decreased to 43% and 37% of wild-type levels, respectively. This accumulation of antenna proteins in relation to the reaction centre cores proteins was already indicated by the decreased Chl *a/b* ratio in the mutant. Western analysis of thylakoid proteins with specific antibodies for the D1 protein of PSII and PSI-F confirmed the trend in the thylakoid composition shown by 2-D protein gel analysis. The abundance of the cyt b_6 and the Rieske protein is decreased to 23% and 29% of wild-type levels, respectively, which indicated that these proteins are decreased stoichiometrically with respect to the PSII and PSI core centres in the mutant. As already shown by Western analysis (Figure 3.10), there was no detectable amount of the δ-subunit of the chloroplast ATP synthase. Interestingly, neither did the α- and the β-subunits of the CF_1 complex, nor the a- and b-subunits of the CF_0 complex of the ATPase, accumulate to detectable amounts in the *atpd-1* plants as shown by 2-D PAGE and Western analyses (Figure 3.13, Table 3.6). This indicates a destabilisation of the entire ATP synthase complex in this mutant.

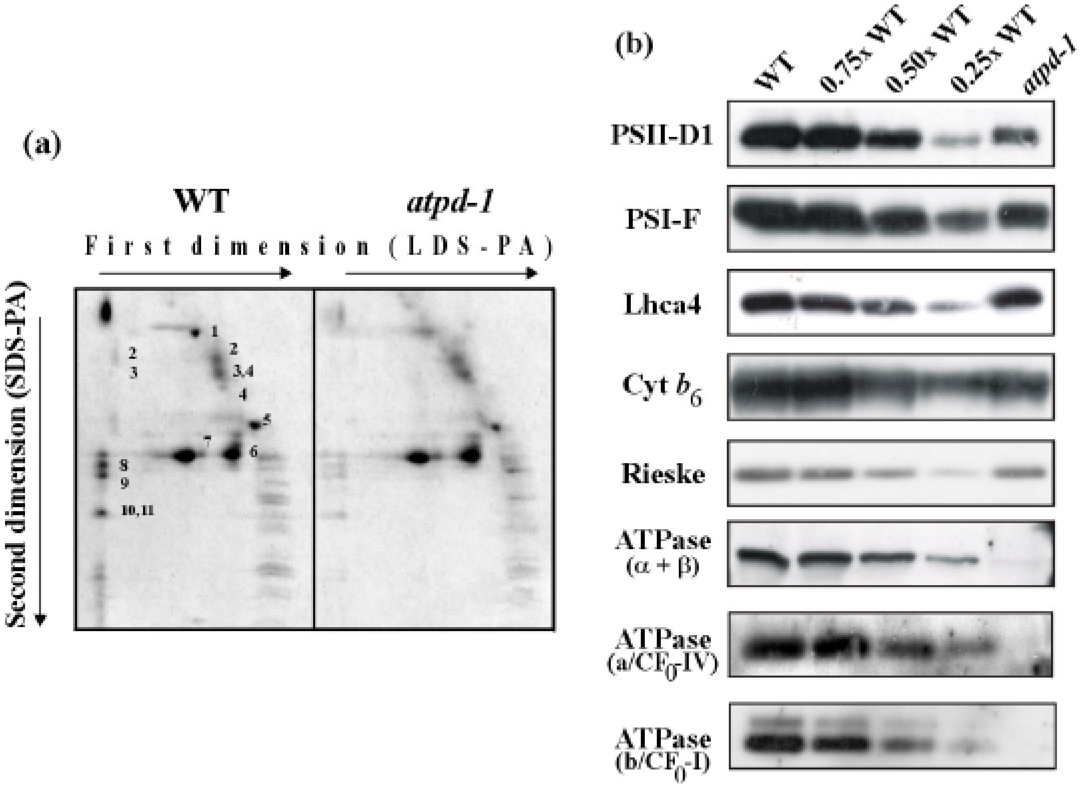

Figure 3.13 Protein composition of the thylakoid membranes in wild-type and *atpd-1* mutant plants.

(a) Thylakoid membranes corresponding to 30 µg of chlorophyll from wild-type and *atpd-1* mutant plants were fractionated first by electrophoresis on a non-denaturing LDS-PA gel and then on a denaturing SDS-PA gel. Positions of wild-type thylakoid proteins previously identified by Western analyses with appropriate antibodies (Pesaresi et al., 2001) are indicated by numbers to the right of the corresponding spots: 1, α- and β-subunits of the ATPase complex; 2, D1-D2 dimers; 3, CP47; 4, CP43; 5, oxygen-evolving complex (OEC); 6, LHCII monomer; 7, LHCII trimer; 8, PSI-D; 9, PSI-F; 10, PSI-C; 11, PSI-H.

(b) Samples of thylakoid membranes equivalent to 5 µg chlorophyll of wild-type (WT) and *atpd-1* were fractionated by 1–D SDS-PAGE. Decreasing amounts of wild-type thylakoid membranes (3.75 µg; 2.5 µg; 1.25 µg chlorophyll) were loaded in the lanes marked 0.75x, 0.5x and 0.25x WT. Replicate filters were probed with the corresponding antibodies. The alterations observed in the *atpd-1* mutant compared to the wild-type are quantified in Table 3.6.

Table 3.6 Analyses of thylakoid protein levels and total chlorophyll content (in nmol Chl (*a* + *b*) g^{-1} fresh weight) in wild-type (WT) and *atpd-1* mutant plants.

Values for proteins are average optical densities (± SD) measured from three independent 2-D protein gel analyses (PSII core (spots 2, 3 and 4), PSI (spots 8, 9, 10 and 11), ATPase (α+β) and LHCII (spots 6 and 7); see also Figure 3.13a) or from three independent Western analyses* (PSII-D1*, PSI-F*, ATPase ($\alpha + \beta$, a, b)* and Cyt b_6*; see also Figure 3.13b). Relative levels as given in column 4 are calculated by the given formula ([OD_{atpd-1}/OD_{WT}] x chlorophyll correction factor (0.45)) and these are the relative values for the mutants in percentage based on g fresh leaf weight.

Pigment/protein	**Absolute optical density values**		**Relative level in**
	WT	***atpd-1***	***atpd-1* (%)**
Chl *a* + *b*	1999 ± 40	894 ± 11	45
PSII core	3.94 ± 0.04	2.55 ± 0.30	29
PSII-D1*	1.10 ± 0.13	0.47 ± 0.06	19
OEC	1.83 ± 0.03	0.76 ± 0.02	19
PSI	3.33 ± 0.07	1.23 ± 0.06	17
PSI-F*	0.75 ± 0.07	0.31 ± 0.04	19
ATPase ($\alpha + \beta$)	1.58 ± 0.10	0	0
ATPase (a)*	1.04 ± 0.14	0	0
ATPase (b)*	1.45 ± 0.08	0	0
ATPase ($\alpha + \beta$)*	1.51 ± 0.12	0	0
cyt b_6*	1.63 ± 0.01	0.84 ± 0.001	23
Rieske*	1.73 ± 0.12	1.12 ± 0.07	29
LHCII	10.64 ± 0.25	10.3 ± 0.36	43
Lhca4*	2.25 ± 0.18	1.83 ± 0.12	37

3.2.6 Photosystems are functional in *atpd-1* mutants, but linear electron transport is impaired

The rate of photosynthetic electron flow in the *atpd-1* mutants was measured by monitoring parameters of chlorophyll fluorescence, fluorescence induction kinetics and the oxidation state of P700 under continuous illumination of leaves from wild-type and mutant plants (Table 3.7, Figure 3.14, Figure 3.16).

Table 3.7 Spectroscopic analysis of wild-type (WT, n = 5) and *atpd-1* mutant (n = 5) plants.

Mean values (± SD) are shown. F_V/F_M, maximum quantum yield of PSII; Φ_{II}, effective quantum yield of PSII; 1-qP, fraction of Q_A (the primary electron acceptor of PSII) present in the reduced state; NPQ, non-photochemical quenching.

Parameter	**WT**	***atpd-1***
F_V/F_M	0.82 ± 0.01	0.39 ± 0.01
Φ_{II}	0.77 ± 0.01	0.23 ± 0.02
1-qP	0.04 ± 0.01	0.14 ± 0.06
NPQ	0.07 ± 0.01	0.26 ± 0.03

The potential quantum efficiency of PSII (F_V/F_M) was substantially reduced in the mutant (0.39 ± 0.01) with respect to the wild-type (0.82 ± 0.01), indicating the presence of inactive PSII centres. The effective quantum yield of PSII (Φ_{II}) showed a strong decrease in the mutant (0.23 ± 0.02) compared to the wild-type (0.77 ± 0.01) which was even stronger at increasing light intensities (Figure 3.14). This indicates a severe pertubation in electron flow which is consistent with the high photosensitivity of the mutant.

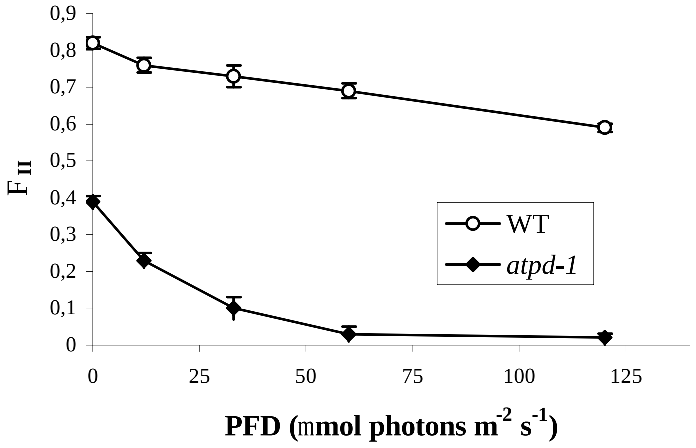

Figure 3.14 Effective quantum yield of PSII in wild-type and *atpd-1* plants illuminated at increasing light intensities.

Five wild-type (WT) and five mutant plants were kept for 30 minutes in the dark prior to measurements. Bars indicate standard deviations.

In addition, the fraction of Q_A (the primary electron acceptor of PSII) present in the reduced state (1-qP) was increased in the mutant (0.14 ± 0.03) in comparison to the wild-type (0.04 ± 0.01), implying a block in subsequent electron transfer steps. The non-photochemical quenching (NPQ) was increased in the *atpd-1* mutants (0.26 ± 0.03) compared to the wild-type (0.07 ± 0.01), indicating an increased acidification of the thylakoid lumen. Measuring the qE, the energy-dependent component of NPQ, indicated that the main portion of NPQ is due to qE (Figure 3.15). In additon to this, the maximum values for qE were inducible in the mutant at much lower light intensities (about 100-150 µmol photons m^{-2} s^{-1}) than those required for wild-type plants (about 600-900 µmol photons m^{-2} s^{-1}), indicating that maximal lumen acidification is obtained at significantly lower PFDs in the mutants (Figure 3.15).

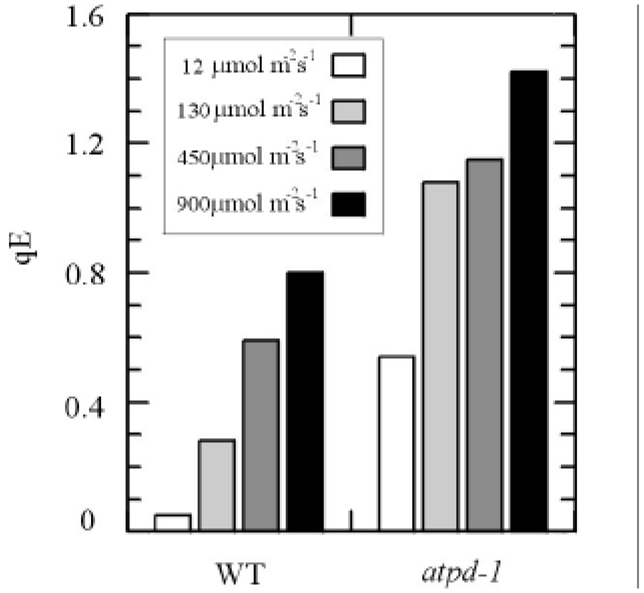

Figure 3.15 qE values in wild-type (WT) and *atpd-1*plants at increasing actinic light intensities.

This result is consistent with the presence of an increased VAZ-pool and the high de-epoxidation state of the VAZ-pool (Table 3.5) and could be related to the loss of ATPase function in the mutant. The oxidation state of P700 in intact leaves at different actinic light intensities was determined by measuring the absorbance changes at 820 nm (Figure 3.16). In *atpd-1* plants, the maximum oxidation of P700 was reached at much lower PFDs indicating that the electron transport was saturated at lower light intensities than in the wild-type.

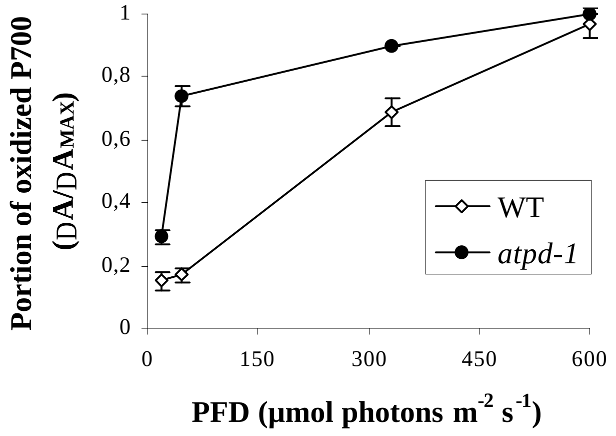

Figure 3.16 Steady-state levels of oxidized reaction centre chlorophyll in PSI (P700$^+$) in wild-type and *atpd-1* mutant plants.

After five minutes of illumination with actinic light the steady-state level of P700$^+$ was measured for wild-type and *atpd-1* mutant plants (n = 3 each). Mean values are shown, bars indicate standard deviations.

Using artificial electron acceptors and donors, the activity of both photosystems was recorded. (Table 3.8). The activity of PSI and PSII and the rate of the uncoupled linear electron transport was monitored by oxygen electrode measurements in isolated thylakoid membranes of wild-type and mutant plants.

Table 3.8 Activity of PSII and PSI, and the rate of uncoupled linear electron transport in WT and *atpd-1* thylakoids.

Values of average oxygen evolution (PSII activity and linear electron transport) or consumption (PSI activity) (± SD) in µmol O_2 (mg Chl^{-1}) h^{-1} were derived from three independent measurements of thylakoids equivatlent to 10 µg chlorophyll ml^{-1}. The relative levels in column 4 were calculated by the given formula ([activity$_{atpd\text{-}1}$/activity$_{WT}$] x chlorophyll correction factor (0.45)) and they express relative values for the mutants in percentage based on gram fresh leaf weight.

Parameter	**Absolute values (µmol O_2 (mg Chl^{-1}) h^{-1})**		**Relative level in *atpd-1* (%)**
	WT	***atpd-1***	
PSII activity	137 ± 7	84 ± 7	28
PSI activity	147 ± 7	88 ± 7	27
Linear electron transport (uncoupled)	85 ± 7	54 ± 2	29

The relative levels of PSI and PSII activity were reduced to 27% and 28%, respectively, indicating that residual levels of functional PSI and PSII accumulate in the mutant. The uncoupled linear electron flow was reduced to 29% compared with the wild-type. These reductions are in line with the reduced protein levels of PSII, the cyt b_6/f complex and PSI in the mutant analysed by 2-D gel electrophoresis and Western blot anaylses (Figure 3.13, Table 3.6). These results indicate that the complexes are functional in mutant plants and the observed decrease in electron transport rates is due to the reduced protein levels in the *atpd-1* mutant.

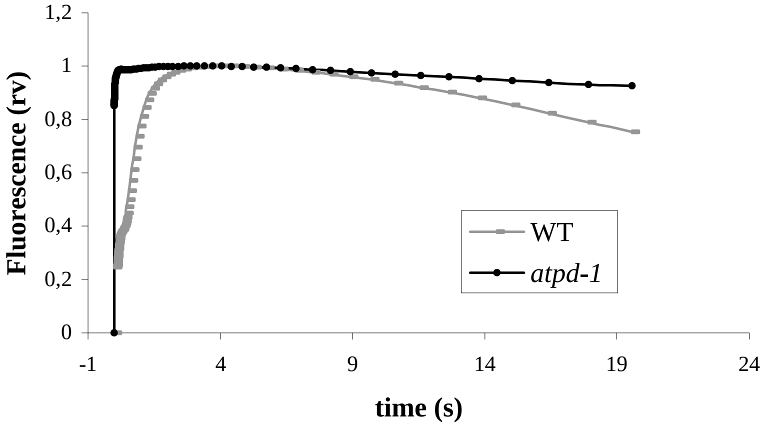

Figure 3.17 Fluorescence induction kinetics of intact leaves of wild-type and *atpd-1* leaves.

Plants were dark kept o/n before being exposed to a saturating red light pulse (max. 680 nm) for 400 ms that fully reduced Q_A. Values are the averages of three repetitions with a standard deviation less than 5%.

However, measuring the electron transport in intact leaves by fluorescence induction kinetics provided interesting results for the *atpd-1* mutant. The mutant shows a rapid increase in fluorescence after 5.5 x 10^{-5} s (0.85) whereas in the wild-type the fluorescence is much lower (0.25). In addition, the wild-type dispays an initial rapid increase in fluorescence to a relative value of approximately 0.3 after 0.05 s and then a slower increase in fluorescence, before reaching a maximum after approximately 4 s. This second, slower increase in fluorescence, is caused by electron flow from PSII to PSI acceptors. However, the *atpd-1* mutant does not show this slower increase, indicating that no electron flow from PSII to PSI acceptors exists and therefore no linear electron transport. Moreover, the maximal fluorescence is reached earlier in the mutant (after 0.9 s) than in the wild-type (after 4 s) implying that the system is saturated immediately in the *atpd-1* mutant and/or a possible reduction in the plastoquinol pool. After reaching the maximal fluorescence in wild-type and mutant leaves a decay of the curve due to NPQ and activity of the Calvin cycle is visible. As already shown by spectroscopic analysis (Table 3.7) the NPQ is increased in the *atpd-1* mutant. This means, that the lower decay in the fluorescence induction curve for the mutant in comparison to the wild-type is possibly due to a decreased activity in the Calvin cycle. Since linear electron flow is absent, the observed increase in ΔpH, which results in the increased level of non-photochemical quenching in the mutant (Table 3.7), is most probably due to cyclic electron flow in the absence of proton gradient dissipation (ATP synthesis).

These results are consistent with an impaired, but not entirely blocked, cyclic electron flow. Due to the supression of proton flow through the ATP synthase, electron flow is saturated at significantly lower light intensities than in wild-type plants, resulting in an increased lumen acidification and an increased thermal energy dissipation at low light.

3.3 mRNA expression analysis for nucleus-encoded chloroplast proteins in the mutants *petc-2* and *atpd-1*

The data presented above showed that the absence of either the Rieske protein (*petc-2* mutant) or of the δ-subunit of the chloroplast ATP synthase (*atpd-1* mutant) strongly impairs photosynthesis. However, the two mutations have quite different effects on photosynthetic electron flow and the composition of thylakoid membranes. To test for further differences in the effects of the two mutations on photosynthesis and other chloroplast functions, the expression of nuclear genes contributing to chloroplast functions were analysed by determining the relative mRNA levels by DNA array analysis. Therefore the expression of 3292 nuclear genes were considered of which 81% are coding for chloroplast-targeted proteins. The expression patterns of the two mutants *petc-2* and *atpd-1* were compared with the expression pattern seen in wild-type plants as described in material and methods. As additional controls the *psae1-1*, *psad1-1*, *psan-1* and *psao-1* lines (Varotto et al., 2000; Richly et al., 2003 and unpublished results of our laboratory) bearing knock-out alleles of the PSI genes *PsaE1*, *PsaD1*, *PsaN* and *PsaO* were also included in this analysis. Differential gene expression values (mutants versus wild-type) were determined by comparing hybridization signals. In all six mutant genotypes, a set of 344 genes was identified, all of which were expressed at significantly different levels from wild-type in at least 5 of the 6 genotypes. The hierarchical clustering of the 344 gene expression profiles revealed that the expression pattern of *petc-1* and *atpd-1* were substantially different: the *petc-2* profile was related to that of *psad1-1* and *psae1-1*, while the pattern of *atpd-1* was more similar to that of *psan-1* or *psao-1* (Figure 3.18a and appendix 7.1).

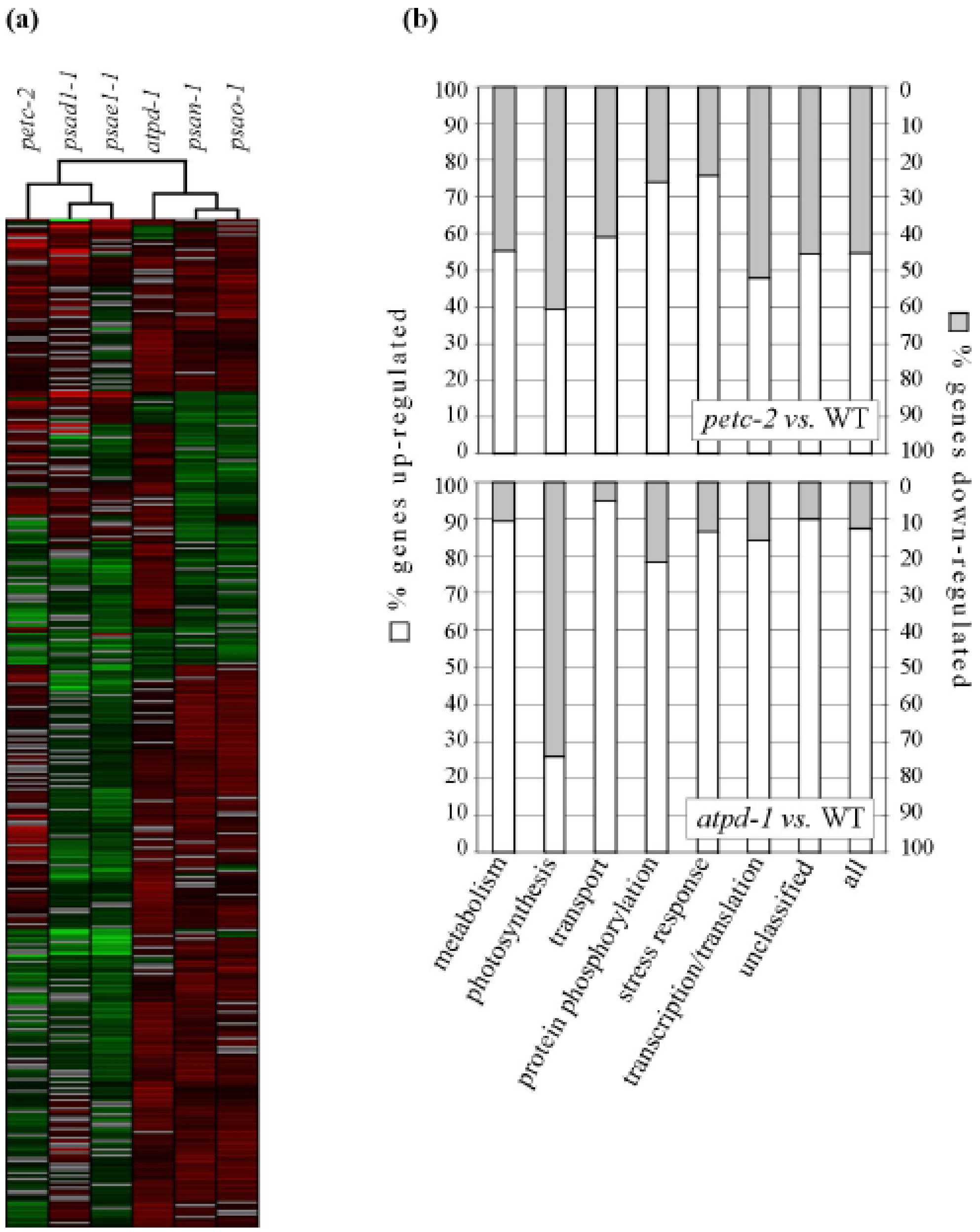

Figure 3.18 Effects of *petc-2* and *atpd-1* mutations on the accumulation of nuclear transcripts for chloroplast proteins.

(a) Hierarchical clustering of the expression profiles of 344 genes that show significant differential expression in at least five of the six mutants *petc-2*, *atpd-1*, *psae1-1*, *psad1-1*, *psan-1* and *psao-1*. The cladogram at the top summarizes the degree of relatedness between the transcriptome responses in the six genotypes. Colours indicate up (red)- or down (green)-regulation of gene expression. Grey lines indicate non-significant differential expression. For a more detailed image, including gene accession numbers and annotations see appendix 7.1.

(b) Fraction of up- and down-regulated genes in 7 major functional categories. For a complete list of differentially expressed genes see appendix 7.3.

Direct comparison of the differential expression profiles of *petc-2* and *atpd-1* plants revealed that among all genes differentially expressed in the two genotypes, 451 genes showed the same trend (379 up- and 72 down-regulated). A further set of 346 genes showed opposite trends in transcriptional regulation in the two lines: 49 genes were up-regulated in *petc-2* and down-regulated in *atpd-1*, whereas 297 genes were down-regulated in *petc-1* but up-regulated in *atpd-1* (see appendix 7.2).

The significantly differentially expressed genes in *petc-2* and *atpd-1* were grouped into 7 major functional categories, including metabolism, photosynthesis, transport, protein phosphorylation, stress response, transcription and translation and unclassified proteins (Figure 3.18b). Also by this analysis the two mutants showed a quite different trend in gene regulation: in *petc-2*, a balanced response of the nuclear chloroplast transcriptome was observed, with about an equal fraction of genes being up- or down-regulated (636 and 524 genes, respectively). Genes for photosynthesis were down-regulated with a higher frequency than others, while genes for protein phosphorylation and stress response represented the most up-regulated group of genes in this genotype. On the contrary, in the *atpd-1* mutant 87% of the differentially regulated genes were up-regulated. Most of the different functional gene classes followed this trend, with the exception of genes coding for proteins involved in photosynthesis (26% of which were up-regulated).

These results show that the two photosynthetic mutations, *petc-2* and *atpd-1*, result into very different transcriptional responses of the nuclear chloroplast transcriptome.

4 DISCUSSION

4.1 The *petc-2* mutant

In the *petc-2* mutant the expression of the *PetC* gene was abolished due to a *Ds* element insertion in the promoter region of the gene. The absence of the *PetC* mRNA and the resulting Rieske protein was shown by Northern and Western blot analyses. Crosses between heterozygous *petc-1*, *-2*, and *–3* plants resulted in progenies that segregated with a 1 to 3 ratio for the mutant phenotype, demonstrating that the three mutations are allelic and that the observed phenotype was due to the loss of the Rieske protein. The effects of this mutation on photosynthesis, thylakoid composition and nuclear chloroplast gene expression were analysed in this work.

Greenhouse-grown *petc-2* plants were seedling-lethal as they are photosynthetically incompetent. The plants could, however, be propagated heterotrophically and mutant plants displayed a pigmentation defective phenotype, which was even more severe when the mutants were grown under increased light conditions. This photosensitivity could have caused the over-proportional increase in the VAZ-pool observed in *petc-2*. The phenotype of the Arabidopsis *petc-2* mutants is reminiscent of both the tobacco mutants with disrupted chloroplast *petA*, *petB* and *petD* genes (Monde et al., 2000) and the maize mutants *crp1*, *pet2* and *pet3* (Barkan et al., 1994; Voelker and Barkan, 1995), all of which displayed a pale-green phenotype, a reduction in chlorophyll concentration and all lacked a functional cyt b_6/f complex. However, a similar reduction in chlorophyll accumulation was not observed in the corresponding Chlamydomonas mutants (Kuras and Wollman, 1994), possibly indicative of different control mechanisms between Chlamydomonas and higher plants.

4.1.1 The absence of the Rieske protein blocks the linear electron transport

The observed hcf phenotype indicates a block in the intersystem electron flow. The effect of the absence of the Rieske protein on photosynthesis was further analysed by monitoring parameters of chlorophyll fluorescence, fluorescence induction kinetics and steady-state levels of the oxidized reaction centre chlorophyll in PSI. The maximum quantum yield of PSII (F_V/F_M) was substantially reduced indicating the presence of inactive PSII centres.

The strong reduction in the effective quantum yield of PSII, Φ_{II}, and its pronounced decrease with increasing light intensities imply a severe perturbation of electron flow, which is consistent with the high photosensitivity of the mutant. A substantial overreduction of the plastoquinone pool (reduced photochemical quenching) was observed for the mutant plants, and the reaction centre of PSI, P700, was fully oxidized even at low light intensities, implying that the electron transport from PSII to PSI though the cyt b_6/f complex is completely suppressed. The almost complete suppression of non-photochemical quenching, NPQ, in the *petc-2* mutant indicates a decrease in the thylakoid lumen acidification, as an acidified thylakoid lumen is required for inducing NPQ. Similar effects on the level of photochemical and non-photochemical quenching were observed for tobacco Rieske antisense plants (Price et al., 1995) and for the point mutation mutant, *pgr1*, in the Arabidopsis *PetC* gene (Munekage et al., 2001).

4.1.2 The Rieske protein is involved in the stability of the cytochrome b_6/f complex and has an effect on the thylakoid composition

Western blot analyses confirmed the absence of the Rieske protein in the *petc-2* mutant. To test which role the Rieske protein plays in the stability of the entire complex, Western blot analyses were performed. An antibody against the cyt b_6 subunit was chosen, as this subunit is very likely to be diagnostic for the entire complex. It had earlier been shown in the tobacco mutant Δ*petB* that the absence of the cyt b_6 protein results in a loss of the entire cyt b_6/f complex (Monde et al., 2000). As the *petc-2* mutant displays a strong decrease of the cyt b_6 protein (to 4% of wild-type level) it is very likely that the absence of the Rieske protein leads to a strong decrease in the entire cyt b_6/f complex. However, no other antibodies specific for additional cyt b_6/f subunits were available in our laboratory, therefore the protein level of no other subunit of the cyt b_6/f complex could be tested. But the data presented here clearly indicate that the Rieske protein is essential for the stable assembly of this thylakoid membrane complex in Arabidopsis. This finding is compatible with previous analyses carried out in maize (Miles, 1982), Oenothera (Stubbe and Herrmann, 1982) and Lemna (Bruce and Malkin, 1991) mutants defective in the assembly of cyt b_6/f, and thus supports the conclusion of other authors, that the Rieske protein is required for the assembly of the cyt b_6/f complex. Bruce and Malkin, (1991) suggested an “all-or-none” mechanism for the assembly of this chloroplast complex, which seems more likely to take place, whereby all components must be present for the stabilization of the entire complex. However, in the Chlamydomonas *petc*-Δ1 mutant, lacking the Rieske protein, all other subunits of the cyt b_6/f complex assemble even in the absence of the Rieske protein and the complex could be isolated as a dimer (de Vitry et al., 1999). This implies that in algae different regulatory mechanisms, in the transcription or translation or in the degradation of unassembled proteins in response to the missing Rieske protein, operate. However, on the basis of this work, it cannot be decided if the knock-out of the Rieske protein in the *petc-2* mutant influences (i) the transcription, (ii) the translation of the other subunits of this complex, or (iii) if the absence of the cyt b_6 protein is due to the proteolytic degradation of unassembled protein.

PSI core centre, LHCII and LHCI proteins had reduced levels similar in magnitude to the reduction in chlorophyll and furthermore little PSII was detectable in the *petc-2* mutant. This change in the stoichiometry of the photosystems was also indicated by the reduced Chl *a/b* ratio and the reduced β-carotene levels. This accumulation of antenna proteins relative to the reaction centre core proteins is in line with the increased xanthophyll content. Such a relative increase in the antenna proteins was also seen in the tobacco Rieske antisense plants with diminished cyt b_6/f complex content (Price et al., 1995) and is also observed during shade acclimation (Anderson, 1986; Anderson et al., 1988). Price et al., (1995) suggested that the relative increase in antenna proteins in the antisense plants could be due to their reduced ability for intersystem electron transport, thus explaining the relative increase of the antenna proteins in the *petc-2* mutants.

It was observed in this work that in the *petc-2* mutant, where there is little turn-over of the chemically reduced plastoquinol pool, the D1 protein is decreased over-proportionally with respect to the entire PSII complex. This could be due to an increased photoinhibition in these mutant plants. This is in contrast to the analysis of Shochat et al., (1990) of a Chlaymdomonas cyt b_6/f-less mutant where it was concluded that continuous PQ/PQH_2 turnover (redox reactions of the plastoquinol pool) is essential for the degradation of the D1 protein. In the *petc-2* mutant there is no cyt b_6/f complex present to oxidize the plastoquinol pool. However, the plastoquinol pool could be at least partly be oxidized by chlororespiration, an alternative oxidase activity, that can remove electrons from the plastoquinol pool, thus providing a turn-over of the plastoquinol pool (Niyogi, 2000; Bennoun, 1982; Cournac et al., 2000). Under normal conditions the electron flow to oxygen via the plastid oxidase is only marginal, but when the plastoquinol pool becomes highly reduced the plastid oxygenase becomes highly active and thereby prevents the over-reduction of the plastoquinol pool (Cournac et al., 2002). Thus, providing a plausible explaination for the observed over-proportional decrease of the D1 protein in the *petc-2* mutant.

4.1.3 The disruption of the cyt b_6/f complex causes a relative increase of the chloroplast ATP synthase

In the *petc-2* mutant the accumulation of the α- and β-subunits of the chloroplast ATP synthase were reduced to about 60% of the wild-type level based on fresh weight. Relative to chlorophyll levels the ATP synthase showed an accumulation of approximately 135% of the wild-type levels. Interestingly, a similar effect was observed in a tobacco Rieske antisense plant where an increased level of the δ-subunit to 163% was observed in combination with an increased level of ATP hydrolysis (115%) (Price et al., 1995). It has been suggested that, in such mutants, the ATP synthase is directly involved in maintaining a transthylakoid ΔpH gradient at the expense of ATP consumption. It is known that the chloroplast ATP synthase can potentially hydrolize ATP when the transmembrane electrochemical potential difference is small (Hisabori et al., 2002). One reason for generating a ΔpH at the cost of ATP hydrolysis could be to faciliate the import of thylakoid proteins by the pH-dependent twin-arginine translocation (Tat) pathway. It was shown *in vitro* that the import of proteins via this pathway requires a ΔpH (Robinson et al., 2001). However, Finazzi et al., (2003) have shown recently in Chlamydomonas and barley that it is likely that thylakoid targeting of Tat passenger proteins like the Rieske protein (Madueno et al., 1994; Molik et al., 2001) or the 16- and 23-kDa subunits of the oxygen-evolving complex of PSII (Mould and Robinson, 1991; Cline et al., 1992) show no ΔpH dependence *in vivo*. Therefore, it is unclear if the relative increase in the quantity of the ATP synthase in the *petc-2* mutants can be interpreted as a mechanism to maintain the ΔpH for protein import via the Tat pathway. Alternatively, another reason for maintaining the ΔpH in the mutant plants is that it is thought that a ΔpH is necessary to activate the elongation step of translation in the chloroplasts of vascular plants (Muhlbauer and Eichacker, 1998).

4.2 The *atpd-1* mutant

The *atpd-1* mutant was identified based on its seedling-lethal phenotype (Budziszewski et al., 2001). In the mutant the expression of the *AtpD* gene was abolished due to a T-DNA insertion in the promoter region of the gene. The absence of the *AtpD* mRNA and the resulting protein, the δ-subunit of the chloroplast ATP synthase, was shown by Northern and Western analyses. The wild-type phenotype could be restored in the *atpd-1* mutant plants by introducing the *AtpD* gene under the control of the 35S promoter in the mutant plants thus proving that the observed phenotype was due to the lack of the δ-subunit of the ATP synthase. The seedling-lethal phenotype, alone, indicates that loss of ATP synthase function results in a block in the photosynthetic electron flow. Measuring membrane potential changes in intact leaves have shown that dissipation of the ΔpH in the *atpd-1* mutants results most likely only from proton leakage and that there is no active ATP synthase channel. However, mutant plants could be propagated on medium supplemented with 2% sucrose. The effects on photosynthesis, the thylakoid composition and nuclear chloroplast gene expression of the knock-out of the *AtpD* gene in Arabidopsis were analysed in this work.

4.2.1 The d-subunit is important for the stability of the chloroplast ATP synthase

To study the effect of the absence of the δ-subunit on the stability of the ATP synthase, Western analyses were performed. The a- and b-subunits of the CF_0 complex did not accumulate to detectable amounts in the mutants. Also the α- and β-subunits of the CF_1 complex could not be detected in thylakoid membranes. This indicates that the absence of the δ-subunit leads to a loss of the entire ATP synthase complex. The increased VAZ-pool in the mutant - even at low light intensities - and the increased level of de-epoxidation of the VAZ-pool are indicative of an increased ΔpH across the thylakoid membrane. This luminal acidification is most likely caused by the fact that the mutant plants cannot translocate protons across the thylakoid membrane by ATP synthase activity. Mutational analyses of the homologs of chloroplast ATPase-δ in *E. coli* (Hazard and Senior, 1994, 1994; Stack and Cain, 1994) or yeast (Prescott et al., 1994; Straffon et al., 1998) indicated that this protein is essential for the function of the ATPase complex.

4.2.2 Absence of a functional ATP synthase changes the thylakoid composition and favours a limited cyclic electron transport

Upon UV-illumination the mutant plants display a hcf phenotype, indicating a severe effect on photosynthesis. Therefore the effects on photosynthesis in the *atpd-1* mutant were further analysed by monitoring parameters of chlorophyll fluorescence, fluorescence induction kinetics and steady-state levels of the oxidized reaction centre chlorophyll in PSI.

The mutants displayed a substantially reduced maximum quantum efficiency of PSII, F_V/F_M, indicating the presence of inactive PSII centres. Moreover, the strong reduction in the effective quantum yield of PSII, Φ_{II}, became even more pronounced at increasing light intensities. This is indicative of a severe perturbation of electron flow from PSII to PSI. The increased fraction of reduced plastoquinol Q_A indicates an impaired electron flow downstream of PSII. It has been shown in isolated thylakoids that when the pH is lowered from 7.5 to 5.5 the oxidation of plastoquinol is decreased 10-fold (Kramer et al., 1999). This leads, of course, to a slow down of the photosynthetic electron transport, which means that the electron transport can be controlled by the luminal pH (Kramer et al., 2003). However, in intact leaves these observations could not be made (Kramer et al., 1999). Kramer et al., (1999) therefore suggested that under normal conditions plants maintain a luminal pH at levels that do not substantially suppress cyt b_6/f activity. Therefore, it might be that in the *atpd-1* mutants these mechanisms, that control the luminal pH, are impaired resulting in a high ΔpH in this mutant and, as a consequence, in an impaired electron flow. Such an impaired electron flow had already been indicated by the fact that in intact leaves the fraction of oxidized P700 is increased at low light intensities and the maximum oxidation of P700 was reached at much lower light intensities in the mutants.

By using gramidicin D, which forms a pore or channel in the membrane and thus eliminates the ΔpH gradient, it was shown that linear electron flow is possible in the mutant. Similar results were shown for the Chlamydomonas deletion mutants Δ*atpA* and Δ*atpB* (Fiedler et al., 1997). In these mutants both photosystems were fully active, but linear electron transport was only detectable in mutant thylakoids by using the uncoupler nigericin. However, in this thesis fluorescence induction kinetics of intact leaves have been used to show that it is very likely that *in vivo* only cyclic electron transport takes place in the mutant plants, resulting in an increased ΔpH in the *atpd-1* mutant.

In addition to the impaired electron flow, a marked alteration of the thylakoid protein composition was observed in the mutant plants. As already indicated by the decreased Chl *a/b* ratio in mutant plants there is an increased accumulation of the antenna proteins in relation to reaction centre core proteins. It was shown that cultivating plants at low concentrations of PSII inhibitors, which decreases the electron transport, triggers an increase in the light harvesting proteins (Anderson, 1986). It could, therefore, be that the impaired electron transport in the plant causes the relative increase in the antenna proteins in *atpd-1* mutant plants.

4.2.3 The low luminal pH in the *atpd-1* mutant induces non-photochemical quenching even at low light intensities

In the *atpd-1* mutant plants a strong increase in NPQ was observed at low light intensities. The major portion of this NPQ was shown to be composed of the ΔpH-dependent component, qE, this suggests an increase in acidification of the thylakoid lumen. A decrease of the luminal pH – as observed in the *atpd-1* mutant – activates the violaxanthin de-epoxidase, which converts violaxanthin to antheraxanthin and zeaxanthin (Niyogi et al., 1998) leading to the high de-epoxidation state of the VAZ-pool observed in the *atpd-1* mutant. These results indicate that in the *atpd-1* mutants, even at low light intensities, the luminal pH is high enough to initiate non-photochemical quenching. The Chlamydomonas mutant ac46, having a defect in the production or stability of the *atpH* mRNA, exhibited a loss of the CF_0 complex of the ATP synthase. In contrast to the data presented here no qE could be measured, although the Chlamydomonas mutant should theoretically accumulate a large electrochemical gradient upon illumination (Majeran et al., 2001). As the Chlaymdomonas mutants were grown under even lower light intensities than the *atpd-1* mutants, the cultivating light for Chlamydomonas could be too low to induce the formation of antheraxanthin and zeaxanthin. Moreover, the formation of antheraxanthin and zeaxanthin depends not only on the ΔpH, but also on the light intensities used for cultivating the plants (Demmig-Adams et al., 1995) or algae (Niyogi et al., 1997).

These results indicate that in *atpd-1* plants the photosystems, cyt b_6/f, and thus linear electron flow, are still functional, while the chloroplast ATPase is missing. Since the transthylakoid protein gradient cannot be utilized to drive ATP synthesis, increased acidification of the lumen lead to an increased non-photochemical quenching of excitation energy at low light intensities as observed for the mutant.

4.3 Effects on plastid signalling in the *petc-2* and *atpd-1* mutants

The majority of chloroplast proteins are encoded in the nucleus (Abdallah et al., 2000), therefore, communication between the two organelles is necessary. Expression profiling of more than 3000 nuclear genes, most of them coding for chloroplast functions, in this study, showed that different transcriptional responses of the nuclear chloroplast transcriptome were induced by the two mutations, *petc-2* and *atpd-1*. Since photosynthesis was abolished in both genotypes, many secondary effects due to loss of photoautotrophy should be similar in the mutants. This allows to conclude that many, if not most, differences in the expression profile of *petc-2* and *atpd-1* could be due to different types of plastid signaling pathways which are triggered by the physiological effects of the two mutations. So far there are at least two retrograde (from the plastid to the nucleus) signalling pathways identified, that control nuclear gene expression (Surpin et al., 2002; Pfannschmidt, 2003). Intermediates of the tetrapyrrole biosynthetic pathway (Strand et al., 2003), as well as the redox state of the photosynthetic apparatus (Pfannschmidt, 2003), have been associated with the generation of plastid signals which result in the modulation of the transcription of nuclear-encoded chloroplast proteins. The molecular mechanisms of these signals has remained thus far unknown (Strand et al., 2003).

In the *petc-2* mutant the reduction state of Q_A, the primary electron acceptor of PSII, is, in fact, substantially increased as observed in the *psad-1* (personal communication, D. Leister) and in *psae1-1* (Varotto et al., 2000) mutants, but not in *atpd-1* (this study) and *psao-1* (personal communication, D. Leister), as well as in PSI-N mutants (Haldrup et al., 1999). This different redox state of thylakoids in the two mutants (*petc-2* and *atpd-1*) could be responsible for the different transcriptional responses. Another possibility is that the different level of luminal acidification in the two mutants is sensed and produces, at least indirectly, a signal which modulates nuclear gene transcription of the chloroplast targeted proteins, resulting in differing responses.

4.4 Outlook

It is obvious that the destabilization of the entire cyt b_6/f and chloroplast ATP synthase complexes by loss of the Rieske or ATPase-δ-subunit proteins, respectively, complicates the functional analysis of the specific role(s) of the *PetC* and *AtpD* gene products. As a starting point for future functional studies *in planta*, the *petc-2* and *atpd-1* knock-out mutants characterized in this study should be complemented with mutagenized versions of these proteins which retain the ability to stabilize their multi-protein complexes, while being impaired by targeted mutations at specific sites affecting their specific functions.

5 SUMMARY / ZUSAMMENFASSUNG

In *Arabidopsis thaliana*, the nuclear genes *PetC* and *AtpD* code for the Rieske protein of the cytochrome b_6/f complex and the δ-subunit of the chloroplast ATPase, respectively. Knock-out alleles for each of these loci have been identified by forward and reverse genetics. Greenhouse-grown *petc-2* and *atpd-1* mutants are seedling-lethal, while heterotrophically propagated plants display a high-chlorophyll-fluorescence phenotype, indicating that the products of *PetC* and *AtpD* are essential for photosynthesis. Additional effects of the mutations in axenic culture include altered leaf coloration and increased photosensitivity. Lack of the Rieske protein destabilizes the cytochrome b_6/f complex, and also affects the level of other thylakoid proteins, particularly those of photosystem II. In *petc-2*, linear electron flow is blocked, leading to an altered redox state of both the primary quinone acceptor Q_A in photosystem II, and the reaction centre chlorophyll P700 in photosystem I. Absence of the chloroplast ATPase-δ-subunit destabilizes the ATP synthase complex, whereas residual accumulation of the cytochrome b_6/f complex and of the photosystems still allows electron flow. In *atpd-1*, the increase in non-photochemical quenching of chlorophyll fluorescence and a higher de-epoxidation state of xanthophyll cycle pigments under low light is compatible with increased lumen acidification associated with the defect in chloroplast ATPase activity. Further and clear differences between the two mutations are evident when mRNA expression profiles of nucleus-encoded chloroplast proteins were considered, suggesting that the physiological states conditioned by the two mutations trigger different modes of plastid signaling and nuclear response.

Bei *Arabidopsis thaliana* kodieren die Kern-Gene *PetC* und *AtpD* für das Rieske Protein des Cyt b_6/f Komplexes bzw. für die δ-Untereinheit der chloroplastidären ATP Synthase. Null Allele für diese beiden Loci wurden mittels „Forward“ und „Reverse“ Genetik identifiziert. Im Gewächshaus kultivierte Pflanzen sind keimlings lethal, während heterotroph kultivierte Pflanzen hingegen einen „high-chlorophyll-fluorescence“ Phänotyp zeigen. Dies weist darauf hin, daß die Produkte der *PetC* und *AtpD* Gene essentiell für die Photosynthese sind. In Sterilkultur wurden auch eine veränderte Pigmentierung der Blätter und erhöhte Photoinhibition beobachtet. Das Fehlen des Rieske Proteins destabilisiert den Cyt b_6/f Komplex und bewirkt eine veränderte Zusammensetzung der Thylakoidmembran Proteine Komplexe, besonders die von PSII. Bei der *petc-2* Mutante ist der lineare Elektronenfluß blockiert, was zu einem verändertem Redoxstatus des primären Akzeptor

Q_A von PSII und des P700 Chlorophyll im Reaktionszentrums in PSI führt. Das Fehlen der δ-Untereinheit der chloroplastidären ATP Synthase führt zu einer Destabilisierung des ATP Synthase Komplexes. Der Cyt b_6/f Komplex und die Photosysteme hingegen sind vorhanden und erlauben unter bestimmten Bedingungen einen photosynthetischen Elektronenfluß. Bei der *atpd-1* Mutante wurde ein erhöhtes nicht-photosynthetisches Quenching der Chlorophyll Fluoreszenz and ein höherer De-epoxidationsstatus der Xanthophyll Zyklus Pigmente bei Niedrig-Licht Bedingungen beobachtet. Dies ist stimmig mit einer erhöhten Azidifizierung des Thylakoidlumens bedingt durch den Defekt in der chloroplastidären ATP Synthase. Weitere und klare Unterschiede zwischen den zwei Mutanten wurden bei Untersuchung von mRNA Expressionsprofilen von Kern kodierten Chloroplasten Proteinen deutlich: die veränderte Chloroplastenphysiologie beider Mutanten löst verschiedene Plastiden Signale und Kern-Antworten aus.

6 REFERENCES

Abdallah F, Salamini F, Leister D (2000) A prediction of the size and evolutionary origin of the proteome of chloroplasts of Arabidopsis. Trends Plant Sci **5:** 141-142

Anderson JM (1986) Photoregulation of the composition, function and structure of thylakoid membranes. Annu Rev Plant Physiology **37:** 93-136

Anderson JM, Chow WS, Goodchild DJ (1988) Thylakoid membrane organization in sun/shade acclimation. Australian Journal of Plant Physiology **15:** 11-26

Barkan, A, Miles, D, Taylor, WC (1986) Chloroplast gene expression in nuclear, photosynthetic mutants of maize. Embo J **5:** 1421-1427

Barkan A, Walker M, Nolasco M, Johnson D (1994) A nuclear mutation in maize blocks the processing and translation of several chloroplast mRNAs and provides evidence for the differential translation of alternative mRNA forms. Embo J **13:** 3170-3181

Barth C, Krause GH, Winter K (2001) Responses of photosystem I compared with photosystem II to high-light stress in tropical shade and sun leaves. Plant Cell Environ **24:** 163-176

Bassi R, dal Belin Peruffo A, Barbato R, Ghisi R (1985) Differences in chlorophyll-protein complexes and composition of polypeptides between thylakoids from bundle sheaths and mesophyll cells in maize. Eur J Biochem **146:** 589-595

Bassi R, Pineau B, Dainese P, Marquardt J (1993) Carotenoid-binding proteins of photosystem II. Eur J Biochem **212:** 297-303

Beckers G, Berzborn RJ, Strotmann H (1992) Zero-length crosslinking between subunits δ and I of the H^+-translocating ATPase of chloroplasts. Biochim Biophys Acta **1101:** 97-104

Bennoun P (1982) A respiratory chain in the thylakoid membranes of *Chlamydomonas reinhardtii*. Prog Clin Biol Res **102 Pt B:** 291-298

Berthold DA, Schmidt CL, Malkin R (1995) The deletion of *petG* in *Chlamydomonas reinhardtii* disrupts the cytochrome *bf* complex. J Biol Chem **270:** 29293-29298

Boettcher B, Schwarz L, Graber P (1998) Direct indication for the existence of a double stalk in CF_0F_1. J Mol Biol **281:** 757-762

Boronowsky U, Wenk S, Schneider D, Jager C, Rogner M (2001) Isolation of membrane protein subunits in their native state: evidence for selective binding of chlorophyll and carotenoid to the b_6 subunit of the cytochrome b_6f complex. Biochim Biophys Acta **1506:** 55-66

Boyer PD (1999) What makes ATP synthase spin? Nature **402:** 247, 249

Breyton C, Tribet C, Olive J, Dubacq JP, Popot JL (1997) Dimer to monomer conversion of the cytochrome b_6f complex. Causes and consequences. J Biol Chem **272:** 21892-21900

Breyton C (2000) The cytochrome b_6f complex: structural studies and comparison with the bc_1 complex. Biochim Biophys Acta **1459:** 467-474

Bruce BD, Malkin R (1991) Biosynthesis of the chloroplast cytochrome b_6f complex: studies in a photosynthetic mutant of *Lemna*. Plant Cell **3:** 203-212

Budziszewski GJ, Lewis SP, Glover LW, Reineke J, Jones G, Ziemnik LS, Lonowski J, Nyfeler B, Aux G, Zhou Q, McElver J, Patton DA, Martienssen R, Grossniklaus U, Ma H, Law M, Levin JZ (2001) Arabidopsis genes essential for seedling viability: isolation of insertional mutants and molecular cloning. Genetics **159:** 1765-1778

Chomczynski P, Sacchi N (1987) Single-step method of RNA isolation by acid guanidinium thiocyanate-phenol-chloroform extraction. Anal Biochem **162:** 156-159

Clayton RK (1980) Photosynthesis: Physical mechanisms and chemical patterns. Cambridge University Press Cambridge, England

Cline K, Ettinger WF, Theg SM (1992) Protein-specific energy requirements for protein transport across or into thylakoid membranes. Two lumenal proteins are transported in the absence of ATP. J Biol Chem **267:** 2688-2696

Cline K, Henry R, Li C, Yuan J (1993) Multiple pathways for protein transport into or across the thylakoid membrane. Embo J **12:** 4105-4114

Clough SJ, Bent AF (1998) Floral dip: a simplified method for *Agrobacterium*-mediated transformation of *Arabidopsis thaliana*. Plant J **16:** 735-743

Cournac L, Redding K, Ravenel J, Rumeau D, Josse EM, Kuntz M, Peltier G (2000) Electron flow between photosystem II and oxygen in chloroplasts of photosystem I-deficient algae is mediated by a quinol oxidase involved in chlororespiration. J Biol Chem **275:** 17256-17262

Cournac L, Latouche G, Cerovic Z, Redding K, Ravenel J, Peltier G (2002) In vivo interactions between photosynthesis, mitorespiration, and chlororespiration in *Chlamydomonas reinhardtii*. Plant Physiol **129:** 1921-1928

Cramer WA, Furbacher PN, Szczepaniak A, Tae G-S (1991) Electron transport between photosystem II and photosystem I. In CP Lee, ed, Current Topics in Bioenergetics, Academic Press, San Diego **16:** 179-222

Crofts AR, Meinhardt SW, Jones KR, Snozzi M (1983) The Role of the Quinone Pool in the Cyclic Electron-Transfer Chain on *Rhodopseudomonas-Sphaeroides* - a Modified Q-Cycle Mechanism. Biochim Biophys Acta **723:** 202-218

de Vitry C (1994) Characterization of the Gene of the Chloroplast Rieske Iron-Sulfur Protein in *Chlamydomonas reinhardtii*. J Biol Chem **269:** 7603-7609

de Vitry C, Finazzi G, Baymann F, Kallas T (1999) Analysis of the nucleus-encoded and chloroplast-targeted rieske protein by classic and site-directed mutagenesis of *Chlamydomonas*. Plant Cell **11:** 2031-2044

Demmig-Adams B, Adams WW, Heber U, Neimanis S, Winter K, Krüger A, Czygan F-C, Bilger W, Bjorkman O (1990) Inhibition of zeaxanthin formation and of rapid changes in radiationless energy dissipation by dithioreitol in spinach leaves and chloroplasts. Plant Physiol **92:** 293-301

Demmig-Adams B, Adams WW, Logan BA, Verhoeven AS (1995) Xanthophyll Cycle-Dependent Energy-Dissipation and Flexible Photosystem-II Efficiency in Plants Acclimated to Light Stress. Austr J Plant Physiol **22:** 249-260

Devenish RJ, Prescott M, Roucou X, Nagley P (2000) Insight into ATP synthase assembly and function through the molecular genetic manipulation of subunits of the yeast mitochondrial enzyme complex. Biochim Biophys Acta **1458:** 428-442

Douglas SE (1998) Plastid evolution: origins, diversity, trends. Curr. Opin. Genet. Dev. **8:** 655-661

Engelbrecht S, Junge W (1988) Purified Subunit-δ of Chloroplast Coupling Factor-CF_1 Reconstitutes Photophosphorylation in Partially CF_1-Depleted Membranes. Europ J Biochem **172:** 213-218

Engelbrecht S, Junge W (1990) Subunit-δ of H^+-ATPases - at the Interface between Proton Flow and ATP Synthesis. Biochim Biophys Acta **1015:** 379-390

Engelbrecht S, Reed J, Penin F, Gautheron DC, Junge W (1991) Subunit δ of chloroplast F_0F_1-ATPase and OSCP of mitochondrial F_0F_1-ATPase: a comparison by CD-spectroscopy. Z Naturforsch [C] **46:** 759-764

Engelbrecht S, Junge W (1997) ATP synthase: a tentative structural model. FEBS Lett **414:** 485-491

Farber A, Young AJ, Ruban AV, Horton P, Jahns P (1997) Dynamics of Xanthophyll-Cycle Activity in Different Antenna Subcomplexes in the Photosynthetic Membranes of Higher Plants (The Relationship between Zeaxanthin Conversion and Nonphotochemical Fluorescence Quenching). Plant Physiol **115:** 1609-1618

Fiedler HR, Schlesinger J, Strotmann H, Shavit N, Leu S (1997) Characterisation of *atpA* and *atpB* deletion mutants produced in *Chlamydomonas reinharddtii* cw15: electron transport and photophosphorylation activities in isolated thylakoids. Biochim Biophys Acta **1319:** 109-118

Finazzi G, Chasen C, Wollman FA, de Vitry C (2003) Thylakoid targeting of Tat passenger proteins shows no ΔpH dependence *in vivo*. Embo J **22:** 807-815

Fromme P, Boekema EJ, Graber P (1987) Isolation and Characterization of a Supramolecular Complex of Subunit-Iii of the ATPSynthase from Chloroplasts. Z Naturforsch [C] **42:** 1239-1245

Futai M, Noumi T, Maeda M (1989) ATP synthase (H+-ATPase): results by combined biochemical and molecular biological approaches. Annu Rev Biochem **58:** 111-136

Genty B, Barrell JM, Baker NR (1989) The relationship between quantum yield of phototsynthetic electron tranport and quenching of chlorophyll fluorescence. Biochim Biophys Acta **990:** 87-92

Groth G, Strotmann H (1999) New results about structure, function and regulation of the chloroplast ATP synthase (CF_0CF_1). Physiologia Plantarum **106:** 142-148

Hager M, Biehler K, Illerhaus J, Ruf S, Bock R (1999) Targeted inactivation of the smallest plastid genome-encoded open reading frame reveals a novel and essential subunit of the cytochrome cyt b_6f complex. Embo J **18:** 5834-5842

Haldrup A, Naver H, Scheller HV (1999) The interaction between plastocyanin and photosystem I is inefficient in transgenic Arabidopsis plants lacking the PSI-N subunit of photosystem I. Plant J **17:** 689-698

Hamel P, Olive J, Pierre Y, Wollman FA, de Vitry C (2000) A new subunit of cytochrome b_6f complex undergoes reversible phosphorylation upon state transition. J Biol Chem **275:** 17072-17079

Hanahan D (1983) Studies on Transformation of *Escherischia coli* with Plasmids. J Mol Biol **166:** 557-580

Hatefi Y (1985) The mitochondrial electron transport and oxidative phosphorylation system. Annu Rev Biochem **54:** 1015-1069

Hauska G, Schutz M, Buttner M (1996) Oxygenic Photosynthesis: The light reactions. Kluwer Academic Publishers, Dordrecht, the Netherland**:** 377-398

Hazard AL, Senior AE (1994) Defective energy coupling in δ-subunit mutants of *Escherichia coli* F_1F_0-ATP synthase. J Biol Chem **269:** 427-432

Hazard AL, Senior AE (1994) Mutagenesis of subunit δ from *Escherichia coli* F_1F_0-ATP synthase. J Biol Chem **269:** 418-426

Hill R, Bendall F (1960) Function of the two cytochrome components in chloroplast: a working hypothesis. Nature **186:** 136-137

Hisabori T, Konno H, Ichimura H, Strotmann H, Bald D (2002) Molecular devices of chloroplast F_1-ATP synthase for the regulation. Biochim Biophys Acta **1555:** 140-146

Hope AB (1993) The chloroplast cytochrome *bf* complex: a critical focus on function. Biochim Biophys Acta **1143:** 1-22

Inohara N, Iwamoto A, Moriyama Y, Shimomura S, Maeda M, Futai M (1991) Two genes, *atpC1* and *atpC2*, for the γ subunit of *Arabidopsis thaliana* chloroplast ATP synthase. J Biol Chem **266:** 7333-7338

Jahns P, Graf M, Munekage Y, Shikanai T (2002) Single point mutation in the Rieske iron-sulfur subunit of cytochrome b_6f leads to an altered pH dependence of plastoquinol oxidation in Arabidopsis. FEBS Lett **519:** 99-102

Joliot P, Beal D, Frilley B (1980) Une nouvelle methode spectrophotometrique destine a l'etude des reactions photosynthetiques. J Chim Phys **77:** 209-216

Joliot P, Joliot A (2001) Electrogenic events associated with electron and proton transfer within the cytochrome b_6/f complex. Biochim Biophys Acta **1503:** 369-376

Joliot P, Joliot A (2002) Cyclic electron transfer in plant leaf. Proc Natl Acad Sci U S A **99:** 10209-10214

Junge W, Engelbrecht S, Griwatz C, Groth G (1992) The Chloroplast H^+-ATPase: Partial Reactions of the proton. J Exp Biol **172:** 461-474

Junge W, Lill H, Engelbrecht S (1997) ATP synthase: an electrochemical transducer with rotatory mechanics. Trends Biochem Sci **22:** 420-423

Junge W, Panke O, Cherepanov DA, Gumbiowski K, Muller M, Engelbrecht S (2001) Inter-subunit rotation and elastic power transmission in F_0F_1-ATPase. FEBS Lett **504:** 152-160

Ketcham SR, Davenport JW, Warncke K, McCarty RE (1984) Role of the γ subunit of chloroplast coupling factor 1 in the light-dependent activation of photophosphorylation and ATPase activity by dithiothreitol. J Biol Chem **259:** 7286-7293

Knight JS, Duckett CM, Sullivan JA, Walker AR, Gray JC (2002) Tissue-specific, light-regulated and plastid-regulated expression of the single-copy nuclear gene encoding the chloroplast Rieske FeS protein of *Arabidopsis thaliana*. Plant Cell Physiol **43:** 522-531

Koncz C, Mayerhofer R, Koncz-Kalman Z, Nawrath C, Reiss B, Redei GP, Schell J (1990) Isolation of a gene encoding a novel chloroplast protein by T-DNA tagging in *Arabidopsis thaliana*. Embo J **9:** 1337-1346

Kramer DM, Sacksteder, CA, Cruz JA (1999) How acidic is the lumen? Photosyn Res **60:** 153-163

Kramer DM, Cruz JA, Kanazawa A (2003) Balancing the central roles of the thylakoid proton gradient. Trends Plant Sci **8:** 27-32

Krause GH, Weis E (1991) Chlorophyll fluorescence and photosynthesis: the basics. Annu Rev Plant Physiol Plant Mol Biol **42:** 313-349

Kuras R, Wollman FA (1994) The assembly of cytochrome b_6f complexes: an approach using genetic transformation of the green alga *Chlamydomonas reinhardtii*. Embo J **13:** 1019-1027

Kurth J, Varotto C, Pesaresi P, Biehl A, Richly E, Salamini F, Leister D (2002) Gene-sequence-tag expression analyses of 1,800 genes related to chloroplast functions. Planta **215:** 101-109

Lavergne J, Briantais J-M (1995) Photosystem II heterogeneity. In DR Ort, CF Yocum, eds, Advances in Photosynthesis. Oxygenic Photosynthesis: The Light Reactions. Kluwer Academic Publishers, Dotrecht, The Netherlands: 265-287

Lemaire C, Wollman FA (1989) The chloroplast ATP synthase in *Chlamydomonas reinhardtii*. II. Biochemical studies on its biogenesis using mutants defective in photophosphorylation. J Biol Chem **264:** 10235-10242

Lill H, Hensel F, Junge W, Engelbrecht S (1996) Cross-linking of engineered subunit δ to $(\alpha\beta)_3$ in chloroplast F-ATPase. J Biol Chem **271:** 32737-32742

Liu YG, Mitsukawa N, Oosumi T, Whittier RF (1995) Efficient isolation and mapping of *Arabidopsis thaliana* T-DNA insert junctions by thermal asymmetric interlaced PCR. Plant J **8:** 457-463

Madueno F, Napier JA, Cejudo FJ, Gray JC (1992) Import and processing of the precursor of the Rieske FeS protein of tobacco chloroplasts. Plant Mol Biol **20:** 289-299

Madueno F, Bradshaw SA, Gray JC (1994) The thylakoid-targeting domain of the chloroplast Rieske iron-sulfur protein is located in the N-terminal hydrophobic region of the mature protein. J Biol Chem **269:** 17458-17463

Majeran W, Olive J, Drapier D, Vallon O, Wollman FA (2001) The light sensitivity of ATP synthase mutants of *Chlamydomonas reinhardtii*. Plant Physiol **126:** 421-433

Meurer J, Meierhoff K, Westhoff P (1996) Isolation of high-chlorophyll-fluorescence mutants of *Arabidopsis thaliana* and their characterisation by spectroscopy, immunoblotting and northern hybridisation. Planta **198:** 385-396

Miles D (1982) The use of mutations to probe photosynthesis in higher plants. In M Edelman, RB Hallick, N-H Chua, eds, Methods in Chloroplast Molecular Biology Elsevier Biomedical Press, Amsterdam: 75-107

Mills DA, Richter ML (1991) Nucleotide binding to the isolated β subunit of the chloroplast ATP synthase. J Biol Chem **266:** 7440-7444

Mills JD (1995) The Regulation of Chloroplast ATP Synthase, CF_0-CF_1. in Ort, D. R., Yocum, C. Y.: Adv Photosyn **4:** 469-485

Mitchell P (1975) Protonmotive Q-cycle-general formulation. FEBS Lett **59:** 137-139

Molik S, Karnauchov I, Weidlich C, Herrmann RG, Klosgen RB (2001) The Rieske Fe/S protein of the cytochrome b_6f complex in chloroplasts: missing link in the evolution of protein transport pathways in chloroplasts? J Biol Chem **276:** 42761-42766

Monde RA, Zito F, Olive J, Wollman FA, Stern DB (2000) Post-transcriptional defects in tobacco chloroplast mutants lacking the cytochrome b_6f complex. Plant J **21:** 61-72

Monticello RA, Brusilow WS (1994) Role of the δ subunit in enhancing proton conduction through the F_0 of the *Escherichia coli* F_1F_0 ATPase. J Bacteriol **176:** 1383-1389

Mould RM, Robinson C (1991) A proton gradient is required for the transport of two lumenal oxygen-evolving proteins across the thylakoid membrane. J Biol Chem **266:** 12189-12193

Muhlbauer SK, Eichacker LA (1998) Light-dependent formation of the photosynthetic proton gradient regulates translation elongation in chloroplasts. J Biol Chem **273:** 20935-20940

Muller P, Li XP, Niyogi KK (2001) Non-photochemical quenching. A response to excess light energy. Plant Physiol **125:** 1558-1566

Munekage Y, Takeda S, Endo T, Jahns P, Hashimoto T, Shikanai T (2001) Cytochrome b_6f mutation specifically affects thermal dissipation of absorbed light energy in Arabidopsis. Plant J **28:** 351-359

Nalin CM, McCarty RE (1984) Role of a disulfide bond in the γ subunit in activation of the ATPase of chloroplast coupling factor 1. J Biol Chem **259:** 7275-7280

Nitschke W, Joliot P, Liebl U, Rutherford AW, Hauska G, Muller A, Riedel A (1992) The pH-Dependence of the Redox Midpoint Potential of the 2fe2s Cluster from Cytochrome-b_6f Complex (the Rieske Center). Biochim Biophys Acta **1102:** 266-268

Niyogi KK, Bjorkman O, Grossman AR (1997) Chlamydomonas Xanthophyll Cycle Mutants Identified by Video Imaging of Chlorophyll Fluorescence Quenching. Plant Cell **9:** 1369-1380

Niyogi KK, Grossman AR, Bjorkman O (1998) Arabidopsis mutants define a central role for the xanthophyll cycle in the regulation of photosynthetic energy conversion. Plant Cell **10:** 1121-1134

Niyogi KK (2000) Safety valves for photosynthesis. Curr Opin Plant Biol **3:** 455-460

Noctor G, Ruban AV, Horton P (1993) Modulation of ΔpH-dependent nonphotochemical quenching of chlorophyll fluorescence in isolated chloroplasts. Biochim Biophys Acta **1183:** 339-344

Ort DR, Oxborough K (1992) In Situ Regulation of Chloroplast Coupling Factor Activity Annu Rev Plant Mol Biol **43:** 269-291

Ovchinnikov YA, Modyanov NN, Grinkevich VA, Aldanova NA, Trubetskaya OE, Nazimov IV, Hundal T, Ernster L (1984) Amino acid sequence of the oligomycin sensitivity-conferring protein (OSCP) of beef-heart mitochondria and its homology with the delta-subunit of the F_1-ATPase of *Escherichia coli*. FEBS Lett **166:** 19-22

Palomares R, Herrmann RG, Oelmuller R (1991) Different blue-light requirement for the accumulation of transcripts from nuclear genes for thylakoid proteins in *Nicotiana tabacum* and *Lycopersicon esculentum*. J Photochem Photobiol B **11:** 151-162

Patrie WJ, McCarty RE (1984) Specific binding of coupling factor 1 lacking the δ and ε subunits to thylakoids. J Biol Chem **259:** 11121-11128

Pesaresi P, Varotto C, Meurer J, Jahns P, Salamini F, Leister D (2001) Knock-out of the plastid ribosomal protein L11 in Arabidopsis: effects on mRNA translation and photosynthesis. Plant J **27:** 179-189

Peter GF, Thornber JP (1991) Biochemical composition and organization of higher plant photosystem II light-harvesting pigment-proteins. J Biol Chem **266:** 16745-16754

Pfannschmidt T (2003) Chloroplast redox signals: how photosynthesis controls its own genes. Trends Plant Sci **8:** 33-41

Pierre Y, Breyton C, Kramer D, Popot JL (1995) Purification and characterization of the cytochrome b_6f complex from *Chlamydomonas reinhardtii*. J Biol Chem **270:** 29342-29349

Pierre Y, Breyton C, Lemoine Y, Robert B, Vernotte C, Popot JL (1997) On the presence and role of a molecule of chlorophyll a in the cytochrome b_6f complex. J Biol Chem **272:** 21901-21908

Porra R, Thompson W, Kriedemann P (1989) Determination of accurate extiction coefficients and simultaneous equations for assaying chlorophyll *a* and *b* exctracted with four different solvents: verification of the concentration of chlorophyll standards by atomic absorption spectroscopy. Biochim Biophys Acta **975:** 384-394

Prescott M, Bush NC, Nagley P, Devenish RJ (1994) Properties of Yeast-Cells Depleted of the OSCP Subunit of Mitochondrial ATP Synthase by Regulated Expression of the *Atp5* Gene. Biochemistry and Molecular Biology International **34:** 789-799

Price GD, Yu JW, Voncaemmerer S, Evans JR, Chow WS, Anderson JM, Hurry V, Badger MR (1995) Chloroplast Cytochrome b_6f and ATP Synthase Complexes in Tobacco - Transformation with Antisense RNA against Nuclear-Encoded Transcripts for the Rieske FeD and ATP-δ Polypeptides. Austr J Plant Physiol **22:** 285-297

Renger G, Govindjee (1985) The Mechanism of Photosynthetic Water Oxidation. Photosyn Res **6:** 33-55

Richly E, Kurth J, Leister D (2002) Mode of amplification and reorganization of resistance genes during recent *Arabidopsis thaliana* evolution. Mol Biol Evol **19:** 76-84

Richly E, Dietzmann A, Biehl A, Kurth J, Laloi C, Apel K, Salamini F, Leister D. (2003) Covariations in the nuclear chloroplast transcriptome reveal a regulatory master-switch. EMBO Rep **4** 1-8

Richter ML, Hein R, Huchzermeyer B (2000) Important subunit interactions in the chloroplast ATP synthase. Biochim Biophys Acta **1458:** 326-342

Robertson D, Woessner JP, Gillham NW, Boynton JE (1989) Molecular characterization of two point mutants in the chloroplast *atpB* gene of the green alga *Chlamydomonas reinhardtii* defective in assembly of the ATP synthase complex. J Biol Chem **264:** 2331-2337

Robinson C, Thompson SJ, Woolhead C (2001) Multiple pathways used for the targeting of thylakoid proteins in chloroplasts. Traffic **2:** 245-251

Rodgers AJ, Wilkens S, Aggeler R, Morris MB, Howitt SM, Capaldi RA (1997) The subunit δ-subunit b domain of the *Escherichia coli* F_1F_0 ATPase. The b subunits interact with F_1 as a dimer and through the δ subunit. J Biol Chem **272:** 31058-31064

Rutherford AW, Heathcope P (1985) Primary photochemistry in photosystem I. Photosynth Res**:** 295-316

Salter AH, Newman BJ, Napier JA, Gray JC (1992) Import of the precursor of the chloroplast Rieske iron-sulphur protein by pea chloroplasts. Plant Mol Biol **20:** 569-574

Sambrook J, Fritsch EF, Maniatis T (1989) Molecular cloning: A laboratory manual. Cold Spring Harbor Laboratory Press Ed., New York

Sanguinetti CJ, Dias Neto E, Simpson AJ (1994) Rapid silver staining and recovery of PCR products separated on polyacrylamide gels. Biotechniques **17:** 914-921

Sauer K (1975) Primary events and the trapping of energy. In: Bioenergetics of Photosynthesis, Govindjee, ed. Academic Press, New York: 116-181

Schagger H, von Jagow G (1987) Tricine-sodium dodecyl sulfate-polyacrylamide gel electrophoresis for the separation of proteins in the range from 1 to 100 kDa. Anal Biochem **166:** 368-379

Schreiber U, Schliwa U, Bilger W (1986) Continuous recording of photochemical and non-photochemical chlorophyll fluorescence quenching with a new type of modulation fluorometer. Photosynth Res **10:** 51-62

Shochat S, Adir N, Gal A, Inoue Y, Mets L, Ohad I (1990) Photoinactivation of photosystem II and degradation of the D 1 protein are reduced in a cytochrome b_6f-less mutant of *Chlamydomonas reinhardtii*. Z Naturforsch [C] **45:** 395-401

Smart EJ, Selman BR (1991) Isolation and Characterization of a *Chlamydomonas reinhardtii* Mutant Lacking the γ-Subunit of Chloroplast Coupling Factor-I (CF_1). Mol Cell Biol **11:** 5053-5058

Smart EJ, Selman BR (1993) Complementation of a *Chlamydomonas reinhardtii* mutant defective in the nuclear gene encoding the chloroplast coupling factor 1 (CF_1) γ-subunit (*atpC*). J Bioenerg Biomembr **25:** 275-284

Stack AE, Cain BD (1994) Mutations in the δ subunit influence the assembly of F_1F_0 ATP synthase in *Escherichia coli*. J Bacteriol **176:** 540-542

Straffon AF, Prescott M, Nagley P, Devenish RJ (1998) The assembly of yeast mitochondrial ATP synthase: subunit depletion *in vivo* suggests ordered assembly of the stalk subunits b, OSCP and d. Biochim Biophys Acta **1371:** 157-162

Strand A, Asami T, Alonso J, Ecker JR, Chory J (2003) Chloroplast to nucleus communication triggered by accumulation of Mg-protoporphyrinIX. Nature **421:** 79-83

Stubbe W, Herrmann RG (1982) Selection and maintenance of plastome mutants and interspecific genome/plastome hybrids in *Oenothera*. In M Edelman, RB Hallick, N-H Chua, eds, Methods in Chloroplast Molecular Biology. Elsevier Biomedical Press, Amsterdam: 149-165

Sturn A, Quackenbush J, Trajanoski Z (2002) Genesis: cluster analysis of microarray data. Bioinformatics **18:** 207-208

Surpin M, Larkin RM, Chory J (2002) Signal transduction between the chloroplast and the nucleus. Plant Cell **14 Suppl:** S327-338

Takahashi Y, Rahire M, Breyton C, Popot JL, Joliot P, Rochaix JD (1996) The chloroplast *ycf7* (petL) open reading frame of *Chlamydomonas reinhardtii* encodes a small functionally important subunit of the cytochrome b_6f complex. Embo Journal **15:** 3498-3506

Thiele A, Winter K, Krause GH (1997) Low Inactivation of D1 Protein of Photosystem II in Young Canopy Leaves of *Anacardium excelsum* under High-Light Stress. J Plant Physiol **151:** 286-292

Van Walraven HS, Strotmann H, Schwarz O, Rumberg B (1996) The H^+/ATP coupling ratio of the ATP synthase from thiol-modulated chloroplasts and two cyanobacterial strains is four. FEBS Lett **379:** 309-313

Varotto C, Pesaresi P, Meurer J, Oelmuller R, Steiner-Lange S, Salamini F, Leister D (2000) Disruption of the Arabidopsis photosystem I gene *psaE1* affects photosynthesis and impairs growth. Plant J **22:** 115-124

Voelker R, Barkan A (1995) Nuclear genes required for post-translational steps in the biogenesis of the chloroplast cytochrome b_6f complex in maize. Mol Gen Genet **249:** 507-514

Walker JE, Cozens, A.L. (1986) Evolution of ATP synthase. Chem Scripta **26:** 263-272

Wilkens S, Rodgers A, Ogilvie I, Capaldi RA (1997) Structure and arrangement of the δ subunit in the *E. coli* ATP synthase (ECF_1F_0). Biophys Chem **68:** 95-102

Wisman E, Hartmann U, Sagasser M, Baumann E, Palme K, Hahlbrock K, Saedler H, Weisshaar B (1998) Knock-out mutants from an *En-1* mutagenized Arabidopsis thaliana population generate phenylpropanoid biosynthesis phenotypes. Proc Natl Acad Sci U S A **95:** 12432-12437

Yamamoto H, Bassi R (1996) Carotenoids: localization and function. In DR Ort, CF Yocum, eds, Oxygenic Photosynthesis. Kluwer Academic Publishers, Dordrecht, The Netherlands: 539-583

Zhang H, Huang D, Cramer WA (1999) Stoichiometrically bound β-carotene in the cytochrome b_6f complex of oxygenic photosynthesis protects against oxygen damage. J Biol Chem **274:** 1581-1587

7 APPENDIX

7.1 Detailed image of hierarchical clustering of the expression profiles

344 genes that show significant differential expression in at least five of the six mutants *petc-2*, *atpd-1*, *psae1-1*, *psad1-1*, *psan-1* and *psao-1*. The cladogram at the top summarizes the degree of relatedness between the transcriptome responses in the six genotypes. Colors indicate up (red)- or down (green)-regulation of gene expression. Grey lines indicate non-significant differential expression (see also Figure 3.18a)

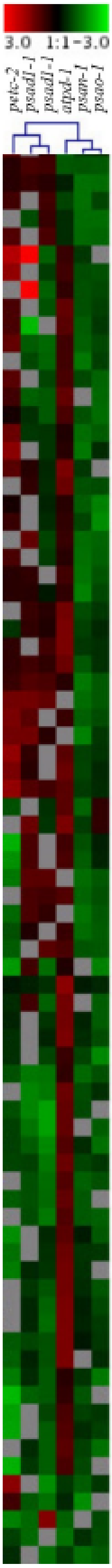

At4g14690	early light-induced protein ELIP.2 (Lil1.2)
At1g54580	acyl-carrier protein (ACP). putative
At1g06680	PsbP1 (3 mRNAs)
At2g01380	hypothetical protein
At1g58290	glutamyl-tRNA reductase. putative
At4g27990	putative protein
At2g01480	axi 1-like protein
At2g16570	amidophosphoribosyltransferase
At4g15910	drought-induced protein like
At1g68690	protein kinase. putative
At1g09780	putative 2.3-bisphosphoglycerate-independent phosphoglycerate mutase
At1g15140	unknown protein
At4g23190	serine/threonine kinase - like protein
At1g52220	unknown protein
At1g67810	putative protein
At2g18900	unknown protein
At1g01500	hypothetical protein
At5g07540	glycine-rich protein atGRP-6
At4g17440	hypothetical protein
At4g35510	putative protein
At5g49020	arginine methyltransferase-like protein
At2g29980	omega-3 fatty acid desaturase
At4g35170	putative protein
At1g05610	putative ADP-glucose pyrophosphorylase. small subunit precursor
At3g18190	chaperonin subunit. putative
At2g33740	putative related to microbial divalent cation tolerance proteins
At3g44990	xyloglucan endo-transglycosylase
At4g13260	putative protein
At1g01290	molybdopterin biosynthesis CNX3 protein. putative
At1g62250	unknown protein
At5g54600	chloroplast ribosomal protein L24
At5g03940	signal recognition particle 54CP (SRP54) protein precursor
At2g13590	pseudogene; similar to GB:AAA75253
At2g22890	unknown protein
At2g37510	putative RNA-binding protein
At1g12900	putative calcium-binding protein. calreticulin
At4g16490	hypothetical protein
At1g10830	unknown protein
At1g04360	hypothetical protein
At4g34310	hypothetical protein
At1g42970	glyceraldehyde-3-phosphate dehydrogenase
At1g30480	DNA damage repair protein. putative
At3g22840	early light-induced protein ELIP.1 (Lil1.1)
At1g30120	pyruvate dehydrogenase E1 beta subunit. putative
At2g40980	unknown protein
At1g33250	unknown protein
At4g15410	phosphatase like protein
At2g31170	putative cysteinyl-tRNA synthetase
At1g70990	hypothetical protein
At1g19870	hypothetical protein
At5g07770	unknown protein
At2g24070	unknown protein
At2g02770	unknown protein
At1g54690	histone H2A. putative
At1g31160	putative protein kinase C inhibitor (Zinc-binding protein)
At4g26900	glutamine amidotransferase/cyclase
At1g79840	homeobox protein (GLABRA2)
At1g65010	hypothetical protein
At1g72010	unknown protein
At3g24430	mrp protein. putative
At2g36010	putative E2F5 family transcription factor
At5g64290	2-oxoglutarate/malate translocator; corrected anotation: glutamate/malate translocator (Di
At2g24730	pseudogene
At2g45770	putative signal recognition particle receptor (alpha subunit)
At1g70710	endo-1.4-beta-glucanase
At2g01580	hypothetical protein
At4g03150	hypothetical protein
At5g40470	putative protein
At2g36480	hypothetical protein
At1g13280	allene oxide cyclase. putative
At4g33030	sulfolipid biosynthesis protein SQD1
At4g39000	putative endo-1.4-beta-glucanase
At2g42070	unknown protein
At1g67770	putative ABC transporter
At2g28760	putative nucleotide-sugar dehydratase
At2g39000	unknown protein
At1g61520	Lhca3
At4g21280	PsbQ1 (1 mRNA)
At4g32340	putative protein

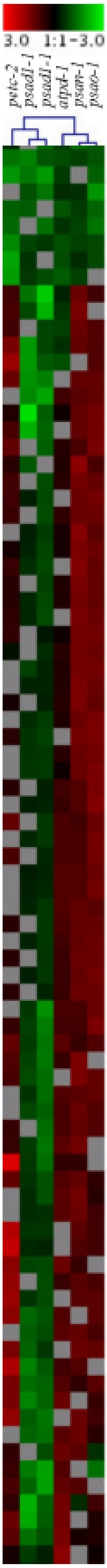

At4g28750	PsaE1 (2 mRNAs)
At2g20260	PsaE2 (2 mRNAs)
At4g31990	aspartate aminotransferase (chloroplast), priming uncertain
At5g54270	Lhcb3 chlorophyll a/b binding protein (gb|AAD28773.1)
At5g11550	putative protein
At2g21660	glycine-rich RNA binding protein 7
At1g12090	hypothetical protein
At2g28900	OuterEnvelopeProtein24
At1g54520	unknown protein
At5g50280	putative protein
At4g01800	putative SecA-type chloroplast protein transport factor
At3g27690	Lhcb2.4
At2g34640	unknown protein
At1g50880	hypothetical protein
At5g54360	unknown protein
At2g31800	putative protein kinase
At2g15870	putative retroelement pol polyprotein
At5g02250	ribonuclease II-like protein
At4g31180	aspartate--tRNA ligase - like protein
At5g22830	putative protein
At3g42060	putative protein
At3g59100	putative protein
At1g56200	unknown protein
At4g32040	homeodomain containing protein 1
At1g25410	tRNA isopentenyl transferase, putative
At3g57110	hypothetical protein
At3g30780	hypothetical protein
At5g63290	oxygen-independent coproporphyrinogen-like protein
At5g32490	putative protein
At1g27610	hypothetical protein
At3g14890	DNA nick sensor, putative
At3g18680	uridylate kinase, putative
At5g44820	putative protein
At3g42200	putative protein
At4g30150	hypothetical protein
At1g67800	unknown protein
At5g17680	disease resistance protein RPP1-WsB - like protein
At4g24930	proteomics: thylakoid lumen protein
At1g68890	putative menaquinone biosynthesis protein
At4g03410	hypothetical protein
At3g16260	hypothetical protein
At3g48320	cytochrome P450 - like protein
At1g72020	unknown protein
At1g07780	phosphoribosylanthranilate isomerase
At5g15280	putative protein
At5g17280	putative protein
At5g46560	unknown protein
At1g47730	hypothetical protein
At5g56250	unknown protein
At3g52190	putative protein
At5g26880	putative protein
At1g79460	ent-kaurene synthase, putative
At4g28590	hypothetical protein
At5g38680	putative protein
At5g01920	putative protein
At4g08790	nitrilase 1 like protein
At3g02750	putative protein phosphatase-2C (PP2C)
At3g01170	unknown protein
At3g26840	unknown protein
At1g07160	protein phosphatase 2C, putative
At5g52810	putative protein
At3g18770	unknown protein
At4g34100	putative protein
At3g25840	protein kinase, putative
At5g03415	transcription factor - like protein
At4g20090	membrane-associated salt-inducible-like protein
At4g00170	putative proline-rich protein
At3g56040	putative protein
At4g33350	Tic110
At5g13340	putative protein
At1g31410	hypothetical protein
At4g32130	hypothetical protein
At4g21460	putative protein
At4g14210	phytoene dehydrogenase precursor (phytoene desaturase)
At5g45290	unknown protein
At5g57390	putative protein
At3g56410	putative protein
At5g28750	Tha4 protein - like
At3g42100	putative protein
At2g11380	pseudogene
At4g13550	putative protein
At3g08720	putative ribosomal-protein S6 kinase (ATPK19)
At4g03310	hypothetical protein

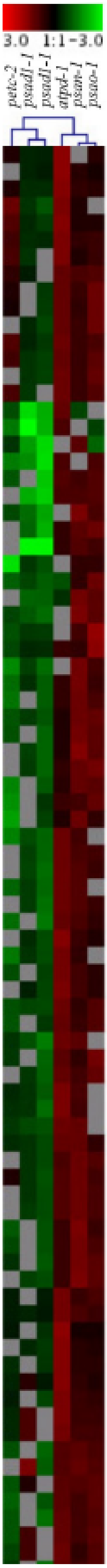

At4g27250	putative protein
At1g05530	putative UDP-glucose:indole-3-acetate beta-D-glucosyltransferase
At3g47650	putative protein
At4g31530	putative protein
At2g30460	putative integral membrane protein
At5g41380	putative protein
At1g35510	growth regulator, putative
At3g14900	hypothetical protein
At4g26220	caffeoyl-CoA O-methyltransferase - like protein
At4g04350	putative leucyl tRNA synthetase
At1g44110	mitotic cyclin a2-type, putative
At3g10350	putative ATPase
At5g38190	putative protein
At5g65250	unknown protein
At5g64940	ABC transporter-like
At4g16590	cellulose synthase like protein
At4g23170	putative protein
At1g66890	hypothetical protein
At2g29670	unknown protein
At3g11490	putative rac GTPase activating protein
At1g56180	hypothetical protein
At5g13840	cell cycle switch protein
At1g28280	hypothetical protein
At5g64860	4-alpha-glucanotransferase
At1g54930	hypothetical protein
At4g16780	DNA-binding homeotic protein Athb-2
At4g32640	putative protein
At5g11890	putative protein
At5g22270	putative protein
At1g30320	hypothetical protein
At5g64090	unknown protein
At1g80450	unknown protein
At3g55070	putative protein
At1g69240	putative alpha/beta hydrolase
At5g55570	unknown protein
At3g10620	putative diadenosine 5',5'''-P1,P4-tetraphosphate hydrolase
At1g68840	putative DNA-binding protein (RAV2-like)
At5g57990	putative protein
At2g17300	unknown protein
At5g19900	putative protein
At1g80830	metal ion transporter
At3g56250	putative protein
At3g14490	terpene synthase-related protein, putative
At2g34700	putative proline-rich glycoprotein
At1g50020	tubulin alpha-6 chain, putative
At5g27070	putative protein
At4g02290	putative endo-1,4-beta glucanase
At2g19240	hypothetical protein
At3g54610	histon acetyltransferase HAT1
At5g12860	2-oxoglutarate/malate translocator (DiT1) protein
At1g08050	unknown protein
At3g16000	myosin heavy chain-like protein
At1g31790	hypothetical protein
At2g24210	putative limonene cyclase
At1g10510	unknown protein
At3g30190	hypothetical protein
At3g18870	hypothetical protein
At5g15530	biotin carboxyl carrier protein precursor-like protein
At1g33780	hypothetical protein
At5g19500	putative protein
At5g61450	putative protein
At3g44050	kinesin -like protein
At1g09840	shaggy-like protien kinase, kappa
At4g34590	bZIP transcription factor ATB2
At5g35100	putative protein
At1g79250	serine/threonine protein kinase, putative
At3g13850	hypothetical protein
At2g17265	homoserine kinase; 3-hydroxy-3-methylglutaryl-coenzyme A reductase 2
At3g20230	hypothetical protein
At1g50960	gibberellin 20-oxidase, putative
At1g32010	hypothetical protein
At5g10910	putative protein
At1g15070	unknown protein, 3' partial
At2g39710	unknown protein
At2g23330	putative retroelement pol polyprotein
At1g32760	unknown protein
At4g25540	putative DNA mismatch repair protein
At1g05650	putative polygalacturonase
At1g30700	putative reticuline oxidase-like protein
At4g29920	putative protein
At1g44350	putative IAA-amino acid hydrolase
At1g79360	hypothetical protein
At3g03630	O-acetylserine (thiol) lyase

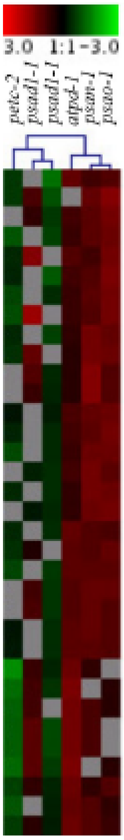

At1g79960	hypothetical protein
At3g53860	putative protein
At4g25720	glutamine cyclotransferase precursor - like protein
At5g03910	ABC transporter -like protein
At3g52550	hypothetical protein
At3g11150	hypothetical protein
At3g18420	unknown protein
At1g30100	9-cis-epoxycarotenoid dioxygenase. putative; neoxanthin cleavage enzyme - like
At5g44750	putative protein
At1g12520	unknown protein
At4g35680	putative protein
At1g63720	hypothetical protein
At3g04680	unknown protein
At3g17700	hypothetical protein
At1g62010	hypothetical protein
At3g45850	kinesin-related protein - like
At3g57950	putative protein
At1g68070	putative RING zinc finger protein
At3g47200	putative protein
At5g07900	putative protein
At1g27660	hypothetical protein
At5g46390	carboxy-terminal proteinase D1-like protein
At1g79480	hypothetical protein
At4g29490	putative protein. fragment
At5g48370	putative protein
At2g40400	unknown protein
At3g48110	glycine--tRNA ligase precursor. chloroplast (edd1)
At4g19490	putative protein
At4g24860	putative protein
At4g24860	putative protein
At4g19100	putative protein
At4g10750	putative aldolase
At3g62520	putative protein
At3g06850	branched chain alpha-keto acid dehydrogenase E2 subunit

7.2 Direct comparison of the differential expression profiles of *petc-2* and *atpd-1* plants

MIPS-code/GI	*petc-2* vs. WT	*atpd-1* vs. WT
up-regulated in both mutants		
At4g29060	2.09	1.65
At4g33170	1.28	4.55
At4g35170	2.23	2.26
At4g27990	3.55	2.13
At2g39670	1.48	2.78
At2g03220	1.29	1.57
At4g38660	1.55	1.86
At4g27510	1.62	7.93
At2g23800	1.45	1.58
At1g17740	1.40	6.26
At4g23890	1.61	1.51
At4g37890	1.66	7.24
At5g23070	1.46	5.40
At4g32040	1.32	1.67
At5g61450	1.28	2.78
At4g14910	1.31	3.48
At4g00170	2.03	1.60
At2g37330	1.58	2.08
At4g19900	1.73	13.20
At3g54900	1.45	1.61
At3g63410	4.41	1.61
At5g53920	1.52	13.39
At3g04650	2.13	4.05
At4g26860	1.39	2.54
At4g19010	1.47	3.68
At5g36860	1.95	10.44
At5g04770	1.32	2.45
At3g18190	1.51	2.71
At1g35510	2.50	15.91
At5g19850	1.31	4.64
At2g28070	1.38	3.39
At4g24840	1.31	2.56
At3g57780	1.29	2.32
At4g20360	1.42	1.53
At2g37230	1.58	1.38
At4g17070	2.25	8.18
At2g41460	1.34	3.96
At4g23190	1.43	1.72
At4g13550	2.07	4.23
At2g04240	2.32	3.28
At1g73110	1.50	2.81
At4g15910	1.65	3.35
At1g73150	1.29	4.07
At3g53350	1.74	2.29
At4g17650	1.52	3.59
At2g33980	1.81	6.08
At1g44575	1.35	2.04
At3g58990	1.29	1.77
At5g23120	1.37	1.56
At5g61440	1.31	5.34
At4g27670	1.30	2.12
At2g35600	1.90	3.68
At3g57110	1.32	1.44
At5g66210	1.47	5.57
At4g03410	1.57	1.78
At5g56050	1.76	5.49
At5g62840	1.41	3.28
At5g41380	1.64	4.48
At2g18820	1.64	5.02
At5g45980	1.37	2.61
At2g37750	1.67	1.68
At3g48000	1.44	2.06
At2g43870	2.60	2.43
At4g28840	1.42	2.78
At4g03310	1.35	16.19
At4g27250	1.31	7.04
At2g01760	1.50	4.89
At1g22680	3.27	2.33
At5g06290	1.29	1.45
At5g52810	2.03	2.94
At4g39940	5.28	2.14
At3g48320	1.84	2.78
At5g52250	2.75	1.89
At3g44570	2.27	2.57
At3g01370	1.70	4.19
At2g31040	1.89	1.71
At1g02060	1.59	13.41
At4g09620	2.81	4.08
At3g03880	1.43	3.12
At4g07990	2.86	10.24
At2g35650	1.40	4.79
At3g50770	1.41	4.72
At1g72520	1.82	1.89
At5g04600	2.68	1.36
At3g58190	1.71	6.47
At2g37040	1.86	5.33
At2g38470	1.45	5.61
At1g48490	1.67	1.95
At1g05190	1.44	3.82
At4g02740	1.35	3.96
At1g05140	3.70	4.36
At4g13260	1.39	3.95
At1g79380	1.39	1.70
At1g04570	1.47	2.83
At5g13280	1.44	3.60
At2g44570	1.30	1.85
At1g30950	2.00	1.36
At1g51350	1.53	5.25
At3g27740	1.59	2.94
At1g22040	1.41	3.58
At1g20070	2.30	10.38
At3g22700	1.54	4.30
At5g02860	1.51	3.51
At5g49910	1.43	1.46
At4g27020	3.80	23.44
At4g11170	1.62	2.85
At5g06670	1.71	1.79
At1g78630	1.56	2.05
At1g74220	2.00	2.70
At2g37510	2.69	4.75
At1g65370	1.33	4.44
At4g08900	2.19	1.46
At2g39360	1.71	2.97
At1g05610	1.39	2.20
At2g33250	1.95	2.38
At4g08940	1.33	2.09
At4g11090	3.98	1.95
At5g04590	1.64	1.39
At2g38310	3.51	1.53
At2g21860	1.42	1.77
At3g21865	1.49	4.47
At2g45310	1.31	2.12
At4g25290	2.51	3.09
At2g31800	1.33	1.38
At4g25120	1.58	2.02
At3g22690	1.60	2.13
At2g17120	1.79	7.81
At4g35510	1.38	2.30
At3g57440	3.05	7.61
At4g00650	1.43	3.51
At3g26940	1.42	1.67
At5g66530	2.06	2.02
At3g49350	1.48	16.29
At4g08600	1.52	8.34
At1g01290	1.57	5.61
At2g17540	4.14	4.28
At2g26790	1.32	2.70
At3g02875	1.29	2.47
At2g32920	1.44	2.97
At4g25050	1.38	1.99
At4g29890	2.07	4.93
At2g23230	1.71	2.61
At4g26780	2.15	12.47
At2g22890	2.60	2.95
At3g21810	1.68	3.17
At1g20510	1.48	4.69
At3g07100	2.85	1.64
At2g41040	2.47	3.79
At1g65080	1.53	5.53
At3g63190	1.54	1.75
At3g02040	1.86	5.89
At1g24040	1.71	2.00
At5g19000	1.37	3.58
At4g17330	1.44	5.64
At4g22760	1.37	3.18
At4g32130	2.57	1.88
At4g04350	1.30	5.27
At4g32060	2.08	10.16
At1g24150	1.32	1.78

MIPS-code/GI	*petc-2* vs. WT	*atpd-1* vs. WT
up-regulated in both mutants		
At2g35400	1.41	2.16
At3g26630	3.39	1.46
At4g33350	1.99	2.10
At1g78160	1.45	6.03
At3g23940	2.14	3.16
At3g10350	2.20	6.30
At5g44820	1.51	2.77
At3g01170	1.37	2.10
At1g32900	2.04	1.77
At1g66670	1.72	5.55
At4g20090	2.46	3.32
At5g32490	1.73	1.49
At5g65840	1.87	6.74
At4g27580	1.36	4.07
At4g34440	1.34	1.41
At1g23210	1.32	11.41
At4g22320	2.32	4.03
At1g64780	1.47	5.64
At5g07540	2.07	5.59
At1g69370	1.44	1.83
At2g43050	1.29	1.98
At1g13990	1.36	1.35
At4g18370	1.30	1.35
At5g58330	1.33	8.17
At1g12900	2.29	2.43
At2g19940	1.53	1.64
At4g24280	1.36	2.27
At3g15780	1.42	4.01
At1g01730	1.79	1.90
At4g39540	1.66	3.07
At2g19870	1.42	16.07
At4g39980	1.36	5.87
At3g58610	1.54	2.30
At4g39030	1.40	7.29
At4g29540	1.49	4.05
At2g11380	1.55	5.10
At1g34300	1.44	4.44
At4g21210	1.33	1.45
At4g29670	2.83	12.87
At2g31160	1.38	2.01
At4g29750	1.31	2.13
At2g47860	1.37	1.72
At2g47910	1.37	3.02
At1g52220	1.36	2.35
At5g03940	1.56	1.47
At4g34830	1.62	2.75
At4g34200	1.51	2.17
At4g10060	1.47	5.09
At5g10980	1.31	1.43
At5g48990	1.53	2.28
At1g06730	1.34	1.45
At1g18890	1.49	1.95
At4g38970	2.01	2.41
At5g14840	1.86	2.68
At3g42100	1.36	2.08
At4g36190	1.77	1.97
At2g04790	1.67	7.75
At5g38680	1.57	1.80
At5g38190	1.88	5.83
At1g07160	3.62	1.70
At4g18810	1.34	1.89
At2g33230	2.86	1.62
At4g26220	1.36	5.12
At1g62180	1.41	5.71
At2g01150	1.39	1.49
At3g09600	1.55	1.38
At2g33100	2.18	3.75
At4g26310	1.66	2.74
At4g20120	1.34	1.45
At4g01650	2.94	2.33
At3g44670	1.34	2.66
3834303	1.81	1.54
At1g21670	1.35	13.27
At3g44880	1.37	12.79
At2g18900	1.78	1.36
At2g15820	2.21	5.58
At2g18940	1.29	1.53
At2g24820	1.38	2.76
At1g03260	1.70	2.09
At2g22230	1.46	3.13
At2g30570	1.42	2.77
At1g75690	1.39	3.38
At2g27360	1.30	3.93
At2g18980	1.61	1.36
At1g03230	1.41	1.60
At2g30460	2.99	21.31
At2g27290	1.28	4.04
At1g50770	2.38	4.18
At3g59100	1.49	1.85
At3g63130	1.30	2.58
At5g02250	1.76	1.60
At5g13090	1.33	2.02
At1g16880	1.28	1.42
At5g06990	3.72	1.75
At2g04030	1.52	7.87
At2g22210	1.31	2.54
At3g63320	1.66	1.43
At1g01500	2.19	1.51
At1g79460	1.35	1.85
At4g25970	1.38	1.98
At5g26030	2.15	4.15
At2g43100	1.36	2.68
At2g11100	1.29	6.77
At5g51460	1.80	1.67
At1g54710	1.54	2.46
At3g47650	1.45	11.81
At4g31530	2.32	5.66
At5g04140	1.85	4.04
At2g02740	1.55	1.68
At4g30910	1.34	4.11
At4g36150	1.31	3.82
At4g20740	1.33	4.87
At2g01480	1.88	1.69
At4g08280	1.30	2.27
At4g20930	2.61	7.57
At2g16460	3.15	3.06
At4g20690	1.89	1.39
At5g17280	1.35	2.30
At4g29790	1.41	1.96
At1g80480	1.63	1.61
At5g49590	1.40	24.60
At4g09700	1.70	1.65
At4g24930	1.49	2.61
At4g28590	1.66	2.39
At4g31180	1.35	1.45
At4g20230	3.34	2.07
At4g12390	2.30	14.97
At1g21600	1.80	4.02
At1g10960	2.55	1.40
At4g23200	1.29	1.42
At5g35360	1.44	4.82
At1g08770	1.60	2.08
At2g05590	2.49	1.68
At1g62250	1.40	1.46
At5g39210	1.49	3.22
At1g11470	1.47	3.86
At4g22590	1.70	9.76
At1g09780	1.45	1.63
At3g07670	1.68	1.80
At3g56410	1.31	2.68
At3g52190	1.49	2.82
At1g47520	1.52	6.54
At3g26840	1.35	2.27
At3g03580	1.43	3.33
At5g22830	1.35	1.42
At5g04360	1.57	1.37
At3g63340	1.32	1.37
At3g22780	1.62	4.21
At5g46580	1.37	2.80
At5g57930	1.51	3.90
At3g24260	1.51	2.68
At3g22430	1.30	2.96
At2g21230	1.46	1.59
At2g38340	1.35	1.35
At4g36010	1.74	6.20
At2g42310	1.52	1.55
At3g44310	1.44	1.63
At5g28750	1.41	2.41
At1g49970	1.38	6.08

MIPS-code/GI	***petc-2*** **vs. WT**	***atpd-1*** **vs. WT**
up-regulated in both mutants		
At2g28880	1.34	1.82
At3g54870	2.25	1.36
At1g55630	1.31	3.40
At4g01280	2.25	1.89
At4g34730	1.78	2.02
At3g47100	2.41	3.45
At4g21460	1.78	2.01
At1g59940	1.68	6.58
At1g05385	1.32	1.42
At3g56710	1.38	1.54
At3g05710	1.38	5.74
At2g48130	1.38	1.76
At1g15850	1.43	4.23
At4g39690	5.45	1.60
At1g19050	1.59	1.51
At4g31870	1.55	4.27
At5g49450	1.36	2.77
At3g30780	1.52	1.85
At5g61950	4.79	3.09
At4g23450	1.39	2.86
At5g64940	1.54	2.78
At1g27540	1.37	2.44
At1g67810	1.39	4.51
At1g27380	1.28	7.05
At5g52530	2.85	2.29
At1g73650	1.70	1.99
At1g65070	1.30	3.13
At1g06280	2.80	3.49
At5g58560	1.32	2.68
At2g26280	1.48	1.50
At3g56910	1.94	1.59
At5g42070	1.34	6.92
At4g13430	2.04	1.77
At5g17710	1.49	2.04
cob	1.43	3.21
At4g37200	1.41	2.69
At5g24120	1.36	1.60
At1g54120	1.77	2.21
At4g11980	1.49	17.22
At4g14210	2.30	3.54
At1g68690	1.48	2.32
At1g27210	4.79	3.81
At4g12770	1.55	1.67
At3g58010	1.41	2.19
At5g30460	1.31	1.71
At5g54430	1.71	2.01
At3g08720	2.33	7.17
At1g03060	1.69	2.57
At5g49020	2.04	3.16
At3g60000	2.35	1.94
At1g47730	1.51	2.88
At3g23400	1.51	1.86
At5g19220	1.78	3.55

MIPS-code/GI	***petc-2*** **vs. WT**	***atpd-1*** **vs. WT**
up-regulated in both mutants		
At3g14900	1.72	7.63
At1g24130	1.29	3.08
At1g70180	1.55	1.41
At2g34470	1.81	2.61
At4g37270	1.39	3.02
At2g13150	2.48	3.09
At2g34540	1.38	1.37

MIPS-code/GI	***petc-2*** **vs. WT**	***atpd-1*** **vs. WT**
down-regulated in both mutants		
At5g54190	0.67	0.46
At4g23930	0.68	0.69
At3g50820	0.70	0.49
At1g70350	0.74	0.50
At1g12090	0.33	0.39
At3g15360	0.54	0.55
At1g80600	0.72	0.47
At3g22970	0.63	0.65
At2g37220	0.72	0.66
At5g23440	0.49	0.52
At4g17460	0.73	0.63
At2g42540	0.25	0.27
At4g19710	0.75	0.65
At1g74960	0.71	0.54
At5g66570	0.59	0.17
At5g54270	0.65	0.52
At4g03520	0.56	0.60
At2g28900	0.42	0.40
At4g09650	0.54	0.45
At4g12520	0.65	0.72
At3g05880	0.23	0.17
At1g02730	0.15	0.63
At3g43700	0.54	0.56
At1g61520	0.60	0.51
At1g51400	0.53	0.14
At3g12120	0.68	0.40
At2g20020	0.71	0.62
At2g06030	0.14	0.58
At3g62030	0.69	0.59
At3g53460	0.78	0.55
At2g39270	0.57	0.51
At1g02560	0.70	0.39
At2g45180	0.64	0.54
At4g30620	0.75	0.40
At5g05590	0.68	0.38
At1g77490	0.44	0.44
At3g21055	0.72	0.16
At5g44680	0.61	0.53
3695380	0.75	0.74
At3g26740	0.54	0.24
At2g34420	0.77	0.32
At5g62000	0.76	0.49
At5g11480	0.75	0.36
At1g48860	0.59	0.53
At1g75380	0.66	0.61
At1g20340	0.77	0.63
At2g24090	0.58	0.47
At4g16780	0.58	0.45
At1g80130	0.36	0.63
At5g19140	0.38	0.49
At3g47470	0.72	0.40
At1g32060	0.39	0.42
At2g24020	0.70	0.72

MIPS-code/GI	*petc-2* vs. WT	*atpd-1* vs. WT
down-regulated in both mutants		
At2g04700	0.61	0.42
At2g21660	0.34	0.32
At2g25320	0.67	0.63
At2g42530	0.14	0.21
At2g15890	0.25	0.27
At5g43930	0.48	0.55
At3g60490	0.59	0.70
At4g05180	0.55	0.21
At2g36410	0.58	0.30
At5g11550	0.61	0.65
At1g03970	0.78	0.63
At4g21280	0.71	0.36
At4g32340	0.77	0.54
At4g28750	0.59	0.53
At2g20260	0.60	0.68
At3g66654	0.61	0.52
At3g08760	0.59	0.73
At1g79040	0.52	0.42
At1g55670	0.60	0.26

MIPS-code/GI	*petc-2* vs. WT	*atpd-1* vs. WT
up/down		
At5g13630	2.34	0.66
At2g25080	1.46	0.52
At2g34640	2.03	0.52
At4g14690	1.30	0.36
At1g08380	1.51	0.58
At1g25220	1.28	0.56
At1g55490	1.46	0.57
At2g14750	1.35	0.40
At4g02520	1.54	0.71
At2g05100	1.90	0.30
At2g05070	2.21	0.27
At3g27690	1.75	0.68
At4g24770	1.80	0.67
At1g48880	3.06	0.29
rpoC1	1.45	0.50
At4g12500	1.87	0.69
At4g03920	1.44	0.67
At1g58290	1.67	0.59
At4g08870	2.59	0.60
At4g34350	2.95	0.42
At5g52440	1.75	0.47
At3g48850	1.39	0.46
At4g32020	1.43	0.55
At4g33780	1.87	0.71
At2g47730	1.53	0.45
At5g14320	1.34	0.58
3695393	2.41	0.58
At2g35240	1.32	0.58
At1g17420	2.19	0.69
At4g10810	1.85	0.67
At2g43090	1.38	0.46
At2g14890	1.37	0.28
At1g54520	1.35	0.74
At1g06680	1.37	0.56
At4g01800	1.29	0.65
At1g79050	2.84	0.57
At1g54580	1.32	0.68
At1g54630	2.00	0.62
rbcL	1.30	0.27
At2g40000	1.46	0.66
At2g28760	1.96	0.60
At2g44030	2.65	0.62
At5g50280	1.47	0.59
At3g18110	1.55	0.56
At4g01050	2.29	0.71
At2g39000	1.37	0.70
At4g05070	1.70	0.51
At1g05860	1.76	0.38
At5g23010	1.37	0.34

MIPS-code/GI	*petc-2* vs. WT	*atpd-1* vs. WT
down/up		
At4g38460	0.69	1.91
At2g17265	0.75	7.56
At1g77250	0.78	3.26
At1g09420	0.54	8.94
At2g03200	0.73	2.02
At4g37470	0.72	2.00
At5g02850	0.67	2.60
At1g27610	0.78	2.48
At4g16490	0.61	2.66
At1g67440	0.77	1.41
At2g31350	0.47	2.77
At4g14930	0.46	1.77
At4g16590	0.70	2.16
At2g30880	0.62	1.62
At1g12520	0.77	1.50
At3g57950	0.77	1.71
At1g29070	0.67	2.54
At2g24730	0.38	4.88
At4g16820	0.56	3.28
At4g12620	0.65	8.03
At4g15870	0.55	1.67
At5g07760	0.71	2.67
At4g14620	0.72	1.46
At5g51670	0.63	2.12
At3g55070	0.52	1.60
At3g18870	0.75	3.27
At5g14040	0.78	3.58
At5g48370	0.76	6.05
At4g16080	0.55	1.38
At5g11930	0.76	2.48
At5g15530	0.76	2.49
At5g61200	0.75	1.94
At3g56700	0.59	2.00
At1g48620	0.69	3.04
At1g79360	0.64	2.45
At1g80450	0.46	1.80
At2g44040	0.71	2.75
At3g52150	0.68	1.49
At1g74850	0.71	2.35
At2g41950	0.77	4.03
At1g79960	0.77	2.19
At4g34590	0.68	1.58
At4g17740	0.50	1.94
At4g26900	0.57	3.29
At2g17300	0.50	1.69
At1g03810	0.58	3.53
At2g33430	0.69	1.85
At2g17420	0.31	1.46
At5g57990	0.46	1.57
At3g09490	0.56	1.95
At5g19900	0.45	1.41
At2g19240	0.38	5.11
At3g16000	0.65	2.43

MIPS-code/GI	***petc-2*** **vs. WT**	***atpd-1*** **vs. WT**
down/up		
At1g15410	0.53	2.16
At5g02750	0.42	3.78
At5g12150	0.70	2.45
At4g18540	0.75	3.65
At3g56010	0.71	3.58
At5g50640	0.60	1.71
At3g42490	0.34	9.82
At3g24190	0.76	2.13
At4g04730	0.75	1.42
At4g03150	0.32	14.56
At4g27230	0.74	1.61
At3g09050	0.49	1.81
At5g15700	0.36	4.34
At5g55210	0.73	7.17
At3g03710	0.77	3.63
At3g11490	0.58	2.62
At3g05020	0.71	1.40
At3g03630	0.71	2.68
At1g73250	0.74	1.60
At2g01610	0.73	2.19
At3g11150	0.76	2.18
At1g33250	0.42	1.39
At3g57280	0.40	1.37
At1g27660	0.67	2.50
At5g65490	0.74	9.33
At3g17550	0.56	3.88
At1g60000	0.77	1.96
At2g48090	0.74	6.40
At5g26570	0.29	2.18
At3g01550	0.76	3.74
At3g44720	0.73	2.61
At1g79840	0.57	4.37
At2g30320	0.73	1.74
At2g05180	0.73	1.59
At4g08630	0.69	2.21
At1g80670	0.73	1.84
At2g13810	0.67	6.50
At2g07710	0.67	1.52
At1g75390	0.66	2.58
At4g23140	0.65	2.17
At5g18260	0.78	7.72
At5g10910	0.72	5.48
At3g20970	0.58	1.80
At2g34020	0.61	5.70
At1g30700	0.43	4.74
At4g07960	0.46	9.59
At4g22920	0.75	12.33
At2g37090	0.52	2.86
At2g15470	0.57	2.47
At2g37080	0.63	1.47
At2g31720	0.75	3.85
At2g34370	0.71	1.92
At2g44550	0.54	2.09
At2g40980	0.63	1.96
At1g60550	0.78	1.38
At2g44560	0.67	1.39
At2g15740	0.72	2.77
At3g06860	0.70	1.57
At1g01520	0.77	5.57
At1g61980	0.65	3.52
At1g11820	0.65	2.18
At3g22160	0.76	3.25
At1g62010	0.65	1.80
At3g09070	0.70	3.17
At3g06590	0.50	2.53
At4g04770	0.66	1.96
At5g25900	0.72	3.89
At1g01550	0.73	5.29
At1g30100	0.72	1.50
At1g70990	0.74	5.21
At1g30120	0.39	3.25
At4g37000	0.74	7.74
At2g28450	0.71	2.05
At3g52490	0.73	2.85
At2g43430	0.62	3.09
At2g46590	0.70	2.94
At1g18680	0.40	3.11
At3g06850	0.58	5.40
At5g18910	0.64	6.85
At5g59610	0.43	5.52
At3g54320	0.56	1.50
At2g31170	0.70	4.50
At1g32760	0.71	5.23
At1g12980	0.54	3.64
At2g38450	0.69	4.32
At3g52550	0.77	2.37
At2g26840	0.57	2.94
At4g24860	0.66	2.45
At4g24860	0.59	2.45
At2g37880	0.71	4.98
At4g24860	0.66	1.40
At4g24860	0.59	1.40
At1g50960	0.75	14.39
At2g23330	0.75	4.31
At2g30020	0.60	1.82
At2g32840	0.78	2.39
At2g26900	0.69	3.01
At4g24910	0.78	3.67
At5g56760	0.74	2.57
At4g29920	0.66	1.90
At4g34310	0.34	2.66
At5g44750	0.70	2.09
At3g48110	0.37	7.11
At2g44940	0.40	5.12
At2g39710	0.77	6.24
At5g07900	0.58	5.78
At1g19870	0.60	8.62
At1g21060	0.76	1.90
At1g51560	0.42	1.90
At4g19100	0.50	4.02
At4g30210	0.77	2.41
At4g33520	0.31	1.69
At3g25110	0.75	1.84
At1g44350	0.69	2.12
At4g39970	0.73	2.70
At2g29630	0.75	3.52
At2g29670	0.58	1.81
At5g03910	0.47	2.62
At3g18420	0.48	2.93
At2g33720	0.78	2.44
At4g37380	0.28	2.97
At1g08050	0.61	2.99
At1g30320	0.56	2.25
At4g10750	0.62	4.05
At1g52500	0.62	2.02
At4g33030	0.46	1.95
At2g14880	0.68	2.14
At3g22890	0.61	1.62
At1g13970	0.69	2.05
At4g31430	0.54	1.72
At1g64890	0.74	4.70
At2g20600	0.61	3.49
At1g31160	0.75	2.19
At3g08660	0.71	1.51
At5g61470	0.70	3.11
At3g20230	0.71	10.39
At1g33780	0.60	6.60
At1g43840	0.77	4.65
At1g13280	0.51	1.37
At1g80830	0.53	2.48
At3g30190	0.77	3.83
At5g35100	0.74	1.56
At2g36010	0.21	5.61
At4g39550	0.77	7.80
At1g29910	0.75	3.28
At5g25930	0.72	3.68
At2g24070	0.77	1.35
At4g39050	0.68	2.05
At4g21230	0.66	3.78
At1g15070	0.68	11.93
At1g19890	0.61	4.33
At5g41960	0.60	1.65
At4g19490	0.53	3.62
At4g39000	0.36	2.47
At5g23300	0.55	7.20
At4g26010	0.67	9.51
At1g54690	0.74	1.93
At4g23100	0.75	2.33
At4g01770	0.70	3.53
At3g44990	0.67	4.75
At4g25540	0.66	2.09
At1g79760	0.68	3.86

MIPS-code/GI	*petc-2* vs. WT	*atpd-1* vs. WT
down/up		
At4g18760	0.58	2.79
At5g51770	0.33	2.42
At4g29490	0.78	7.27
At1g69240	0.51	1.57
At5g19280	0.49	3.46
At3g17700	0.71	2.78
At5g56660	0.76	1.61
At1g04360	0.17	3.11
At2g27770	0.76	2.23
At1g80560	0.67	3.15
At3g24810	0.28	4.01
At5g27070	0.58	2.29
At3g09850	0.51	4.45
At4g23170	0.62	1.72
At4g07560	0.72	1.81
At3g62520	0.40	6.79
At1g79250	0.77	1.67
At2g21590	0.71	4.36
At2g32400	0.55	4.64
At2g36480	0.26	2.45
At2g20090	0.57	3.00
At5g55570	0.62	1.38
At2g28755	0.75	2.78
At5g64290	0.46	3.72
At2g28790	0.65	2.72
At3g60860	0.58	2.18
At3g50140	0.46	1.54
At3g54610	0.53	5.31
At4g00610	0.77	2.01
At2g36920	0.70	2.03
At5g64580	0.57	1.62
At1g62110	0.75	3.40
At2g38810	0.64	4.59
At1g51780	0.69	2.67
At5g17840	0.78	2.56
At4g39710	0.69	1.63
At2g44500	0.48	7.04
At5g10330	0.71	3.46
At1g67770	0.37	2.04
At3g51820	0.76	3.07
At1g76240	0.64	2.94
At5g07770	0.73	1.82
At3g28460	0.60	1.73
At2g24210	0.74	2.16
At4g35690	0.72	3.48
At2g38070	0.77	4.82
At4g03800	0.67	2.43
At1g72010	0.64	2.37
At4g13270	0.45	1.58
At1g13460	0.68	4.06
At1g56020	0.61	1.41
At1g55440	0.53	4.31
At1g30920	0.65	2.49
At5g60050	0.48	2.14
At4g24090	0.71	1.52
At4g15410	0.74	14.41
At4g19390	0.75	1.42
At1g79110	0.55	1.82
At5g65350	0.71	1.59
At2g34700	0.50	3.52
At4g37130	0.69	3.77
At4g12000	0.38	10.37
At1g68730	0.76	3.56
At4g14380	0.65	1.51
At2g04540	0.66	1.83
At4g36910	0.57	3.26
At4g36580	0.64	2.01
At1g05030	0.64	2.53
At2g14120	0.64	2.64
At5g40470	0.42	6.66
At2g40400	0.40	3.60
At4g32260	0.71	3.46
At1g16160	0.67	3.62
At5g38290	0.59	10.58
At3g47200	0.72	3.98
At1g31790	0.76	2.58
At4g35450	0.54	1.41
At3g04680	0.75	5.27
At3g50190	0.48	1.58
At3g20920	0.67	6.48
At1g73470	0.38	3.59
At1g70170	0.49	1.49

7.3 Complete list of significantly differentially expressed genes

petc-2 and *atpd-1* genes grouped into 7 major functional categories (see also Figure 3.18b).

petc-2

Metabolism

MIPS-code	Description	Control (WT)	D (data=mutant)	D/C
At4g39940	adenosine-5-phosphosulfate-kinase	0.71	3.76	5.30
At3g55120	chalcone isomerase	0.81	2.76	3.41
At4g20230	terpene cyclase like protein	0.47	1.56	3.32
At2g21330	putative fructose bisphosphate aldolase	0.27	0.85	3.15
At2g33230	putative flavin-containing monooxygenase	0.32	0.91	2.84
At4g20930	3-hydroxyisobutyrate dehydrogenase -like protein	1.11	2.88	2.59
At4g08870	putative arginase	0.12	0.31	2.58
At1g62640	3-ketoacyl-acyl carrier protein synthase III (KAS III)	0.24	0.62	2.58
At4g14210	phytoene dehydrogenase precursor (phytoene desaturase)	1.39	3.2	2.30
At4g08900	arginase	0.1	0.22	2.20
At2g33100	putative cellulose synthase	2.21	4.82	2.18
At5g26030	ferrochelatase-I	0.7	1.5	2.14
At1g32900	starch synthase	0.12	0.25	2.08
At4g29890	choline monooxygenase - like protein	2.01	4.17	2.07
At4g38970	putative fructose-bisphosphate aldolase	1.51	3.03	2.01
At5g36790	p-nitrophenylphosphatase-like protein	0.13	0.26	2.00
At3g57050	cysthationine beta-lyase precursor (CBL)	0.08	0.15	1.88
At4g23660	polyprenyltransferase like protein	0.39	0.73	1.87
At1g25410	tRNA isopentenyl transferase	0.23	0.43	1.87
At5g04140	ferredoxin-dependent glutamate synthase	0.94	1.75	1.86
At3g48320	cytochrome P450 - like protein	0.17	0.31	1.82
At2g37690	putative phosphoribosylaminoimidazole carboxylase	0.27	0.49	1.81
At5g51460	trehalose-6-phosphate phosphatase	1.04	1.87	1.80
At5g19220	glucose-1-phosphate adenylyltransferase	0.2	0.35	1.75
At4g00620	putative tetrahydrofolate synthase	0.07	0.12	1.71
At4g22590	trehalose-6-phosphate phosphatase - like protein	3.86	6.54	1.69
At2g36390	starch branching enzyme II	0.39	0.66	1.69
At5g04590	sulphite reductase	0.36	0.6	1.67
At3g07670	putative ribulose-1	0.11	0.18	1.64
At3g60880	dihydrodipicolinate synthase precursor	6.86	10.79	1.57
At1g01290	molybdopterin biosynthesis CNX3 protein	1.4	2.19	1.56
At4g34200	Phosphoglycerate dehydrogenase - like protein	0.26	0.4	1.54
At5g04360	pullulanase-like protein (starch debranching enzyme)	0.15	0.23	1.53
At2g29690	anthranilate synthase	0.17	0.26	1.53
At3g48560	acetolactate synthase	0.36	0.55	1.53
At4g02520	Atpm24.1 glutathione S transferase	0.69	1.05	1.52
At3g58610	ketol-acid reductoisomerase	0.35	0.53	1.51
At2g47730	glutathione S-transferase (GST6)	0.26	0.39	1.50
At4g19010	4-coumarate-CoA ligase - like	0.24	0.36	1.50
At5g13280	aspartate kinase	0.19	0.28	1.47

At4g29540	UDP-N-acetylglucosamine O-acyltransferase - like protein	0.13	0.19	1.46
At2g23800	pregeranylgeranyl pyrophosphate synthase	0.22	0.32	1.45
At5g35360	acetyl-CoA carboxylase	0.38	0.55	1.45
At3g48000	aldehyde dehydrogenase (NAD+)-like protein	0.64	0.92	1.44
At2g27860	putative dTDP-glucose 4-6-dehydratase	0.46	0.66	1.43
At4g26860	putative Proline synthetase associated protein	0.39	0.55	1.41
At5g04710	aspartyl aminopeptidase	0.05	0.07	1.40
At3g54640	tryptophan synthase alpha chain	0.05	0.07	1.40
At2g43090	3-isopropylmalate dehydratase	0.74	1.03	1.39
At4g25970	putative phosphatidylserine decarboxylase	0.95	1.31	1.38
At4g25050	acyl carrier - like protein	1.09	1.5	1.38
At3g16950	dihydrolipoamide dehydrogenase lpd1	0.08	0.11	1.38
At2g28880	putative para-aminobenzoate synthase and glutamine amidotransferase	0.08	0.11	1.38
At1g25220	anthranilate synthase beta subunit	0.11	0.15	1.36
At2g43100	3-isopropylmalate dehydratase	0.8	1.09	1.36
At2g14750	putative adenosine phosphosulfate kinase	0.14	0.19	1.36
At2g20860	lipoic acid synthase (LIP1)	0.29	0.39	1.34
At5g58330	NADP-dependent malate dehydrogenase	1.03	1.38	1.34
At1g05610	putative ADP-glucose pyrophosphorylase	0.06	0.08	1.33
At1g54580	acyl-carrier protein (ACP)	1.43	1.89	1.32
At4g14910	imidazoleglycerol-phosphate dehydratase	0.46	0.6	1.30
At1g06730	sugar kinase	0.2	0.26	1.30
At3g58990	3-isopropylmalate dehydratase-like protein (small subunit)	1.51	1.95	1.29
At1g74040	putative 2-isopropylmalate synthase	0.14	0.11	0.79
At4g38990	putative endo-1	0.76	0.59	0.78
At1g03630	putative protochlorophyllide reductase	0.53	0.41	0.77
At5g38530	tryptophan synthase beta chain	0.43	0.33	0.77
At1g72810	threonine synthase	0.92	0.7	0.76
At5g11930	glutaredoxin - like protein	1	0.76	0.76
At3g51820	chlorophyll synthetase	0.66	0.5	0.76
At4g23100	gamma-glutamylcysteine synthetase	1.51	1.14	0.75
At5g15530	biotin carboxyl carrier protein precursor-like protein	0.65	0.49	0.75
At4g19710	aspartate kinase-homoserine dehydrogenase - like protein	1.4	1.05	0.75
At2g29630	putative thiamin biosynthesis protein	0.48	0.36	0.75
At3g20330	aspartate carbamoyltransferase precursor	0.12	0.09	0.75
At3g53900	uracil phosphoribosyltransferase-like protein	0.11	0.08	0.73
At5g25900	cytochrome P450 GA3	0.44	0.32	0.73
At3g05020	acyl carrier protein 1 precursor (ACP)	0.5	0.36	0.72
At4g16590	cellulose synthase like protein	0.21	0.15	0.71
At5g10330	histidinol-phosphate aminotransferase-like protein	0.24	0.17	0.71
At3g03630	O-acetylserine (thiol) lyase	0.48	0.34	0.71
At4g29840	threonine synthase	0.77	0.54	0.70
At3g06860	fatty acid multifunctional protein (AtMFP2)	0.53	0.37	0.70
At4g12740	adenine DNA glycosylase like protein	0.49	0.34	0.69
At5g20830	sucrose-UDP glucosyltransferase	0.19	0.13	0.68
At3g44990	xyloglucan endo-transglycosylase	0.68	0.46	0.68
At4g38460	geranylgeranyl pyrophosphate synthase-related protein	0.15	0.1	0.67
At5g20990	molybdopterin biosynthesis CNX1 protein	0.3	0.2	0.67
At1g80600	putative acetylornithine transaminase	0.09	0.06	0.67
At4g36810	geranylgeranyl pyrophosphate synthase	0.72	0.47	0.65
At2g29990	putative NADH dehydrogenase (ubiquinone oxidoreductase)	0.63	0.39	0.62

At3g22890	ATP sulfurylase	0.41	0.25	0.61
At2g43430	putative glyoxalase II	0.32	0.19	0.59
At1g42970	glyceraldehyde-3-phosphate dehydrogenase	1.94	1.14	0.59
At1g11870	putative seryl-tRNA synthetase	0.45	0.26	0.58
At2g15470	putative polygalacturonase	0.4	0.23	0.58
At3g06850	branched chain alpha-keto acid dehydrogenase E2 subunit	0.77	0.44	0.57
At4g26900	glutamine amidotransferase/cyclase	1.77	1.01	0.57
At4g16820	triacylglycerol lipase like protein	0.58	0.32	0.55
At4g15870	delta-cadinene synthase like protein	1.97	1.08	0.55
At1g08510	acyl-(acyl carrier protein) thioesterase	0.19	0.1	0.53
At1g04610	putative dimethylaniline monooxygenase	0.16	0.08	0.50
At4g33030	sulfolipid biosynthesis protein SQD1	0.19	0.09	0.47
At4g07960	putative glucosyltransferase	251.97	114.84	0.46
At5g10100	trehalose-6-phosphate phosphatase -like protein	0.59	0.26	0.44
At2g02970	putative nucleoside triphosphatase	1.15	0.47	0.41
At1g30120	pyruvate dehydrogenase E1 beta subunit	1.42	0.55	0.39
At2g31950	molybdopterin synthase (CNX2)	0.57	0.22	0.39
At5g19140	aluminium-induced protein - like	0.37	0.14	0.38
At4g39000	putative endo-1	0.86	0.31	0.36
At2g17420	thioredoxin reductase	2.05	0.65	0.32
At1g14230	putative nucleoside triphosphatase	1.66	0.5	0.30
At1g08490	nitrogen fixation protein (nifS)	1.31	0.38	0.29
At2g43750	cysteine synthase (cpACS1)	0.4	0.06	0.15

Photosynthesis

At2g39730	Rubisco activase	0.16	0.49	3.06
At1g10960	PetF2; ferredoxin precusor isolog (1 mRNA)	1.8	4.59	2.55
At2g05070	Lhcb2.2	2.61	5.75	2.20
At2g05100	Lhcb2.1 (oder Lhcb2.3)	5.09	9.66	1.90
At3g27690	Lhcb2.4	16.31	28.47	1.75
At1g30380	PsaK	1.21	2.1	1.74
At1g19150	Lhca6	0.2	0.33	1.65
At1g08380	PsaO	6.7	10.09	1.51
At1g73110	rubisco activase	0.92	1.38	1.50
At2g30570	PsbW	18.52	26.24	1.42
At1g55490	Rubisco subunit binding-protein beta subunit	0.13	0.18	1.38
At1g06680	PsbP1 (3 mRNAs)	2.29	3.13	1.37
At1g44575	PsbS protein	0.47	0.63	1.34
At2g34420	Lhcb1.5	30.37	23.35	0.77
At1g20340	PetE2 (plastocyanin) (5 mRNAs)	0.81	0.62	0.77
At1g29910	Lhcb1.2 (LHCP AB 180)	48.54	36.4	0.75
At3g21055	PsbT1	2.33	1.68	0.72
At3g47470	Lhca4	13.83	9.95	0.72
At4g32260	AtpG; ATP synthase beta\\\' chain (old nomenclature: subunit II)	3.06	2.18	0.71
At4g21280	PsbQ1 (1 mRNA)	6.03	4.28	0.71
At3g50820	PsbO2	2.85	2	0.70
At3g61470	Lhca2	2.31	1.55	0.67
At5g54270	Lhcb3 chlorophyll a/b binding protein	6.19	4.04	0.65
At2g20260	PsaE2 (2 mRNAs)	3.41	2.06	0.60
At1g55670	PsaG	6.29	3.78	0.60
At1g61520	Lhca3	4.98	2.99	0.60

At5g66570	PsbO1	5.71	3.39	0.59
At4g28750	PsaE1 (2 mRNAs)	3.33	1.95	0.59
At4g05180	PsbQ2 (1 mRNA)	6.93	3.8	0.55
At4g09650	AtpD; ATP synthase delta subunit	0.74	0.4	0.54
At1g51400	PsbT2 (2 mRNAs)	2.7	1.44	0.53
At1g79040	PsbR	9.45	4.93	0.52
At4g17740	PSII D1 protein processing enzyme	0.33	0.17	0.52

Transport

At5g09930	ABC transporter	0.12	0.45	3.75
At5g64840	ABC transporter protein 1-like	0.22	0.74	3.36
At5g52250	putative protein	3.55	9.75	2.75
At2g44030	hypothetical protein	0.81	2.14	2.64
At4g25290	hypothetical protein	0.27	0.68	2.52
At3g10350	putative ATPase	1.41	3.11	2.21
At5g55630	outward rectifying potassium channel KCO	0.26	0.57	2.19
At5g59250	D-xylose-H+ symporter - like protein	0.16	0.33	2.06
At3g10670	putative ABC transporter ATPase	0.03	0.06	2.00
At4g33350	Tic110	13	25.94	2.00
At4g32650	potassium channel protein AtKC	0.18	0.32	1.78
At2g38170	high affinity Ca2+ antiporter	0.16	0.27	1.69
At1g03060	putataive transport protein	0.21	0.35	1.67
At4g12030	putative transport protein	0.1	0.16	1.60
At5g64940	ABC transporter-like	1.93	2.96	1.53
At4g24390	transport inhibitor response-like protein	4.6	6.73	1.46
At1g64780	ammonium transporter	0.39	0.57	1.46
At2g18710	putative preprotein translocase SECY protein	0.07	0.1	1.43
At4g00630	putative potassium/H+ antiporter	0.12	0.17	1.42
At3g48850	mitochondrial phosphate transporter	0.43	0.6	1.40
At2g28070	putative ABC transporter	0.18	0.25	1.39
At2g24820	Toc75	0.6	0.82	1.37
At4g37270	Cu2+-transporting ATPase-like protein	0.25	0.34	1.36
At4g01800	putative SecA-type chloroplast protein transport factor	0.28	0.37	1.32
At5g04770	amino acid transporter-like protein	0.43	0.56	1.30
At5g59030	copper transport protein	0.14	0.18	1.29
At5g14040	mitochondrial phosphate translocator	0.88	0.69	0.78
At4g01810	putative protein transport factor	0.12	0.09	0.75
At3g08580	adenylate translocator	2.3	1.71	0.74
At3g01550	putative phosphate/phosphoenolpyruvate (PPT) translocator	0.3	0.22	0.73
At4g37130	nucleoporin-like protein	0.49	0.34	0.69
At2g26900	putative Na+ dependent ileal bile acid transporter	0.32	0.22	0.69
At4g32500	potassium channel - protein	1.03	0.69	0.67
At4g04770	putative ABC transporter	0.83	0.54	0.65
At1g05030	putative sugar transporter protein	0.4	0.26	0.65
At2g32400	putative ligand-gated ion channel subunit	0.89	0.49	0.55
At1g80830	metal ion transporter	0.58	0.31	0.53
At5g03910	ABC transporter -like protein	1.62	0.76	0.47
At5g64290	2-oxoglutarate/malate translocator; corrected anotation: glutamate/malate translocator (Di	0.78	0.36	0.46
At2g31530	putative preprotein translocase SECY protein	0.39	0.17	0.44
At5g54800	glucose-6-phosphate/phosphate translocator (GPT)	0.53	0.2	0.38

At1g67770	putative ABC transporter	1.39	0.52	0.37
At4g03320	Tic20.1	0.61	0.22	0.36
At4g33520	metal-transporting P-type ATPase	3.9	1.22	0.31

Protein phosphorylation

At1g07160	protein phosphatase 2C	0.04	0.15	3.75
At3g25840	protein kinase	0.17	0.5	2.94
At2g39360	putative protein kinase	0.8	1.37	1.71
At1g72540	putative protein kinase	0.06	0.1	1.67
At4g39540	shikimate kinase - like protein	0.11	0.18	1.64
At1g18890	calcium-dependent protein kinase	0.33	0.49	1.48
At1g68690	protein kinase	0.23	0.34	1.48
At3g26940	protein kinase	0.18	0.26	1.44
At4g23190	serine/threonine kinase - like protein	0.17	0.24	1.41
At5g66210	calcium-dependent protein kinase	0.15	0.21	1.40
At4g34440	putative serine/threonine protein kinase	0.22	0.3	1.36
At2g45910	putative protein kinase	0.8	1.09	1.36
At2g31800	putative protein kinase	0.37	0.49	1.32
At4g23200	serine /threonine kinase - like protein	0.29	0.38	1.31
At1g31160	putative protein kinase C inhibitor (Zinc-binding protein)	0.35	0.27	0.77
At5g02290	serine/threonine-specific protein kinase NAK	0.17	0.13	0.76
At1g79250	serine/threonine protein kinase	0.72	0.55	0.76
At2g17265	homoserine kinase; 3-hydroxy-3-methylglutaryl-coenzyme A reductase 2	1.1	0.82	0.75
At4g15410	phosphatase like protein	8.47	6.25	0.74
At5g25930	receptor-like protein kinase - like	15.73	11.28	0.72
At4g21230	receptor kinase - like protein	0.52	0.34	0.65
At4g23140	serine/threonine kinase - like protein	1.04	0.68	0.65
At5g18910	protein kinase - like protein	1	0.64	0.64
At2g30020	putative protein phosphatase 2C	0.51	0.3	0.59
At3g08760	putative protein kinase	0.68	0.4	0.59
At4g25160	putative Ser/Thr protein kinase	1.55	0.77	0.50
At4g36950	MAP3K-like protein kinase	1.2	0.59	0.49

Stress response

At4g29670	thioredoxin-like protein	0.97	2.75	2.84
At4g20090	membrane-associated salt-inducible-like protein	2.35	5.77	2.46
At1g05480	hypothetical protein	0.44	1.08	2.45
At4g36430	peroxidase like protein	0.24	0.52	2.17
At4g37910	heat shock protein 70 like protein	0.88	1.89	2.15
At5g18360	disease resistance protein -like	0.43	0.74	1.72
At4g15910	drought-induced protein like	0.12	0.2	1.67
At4g11170	RPP1-WsA-like disease resistance protein	0.92	1.49	1.62
At4g25130	protein-methionine-S-oxide reductase	0.21	0.34	1.62
At2g18980	peroxidase (ATP22a)	1.04	1.67	1.61
At4g31870	glutathione peroxidase - like protein	0.19	0.29	1.53
At2g04030	putative heat shock protein	0.56	0.84	1.50
At3g18190	chaperonin subunit	0.37	0.55	1.49
At5g15450	ClpB heat shock protein-like	0.15	0.22	1.47
At2g40000	putative nematode-resistance protein	1.27	1.85	1.46
At5g49910	heat shock protein 70	1.62	2.31	1.43

At2g25080	putative glutathione peroxidase	0.26	0.37	1.42
At4g24280	Hsp70-like protein	1	1.36	1.36
At3g13470	chaperonin 60 beta	0.31	0.42	1.35
At3g44670	disease resistance protein homlog	0.74	0.99	1.34
At2g26790	putative salt-inducible protein	0.56	0.74	1.32
At4g36150	putative disease resistance protein	1.01	1.33	1.32
At2g18940	putative salt-inducible protein	0.23	0.3	1.30
At4g27670	heat shock protein 21	0.33	0.43	1.30
At5g61440	thioredoxin-like 3	0.34	0.44	1.29
At1g10910	membrane-associated salt-inducible protein isolog	0.19	0.14	0.74
At1g75380	wound-responsive protein	1.38	0.9	0.65
At1g09420	putative glucose-6-phosphate dehydrogenase	1.21	0.66	0.55
At2g19280	putative salt-inducible protein	3.2	1.56	0.49
At1g77490	thylakoid-bound ascorbate peroxidase	0.27	0.12	0.44
At2g42540	cold-regulated protein cor15a precursor	1.22	0.3	0.25
At3g05880	low temperature and salt responsive protein LTI6A	2.96	0.69	0.23
At2g42530	cold-regulated protein cor15b precursor	0.8	0.11	0.14

Transcription/Translation

At5g03415	transcription factor - like protein	0.09	0.47	5.22
At1g48880	hypothetical protein	0.46	1.41	3.07
At2g37510	putative RNA-binding protein	0.28	0.75	2.68
At5g04600	RNA binding protein - like	0.06	0.16	2.67
At2g13150	putative bZIP transcription factor	0.43	1.06	2.47
At3g04450	transfactor	0.08	0.19	2.38
At3g08720	putative ribosomal-protein S6 kinase (ATPK19)	1.04	2.43	2.34
At4g01280	putative myb-related DNA-binding protein	0.09	0.21	2.33
At2g04240	putative RING zinc finger protein	1.98	4.59	2.32
At1g14410	DNA-binding protein p24	0.05	0.1	2.00
At3g56910	ribosomal protein PSRP5	2.76	5.34	1.93
At4g21660	spliceosome associated protein - like	0.5	0.92	1.84
At4g24770	RNA-binding protein RNP-T precursor	1.88	3.39	1.80
At3g18290	zinc finger protein	0.08	0.14	1.75
At5g54600	chloroplast ribosomal protein L24	0.9	1.55	1.72
At1g48490	transcription factor IRE	0.36	0.6	1.67
At3g58570	ATP-dependent RNA helicase-like protein	0.08	0.13	1.63
At3g22780	putative DNA binding protein	0.55	0.88	1.60
At2g39100	putative C3HC4-type RING zinc finger protein	0.42	0.66	1.57
At1g78630	putative chloroplast ribosomal protein L13	0.65	1.01	1.55
At3g09600	putative MYB-related protein	0.15	0.23	1.53
At5g53920	ribosomal protein L11 methyltransferase-like protein	0.38	0.57	1.50
At2g21230	putative bZIP transcription factor	0.45	0.66	1.47
At2g38470	putative WRKY-type DNA-binding protein	0.39	0.57	1.46
rpoC1	plastid gene product; RNA polymerase	1.92	2.78	1.45
At2g22360	putative DnaJ protein	0.25	0.36	1.44
At4g30680	translation initiation factor-like protein	0.16	0.23	1.44
At1g05190	putative chloroplast ribosomal protein L6	1.05	1.5	1.43
At2g37600	60S ribosomal protein L36	0.29	0.41	1.41
At1g78160	putative RNA-binding protein	0.17	0.24	1.41
At4g20360	translation elongation factor EF-Tu precursor	0.34	0.48	1.41
At2g01150	RING-H2 zinc finger protein (RHA2b)	0.79	1.1	1.39

At1g80420	putative DNA repair protein	0.18	0.25	1.39
At2g47520	putative AP2 domain transcription factor	0.26	0.36	1.38
At1g64510	putative chloroplast plastid ribosomal protein S6	0.56	0.77	1.38
At2g38340	DREB-like AP2 domain transcription factor	0.11	0.15	1.36
At5g14320	very similar to chloroplast ribosomal protein S13	1.64	2.2	1.34
At5g45110	regulatory protein NPR1-like; transcription factor inhibitor I kappa B-like protein	0.18	0.24	1.33
At4g32040	homeodomain containing protein 1	0.37	0.49	1.32
At4g04350	putative leucyl tRNA synthetase	0.28	0.37	1.32
At5g10980	histon H3 protein	0.69	0.91	1.32
At2g41460	DNA-(apurinic or apyrimidinic site) lyase (ARP)	0.22	0.29	1.32
At5g14460	tRNA synthase - like protein	0.13	0.17	1.31
At5g26710	glutamyl-tRNA synthetase	1.66	2.15	1.30
At1g49400	40S ribosomal protein S17	0.14	0.18	1.29
At5g02320	myb-like protein	1.01	1.29	1.28
At3g58140	phenylalanine-tRNA synthetase-like protein	0.26	0.33	1.27
At1g13960	putative DNA-binding protein	0.04	0.05	1.25
At3g53460	RNA-binding protein cp29 protein	1.16	0.9	0.78
At4g26770	putative CDP-diacylglycerol synthetase	0.26	0.2	0.77
At1g60000	nucleic acid-binding protein	0.91	0.7	0.77
At3g03710	putative polynucleotide phosphorylase	0.56	0.43	0.77
At1g68730	putative transcription factor	1.11	0.85	0.77
At3g08000	putative RNA-binding protein	0.17	0.13	0.76
At1g01520	myb-related protein	0.25	0.19	0.76
At4g04730	putative zinc finger protein	0.53	0.4	0.75
At1g73250	GDP-4-keto-6-deoxy-D-mannose-3	0.44	0.33	0.75
At1g54690	histone H2A	0.64	0.48	0.75
At4g34590	bZIP transcription factor ATB2	0.08	0.06	0.75
At1g03970	G-box binding factor	0.19	0.14	0.74
At4g27230	histone H2A- like protein	0.45	0.33	0.73
At2g30320	putative pseudouridine synthase	0.86	0.63	0.73
At2g15740	putative C2H2-type zinc finger protein	0.66	0.48	0.73
At2g28450	putative RNA methyltransferase	0.33	0.24	0.73
At4g17460	homeobox-leucine zipper protein HAT1	0.98	0.71	0.72
At2g03200	putative chloroplast nucleoid DNA-binding protein	0.9	0.65	0.72
At2g37220	putative RNA-binding protein	2.05	1.48	0.72
At5g65350	histone H3	2.59	1.85	0.71
At1g80670	mRNA export protein	0.28	0.2	0.71
At5g15760	ribosomal protein PSRP3	0.73	0.52	0.71
At2g31170	putative cysteinyl-tRNA synthetase	0.17	0.12	0.71
At2g46590	putative DOF zinc finger protein	0.71	0.5	0.70
At4g39410	putative WRKY DNA-binding protein	0.26	0.18	0.69
At1g29070	putative plastid ribosomal protein L34	0.41	0.28	0.68
At3g52150	chloroplast ribosomal protein PSRP2	1.09	0.74	0.68
At1g13460	B\\\' regulatory subunit of protein phosphatase 2A	0.52	0.35	0.67
At1g80560	putative 3-isopropylmalate dehydrogenase	0.47	0.31	0.66
At1g75390	bZIP transcription factor ATB2	0.94	0.62	0.66
At4g25540	putative DNA mismatch repair protein	1.35	0.89	0.66
At1g48350	putative chloroplast ribosomal protein L18	0.7	0.46	0.66
At2g38810	histone H2A	0.56	0.36	0.64
At4g12620	origin recognition complex subunit 1 -like protein	0.36	0.23	0.64
At4g20980	translation initiation factor eIF3 - like protein	0.11	0.07	0.64

At1g35560	DNA binding protein	0.33	0.21	0.64
At1g13270	methionine aminopeptidase I (MAP1)	0.55	0.34	0.62
At2g39990	26S proteasome regulatory subunit	0.18	0.11	0.61
At1g19890	histone H3	1.21	0.73	0.60
At2g24090	putative chloroplast ribosomal protein L35	0.34	0.2	0.59
At4g03090	NDX1 homeobox protein homolog	0.17	0.1	0.59
At4g16780	DNA-binding homeotic protein Athb-2	0.9	0.52	0.58
At3g60490	transcription factor - like protein	0.07	0.04	0.57
At3g54210	putative chloroplast ribosomal protein L17	1.13	0.64	0.57
At1g79840	homeobox protein (GLABRA2)	0.25	0.14	0.56
At1g34380	DNA polymerase type I	0.87	0.47	0.54
At3g54610	histon acetyltransferase HAT1	1.82	0.97	0.53
At1g14580	zinc finger protein	40.69	18.15	0.45
At2g44940	putative AP2 domain transcription factor	1.61	0.65	0.40
At5g15700	DNA-directed RNA polymerase (mitochondrial)	0.39	0.14	0.36
At2g21660	glycine-rich RNA binding protein 7	13.75	4.69	0.34
At2g36010	putative E2F5 family transcription factor	4.09	0.84	0.21

Unclassified

At4g11230	respiratory burst oxidase homolog F - like protein	0.3	2.94	9.80
At4g39690	putative protein	0.86	4.68	5.44
At5g61950	putative protein	0.08	0.4	5.00
At1g27210	unknown protein	3.33	15.95	4.79
At3g63410	putative chloroplast inner envelope protein	0.56	2.49	4.45
At2g17540	unknown protein	1.1	4.53	4.12
At4g12470	pEARLI 1-like protein	0.39	1.57	4.03
At3g56290	putative protein	0.05	0.2	4.00
At4g11090	putative protein	0.53	2.11	3.98
At4g27020	putative protein	3.98	15.14	3.80
At1g05140	unknown protein	0.94	3.5	3.72
At5g06990	putative protein	0.18	0.67	3.72
At4g27990	putative protein	0.42	1.51	3.60
At2g38310	unknown protein	0.63	2.23	3.54
At3g26630	unknown protein	1.1	3.72	3.38
At1g09940	putative glutamyl-tRNA reductase 2 precursor	0.14	0.47	3.36
At1g22680	hypothetical protein	0.98	3.21	3.28
At4g12490	pEARLI 1-like protein	0.51	1.67	3.27
At2g16460	unknown protein	2.06	6.48	3.15
At3g57440	hypothetical protein	0.47	1.43	3.04
At3g52760	putative protein	1.42	4.27	3.01
At3g56040	putative protein	0.02	0.06	3.00
At2g30460	putative integral membrane protein	2.35	7.05	3.00
At4g34350	putative protein	0.79	2.35	2.97
At4g01650	hypothetical protein	2.64	7.76	2.94
At5g52530	putative protein	0.69	1.97	2.86
At1g06280	hypothetical protein	0.23	0.65	2.83
At4g09620	putative protein	0.56	1.58	2.82
At1g79050	replicase	0.3	0.84	2.80
At4g07990	hypothetical protein	0.1	0.27	2.70
At1g23730	putative carbonic anhydrase	0.03	0.08	2.67
At3g07100	putative Sec24-like COPII protein	0.06	0.16	2.67

At4g32130	hypothetical protein	0.18	0.47	2.61
At2g22890	unknown protein	0.58	1.5	2.59
At2g43870	putative polygalacturonase	0.36	0.93	2.58
At4g21990	PRH26 protein	0.57	1.46	2.56
At1g76620	unknown protein	0.74	1.88	2.54
At1g31410	hypothetical protein	0.2	0.5	2.50
At3g08010	unknown protein	0.02	0.05	2.50
At1g35510	growth regulator	0.74	1.84	2.49
At2g41040	hypothetical protein	0.75	1.86	2.48
At3g47100	hypothetical protein	0.19	0.47	2.47
At2g26110	unknown protein	0.64	1.55	2.42
3695393	contains similarity to retroviral aspartyl proteases	1.44	3.48	2.42
rpoB	plastid gene product; RNA polymerase	4.4	10.51	2.39
At1g72430	hypothetical protein	1.01	2.4	2.38
At1g50490	cyclin-specific ubiquitin carrier protein	2.48	5.88	2.37
At3g60000	putative protein	0.25	0.59	2.36
At5g55580	putative protein	0.67	1.58	2.36
At1g50770	hypothetical protein	0.38	0.89	2.34
At5g13630	cobalamin biosynthesis protein	1.04	2.42	2.33
At5g26110	endopeptidase - like protein	0.95	2.21	2.33
At4g31530	putative protein	32.42	75.31	2.32
At1g12900	putative calcium-binding protein	0.84	1.94	2.31
At3g03760	unknown protein	0.91	2.1	2.31
At1g20070	hypothetical protein	1.69	3.9	2.31
At4g12390	putative protein	1.89	4.35	2.30
At4g01050	hypothetical protein	0.37	0.85	2.30
At4g22320	hypothetical protein	0.27	0.62	2.30
At1g03160	fructokinase	0.69	1.58	2.29
At1g17420	lipoxygenase	0.07	0.16	2.29
At1g01500	hypothetical protein	0.15	0.34	2.27
At3g44570	putative protein	0.34	0.77	2.26
At3g54870	kinesin-like protein	0.31	0.7	2.26
At2g34330	unknown protein	0.08	0.18	2.25
At4g17070	hypothetical protein	3.67	8.25	2.25
At2g26190	unknown protein	0.13	0.29	2.23
At2g15820	unknown protein	5.45	12.04	2.21
At1g27560	unknown protein	2.9	6.39	2.20
At2g05590	hypothetical protein	0.05	0.11	2.20
At4g35170	putative protein	0.05	0.11	2.20
At1g23500	hypothetical protein	0.2	0.43	2.15
At4g26780	grpE like protein	7.86	16.87	2.15
At3g04650	unknown protein	0.84	1.79	2.13
At1g34270	unknown protein	0.09	0.19	2.11
At4g13550	putative protein	0.42	0.88	2.10
At4g29060	putative protein	2.13	4.46	2.09
At4g32060	putative protein	3.37	7.01	2.08
At4g00170	putative proline-rich protein	0.14	0.29	2.07
At2g13590	pseudogene; similar to GB:AAA75253	0.15	0.31	2.07
At5g66530	apospory-associated protein C-like	0.18	0.37	2.06
At4g11960	putative protein	2.01	4.11	2.04
At5g07540	glycine-rich protein atGRP-6	0.46	0.94	2.04

At4g13430	putative protein	0.46	0.94	2.04
At5g49020	arginine methyltransferase-like protein	0.47	0.96	2.04
At5g52810	putative protein	0.58	1.18	2.03
At1g74220	hypothetical protein	0.34	0.69	2.03
At1g54630	hypothetical protein	0.94	1.89	2.01
At2g34640	unknown protein	0.14	0.28	2.00
At2g28760	putative nucleotide-sugar dehydratase	0.23	0.46	2.00
3834303	hypothetical protein	0.02	0.04	2.00
At1g30950	putative unusual floral organ (UFO)	1.44	2.87	1.99
At5g36860	putative protein	1.38	2.7	1.96
At4g20690	putative protein	0.18	0.35	1.94
At2g35600	hypothetical protein	0.15	0.29	1.93
At3g63300	putative protein	0.14	0.27	1.93
At2g33250	unknown protein	0.21	0.4	1.90
At2g43970	unknown protein	0.97	1.84	1.90
At5g38190	putative protein	0.48	0.91	1.90
At2g42870	unknown protein	0.19	0.36	1.89
At2g37040	phenylalanine ammonia lyase (PAL1)	0.19	0.36	1.89
At1g47230	cyclin	0.44	0.83	1.89
At4g12500	pEARLI 1-like protein	0.68	1.28	1.88
At2g01480	axi 1-like protein	0.25	0.47	1.88
At2g31040	hypothetical protein	0.08	0.15	1.88
At1g21600	unknown protein	0.16	0.3	1.88
At4g33780	putative protein	2.53	4.73	1.87
At5g14840	putative protein	0.38	0.71	1.87
At5g65840	unknown protein	0.53	0.99	1.87
At2g15680	putative calmodulin-like protein	0.79	1.47	1.86
At3g02040	hypothetical protein	2.64	4.91	1.86
At4g10810	putative protein	13.67	25.36	1.86
At1g72520	putative lipoxygenase	0.2	0.37	1.85
At5g58870	cell division protein - like	0.26	0.48	1.85
At5g03110	putative protein	0.06	0.11	1.83
At2g26220	pseudogene; similar to AraPPT	14.63	26.74	1.83
At2g04530	hypothetical protein	0.43	0.78	1.81
At1g23360	spore germination protein c2	0.63	1.14	1.81
At2g33980	hypothetical protein	0.68	1.23	1.81
At4g25190	putative protein	0.31	0.56	1.81
At2g18900	unknown protein	0.56	1.01	1.80
At4g28430	hypothetical protein	0.15	0.27	1.80
At2g34470	putative urease accessory protein	0.25	0.45	1.80
At5g65480	putative protein	0.25	0.45	1.80
At2g17120	unknown protein	3.08	5.53	1.80
At1g01730	unknown protein	0.72	1.29	1.79
At1g54120	hypothetical protein	0.23	0.41	1.78
At4g21460	putative protein	0.64	1.14	1.78
At5g25380	cyclin 3a	0.45	0.8	1.78
At4g34730	putative protein	0.48	0.85	1.77
At4g36190	putative protein	1.59	2.81	1.77
At5g56050	unknown protein	0.55	0.97	1.76
At2g17070	hypothetical protein	2.02	3.56	1.76
At4g20850	putative protein	0.25	0.44	1.76

At4g36010	thaumatin-like protein	0.64	1.12	1.75
At1g66670	ATP-dependent Clp protease (nClpP3)	0.12	0.21	1.75
At5g32490	putative protein	0.35	0.61	1.74
At3g53350	putative protein	0.92	1.6	1.74
At3g47380	putative protein	0.83	1.44	1.73
At5g52440	HCF106	0.49	0.85	1.73
At2g37660	unknown protein	0.94	1.63	1.73
At3g42060	putative protein	0.11	0.19	1.73
At5g02250	ribonuclease II-like protein	0.11	0.19	1.73
At4g19900	putative protein	8.6	14.85	1.73
At3g01370	unknown protein	0.32	0.55	1.72
At1g24040	unknown protein	0.39	0.67	1.72
At5g45290	unknown protein	0.14	0.24	1.71
At3g04890	hypothetical protein	0.07	0.12	1.71
At5g54430	putative protein	1.39	2.38	1.71
At3g14900	hypothetical protein	0.71	1.21	1.70
At3g63320	putative protein	0.27	0.46	1.70
At1g73650	unknown protein	0.47	0.8	1.70
At2g27440	putative rac GTPase activating protein	0.1	0.17	1.70
At4g05070	expressed protein	0.42	0.71	1.69
At1g59940	response regulator 3	1.15	1.94	1.69
At5g11270	putative protein	0.19	0.32	1.68
At4g02480	unknown protein	0.19	0.32	1.68
At3g11170	omega-3 fatty acid desaturase	0.47	0.79	1.68
At1g68725	hypothetical protein	1.22	2.05	1.68
At2g04790	hypothetical protein	0.84	1.41	1.68
At1g58290	glutamyl-tRNA reductase	0.4	0.67	1.68
At1g05860	hypothetical protein	0.03	0.05	1.67
At5g06670	kinesin heavy chain-like protein	0.18	0.3	1.67
At1g03260	hypothetical protein	0.06	0.1	1.67
At3g21810	unknown protein	0.12	0.2	1.67
At4g26310	putative protein	0.79	1.31	1.66
At4g37890	putative protein	0.7	1.16	1.66
At2g18820	putative non-LTR retroelement reverse transcriptase	0.29	0.48	1.66
At5g12040	putative protein	0.26	0.43	1.65
At2g37750	unknown protein	0.28	0.46	1.64
At5g63290	oxygen-independent coproporphyrinogen-like protein	0.47	0.77	1.64
At3g58190	putative protein	0.11	0.18	1.64
At4g09700	putative protein	0.11	0.18	1.64
At4g14070	AMP-binding protein	0.22	0.36	1.64
At5g03940	signal recognition particle 54CP (SRP54) protein precursor	0.11	0.18	1.64
At4g28590	hypothetical protein	0.19	0.31	1.63
At1g50880	hypothetical protein	0.46	0.75	1.63
At5g41380	putative protein	0.81	1.32	1.63
At4g00300	contains weak similarity to S. cerevisiae BOB1 protein	1.72	2.78	1.62
At1g80480	hypothetical protein	0.26	0.42	1.62
At2g02740	hypothetical protein	0.13	0.21	1.62
At4g17650	putative protein	0.13	0.21	1.62
At4g23890	putative protein	3.45	5.56	1.61
At2g45990	unknown protein	0.18	0.29	1.61
At5g38680	putative protein	0.18	0.29	1.61
At4g34830	putative protein	0.23	0.37	1.61

At4g27510	hypothetical protein	0.4	0.64	1.60
At1g08770	unknown protein	0.4	0.64	1.60
At1g61820	beta-glucosidase	0.05	0.08	1.60
At2g15870	putative retroelement pol polyprotein	3.56	5.64	1.58
At2g37230	unknown protein	0.55	0.87	1.58
At1g02060	unknown protein	1.41	2.23	1.58
At4g25120	putative protein	0.64	1.01	1.58
At3g27740	carbamoyl phosphate synthetase small subunit	0.21	0.33	1.57
At2g37330	unknown protein	0.42	0.66	1.57
At1g19050	response regulator 5	0.14	0.22	1.57
At2g42310	unknown protein	0.07	0.11	1.57
At3g59100	putative protein	0.07	0.11	1.57
At2g23670	hypothetical protein	0.55	0.86	1.56
At4g12770	auxilin-like protein	0.41	0.64	1.56
At5g23240	putative protein	1.11	1.73	1.56
At3g22690	hypothetical protein	0.18	0.28	1.56
At5g05580	temperature-sensitive omega-3 fatty acid desaturase	0.36	0.56	1.56
At4g03410	hypothetical protein	0.65	1.01	1.55
At3g18110	hypothetical protein	0.29	0.45	1.55
At2g35260	unknown protein	0.4	0.62	1.55
At5g48990	putative protein	0.2	0.31	1.55
At1g70180	hypothetical protein	0.11	0.17	1.55
At2g25040	hypothetical protein	0.33	0.51	1.55
At2g19940	putative N-acetyl-gamma-glutamyl-phosphate reductase	0.83	1.28	1.54
At1g65080	hypothetical protein	0.26	0.4	1.54
At4g38660	putative thaumatin-like protein	0.15	0.23	1.53
At2g39670	unknown protein	0.15	0.23	1.53
At2g11380	pseudogene	0.66	1.01	1.53
At4g04480	hypothetical protein	3.96	6.06	1.53
At5g66780	putative protein	0.17	0.26	1.53
At1g47520	polyprotein	0.76	1.16	1.53
At5g23060	putative protein	0.19	0.29	1.53
At3g22700	hypothetical protein	0.21	0.32	1.52
At1g51350	hypothetical protein	1.07	1.63	1.52
At2g26280	unknown protein	0.23	0.35	1.52
At3g06350	putative dehydroquinase shikimate dehydrogenase	0.27	0.41	1.52
At5g02860	putative protein	0.62	0.94	1.52
At3g63190	putative protein	0.33	0.5	1.52
At4g08600	hypothetical protein	2	3.03	1.52
At3g24260	hypothetical protein	1.38	2.09	1.51
At3g23400	unknown protein	0.43	0.65	1.51
At5g57930	putative protein	0.67	1.01	1.51
At3g57630	putative protein	0.18	0.27	1.50
At1g54710	hypothetical protein	0.12	0.18	1.50
At4g24930	proteomics: thylakoid lumen protein	0.44	0.66	1.50
At5g50280	putative protein	0.04	0.06	1.50
At4g22830	predicted protein	0.12	0.18	1.50
At4g25170	putative protein	0.08	0.12	1.50
At2g37710	putative receptor-like protein kinase	0.06	0.09	1.50
At3g30780	hypothetical protein	0.14	0.21	1.50
At5g44820	putative protein	0.2	0.3	1.50
At1g47730	hypothetical protein	0.56	0.84	1.50

At3g10130	unknown protein	0.1	0.15	1.50
At2g42620	unknown protein	7.9	11.81	1.49
At4g11980	putative protein	13.17	19.61	1.49
At1g30680	hypothetical protein	0.31	0.46	1.48
At2g01760	putative two-component response regulator protein	0.29	0.43	1.48
At3g21865	unknown protein	0.77	1.14	1.48
At3g49350	GTPase activating -like protein	0.25	0.37	1.48
At2g21280	unknown protein	0.25	0.37	1.48
At5g39210	hypothetical protein	0.42	0.62	1.48
At4g10060	putative protein	0.78	1.15	1.47
At1g75230	3-methyladenine DNA glycosylase	0.19	0.28	1.47
At1g20510	hypothetical protein	2.41	3.55	1.47
At1g62140	hypothetical protein	0.89	1.31	1.47
At3g52190	putative protein	0.15	0.22	1.47
At4g22370	hypothetical protein	0.45	0.66	1.47
At1g54130	RSH3 (RelA/SpoT homolog)	0.15	0.22	1.47
At5g17710	chloroplast GrpE protein	0.43	0.63	1.47
At5g20070	putative protein	1.25	1.83	1.46
At5g23070	putative protein	0.97	1.42	1.46
At1g69370	chorismate mutase	0.13	0.19	1.46
At5g09820	putative protein	0.13	0.19	1.46
At1g11470	hypothetical protein	0.5	0.73	1.46
At3g47650	putative protein	1.14	1.66	1.46
At5g35220	putative protein	0.22	0.32	1.45
At1g09780	putative 2	0.71	1.03	1.45
At2g26440	putative pectinesterase	1.11	1.61	1.45
At3g44310	nitrilase 1	0.2	0.29	1.45
At5g24020	septum site-determining MinD	0.2	0.29	1.45
At5g43540	unknown protein	0.2	0.29	1.45
At2g32920	putative protein disulfide isomerase	0.49	0.71	1.45
At4g03920	putative protein	0.58	0.84	1.45
At1g08250	hypothetical protein	0.09	0.13	1.44
At2g47940	putative serine protease	0.34	0.49	1.44
At1g34300	hypothetical protein	0.5	0.72	1.44
At4g00650	hypothetical protein	0.25	0.36	1.44
At4g29790	putative protein	0.25	0.36	1.44
At4g17330	G2484-1 protein	1.78	2.56	1.44
At2g22230	putative beta-hydroxyacyl-ACP dehydratase	0.16	0.23	1.44
cob	mitochondrial gene; cytochrome b	1.12	1.61	1.44
At3g54900	putative protein	0.55	0.79	1.44
At5g27280	putative protein	0.39	0.56	1.44
At1g60990	hypothetical protein	0.14	0.2	1.43
At2g35650	putative glucosyltransferase	0.38	0.54	1.42
At1g03230	unknown protein	0.31	0.44	1.42
At3g03880	hypothetical protein	1.29	1.83	1.42
At5g62840	putative protein	0.43	0.61	1.42
At1g15850	mitotic checkpoint protein	0.55	0.78	1.42
At1g04420	hypothetical protein	0.12	0.17	1.42
At4g28840	putative protein	0.36	0.51	1.42
At2g21860	unknown protein	0.36	0.51	1.42
At5g47870	putative protein	0.12	0.17	1.42

At3g32930	unknown protein	0.12	0.17	1.42
At5g01920	putative protein	0.65	0.92	1.42
At3g15780	unknown protein	0.7	0.99	1.41
At4g37200	HCF164; thiol-disulfide interchange like protein	0.46	0.65	1.41
At3g50770	calmodulin-like protein	0.46	0.65	1.41
At1g04570	hypothetical protein	0.17	0.24	1.41
At2g19870	hypothetical protein	0.39	0.55	1.41
At1g62180	5\\\'-adenylylphosphosulfate reductase	0.83	1.17	1.41
At3g03580	hypothetical protein	0.22	0.31	1.41
At5g63570	glutamate-1-semialdehyde 2	0.22	0.31	1.41
At2g31920	hypothetical protein	0.27	0.38	1.41
At1g44446	chlorophyll a oxygenase	0.86	1.21	1.41
At5g28750	Tha4 protein - like	0.32	0.45	1.41
At1g17740	unknown protein	0.2	0.28	1.40
At2g25130	hypothetical protein	0.1	0.14	1.40
At1g73090	hypothetical protein	0.05	0.07	1.40
At4g32020	putative protein	0.25	0.35	1.40
At5g49590	putative protein	0.3	0.42	1.40
At2g46010	hypothetical protein	1.05	1.47	1.40
At1g62250	unknown protein	0.25	0.35	1.40
At1g26150	Pto kinase interactor	0.55	0.77	1.40
At3g42100	putative protein	0.15	0.21	1.40
At1g22040	hypothetical protein	0.38	0.53	1.39
At1g49970	nClpP5	0.33	0.46	1.39
At1g75690	unknown protein	3.33	4.64	1.39
At5g24700	unknown protein	0.23	0.32	1.39
At1g79380	unknown protein	1.23	1.71	1.39
At3g58010	putative protein	0.18	0.25	1.39
At3g01170	unknown protein	0.18	0.25	1.39
At4g20120	hypothetical protein	0.18	0.25	1.39
At4g18810	putative protein	0.18	0.25	1.39
At3g05710	putative syntaxin protein	1.37	1.9	1.39
At5g24120	sigma-like factor	0.44	0.61	1.39
At1g63680	putative UDP-N-acetylmuramoylalanyl-D-glutamate--2	0.13	0.18	1.38
At1g67810	putative protein	2.24	3.1	1.38
At4g39030	putative protein	0.34	0.47	1.38
At4g13260	putative protein	0.34	0.47	1.38
At2g47910	unknown protein	0.34	0.47	1.38
At2g31160	unknown protein	1.26	1.74	1.38
At2g14890	putative proline-rich protein	0.42	0.58	1.38
At1g49510	unknown protein	0.37	0.51	1.38
At4g35510	putative protein	0.53	0.73	1.38
At2g35400	unknown protein	0.32	0.44	1.38
At5g04740	unknown protein	0.08	0.11	1.38
At4g39980	2-dehydro-3-deoxyphosphoheptonate aldolase	0.4	0.55	1.38
At4g31180	aspartate--tRNA ligase - like protein	0.08	0.11	1.38
At3g25770	hypothetical protein	0.27	0.37	1.37
At5g49450	putative protein	0.92	1.26	1.37
At5g17280	putative protein	0.38	0.52	1.37
At4g26220	caffeoyl-CoA O-methyltransferase - like protein	0.41	0.56	1.37
At1g27540	unknown protein	0.52	0.71	1.37
At4g27580	putative protein	0.85	1.16	1.36

At2g48130	unknown protein	0.11	0.15	1.36
At3g59640	putative protein	0.11	0.15	1.36
At5g46580	putative protein	0.22	0.3	1.36
At3g26840	unknown protein	0.11	0.15	1.36
At1g52220	unknown protein	0.69	0.94	1.36
At5g19000	putative protein	1.16	1.58	1.36
At5g23120	HCF136	0.86	1.17	1.36
At3g57120	putative protein	1.03	1.4	1.36
At4g22760	predicted protein	0.14	0.19	1.36
At1g13990	unknown protein	0.56	0.76	1.36
At1g21670	hypothetical protein	0.14	0.19	1.36
At5g42070	putative protein	0.45	0.61	1.36
At5g01590	hypothetical protein	0.31	0.42	1.35
At1g41750	hypothetical protein	0.34	0.46	1.35
At4g03310	hypothetical protein	5.08	6.87	1.35
At2g34540	hypothetical protein	0.2	0.27	1.35
At4g20740	similarity to CRP1	0.4	0.54	1.35
At4g37710	putative protein	0.23	0.31	1.35
At5g27560	putative protein	0.23	0.31	1.35
At4g02740	hypothetical protein	0.23	0.31	1.35
At1g65370	unknown protein	0.23	0.31	1.35
At3g12930	hypothetical protein	0.78	1.05	1.35
At1g51440	hypothetical protein	0.26	0.35	1.35
At3g44880	lethal leaf-spot 1 homolog Lls1	0.29	0.39	1.34
At4g30910	leucyl aminopeptidase - like protein (partial)	0.53	0.71	1.34
At5g66480	putative protein	0.06	0.08	1.33
At4g23450	putative protein	0.15	0.2	1.33
At5g45980	putative protein	0.15	0.2	1.33
At3g19590	mitotic checkpoint protein	0.03	0.04	1.33
At3g11590	unknown protein	0.15	0.2	1.33
At1g54520	unknown protein	0.06	0.08	1.33
At5g39520	putative protein	0.03	0.04	1.33
At3g23490	cyanate lyase (CYN)	2.67	3.56	1.33
At5g03000	putative protein	0.21	0.28	1.33
At2g35240	unknown protein	0.24	0.32	1.33
At4g18370	putative HhoA protease precursor; proteomics: lumenal DegQ protease	0.21	0.28	1.33
At5g61450	putative protein	0.15	0.2	1.33
At2g39000	unknown protein	0.09	0.12	1.33
At2g47860	unknown protein	0.09	0.12	1.33
At2g40310	putative polygalacturonase	0.09	0.12	1.33
At1g05385	expressed protein	0.18	0.24	1.33
At3g07430	unknown protein	0.27	0.36	1.33
At4g15560	DEF (CLA1) protein	0.61	0.81	1.33
At4g08940	hypothetical protein	1.22	1.62	1.33
At4g21210	putative protein	0.49	0.65	1.33
At5g13090	putative protein	0.95	1.26	1.33
At1g23210	hypothetical protein	0.34	0.45	1.32
At2g45310	putative nucleotide sugar epimerase	0.34	0.45	1.32
At3g17930	hypothetical protein	0.99	1.31	1.32
At1g24150	unknown protein	0.84	1.11	1.32
At5g22830	putative protein	0.25	0.33	1.32

At5g63830	unknown protein	0.25	0.33	1.32
At3g57110	hypothetical protein	0.25	0.33	1.32
At3g16855	ARR1 protein	0.25	0.33	1.32
At1g55630	hypothetical protein	0.44	0.58	1.32
At4g08280	putative protein	0.22	0.29	1.32
At4g27250	putative protein	0.98	1.29	1.32
At4g27390	putative protein	0.38	0.5	1.32
At3g44810	hypothetical protein	0.16	0.21	1.31
At1g79460	ent-kaurene synthase	0.16	0.21	1.31
At1g79460	ent-kaurene synthase	0.16	0.21	1.31
At4g29750	putative protein	0.16	0.21	1.31
At5g50920	ATP-dependent Clp protease	3.08	4.03	1.31
At3g63130	RAN GTPase activating protein 1 protein	0.39	0.51	1.31
At3g57780	putative protein	0.52	0.68	1.31
At3g56410	putative protein	0.36	0.47	1.31
At2g27360	putative lipase	0.36	0.47	1.31
At3g13110	serine acetyltransferase (Sat-1)	0.33	0.43	1.30
At2g44570	putative glucanase	0.33	0.43	1.30
rbcL	plastid gene product; large subunit of Rubisco	137.12	178.6	1.30
At3g56710	SigA binding protein	0.1	0.13	1.30
At5g19460	putative protein	0.1	0.13	1.30
At1g21390	hypothetical protein	0.1	0.13	1.30
At2g11100	pseudogene	1.12	1.45	1.29
At3g02875	IAA-amino acid hydrolase (ILR1)	1.29	1.67	1.29
At2g23890	hypothetical protein	0.17	0.22	1.29
At5g30460	putative protein	0.34	0.44	1.29
At4g24840	brefeldin A-sensitive Golgi protein - like	0.24	0.31	1.29
At1g65070	hypothetical protein	0.45	0.58	1.29
At4g33170	putative protein	0.59	0.76	1.29
At2g22210	pseudogene	0.35	0.45	1.29
At3g63340	putative protein	0.07	0.09	1.29
At4g30150	hypothetical protein	0.07	0.09	1.29
At3g22430	hypothetical protein	0.28	0.36	1.29
At5g27300	putative protein	1.62	2.08	1.28
At1g24130	hypothetical protein	0.74	0.95	1.28
At2g43050	putative pectinesterase	0.39	0.5	1.28
At5g19850	putative protein	0.32	0.41	1.28
At2g27290	hypothetical protein	43.52	55.62	1.28
At4g37510	putative protein	0.18	0.23	1.28
At5g58560	putative protein	0.11	0.14	1.27
At1g16880	unknown protein	0.22	0.28	1.27
At1g73150	hypothetical protein	0.23	0.29	1.26
At1g65690	hypothetical protein	0.23	0.29	1.26
At2g47450	CAO (cpSRP43)	0.27	0.34	1.26
At1g27380	hypothetical protein	0.36	0.45	1.25
At4g14690	early light-induced protein ELIP.2 (Lil1.2)	0.07	0.08	1.14
At5g17840	putative protein	0.2	0.16	0.80
At1g10600	hypothetical protein	0.05	0.04	0.80
At1g22240	hypothetical protein	0.19	0.15	0.79
At3g57950	putative protein	0.56	0.44	0.79
At2g24070	unknown protein	0.14	0.11	0.79

At4g19390	putative protein		0.14	0.11	0.79
At5g18260	putative protein		0.73	0.57	0.78
At4g24910	putative protein		0.5	0.39	0.78
At2g32840	hypothetical protein		0.59	0.46	0.78
At1g66890	hypothetical protein		0.59	0.46	0.78
At3g52550	hypothetical protein		0.59	0.46	0.78
At2g41950	hypothetical protein		0.68	0.53	0.78
At1g60550	hypothetical protein		0.36	0.28	0.78
At3g53860	putative protein		0.18	0.14	0.78
At1g27610	hypothetical protein		1.07	0.83	0.78
At3g19540	unknown protein		0.89	0.69	0.78
At1g77250	hypothetical protein		0.8	0.62	0.78
At4g39550	putative protein		1.11	0.86	0.77
At3g57680	carboxyl terminal protease - like protein		0.31	0.24	0.77
At1g79960	hypothetical protein		0.53	0.41	0.77
At1g15490	hypothetical protein		0.22	0.17	0.77
At1g12520	unknown protein		0.22	0.17	0.77
At5g62000	auxin response factor - like protein		0.35	0.27	0.77
At2g39710	unknown protein		1.05	0.81	0.77
At4g38150	putative protein		5.85	4.51	0.77
At4g29490	putative protein		0.48	0.37	0.77
At5g48370	putative protein		0.61	0.47	0.77
At2g24210	putative limonene cyclase		0.13	0.1	0.77
At5g65490	putative protein		0.13	0.1	0.77
At1g43840	hypothetical protein		0.39	0.3	0.77
At1g67440	hypothetical protein		1.47	1.13	0.77
At4g32340	putative protein		0.43	0.33	0.77
At3g11150	hypothetical protein		0.86	0.66	0.77
At4g00610	hypothetical protein		0.6	0.46	0.77
At3g30190	hypothetical protein		0.6	0.46	0.77
At1g19350	unknown protein		0.34	0.26	0.76
At5g11480	putative GTP-binding protein		0.17	0.13	0.76
At2g23330	putative retroelement pol polyprotein		0.55	0.42	0.76
At3g24190	unknown protein		1.01	0.77	0.76
At1g31790	hypothetical protein		1.38	1.05	0.76
At2g38070	hypothetical protein		0.46	0.35	0.76
3695380	partial CDS; contains similarity to Nicotiana tabacum membrane-associated salt-inducible protein		0.71	0.54	0.76
At1g21060	unknown protein		0.25	0.19	0.76
7939562		7939562	0.54	0.41	0.76
At1g64890	unknown protein		0.45	0.34	0.76
At2g38360	unknown protein		0.45	0.34	0.76
At2g27770	hypothetical protein		1.06	0.8	0.75
At5g56660	IAA-amino acid hydrolase		0.69	0.52	0.75
At4g27320	putative protein		0.81	0.61	0.75
At3g22160	unknown protein		0.16	0.12	0.75
At4g30620	putative protein		0.68	0.51	0.75
At1g62110	hypothetical protein		0.48	0.36	0.75
At2g05310	unknown protein		0.24	0.18	0.75
At2g39470	proteomics: thylakoid lumen protein		0.96	0.72	0.75
At1g50960	gibberellin 20-oxidase		0.44	0.33	0.75
At5g13840	cell cycle switch protein		0.32	0.24	0.75

At4g14620	hypothetical protein	0.12	0.09	0.75
At3g19960	myosin	0.28	0.21	0.75
At5g07770	unknown protein	0.28	0.21	0.75
At4g18540	hypothetical protein	0.75	0.56	0.75
At4g00890	hypothetical protein	0.67	0.5	0.75
At5g61200	putative protein	1.02	0.76	0.75
At3g18870	hypothetical protein	0.94	0.7	0.74
At3g04680	unknown protein	0.39	0.29	0.74
At1g70990	hypothetical protein	1.28	0.95	0.74
At2g31720	hypothetical protein	0.31	0.23	0.74
At3g15840	unknown protein	0.31	0.23	0.74
At3g47200	putative protein	0.31	0.23	0.74
At3g18230	unknown protein	1.16	0.86	0.74
At4g22920	hypothetical protein	0.85	0.63	0.74
At1g74940	unknown protein	0.27	0.2	0.74
At5g56760	serine O-acetyltransferase	0.5	0.37	0.74
At2g33720	hypothetical protein	0.23	0.17	0.74
At5g35100	putative protein	0.88	0.65	0.74
At3g44720	putative chloroplast prephenate dehydratase	0.61	0.45	0.74
At2g33280	hypothetical protein	0.61	0.45	0.74
At2g28755	putative dTDP-glucose 4-6-dehydratase	0.38	0.28	0.74
At3g25110	acyl-(acyl carrier protein) thioesterase	0.57	0.42	0.74
At5g60600	putative protein	1.1	0.81	0.74
At2g48090	unknown protein	0.68	0.5	0.74
At2g41330	unknown protein	0.75	0.55	0.73
At1g01550	hypothetical protein	0.97	0.71	0.73
At4g39970	putative protein	1.04	0.76	0.73
At5g55210	putative protein	0.48	0.35	0.73
At1g28960	hypothetical protein	0.22	0.16	0.73
At2g05180	putative cytochrome P450	0.44	0.32	0.73
At2g23230	putative vetispiradiene synthase	0.44	0.32	0.73
At3g52490	putative protein	0.62	0.45	0.73
At4g23110	hypothetical protein	0.62	0.45	0.73
At4g37000	putative protein	0.4	0.29	0.73
At4g37470	putative protein	0.4	0.29	0.73
At3g02730	thioredoxin f1	1.01	0.73	0.72
At3g19370	unknown protein	0.18	0.13	0.72
At2g38950	unknown protein	0.18	0.13	0.72
At5g52660	putative protein	0.36	0.26	0.72
At1g30100	9-cis-epoxycarotenoid dioxygenase	0.9	0.65	0.72
At2g01610	unknown protein	0.43	0.31	0.72
At2g44530	putative phosphoribosyl pyrophosphate synthetase	0.43	0.31	0.72
At2g15440	hypothetical protein	0.57	0.41	0.72
At1g23980	hypothetical protein	0.71	0.51	0.72
At2g06970	hypothetical protein	0.78	0.56	0.72
At1g03660	unknown	1.24	0.89	0.72
At1g74850	hypothetical protein	0.85	0.61	0.72
At4g07560	putative transposon protein	0.53	0.38	0.72
At2g37880	hypothetical protein	0.53	0.38	0.72
At1g70350	hypothetical protein	0.21	0.15	0.71
At4g35980	putative protein	0.14	0.1	0.71

At1g32760	unknown protein	1.47	1.05	0.71
At1g74960	putative 3-ketoacyl-ACP synthase	0.14	0.1	0.71
At1g54320	unknown protein	0.42	0.3	0.71
At5g48590	putative protein	0.14	0.1	0.71
At1g75330	ornithine carbamoyltransferase precursor	0.07	0.05	0.71
At3g56010	putative protein	0.45	0.32	0.71
At1g68450	unknown protein	0.45	0.32	0.71
At5g07760	putative protein	2.93	2.08	0.71
At2g03220	xyloglucan fucosyltransferase AtFT1	2.93	2.08	0.71
At3g20230	hypothetical protein	7.06	5.01	0.71
At5g67030	zeaxanthin epoxidase precursor	7.06	5.01	0.71
At2g24020	unknown protein	0.48	0.34	0.71
At5g38560	putative protein	3.99	2.82	0.71
At1g51390	unknown protein	0.34	0.24	0.71
At1g02560	ATP-dependent Clp protease proteolytic subunit (nClpP1)	0.68	0.48	0.71
At4g35690	putative protein	0.61	0.43	0.70
At2g20020	hypothetical protein	0.88	0.62	0.70
At5g10910	putative protein	0.64	0.45	0.70
At5g12150	putative protein	0.37	0.26	0.70
At5g44750	putative protein	0.37	0.26	0.70
At2g44040	unknown protein	0.47	0.33	0.70
At4g11630	putative protein	0.2	0.14	0.70
At2g14230	hypothetical protein	0.4	0.28	0.70
At3g11050	putative ferritin subunit precursor	0.1	0.07	0.70
At4g01770	hypothetical protein	0.6	0.42	0.70
At2g36920	hypothetical protein	0.83	0.58	0.70
At4g24090	hypothetical protein	0.53	0.37	0.70
At2g33430	plastid protein	0.96	0.67	0.70
At3g09070	unknown protein	0.43	0.3	0.70
At2g21590	putative ADP-glucose pyrophosphorylase large subunit	0.56	0.39	0.70
At2g30100	putative leucine-rich repeat protein	1.91	1.33	0.70
At1g51780	hypothetical protein	1.25	0.87	0.70
At5g61470	putative protein	0.69	0.48	0.70
At3g62030	peptidylprolyl isomerase ROC4	0.46	0.32	0.70
At1g48620	unknown protein	0.46	0.32	0.70
At5g67490	unknown protein	0.46	0.32	0.70
At4g08630	hypothetical protein	0.49	0.34	0.69
At4g39710	proteomics: thylakloid lumen FKBP-like protein	0.55	0.38	0.69
At4g25990	putative protein	0.55	0.38	0.69
At3g12400	hypothetical protein	0.74	0.51	0.69
At5g06140	sorting nexin-like protein	0.93	0.64	0.69
At3g15095	unknown protein	0.16	0.11	0.69
At1g27660	hypothetical protein	0.32	0.22	0.69
At3g08660	putative non-phototropic hypocotyl	0.19	0.13	0.68
At2g25320	unknown protein	0.19	0.13	0.68
At1g13970	hypothetical protein	0.41	0.28	0.68
At3g17700	hypothetical protein	0.22	0.15	0.68
At5g11890	putative protein	1.35	0.92	0.68
At1g02020	hypothetical protein	0.25	0.17	0.68
At2g14880	unknown protein	0.9	0.61	0.68
At1g15070	unknown protein	6.96	4.71	0.68
At4g23930	putative protein	0.34	0.23	0.68

At2g44560	putative glucanase	0.68	0.46	0.68
At3g12120	hypothetical protein	2.86	1.93	0.67
At4g39050	kinesin like protein	0.43	0.29	0.67
At1g79760	hypothetical protein	0.64	0.43	0.67
At4g26010	putative peroxidase	1.72	1.15	0.67
At4g23060	putative protein	0.12	0.08	0.67
At1g44350	putative IAA-amino acid hydrolase	0.21	0.14	0.67
At5g05590	phosphoribosylanthranilate isomerase	0.3	0.2	0.67
At2g07710	hypothetical protein	0.6	0.4	0.67
At3g48420	putative protein	0.09	0.06	0.67
At2g38450	unknown protein	0.33	0.22	0.67
At3g20920	hypothetical protein	0.39	0.26	0.67
At2g13810	putative aspartate aminotransferase	0.39	0.26	0.67
4559339	4559339	3.99	2.64	0.66
At5g54190	NADPH:protochlorophyllide oxidoreductase A	0.62	0.41	0.66
At5g45390	ATP-dependent Clp protease-like protein	0.53	0.35	0.66
At1g76560	hypothetical protein	1.53	1.01	0.66
At5g02850	putative protein	0.41	0.27	0.66
At4g24860	putative protein	0.41	0.27	0.66
At1g30920	F17F8.21	1.23	0.81	0.66
At4g03800	hypothetical protein	0.35	0.23	0.66
At2g04540	3-oxoacyl carrier protein synthase	0.29	0.19	0.66
At1g03680	putative thioredoxin m1	2.29	1.5	0.66
At4g29920	putative protein	0.49	0.32	0.65
At3g16250	putative 2Fe-2S iron-sulfur cluster protein	0.43	0.28	0.65
At1g61980	hypothetical protein	1.06	0.69	0.65
At4g14380	hypothetical protein	0.57	0.37	0.65
At1g62010	hypothetical protein	1.11	0.72	0.65
At2g14120	dynamin-like protein	1.19	0.77	0.65
At1g16160	hypothetical protein	0.17	0.11	0.65
At1g11820	unknown protein	0.34	0.22	0.65
At4g14260	hypothetical protein	0.99	0.64	0.65
At2g45180	putative proline-rich protein	4.2	2.71	0.65
At4g12520	pEARLI 1-like protein	1.04	0.67	0.64
At5g22270	putative protein	1.12	0.72	0.64
At1g77090	proteomics: thylakoid lumen protein	0.14	0.09	0.64
At1g77390	mitotic cyclin a2-type	0.28	0.18	0.64
At4g36580	ATPase-like protein	0.53	0.34	0.64
At3g16000	myosin heavy chain-like protein	0.36	0.23	0.64
At1g72010	unknown protein	0.66	0.42	0.64
At1g61990	hypothetical protein	1.21	0.77	0.64
At1g76240	hypothetical protein	1.1	0.7	0.64
At4g10980	putative protein	0.96	0.61	0.64
At4g37460	putative protein	0.3	0.19	0.63
At1g79360	hypothetical protein	0.9	0.57	0.63
At1g53280	hypothetical protein	0.27	0.17	0.63
At2g37080	putative myosin heavy chain	0.94	0.59	0.63
At3g22970	unknown protein	1.34	0.84	0.63
At2g04700	FTR; ferredoxin-thioredoxin reductase	0.32	0.2	0.63
At3g04260	hypothetical protein	0.69	0.43	0.62
At2g40980	unknown protein	0.53	0.33	0.62

At4g10750	putative aldolase	0.98	0.61	0.62
At5g51670	putative protein	0.45	0.28	0.62
At4g23170	putative protein	18.56	11.5	0.62
At5g55570	unknown protein	1.18	0.73	0.62
At2g30880	unknown protein	0.55	0.34	0.62
At2g28790	putative thaumatin	0.13	0.08	0.62
At5g50640	putative protein	0.26	0.16	0.62
At1g56020	unknown protein	0.78	0.48	0.62
At5g11550	putative protein	2.31	1.42	0.61
At2g44540	putative glucanase	0.44	0.27	0.61
At2g34020	unknown protein	1.03	0.63	0.61
At1g52500	hypothetical protein	0.18	0.11	0.61
At3g66654	unknown protein	0.18	0.11	0.61
At4g11080	98b like protein	0.54	0.33	0.61
At1g19870	hypothetical protein	1.28	0.78	0.61
At4g30210	NADPH-ferrihemoprotein reductase (ATR2)	1.28	0.78	0.61
At1g55420	hypothetical protein	0.46	0.28	0.61
At2g20600	hypothetical protein	1.45	0.88	0.61
At4g16490	hypothetical protein	1.36	0.82	0.60
At1g08050	unknown protein	0.25	0.15	0.60
At2g24490	putative replication protein A1	0.25	0.15	0.60
At1g33780	hypothetical protein	0.95	0.57	0.60
At5g41960	unknown protein	0.15	0.09	0.60
At5g38290	CRS2 -like protein	1.04	0.62	0.60
At3g56700	putative protein	0.32	0.19	0.59
At2g36410	unknown protein	0.32	0.19	0.59
At4g24860	putative protein	0.39	0.23	0.59
At1g01080	ribonucleoprotein	0.17	0.1	0.59
At3g17810	dehydrogenase	0.29	0.17	0.59
At4g15120	hypothetical protein	1.11	0.65	0.59
At4g18760	putative protein	0.79	0.46	0.58
At3g11490	putative rac GTPase activating protein	0.98	0.57	0.58
At5g07900	putative protein	1.38	0.8	0.58
At1g03810	hypothetical protein	0.88	0.51	0.58
At5g44680	putative protein	0.19	0.11	0.58
At1g48860	hypothetical protein	0.19	0.11	0.58
At2g29670	unknown protein	0.57	0.33	0.58
At3g15050	hypothetical protein	0.19	0.11	0.58
At5g11090	putative protein	0.52	0.3	0.58
At3g60860	guanine nucleotide exchange factor - like protein	1.56	0.9	0.58
At3g20970	unknown protein	0.66	0.38	0.58
At2g39270	putative adenylate kinase	0.33	0.19	0.58
At5g27070	putative protein	1.01	0.58	0.57
At5g64580	putative protein	0.61	0.35	0.57
At2g20090	unknown protein	0.61	0.35	0.57
At3g28460	unknown protein	0.07	0.04	0.57
At3g22840	early light-induced protein ELIP.1 (Lil1.1)	0.14	0.08	0.57
At2g26840	unknown protein	0.34	0.19	0.56
At3g09490	hypothetical protein	0.68	0.38	0.56
At1g12250	hypothetical protein	0.52	0.29	0.56
At1g30320	hypothetical protein	0.97	0.54	0.56

At4g03520	m-type thioredoxin	1.94	1.08	0.56
At5g16730	putative protein	0.18	0.1	0.56
At3g54320	aintegumaenta-like protein	0.36	0.2	0.56
At3g17550	hypothetical protein	0.36	0.2	0.56
At1g79110	hypothetical protein	0.83	0.46	0.55
At4g16080	hypothetical protein	1	0.55	0.55
At1g08540	sigma factor	0.71	0.39	0.55
At4g36910	putative protein	0.31	0.17	0.55
ratpBr	plastid gene product; ATP synthase	10.43	5.71	0.55
At3g12970	unknown protein	0.22	0.12	0.55
At5g40160	ankyrin repeat protein EMB506	0.77	0.42	0.55
At3g26740	light regulated protein	9.69	5.26	0.54
At3g15360	thioredoxin m4	1.09	0.59	0.54
At1g80920	J8-like protein	0.37	0.2	0.54
At4g31430	predicted protein	0.5	0.27	0.54
At5g27860	putative protein	0.13	0.07	0.54
At1g12980	hypothetical protein	1.19	0.64	0.54
At1g15410	hypothetical protein	0.28	0.15	0.54
At4g35450	ankyrin repeat-containing protein 2	1.27	0.68	0.54
At1g50040	hypothetical protein	0.73	0.39	0.53
At2g44550	putative glucanase	0.32	0.17	0.53
At5g46640	putative protein	0.32	0.17	0.53
At1g67460	hypothetical protein	0.83	0.44	0.53
At4g19490	putative protein	0.68	0.36	0.53
At2g42300	unknown protein	0.38	0.2	0.53
At1g13280	allene oxide cyclase	0.42	0.22	0.52
At5g42480	putative protein	1.07	0.56	0.52
At3g55070	putative protein	0.65	0.34	0.52
At3g43700	putative protein	0.23	0.12	0.52
At1g55440	hypothetical protein	0.71	0.37	0.52
At1g48570	hypothetical protein	0.48	0.25	0.52
At2g37090	unknown protein	0.5	0.26	0.52
At1g69240	putative alpha/beta hydrolase	0.29	0.15	0.52
At3g09850	hypothetical protein	127.72	65.69	0.51
At5g23300	dihydroorotate dehydrogenase precursor	127.72	65.69	0.51
At4g19100	putative protein	0.39	0.2	0.51
At5g41110	unknown protein	2.5	1.27	0.51
At3g06590	unknown protein	1.28	0.64	0.50
At1g72260	thionin	0.52	0.26	0.50
At2g17300	unknown protein	2.44	1.22	0.50
At2g34700	putative proline-rich glycoprotein	0.24	0.12	0.50
At1g70170	matrix metalloproteinase	0.58	0.29	0.50
At5g19280	kinase associated protein phosphatase	0.24	0.12	0.50
At3g09050	unknown protein	1.14	0.56	0.49
At5g23440	putative protein	0.47	0.23	0.49
At5g12120	putative protein	3.95	1.91	0.48
At2g17230	unknown protein	0.27	0.13	0.48
At3g50190	putative protein	4.93	2.36	0.48
At5g60050	putative protein	1.4	0.67	0.48
At4g14930	hypothetical protein	0.23	0.11	0.48
At3g18420	unknown protein	0.9	0.43	0.48

At5g26600	putative protein	0.42	0.2	0.48
At2g44500	axi 1-like protein	2.9	1.38	0.48
At3g23160	hypothetical protein	0.19	0.09	0.47
At2g31350	putative glyoxalase II	1.67	0.79	0.47
At1g04330	unknown protein	0.72	0.34	0.47
At4g17680	hypothetical protein	2.38	1.12	0.47
At2g37250	putative adenylate kinase	0.32	0.15	0.47
At3g50140	putative protein	5.64	2.58	0.46
At1g80450	unknown protein	0.7	0.32	0.46
At5g43930	putative protein	0.22	0.1	0.45
At5g39860	putative protein	0.11	0.05	0.45
At5g38750	putative protein	1.04	0.47	0.45
At3g23940	dihydroxyacid dehydratase	1.04	0.47	0.45
At5g57990	putative protein	0.29	0.13	0.45
At5g19900	putative protein	0.29	0.13	0.45
At4g13270	hypothetical protein	0.87	0.39	0.45
At3g01700	unknown protein	0.48	0.21	0.44
At5g59610	putative protein	0.81	0.35	0.43
At1g30700	putative reticuline oxidase-like protein	1.49	0.64	0.43
At1g51560	unknown protein	0.47	0.2	0.43
At5g40470	putative protein	2.01	0.85	0.42
At2g28900	outer envelope protein24	0.38	0.16	0.42
At1g33250	unknown protein	2.32	0.97	0.42
At5g02750	putative protein	2.13	0.89	0.42
At4g11780	putative protein	1.54	0.64	0.42
At1g79730	unknown protein	1.95	0.8	0.41
At2g01650	unknown protein	0.22	0.09	0.41
At1g18680	unknown protein	4.72	1.9	0.40
At3g62520	putative protein	1.64	0.66	0.40
At2g40400	unknown protein	0.98	0.39	0.40
At5g64090	unknown protein	0.48	0.19	0.40
At1g32060	phosphoribulokinase precursor	1.79	0.69	0.39
At2g24730	pseudogene	0.78	0.3	0.38
At1g73470	expressed protein	3.23	1.24	0.38
At2g34370	putative selenium-binding protein	3.23	1.24	0.38
At4g12000	putative protein	101.22	38.49	0.38
At2g19240	hypothetical protein	2.34	0.88	0.38
At3g19680	unknown protein	0.16	0.06	0.38
At1g05420	hypothetical protein	1.95	0.72	0.37
At3g48110	glycine--tRNA ligase precursor	2.23	0.82	0.37
At4g25250	putative protein	146.64	52.5	0.36
At1g80130	unknown protein	0.65	0.23	0.35
At3g42490	putative protein	1.29	0.44	0.34
At4g34310	hypothetical protein	1	0.34	0.34
At3g57280	hypothetical protein	0.03	0.01	0.33
At5g61120	putative protein	0.09	0.03	0.33
At1g12090	hypothetical protein	3.1	1.01	0.33
At5g51770	putative protein	0.4	0.13	0.33
At4g03150	hypothetical protein	2.3	0.72	0.31
At5g26570	putative protein	0.23	0.07	0.30
At4g35890	putative protein	1.84	0.55	0.30

At1g54930	hypothetical protein	0.34	0.1	0.29
At3g24810	unknown protein	0.67	0.19	0.28
At4g37380	putative protein	1.37	0.38	0.28
At2g36480	hypothetical protein	4.27	1.12	0.26
At2g15890	unknown protein	2.99	0.74	0.25
At1g02730	hypothetical protein	0.06	0.01	0.17
At2g06030	hypothetical protein	0.06	0.01	0.17
At5g06290	2-Cys peroxiredoxin-like protein	0.06	0.01	0.17
At1g04360	hypothetical protein	1.76	0.29	0.16

atpd-1

MIPS-code	Description	Control (WT)	D (data=mutant)	
Metabolism				
At4g12270	copper amine oxidase like protein (fragment1)	0.06	0.74	12.33
At4g22590	trehalose-6-phosphate phosphatase - like protein	0.49	4.76	9.71
At4g07960	putative glucosyltransferase	10.25	98.31	9.59
At4g24040	trehalase - like protein	0.09	0.84	9.33
At5g27090	putative protein	0.14	1.16	8.29
At5g58330	NADP-dependent malate dehydrogenase	0.18	1.44	8.00
At2g15620	ferredoxin--nitrite reductase	0.22	1.73	7.86
At4g20930	3-hydroxyisobutyrate dehydrogenase -like protein	0.21	1.57	7.48
At4g00490	putative beta-amylase	0.08	0.58	7.25
At1g50390	fructokinase	0.2	1.25	6.25
At1g17740	unknown protein	0.09	0.56	6.22
At4g13050	oleoyl-[acyl-carrier-protein] hydrolase-like protein	0.15	0.92	6.13
At4g38880	amidophosphoribosyltransferase - like protein	0.17	1	5.88
At3g10390	hypothetical protein	0.11	0.64	5.82
At3g10050	threonine dehydratase/deaminase (OMR1)	0.13	0.74	5.69
At1g01290	molybdopterin biosynthesis CNX3 protein	0.32	1.78	5.56
At5g23070	putative protein	0.21	1.15	5.48
At1g74030	putative enolase	0.19	1.03	5.42
At4g20840	reticuline oxidase - like protein	0.18	0.96	5.33
At1g77730	hypothetical protein	0.1	0.53	5.30
At3g06850	branched chain alpha-keto acid dehydrogenase E2 subunit	0.18	0.95	5.28
At3g54660	gluthatione reductase	0.14	0.73	5.21
At4g20210	cadinene synthase like protein	0.17	0.88	5.18
At2g34590	putative pyruvate dehydrogenase E1 beta subunit	0.54	2.79	5.17
At4g29890	choline monooxygenase - like protein	0.63	3.13	4.97
At5g35360	acetyl-CoA carboxylase	0.21	1	4.76
At1g01090	pyruvate dehydrogenase E1 alpha subunit	0.24	1.12	4.67
At3g44990	xyloglucan endo-transglycosylase	0.14	0.65	4.64
At5g19850	putative protein	0.22	1	4.55
At4g10260	fructokinase - like protein	0.08	0.36	4.50
At2g25620	putative protein phosphatase 2C	0.3	1.33	4.43
At4g29120	putative protein	0.18	0.76	4.22
At5g26030	ferrochelatase-I	0.29	1.22	4.21
At3g57610	adenylosuccinate synthetase	0.2	0.83	4.15
At4g13550	putative protein	0.14	0.58	4.14
At5g04140	ferredoxin-dependent glutamate synthase	0.39	1.56	4.00
At4g13260	putative protein	0.31	1.24	4.00

At1g07780	phosphoribosylanthranilate isomerase	0.28	1.11	3.96
At4g25700	beta-carotene hydroxylase	0.38	1.49	3.92
At4g19010	4-coumarate-CoA ligase - like	0.09	0.35	3.89
At3g54090	fructokinase - like protein	0.42	1.63	3.88
At2g30390	putative ferrochelatase precusor	0.29	1.12	3.86
At5g25900	cytochrome P450 GA3	0.18	0.68	3.78
At5g24760	alcohol dehydrogenase - like protein	0.1	0.37	3.70
At2g25710	biotin holocarboxylase synthetase	0.16	0.59	3.69
At3g56090	putative protein	0.12	0.44	3.67
At5g19220	Glucose-1-phosphate adenylyltransferase (ApL1/adg2)	0.18	0.65	3.61
At1g78090	trehalose-6-phosphate phosphatase (AtTPPB)	0.16	0.57	3.56
At4g14210	phytoene dehydrogenase precursor (phytoene desaturase)	0.82	2.9	3.54
At4g14910	imidazoleglycerol-phosphate dehydratase	0.19	0.67	3.53
At4g36390	putative protein	0.21	0.74	3.52
At5g62790	1-deoxy-D-xylulose 5-phosphate reductoisomerase (DXR)	0.25	0.88	3.52
At1g68890	putative menaquinone biosynthesis protein	0.35	1.22	3.49
At5g10330	histidinol-phosphate aminotransferase-like protein	0.11	0.38	3.45
At4g34710	arginine decarboxylase SPE2	0.37	1.24	3.35
At4g33510	2-dehydro-3-deoxyphosphoheptonate aldolase	0.36	1.2	3.33
At4g16820	triacylglycerol lipase like protein	0.22	0.73	3.32
At4g26900	glutamine amidotransferase/cyclase	0.66	2.17	3.29
At1g30120	pyruvate dehydrogenase E1 beta subunit	0.32	1.05	3.28
At4g39230	NAD(P)H oxidoreductase	0.12	0.39	3.25
At4g25910	nitrogen fixation like protein	0.26	0.84	3.23
At1g17160	putative ribokinase	0.56	1.8	3.21
At3g18890	hypothetical protein	0.12	0.38	3.17
At1g03310	putative isoamylase	0.38	1.2	3.16
At2g43430	putative glyoxalase II	0.21	0.66	3.14
At4g39540	shikimate kinase - like protein	0.14	0.44	3.14
At4g24620	glucose-6-phosphate isomerase	0.28	0.86	3.07
At4g20820	reticuline oxidase - like protein	0.17	0.52	3.06
At2g42070	unknown protein	0.19	0.57	3.00
At5g52810	putative protein	0.47	1.4	2.98
At4g34860	invertase - like protein	0.14	0.41	2.93
At1g24360	putative 3-oxoacyl [acyl-carrier protein] reductase	0.13	0.38	2.92
At4g37670	putative protein	0.35	1.01	2.89
At2g33880	putative homeodomain transcription factor	0.65	1.87	2.88
At4g30950	chloroplast omega-6 fatty acid desaturase (fad6)	0.55	1.53	2.78
At3g48320	cytochrome P450 - like protein	0.18	0.49	2.72
At3g03630	O-acetylserine (thiol) lyase	0.21	0.57	2.71
At2g34460	unknown protein	0.3	0.81	2.70
At3g24260	hypothetical protein	0.72	1.93	2.68
At2g43100	3-isopropylmalate dehydratase	0.39	1.04	2.67
At2g43180	putative carboxyphosphonoenolpyruvate mutase	0.29	0.77	2.66
At4g15550	glucosyltransferase like protein	0.28	0.74	2.64
At3g07020	UDP-glucose:sterol glucosyltransferase	0.13	0.34	2.62
At1g10640	polygalacturonase PG1	0.23	0.6	2.61
At1g76760	thioredoxin-like protein	0.19	0.49	2.58
At1g11720	putative glycogen synthase	0.18	0.46	2.56
At4g38550	phospholipase like protein	0.36	0.92	2.56
At5g08100	asparaginase	0.12	0.3	2.50
At4g26860	putative Proline synthetase associated protein	0.28	0.7	2.50

At5g11930	glutaredoxin - like protein	0.59	1.47	2.49
At5g15530	biotin carboxyl carrier protein precursor-like protein	0.33	0.82	2.48
At3g29320	alpha-glucan phosphorylase	0.31	0.77	2.48
At4g39000	putative endo-1	0.32	0.78	2.44
At2g15470	putative polygalacturonase	0.21	0.51	2.43
At5g18660	putative protein	0.35	0.85	2.43
At4g38970	putative fructose-bisphosphate aldolase	0.94	2.28	2.43
At1g12900	putative calcium-binding protein	0.57	1.38	2.42
At1g79480	hypothetical protein	0.31	0.75	2.42
At3g14440	9-cis-epoxycarotenoid dioxygenase	0.15	0.36	2.40
At1g31190	unknown protein	0.15	0.36	2.40
At5g65750	2-oxoglutarate dehydrogenase	0.15	0.36	2.40
At3g22960	pyruvate kinase	0.72	1.72	2.39
At2g33250	unknown protein	0.27	0.64	2.37
At4g23100	gamma-glutamylcysteine synthetase	0.74	1.73	2.34
At4g08790	nitrilase 1 like protein	0.12	0.28	2.33
At3g14050	putative GTP pyrophosphokinase	0.36	0.83	2.31
At2g43760	putative molybdopterin synthase large subunit	0.53	1.21	2.28
At1g05610	putative ADP-glucose pyrophosphorylase	0.11	0.25	2.27
At3g58610	ketol-acid reductoisomerase	0.24	0.54	2.25
At3g50270	anthranilate N-hydroxycinnamoyl/benzoyltransferase - like protein	0.45	1.01	2.24
At4g02260	putative GTP pyrophosphokinase	0.39	0.87	2.23
At4g35640	putative protein	0.14	0.31	2.21
At1g06410	trehalose-6-phosphate synthase	0.35	0.77	2.20
At4g16130	galactokinase like protein	0.77	1.69	2.19
At4g27600	carbohydrate kinase - like protein	0.62	1.35	2.18
At3g47390	putative protein	0.17	0.37	2.18
At4g34200	phosphoglycerate dehydrogenase - like protein	0.46	1	2.17
At5g13450	delta subunit of mitochondrial F1-ATPase	0.3	0.65	2.17
At5g08300	succinyl-CoA-ligase alpha subunit	0.31	0.67	2.16
At5g14980	lysophospholipase -like protein	0.27	0.58	2.15
At4g39940	adenosine-5-phosphosulfate-kinase	0.55	1.18	2.15
At3g25860	dihydrolipoamide S-acetyltransferase	0.4	0.85	2.13
At4g16590	cellulose synthase like protein	0.17	0.36	2.12
At4g00560	putative dTDP-6-deoxy-L-mannose-dehydrogenase	0.24	0.5	2.08
At5g46290	3-oxoacyl-[acyl-carrier-protein] synthase I precursor	0.54	1.11	2.06
At4g20230	terpene cyclase like protein	0.37	0.76	2.05
At5g62220	putative protein	0.49	1	2.04
At2g46090	unknown protein	0.26	0.53	2.04
At5g11650	lysophospholipase - like protein	0.32	0.65	2.03
At5g35790	glucose-6-phosphate dehydrogenase	0.32	0.65	2.03
At4g25080	magnesium-protoporphyrin IX methyltransferase - like protein	0.43	0.87	2.02
At3g56700	putative protein	0.23	0.46	2.00
At4g11010	nucleoside diphosphate kinase 3 (ndpk3)	0.36	0.72	2.00
At4g25970	putative phosphatidylserine decarboxylase	0.82	1.62	1.98
At4g00590	putative glycosylasparaginase	0.32	0.63	1.97
At4g37470	putative protein	0.27	0.53	1.96
At4g16800	enoyl-CoA hydratase	0.17	0.33	1.94
At1g15140	unknown protein	0.24	0.46	1.92
At4g18240	starch synthase-like protein	0.35	0.67	1.91
At5g08280	hydroxymethylbilane synthase	0.51	0.97	1.90

At1g73160	putative glycosyl transferase	0.39	0.74	1.90
At4g38460	geranylgeranyl pyrophosphate synthase-related protein	0.36	0.68	1.89
At2g28880	putative para-aminobenzoate synthase and glutamine amidotransferase	0.09	0.17	1.89
At4g33030	sulfolipid biosynthesis protein SQD1	0.15	0.28	1.87
At5g34930	putative protein	0.79	1.46	1.85
At1g22170	unknown protein	0.32	0.59	1.84
At4g10120	sucrose-phosphate synthase - like protein	0.56	1.03	1.84
At2g30020	putative protein phosphatase 2C	0.29	0.53	1.83
At3g07670	putative ribulose-1	0.22	0.4	1.82
At1g32900	starch synthase	0.3	0.54	1.80
At4g13430	putative protein	0.52	0.92	1.77
At3g58990	3-isopropylmalate dehydratase-like protein (small subunit)	1.06	1.87	1.76
At5g03650	1.4-alpha-glucan branching enzyme precursor	0.64	1.12	1.75
At2g28660	unknown protein	0.23	0.4	1.74
At3g02750	putative protein phosphatase-2C (PP2C)	0.53	0.92	1.74
At4g17360	phosphoribosylglycinamide formyltransferase-like protein	0.41	0.7	1.71
At1g07160	protein phosphatase 2C	0.19	0.32	1.68
At4g15870	delta-cadinene synthase like protein	0.78	1.3	1.67
At5g51460	trehalose-6-phosphate phosphatase	1.02	1.7	1.67
At4g39010	putative endo-1	0.41	0.68	1.66
At4g02780	ent-kaurene synthetase A - like protein	0.39	0.64	1.64
At3g22890	ATP sulfurylase	0.38	0.62	1.63
At2g33230	putative flavin-containing monooxygenase	0.54	0.88	1.63
At3g04790	putative ribose 5-phosphate isomerase	1.31	2.13	1.63
At2g02380	putative glutathione S-transferase	0.15	0.24	1.60
At3g55010	phosphoribosylformylglycinamidine cyclo-ligase precursor	0.36	0.57	1.58
At4g04610	5-adenylylsulfate reductase	1.07	1.69	1.58
At3g29200	chorismate mutase	0.14	0.22	1.57
At3g06860	fatty acid multifunctional protein (AtMFP2)	0.37	0.58	1.57
At2g23800	pregeranylgeranyl pyrophosphate synthase	0.23	0.36	1.57
At3g51160	GDP-D-mannose-4	0.34	0.53	1.56
At4g14680	ATP-sulfurylase	0.62	0.96	1.55
At4g19170	neoxanthin cleavage enzyme-like protein	1.16	1.78	1.53
At4g39210	glucose-1-phosphate adenylyltransferase (APL3)	0.3	0.45	1.50
At4g35630	phosphoserine aminotransferase	0.28	0.42	1.50
At4g10500	putative Fe(II)/ascorbate oxidase	0.63	0.92	1.46
At4g08900	arginase	0.24	0.35	1.46
At1g52420	hypothetical protein	0.48	0.7	1.46
At3g47930	L-galactono-1.4-lactone dehydrogenase - like protein	0.35	0.51	1.46
At2g17420	thioredoxin reductase	0.93	1.35	1.45
At2g40490	putative uroporphyrinogen decarboxylase	0.4	0.58	1.45
At3g59760	cysteine synthase	0.59	0.85	1.44
At1g06730	sugar kinase	0.25	0.36	1.44
At3g04000	putative short-chain type dehydrogenase/reductase	0.26	0.37	1.42
At2g16570	amidophosphoribosyltransferase	0.95	1.35	1.42
At5g04360	pullulanase-like protein (starch debranching enzyme)	0.17	0.24	1.41
At2g44050	7-dimethyl-8-ribityllumazine synthase precursor	0.41	0.57	1.39
At5g04590	sulphite reductase	0.57	0.79	1.39
At5g27380	glutathione synthetase gsh2	0.47	0.65	1.38
At4g20830	reticuline oxidase -like protein	0.79	1.09	1.38
At4g34740	amidophosphoribosyltransferase 2 precursor	0.95	1.31	1.38
At1g24500	unknown protein	0.32	0.44	1.38

At4g16700	decarboxylase like protein	0.92	1.26	1.37
At5g43830	aluminum-induced protein-like	0.19	0.26	1.37
At3g63340	putative protein	0.13	0.17	1.31
At5g49190	sucrose synthase	0.07	0.09	1.29
At4g02520	Atpm24.1 glutathione S transferase	1.37	0.97	0.71
At1g18500	2-isopropylmalate synthase	0.34	0.24	0.71
At4g18440	adenylosuccinate lyase - like protein	0.39	0.27	0.69
At1g56190	phosphoglycerate kinase	1.42	0.93	0.65
At4g19710	aspartate kinase-homoserine dehydrogenase - like protein	2.87	1.85	0.64
At4g08870	putative arginase	0.58	0.35	0.60
At1g29900	carbamoyl phosphate synthetase large chain (carB)	0.44	0.26	0.59
At2g41220	ferredoxin-dependent glutamate synthase (GLU2)	2.77	1.63	0.59
At1g25220	anthranilate synthase beta subunit	0.29	0.17	0.59
At1g18360	lysophospholipase homolog	0.14	0.08	0.57
At3g49680	branched-chain-amino-acid transaminase -like protein	0.59	0.32	0.54
At5g23440	putative protein	0.74	0.39	0.53
At3g26650	glyceraldehyde 3-phosphate dehydrogenase A subunit (GapA)	5	2.59	0.52
At1g80600	putative acetylornithine transaminase	0.27	0.13	0.48
At3g04870	putative zeta-carotene desaturase precursor	0.44	0.21	0.48
At5g19140	aluminium-induced protein - like	0.3	0.14	0.47
At2g43090	3-isopropylmalate dehydratase	1.62	0.75	0.46
At2g47730	glutathione S-transferase (GST6)	0.72	0.32	0.44
At2g31810	putative acetolactate synthase	0.84	0.34	0.40
At2g14750	putative adenosine phosphosulfate kinase	0.64	0.25	0.39
At5g09650	inorganic pyrophosphatase - like protein	0.18	0.07	0.39
At3g12780	phosphoglycerate kinase	14.41	3.83	0.27
At3g45140	lipoxygenase AtLOX2	2.34	0.62	0.26

Photosynthesis

At5g10000	PetF4; putative ferredoxin (0 mRNA)	0.42	1.89	4.50
At4g32260	AtpG; ATP synthase beta\\\' chain (old nomenclature: subunit II)	0.74	2.55	3.45
At1g29910	Lhcb1.2 (LHCP AB 180)	11.73	38.52	3.28
At4g14890	PetF5; ferredoxin (1 mRNA)	0.55	1.63	2.96
At2g30570	PsbW	10.04	27.85	2.77
At1g76570	putative Lhcb1 (similar to Petunia CAB 22R)	0.37	0.97	2.62
At1g15700	AtpC2; ATP synthase gamma subunit (1 mRNA)	0.28	0.66	2.36
At1g15820	Lhcb6 (CP24)	0.64	1.49	2.33
At1g03600	proteomics: putative new PSII subunit	0.49	1.06	2.16
At1g44575	PsbS protein	0.38	0.76	2.00
At4g17740	PSII D1 protein processing enzyme	0.27	0.52	1.93
At4g37230	PsbO-like; probably pseudogene	0.15	0.26	1.73
At4g15510	thylakoid lumenal 21.5 kDa protein (PsbP related)	0.42	0.72	1.71
At5g23120	HCF136	0.73	1.14	1.56
At1g10960	PetF2; ferredoxin precusor isolog (1 mRNA)	2.07	2.91	1.41
At4g10340	Lhcb5 (CP26)	2.61	1.87	0.72
At1g52230	PsaH2	1.06	0.75	0.71
At2g30790	PsbP2 (0 mRNA)	2.4	1.68	0.70
At2g20260	PsaE2 (2 mRNAs)	3.19	2.18	0.68
At3g27690	Lhcb2.4	39.85	26.97	0.68
At1g67740	PsbY	2.52	1.7	0.67
At1g20340	PetE2 (plastocyanin) (5 mRNAs)	1.2	0.76	0.63

At5g38430	ribulose bisphosphate carboxylase small chain 1b precursor (RuBisCO small subunit 1b)	67.35	42.54	0.63
psaA	plastid gene product; PSI-A	32.91	20.73	0.63
At3g54890	Lhca1	19.41	11.92	0.61
At1g08380	PsaO	11.66	6.79	0.58
At1g55490	Rubisco subunit binding-protein beta subunit	0.4	0.23	0.58
At1g06680	PsbP1 (3 mRNAs)	4.65	2.59	0.56
At4g28750	PsaE1 (2 mRNAs)	4.32	2.28	0.53
At5g54270	Lhcb3 chlorophyll a/b binding protein	10.8	5.6	0.52
At5g38420	ribulose bisphosphate carboxylase small chain 2b precursor (RuBisCO small subunit 2b)	64.27	32.92	0.51
At1g61520	Lhca3	10.62	5.43	0.51
At1g76100	PetE1 (plastocyanin) (0 mRNAs)	0.87	0.43	0.49
At3g50820	PsbO2	5.21	2.57	0.49
At3g08940	Lhcb4.2 (CP29)	2.6	1.28	0.49
At5g01530	Lhcb4.1 (CP29)	2.7	1.31	0.49
At1g29920	Lhcb1.1 (LHCP AB 160)	50.86	23.61	0.46
At1g67090	ribulose-bisphosphate carboxylase small unit	55.23	24.04	0.44
At1g79040	PsbR	14.87	6.17	0.41
At2g40100	Lhcb4.3 (CP29)	1.79	0.73	0.41
At3g47470	Lhca4	39.92	15.99	0.40
At1g60950	PetF1; ferredoxin precursor (3 mRNAs)	7.13	2.76	0.39
At4g02770	PsaD1 (4 mRNAs)	18.91	7.21	0.38
At4g21280	PsbQ1 (1 mRNA)	10.97	3.96	0.36
At3g56650	proteomics: thylakoid lumen protein	0.24	0.08	0.33
At2g34420	Lhcb1.5	62.21	20.08	0.32
At5g64040	PsaN	13.44	4.27	0.32
At1g03130	PsaD2 (4 mRNAs)	18.52	5.84	0.32
At2g34430	Lhcb1.4	65.99	20.71	0.31
At2g05100	Lhcb2.1 (oder Lhcb2.3)	33.56	10.05	0.30
At2g05070	Lhcb2.2	19.41	5.29	0.27
rbcL	plastid gene product; large subunit of Rubisco	197.31	53.17	0.27
At2g06520	PsbX	17.43	4.55	0.26
At1g55670	PsaG	14.89	3.83	0.26
At4g05180	PsbQ2 (1 mRNA)	18.31	3.9	0.21
At5g66570	PsbO1	29.11	5.03	0.17
At3g21055	PsbT1	10.23	1.63	0.16
At1g51400	PsbT2 (2 mRNAs)	13.01	1.83	0.14

Transport

At2g30460	putative integral membrane protein	0.2	4.25	21.25
At1g66950	ABC transporter	0.33	5.46	16.55
At3g47760	ABC-type transport protein-like protein	0.07	0.88	12.57
At1g47840	hexokinase	0.17	1.85	10.88
At1g10540	putative permease	0.02	0.19	9.50
At2g45770	putative signal recognition particle receptor (alpha subunit)	0.3	2.74	9.13
At5g12860	2-oxoglutarate/malate translocator (DiT1) protein	0.14	1.15	8.21
At1g09960	putative sucrose/H+ symporter	0.16	1.2	7.50
At1g15520	ABC transporter	0.14	0.91	6.50
At3g10350	putative ATPase	0.38	2.42	6.37
At4g01840	putative potassium channel	0.18	1.02	5.67
At1g64780	ammonium transporter	0.18	1.01	5.61

At1g51350	hypothetical protein	0.25	1.32	5.28
At4g36520	trichohyalin like protein	0.19	1	5.26
At4g32400	adenylate translocator (brittle-1) - like protein	0.21	1.1	5.24
At3g10290	putative protein	0.09	0.42	4.67
At5g13550	sulfate transporter	0.08	0.37	4.63
At2g32400	putative ligand-gated ion channel subunit	0.18	0.83	4.61
At1g06950	Tic110	0.2	0.92	4.60
At3g55150	putative protein	0.59	2.71	4.59
At1g59660	nucleoporin 98-like protein	0.16	0.73	4.56
At2g39190	putative ABC transporter	0.11	0.47	4.27
At3g47440	aquaporin-like protein	0.37	1.58	4.27
At1g78560	unknown protein	0.13	0.54	4.15
At1g04940	Tic20.2	0.2	0.82	4.10
At3g26570	chloroplast envelope-localized phosphate transporter	0.27	1.1	4.07
At4g21820	putative protein	0.2	0.81	4.05
At5g19500	putative protein	0.39	1.56	4.00
At2g17270	putative mitochondrial phosphate translocator protein	0.08	0.32	4.00
At2g29870	putative aquaporin (plasma membrane intrinsic protein)	0.36	1.39	3.86
At1g05450	lipid-transfer protein	0.19	0.72	3.79
At5g27100	ion channel - like protein	0.22	0.81	3.68
At4g37130	nucleoporin-like protein	0.18	0.66	3.67
At5g14040	mitochondrial phosphate translocator	0.27	0.98	3.63
At5g17630	chloroplast Xul-5-P/phosphate translocator (XPT)	0.42	1.52	3.62
At2g29100	putative ligand-gated ion channel protein	0.15	0.52	3.47
At1g59870	ABC transporter	0.16	0.55	3.44
At2g31020	putative oxysterol-binding protein	0.07	0.24	3.43
At2g29650	putative Na+-dependent inorganic phosphate cotransporter	0.15	0.51	3.40
At2g28070	putative ABC transporter	0.21	0.7	3.33
At2g43950	Tic22	0.36	1.13	3.14
At3g57180	putative protein	0.3	0.94	3.13
At1g15500	adenine nucleotide translocase	0.34	1.05	3.09
At4g37270	Cu2+-transporting ATPase-like protein	0.27	0.8	2.96
At2g26900	putative Na+ dependent ileal bile acid transporter	0.11	0.32	2.91
At1g26230	chaperonin precursor	0.16	0.46	2.88
At5g01500	putative protein	0.13	0.36	2.77
At5g64940	ABC transporter-like	0.85	2.35	2.76
At2g24820	Toc75	0.28	0.77	2.75
At1g10390	unknown protein	0.91	2.41	2.65
At2g38060	putative Na+-dependent inorganic phosphate cotransporter	0.25	0.66	2.64
At3g63130	RAN GTPase activating protein 1 protein	0.33	0.86	2.61
At5g03910	ABC transporter -like protein	0.34	0.88	2.59
At1g03060	putataive transport protein	0.24	0.62	2.58
At1g80830	metal ion transporter	0.23	0.58	2.52
At5g26980	tSNARE AtTLG2a	0.26	0.65	2.50
At1g05030	putative sugar transporter protein	0.25	0.62	2.48
At5g04770	amino acid transporter-like protein	0.38	0.94	2.47
At1g79360	hypothetical protein	0.26	0.64	2.46
At5g28750	Tha4 protein - like	0.26	0.62	2.38
At2g26650	K^+ transporter	0.34	0.81	2.38
At5g01490	Ca2+/H+ exchanger-like protein	0.11	0.25	2.27
At2g32390	putative ligand-gated ion channel subunit	0.39	0.88	2.26
At1g15210	putative ABC transporter	0.34	0.76	2.24
At2g17260	putative ligand-gated ion channel protein	0.61	1.34	2.20

At2g16980	putative tetracycline transporter protein	0.36	0.79	2.19
At3g23710	Tic22	0.46	1	2.17
At4g33350	Tic110	11.26	23.61	2.10
At1g08770	unknown protein	0.51	1.06	2.08
At5g43070	putative protein	0.46	0.94	2.04
At4g36580	ATPase-like protein	0.44	0.88	2.00
At4g04850	putative potassium transporter	0.17	0.34	2.00
At4g04770	putative ABC transporter	0.38	0.75	1.97
At2g02590	putative transport protein	0.27	0.52	1.93
At2g27810	putative membrane transporter	0.25	0.48	1.92
At5g03900	putative protein	0.28	0.53	1.89
At2g38330	hypothetical protein	0.33	0.61	1.85
At1g67800	unknown protein	0.34	0.61	1.79
At2g21020	putative major intrinsic (channel) protein	0.09	0.16	1.78
At3g03720	putative cationic amino acid transporter	0.17	0.3	1.76
At3g25410	unknown protein	0.37	0.65	1.76
At1g79380	unknown protein	0.69	1.18	1.71
At4g33520	metal-transporting P-type ATPase	0.98	1.66	1.69
At4g18290	potassium channel protein KAT2	0.19	0.32	1.68
At4g39460	mitochondrial carrier - like protein	0.41	0.69	1.68
At4g12770	auxilin-like protein	0.38	0.63	1.66
At3g07100	putative Sec24-like COPII protein	0.16	0.26	1.63
At2g34390	putative aquaporin (plasma membrane intrinsic protein)	0.34	0.52	1.53
At3g46980	putative protein	0.53	0.81	1.53
At3g25620	membrane transporter	0.2	0.3	1.50
At4g02510	Toc159	0.6	0.88	1.47
At3g44340	putative protein	0.18	0.26	1.44
At4g01800	putative SecA-type chloroplast protein transport factor	0.53	0.35	0.66
At5g52440	HCF106	1.43	0.67	0.47
At3g48850	mitochondrial phosphate transporter	1.58	0.72	0.46
At2g28900	OuterEnvelopeProtein24	0.92	0.37	0.40
At5g11480	putative GTP-binding protein	0.42	0.15	0.36

Protein phosphorylation

At4g15410	phosphatase like protein	0.38	5.51	14.50
At5g59220	protein phosphatase 2C - like	0.05	0.7	14.00
At4g32000	serine/threonine protein kinase like protein	0.08	1.1	13.75
At2g39660	putative protein kinase	0.1	0.99	9.90
At2g28930	putative protein kinase	0.07	0.53	7.57
At2g17265	homoserine kinase; 3-hydroxy-3-methylglutaryl-coenzyme A reductase 2	0.14	1.03	7.36
At3g08720	putative ribosomal-protein S6 kinase (ATPK19)	0.3	2.16	7.20
At5g18910	protein kinase - like protein	0.14	0.97	6.93
At3g19100	CDPK-related kinase	0.23	1.43	6.22
At2g41140	CPDK-related protein kinase	0.08	0.46	5.75
At4g02410	contains similarity to a protein kinase domain	0.58	3.17	5.47
At5g66210	calcium-dependent protein kinase	0.07	0.37	5.29
At4g23150	serine/threonine kinase - like protein	0.36	1.76	4.89
At2g46850	putative Ser/Thr protein kinase	0.19	0.88	4.63
At2g31500	putative calcium-dependent protein kinase	0.16	0.64	4.00
At3g44610	protein kinase-like protein	0.25	0.93	3.72
At4g21230	receptor kinase - like protein	0.21	0.78	3.71

At5g25930	receptor-like protein kinase - like	2.73	10.05	3.68
At5g13280	aspartate kinase	0.17	0.62	3.65
At5g36250	protein phosphatase-2C PP2C-like	0.2	0.72	3.60
At5g47750	protein kinase	0.28	0.95	3.39
At3g54930	protein phosphatase 2A regulatory subunit B\\\'-like protein	0.23	0.77	3.35
At5g19280	kinase associated protein phosphatase	0.12	0.4	3.33
At1g09840	shaggy-like protien kinase	0.17	0.55	3.24
At4g25390	receptor kinase-like protein	0.15	0.46	3.07
At1g11300	serine/threonine kinase	0.16	0.49	3.06
At2g18470	putative protein kinase	0.15	0.45	3.00
At2g39360	putative protein kinase	0.56	1.65	2.95
At3g44050	kinesin -like protein	0.25	0.71	2.84
At1g53700	auxin-induced protein kinase	0.33	0.9	2.73
At4g23180	serine/threonine kinase -like protein	0.58	1.55	2.67
At4g23130	protein kinase - like protein	0.41	1.09	2.66
At3g46920	protein kinase - like protein	0.08	0.21	2.63
At4g31220	protein kinase-like protein	0.23	0.59	2.57
At3g45670	putative protein kinase	0.49	1.23	2.51
At3g51990	putative serine/threonine protein kinase	0.14	0.35	2.50
At1g68690	protein kinase	0.29	0.67	2.31
At4g04570	receptor-like protein kinase	0.29	0.66	2.28
At4g38830	receptor-like protein kinase - like protein	0.41	0.93	2.27
At1g31160	putative protein kinase C inhibitor (Zinc-binding protein)	0.2	0.44	2.20
At4g23140	serine/threonine kinase - like protein	0.47	1.03	2.19
At2g23070	putative casein kinase II catalytic (alpha) subunit	0.37	0.81	2.19
At1g71860	protein tyrosine phosphatase	0.19	0.41	2.16
At1g23540	putative serine/threonine protein kinase	0.73	1.48	2.03
At1g18890	calcium-dependent protein kinase	0.48	0.94	1.96
At4g23280	serine /threonine kinase - like protein	0.66	1.29	1.95
At1g61610	receptor-like kinase	0.33	0.62	1.88
At2g23770	putative protein kinase	0.87	1.53	1.76
At3g18040	putative MAP kinase	0.44	0.76	1.73
At5g55910	serine/threonine-specific protein kinase ATPK64	0.73	1.26	1.73
At4g23190	serine/threonine kinase - like protein	0.37	0.63	1.70
At3g26940	protein kinase	0.22	0.37	1.68
At4g32710	putative protein kinase	0.37	0.62	1.68
At1g79250	serine/threonine protein kinase	0.67	1.12	1.67
At3g27580	serine/threonine-protein kinase	0.6	0.94	1.57
At4g16360	kinase like protein	0.24	0.36	1.50
At3g21220	MAP kinase kinase 5	0.52	0.75	1.44
At4g23200	serine /threonine kinase - like protein	0.65	0.92	1.42
At2g34180	putative protein kinase	0.66	0.93	1.41
At4g34440	putative serine/threonine protein kinase	0.3	0.42	1.40
At2g31800	putative protein kinase	0.33	0.46	1.39
At1g61550	receptor kinase	0.64	0.88	1.38
At1g61590	serine/threonine protein kinase	0.49	0.67	1.37
At5g63310	nucleotide diphosphate kinase Ia	0.32	0.43	1.34
At3g08760	putative protein kinase	0.66	0.48	0.73
At2g17220	putative protein kinase	0.56	0.38	0.68
At3g20410	calmodulin-domain protein kinase CDPK isoform 9	1.29	0.82	0.64
At2g30040	putative protein kinase	0.51	0.28	0.55
At1g32060	phosphoribulokinase precursor	3.75	1.59	0.42

Stress response

At3g44880	lethal leaf-spot 1 homolog Lls1	0.04	0.55	13.75
At4g26010	putative peroxidase	0.14	1.3	9.29
At1g09420	putative glucose-6-phosphate dehydrogenase	0.14	1.25	8.93
At5g11250	RPP1 disease resistance protein – like protein	0.09	0.68	7.56
At2g04030	putative heat shock protein	0.11	0.83	7.55
At4g37890	putative protein	0.22	1.58	7.18
At2g13810	putative aspartate aminotransferase	0.07	0.44	6.29
At2g22330	putative cytochrome P450	0.44	2.76	6.27
At5g59610	putative protein	0.1	0.57	5.70
At2g03740	putative cold-regulated protein	0.27	1.32	4.89
At5g05400	NBS/LRR disease resistance protein	0.15	0.71	4.73
At5g28100	putative protein	0.08	0.37	4.63
At1g71000	heat shock protein DnaJ	0.21	0.93	4.43
At4g31470	pathogenesis-related protein homolog	0.17	0.71	4.18
At4g31870	glutathione peroxidase - like protein	0.12	0.5	4.17
At4g19100	putative protein	0.11	0.44	4.00
At1g78490	cytochrome P450	0.36	1.43	3.97
At4g36150	putative disease resistance protein	0.39	1.49	3.82
At5g53460	NADH-dependent glutamate synthase	0.23	0.82	3.57
At2g03850	putative cold-regulated protein	0.08	0.28	3.50
At4g15910	drought-induced protein like	0.11	0.38	3.45
At4g28730	putative protein	0.16	0.55	3.44
At3g51570	propable disease resistance protein	0.26	0.88	3.38
At3g14490	terpene synthase-related protein	0.17	0.51	3.00
At5g48110	terpene synthase	0.29	0.85	2.93
At4g11170	RPP1-WsA-like disease resistance protein	0.48	1.38	2.88
At2g44800	putative flavonol synthase	0.15	0.42	2.80
At2g26790	putative salt-inducible protein	0.46	1.25	2.72
At3g18190	chaperonin subunit	0.21	0.57	2.71
At3g44670	disease resistance protein homlog	0.42	1.12	2.67
At2g32140	putative disease resistance protein	0.35	0.93	2.66
At2g23230	putative vetispiradiene synthase	1.24	3.22	2.60
At4g19660	putative protein	0.42	1	2.38
At4g08390	stromal ascorbate peroxidase	0.49	1.15	2.35
At3g04210	putative disease resistance protein	1.02	2.3	2.25
At5g18820	chaperonin 60 alpha chain - like protein	0.04	0.09	2.25
At5g15870	putative protein	0.41	0.92	2.24
At2g01610	unknown protein	0.36	0.79	2.19
At2g24210	putative limonene cyclase	0.11	0.24	2.18
At4g27670	heat shock protein 21	0.26	0.55	2.12
At5g17820	peroxidase ATP13a	0.09	0.18	2.00
At5g46470	disease resistance protein-like	0.34	0.65	1.91
At4g38660	putative thaumatin-like protein	0.32	0.6	1.88
At1g79460	ent-kaurene synthase	0.17	0.31	1.82
At4g14690	early light-induced protein ELIP.2 (Lil1.2)	0.4	0.72	1.80
At4g38670	putative thaumatin-like protein	0.4	0.72	1.80
At4g39960	DnaJ - like protein	0.49	0.87	1.78
At1g63880	putative disease resistance protein	0.49	0.86	1.76
At5g62360	DC1.2 homologue - like protein	0.67	1.15	1.72

At2g01480	axi 1-like protein	0.27	0.46	1.70
At1g68840	putative DNA-binding protein (RAV2-like)	0.9	1.45	1.61
At4g13270	hypothetical protein	0.55	0.88	1.60
At2g28190	putative chloroplast Cu/Zn superoxide dismutase (SOD)	0.07	0.11	1.57
At5g17680	disease resistance protein RPP1-WsB - like protein	0.57	0.88	1.54
At2g18940	putative salt-inducible protein	0.5	0.76	1.52
At3g23230	ethylene responsive element binding protein	0.7	1.02	1.46
At5g49910	heat shock protein 70	1.69	2.46	1.46
At2g18980	peroxidase (ATP22a)	1.02	1.38	1.35
At2g40000	putative nematode-resistance protein	1.95	1.28	0.66
At1g75380	wound-responsive protein	2.08	1.27	0.61
At2g25080	putative glutathione peroxidase	0.87	0.45	0.52
At4g05070	expressed protein	2.62	1.34	0.51
At1g77490	thylakoid-bound ascorbate peroxidase	0.31	0.14	0.45
At3g48100	response reactor 2 (ATRR2)	1.64	0.73	0.45
At2g42540	cold-regulated protein cor15a precursor	2.29	0.63	0.28
At2g42530	cold-regulated protein cor15b precursor	1.54	0.32	0.21
At3g05880	low temperature and salt responsive protein LTI6A	7.51	1.27	0.17

Transcription/Translation

At2g47680	putative ATP-dependent RNA helicase A	0.02	0.44	22.00
At4g31210	DNA topoisomerase like- protein	0.06	0.92	15.33
At2g19870	hypothetical protein	0.06	0.91	15.17
At4g19900	putative protein	0.55	7.21	13.11
At5g53920	ribosomal protein L11 methyltransferase-like protein	0.07	0.89	12.71
At5g38290	CRS2 -like protein	0.09	1	11.11
At1g32150	G-Box binding protein	0.07	0.5	7.14
At3g46440	dTDP-glucose 4-6-dehydratases-like protein	0.09	0.62	6.89
At3g62910	translation releasing factor RF-1 -like protein	0.11	0.75	6.82
At3g63140	mRNA binding protein precursor - like	0.08	0.51	6.38
At1g78160	putative RNA-binding protein	0.1	0.6	6.00
At2g40620	putative bZIP transcription factor	0.13	0.76	5.85
At1g01520	myb-related protein	0.08	0.46	5.75
At1g31220	putative phosphoribosylglycinamide formyltransferase	0.2	1.14	5.70
At4g27330	NOZZLE/SPOROCYTELESS	0.21	1.17	5.57
At2g36010	putative E2F5 family transcription factor	0.23	1.28	5.57
At2g38470	putative WRKY-type DNA-binding protein	0.15	0.83	5.53
At2g02070	putative C2H2-type zinc finger protein	2.18	11.69	5.36
At4g04350	putative leucyl tRNA synthetase	0.12	0.64	5.33
At3g54610	histon acetyltransferase HAT1	0.29	1.54	5.31
At4g16750	apetala2 domain TINY like protein	0.27	1.37	5.07
At2g44940	putative AP2 domain transcription factor	0.31	1.57	5.06
At2g42080	unknown protein	0.14	0.7	5.00
At2g38810	histone H2A	0.14	0.66	4.71
At2g37510	putative RNA-binding protein	0.17	0.8	4.71
At2g12900	putative VSF-1-like b-ZIP transcription factor	0.07	0.32	4.57
At1g79840	homeobox protein (GLABRA2)	0.1	0.45	4.50
At1g19890	histone H3	0.33	1.44	4.36
At1g17590	transcription factor	0.17	0.73	4.29
At5g15700	DNA-directed RNA polymerase (mitochondrial)	0.13	0.55	4.23
At3g22780	putative DNA binding protein	0.23	0.96	4.17

At1g47870	transcription factor	0.13	0.54	4.15
At1g13460	B\\\' regulatory subunit of protein phosphatase 2A	0.17	0.69	4.06
At1g05190	putative chloroplast ribosomal protein L6	0.3	1.16	3.87
At4g09050	putative protein	0.18	0.68	3.78
At5g02750	putative protein	0.44	1.66	3.77
At3g16280	putative AP2 domain transcription factor	0.25	0.94	3.76
At3g01470	homeobox-leucine zipper protein HAT5	0.28	1.04	3.71
At5g54090	DNA mismatch repair protein MutS2-like	0.3	1.11	3.70
At3g10690	putative DNA gyrase subunit A	0.2	0.72	3.60
At1g68730	putative transcription factor	0.33	1.18	3.58
At3g03710	putative polynucleotide phosphorylase	0.2	0.71	3.55
At5g02860	putative protein	0.44	1.54	3.50
At4g01310	putative chloroplast ribosomal protein L5	0.22	0.76	3.45
At4g17300	asparagine--tRNA ligase	0.35	1.2	3.43
At1g22660	putative tRNA adenylyltransferase	0.17	0.58	3.41
At4g30690	putative protein	0.29	0.98	3.38
At5g40950	putative chloroplast ribosomal protein L27	1.13	3.74	3.31
At2g04240	putative RING zinc finger protein	0.72	2.37	3.29
At4g20330	putative protein	0.15	0.48	3.20
At1g79080	hypothetical protein	0.23	0.73	3.17
At5g61470	putative protein	0.24	0.75	3.13
At5g59730	putative protein	0.1	0.31	3.10
At2g13150	putative bZIP transcription factor	0.25	0.77	3.08
At1g10480	zinc finger protein 5	0.24	0.73	3.04
At5g08070	putative helix-loop-helix DNA binding protein	0.38	1.14	3.00
At2g46590	putative DOF zinc finger protein	0.34	1.01	2.97
At1g63040	transcription factor DREB1A	0.19	0.56	2.95
At1g26370	hypothetical protein	0.18	0.53	2.94
At2g01440	putative ATP-dependent DNA helicase (RECG)	0.24	0.7	2.92
At2g15740	putative C2H2-type zinc finger protein	0.28	0.78	2.79
At5g49450	putative protein	0.56	1.54	2.75
At1g74970	putative ribosomal protein S9 (secretory pathway prediced)	0.16	0.44	2.75
At1g62680	PPR-repeat protein	0.2	0.55	2.75
At1g71720	putative chloroplast ribosomal protein S1	0.15	0.4	2.67
At2g22090	putative RNA-binding protein	0.41	1.09	2.66
At2g24050	putative eukaryotic initiation factor 4	0.25	0.66	2.64
At5g10370	putative protein	0.28	0.73	2.61
At1g30480	DNA damage repair protein	0.12	0.31	2.58
At1g75390	bZIP transcription factor ATB2	0.61	1.56	2.56
At2g24120	chloroplast single subunit DNA-dependent RNA polymerase	0.57	1.44	2.53
At1g29070	putative plastid ribosomal protein L34	0.23	0.58	2.52
At3g16350	putative MYB family transcription factor	0.36	0.9	2.50
At2g20060	putative chloroplast ribosomal protein L4	0.13	0.32	2.46
At2g18670	putative C3HC4-type RING zinc finger protein	0.22	0.54	2.45
At4g10030	putative protein	0.25	0.61	2.44
At1g08880	putative histone H2A	0.5	1.22	2.44
At3g54620	bZIP transcription factor -like protein	0.19	0.46	2.42
At1g68460	putative tRNA isopentenyl transferase	0.48	1.13	2.35
At2g34520	mitochondrial ribosomal protein S14	0.24	0.56	2.33
At1g06070	transcriptional activator RF2a	0.2	0.46	2.30
At2g18650	putative C3HC4-type RING zinc finger protein	0.58	1.31	2.26
At4g27340	putative protein	0.44	0.97	2.20

At3g03590	hypothetical protein	0.28	0.61	2.18
At2g14880	unknown protein	0.31	0.67	2.16
At3g13180	sun (RNA-binding) protein (fmu protein)	0.26	0.56	2.15
At4g25880	pumilio-like protein	0.26	0.56	2.15
At5g18560	AP2 domain -like protein	0.49	1.04	2.12
At4g25540	putative DNA mismatch repair protein	0.73	1.53	2.10
At5g51990	AP2 domain transcription factor-like protein	0.21	0.44	2.10
At3g19160	tRNA isopentenyl transferase	0.11	0.23	2.09
At4g00150	scarecrow-like 6 (SCL6)	0.55	1.15	2.09
At1g13970	hypothetical protein	0.33	0.68	2.06
At1g78630	putative chloroplast ribosomal protein L13	0.56	1.15	2.05
At1g50200	alanine--tRNA ligase	0.39	0.8	2.05
At4g21460	putative protein	0.58	1.18	2.03
At2g28450	putative RNA methyltransferase	0.32	0.65	2.03
At1g67770	putative ABC transporter	0.41	0.83	2.02
At2g03200	putative chloroplast nucleoid DNA-binding protein	0.5	1.01	2.02
At3g16080	putative chloroplast ribosomal protein (L37e signature)	0.83	1.63	1.96
At1g48490	transcription factor IRE	0.26	0.51	1.96
At2g37580	putative C3HC4-type RING zinc finger protein	0.54	1.05	1.94
At1g60000	nucleic acid-binding protein	0.47	0.91	1.94
At4g01280	putative myb-related DNA-binding protein	0.15	0.29	1.93
At1g54690	histone H2A	0.45	0.86	1.91
At3g52380	RNA-binding protein cp33 precursor	0.73	1.39	1.90
At4g14220	RING-H2 finger protein RHF1a	0.14	0.26	1.86
At1g52300	60S ribosomal protein L37	0.92	1.7	1.85
At1g80670	mRNA export protein	0.19	0.35	1.84
At4g39250	putative protein	0.26	0.47	1.81
At4g34290	putative protein	0.25	0.45	1.80
At2g34830	putative WRKY-type DNA-binding protein	0.39	0.7	1.79
At2g30320	putative pseudouridine synthase	0.67	1.16	1.73
At3g53920	sigma factor SigC	0.25	0.43	1.72
At2g13440	GIDA-like protein	0.45	0.76	1.69
At4g32040	homeodomain containing protein 1	0.48	0.8	1.67
At3g14890	DNA nick sensor	0.09	0.15	1.67
At1g29280	DNA binding protein	0.45	0.75	1.67
At4g00730	homeodomain protein AHDP	0.42	0.7	1.67
At3g01790	putative chloroplast ribosomal protein L13	0.41	0.68	1.66
At2g45330	unknown protein	0.32	0.53	1.66
At4g29060	putative protein	1.62	2.68	1.65
At1g68990	DNA-directed RNA polymerase (mitochondrial precursor)	0.55	0.9	1.64
At2g39380	hypothetical protein	0.49	0.8	1.63
At4g11120	putative translation elongation factor ts	0.24	0.39	1.63
At4g27230	histone H2A- like protein	0.61	0.98	1.61
At5g65350	histone H3	1.39	2.22	1.60
At1g73250	GDP-4-keto-6-deoxy-D-mannose-3	0.32	0.51	1.59
At2g21230	putative bZIP transcription factor	0.54	0.85	1.57
At4g34590	bZIP transcription factor ATB2	0.16	0.25	1.56
At4g20360	translation elongation factor EF-Tu precursor	0.32	0.49	1.53
At4g01250	putative DNA-binding protein	0.17	0.26	1.53
At1g68880	putative bZIP transcription factor	0.65	0.98	1.51
At3g52150	chloroplast ribosomal protein PSRP2	0.72	1.08	1.50
At2g01150	RING-H2 zinc finger protein (RHA2b)	1.09	1.62	1.49

At5g15390	rRNA methylase - like protein	0.4	0.59	1.48
At4g31180	aspartate--tRNA ligase - like protein	0.2	0.29	1.45
At4g04730	putative zinc finger protein	0.57	0.82	1.44
At5g10980	histon H3 protein	0.91	1.3	1.43
At1g64860	plastid RNA polymerase sigma-subunit (SIG2)	0.62	0.87	1.40
At3g09600	putative MYB-related protein	0.31	0.43	1.39
At4g29860	putative protein	0.21	0.29	1.38
At1g53670	transcriptional regulator	0.21	0.29	1.38
At2g07750	putative ATP-dependent RNA helicase	0.32	0.44	1.38
At2g38340	DREB-like AP2 domain transcription factor	0.23	0.31	1.35
At5g04600	RNA binding protein - like	0.12	0.16	1.33
At1g79850	chloroplast ribosomal protein S17; HCF60 (maize)	0.85	0.62	0.73
At1g66810	C-x8-C-x5-C-x3-H type Zinc finger protein	0.81	0.59	0.73
At5g50250	RNA-binding protein-like	1.14	0.81	0.71
At3g60490	transcription factor - like protein	0.23	0.16	0.70
At5g55300	DNA topoisomerase I	1.51	1.05	0.70
At4g24770	RNA-binding protein RNP-T precursor	3.36	2.24	0.67
At2g37220	putative RNA-binding protein	2.19	1.44	0.66
At1g02680	transcription factor TFIID	0.36	0.23	0.64
At1g74840	myb-related transcription activator	0.8	0.51	0.64
At1g03970	G-box binding factor	0.38	0.24	0.63
At4g17460	homeobox-leucine zipper protein HAT1	2.1	1.32	0.63
At3g20910	CCAAT-binding factor B chain	1.52	0.91	0.60
At5g14320	very similar to chloroplast ribosomal protein S13	3.7	2.16	0.58
At5g19210	eIF-4AII - like protein	0.11	0.06	0.55
At3g53460	RNA-binding protein cp29 protein	1.8	0.98	0.54
At1g09200	histone H3	2.31	1.24	0.54
rpoC1	plastid gene product; RNA polymerase	4.96	2.47	0.50
At5g62000	auxin response factor - like protein	0.65	0.32	0.49
At4g40040	Histon H3	2.88	1.39	0.48
At3g58120	putative protein	0.56	0.27	0.48
At2g24090	putative chloroplast ribosomal protein L35	0.79	0.37	0.47
At1g32990	chloroplast ribosomal protein L11	1.7	0.79	0.46
At4g16780	DNA-binding homeotic protein Athb-2	1.89	0.85	0.45
At3g27850	putative chloroplast 50S ribosomal protein L12-C	4.94	2.1	0.43
At2g33450	putative chloroplast ribosomal protein L28	2.61	0.97	0.37
At2g21660	glycine-rich RNA binding protein 7	18.94	6.12	0.32
At2g38140	chloroplast ribosomal protein PSRP4	0.09	0.02	0.22

unclassified

At4g27020	putative protein	0.45	10.64	23.64
At5g49590	putative protein	0.05	1.14	22.80
At4g20750	hypothetical protein	0.04	0.75	18.75
At4g13680	hypothetical protein	0.11	2.01	18.27
At3g49350	GTPase activating -like protein	0.03	0.54	18.00
At4g11980	putative protein	0.78	13.43	17.22
At1g35510	growth regulator	0.1	1.64	16.40
At4g03310	hypothetical protein	0.37	6.03	16.30
At4g11680	putative protein	0.56	8.41	15.02
At4g12390	putative protein	0.21	3.13	14.90
At1g50960	gibberellin 20-oxidase	0.04	0.57	14.25

At4g03150	hypothetical protein	0.07	0.99	14.14
At1g21670	hypothetical protein	0.02	0.28	14.00
At1g02060	unknown protein	0.16	2.11	13.19
At4g29670	thioredoxin-like protein	0.13	1.68	12.92
At3g20930	unknown protein	0.16	2.03	12.69
At4g26780	grpE like protein	0.87	10.81	12.43
At1g05530	putative UDP-glucose:indole-3-acetate beta-D-glucosyltransferase	1.57	19.24	12.25
At1g15070	unknown protein	0.41	4.94	12.05
At4g22920	hypothetical protein	0.09	1.08	12.00
At4g04370	hypothetical protein	0.1	1.17	11.70
At3g47650	putative protein	0.15	1.74	11.60
At5g40070	putative protein	0.15	1.7	11.33
At2g42750	unknown protein	0.07	0.78	11.14
At3g05970	putative long-chain-fatty-acid--CoA ligase	0.23	2.55	11.09
At1g23210	Hypothetical protein	0.05	0.54	10.80
At3g47860	putative protein	0.08	0.85	10.63
At5g36860	putative protein	0.18	1.91	10.61
At1g63610	unknown protein	0.12	1.27	10.58
At4g12000	putative protein	2.94	30.51	10.38
At3g20230	hypothetical protein	0.44	4.56	10.36
At2g34130	En/Spm-like transposon protein	0.23	2.38	10.35
At1g20070	hypothetical protein	0.32	3.31	10.34
At4g32060	putative protein	0.31	3.18	10.26
At1g32010	hypothetical protein	0.09	0.89	9.89
At4g18180	polygalacturonase-like protein	0.2	1.95	9.75
At2g46050	hypothetical protein	0.11	1.07	9.73
At2g23160	hypothetical protein	0.13	1.26	9.69
At2g45270	putative O-sialoglycoprotein endopeptidase	0.07	0.67	9.57
At1g20060	hypothetical protein	0.11	1.04	9.45
At5g48470	unknown protein	0.12	1.13	9.42
At5g65770	nuclear matrix constituent protein 1 (NMCP1)-like	0.22	2.07	9.41
At3g42490	putative protein	0.08	0.75	9.38
At1g22650	putative invertase	0.08	0.75	9.38
At5g24390	GTPase activator-like protein of Rab-like small GTPases	0.14	1.29	9.21
At1g68750	putative phosphoenolpyruvate carboxylase	0.06	0.55	9.17
At4g13070	putative protein	0.11	1	9.09
At4g07990	hypothetical protein	0.04	0.36	9.00
At3g17690	hypothetical protein	0.07	0.63	9.00
At1g19870	hypothetical protein	0.17	1.5	8.82
At5g35840	phytochrome C	0.33	2.89	8.76
At3g02620	putative stearoyl-acyl carrier protein desaturase	0.07	0.61	8.71
At4g08600	hypothetical protein	0.3	2.51	8.37
At5g65490	putative protein	0.03	0.25	8.33
At4g14330	kinesin like protein	0.11	0.91	8.27
At4g17070	hypothetical protein	0.75	6.16	8.21
At3g25680	hypothetical protein	0.1	0.8	8.00
At4g12620	origin recognition complex subunit 1 -like protein	0.07	0.56	8.00
At1g31080	hypothetical protein	0.06	0.48	8.00
At4g39550	putative protein	0.2	1.58	7.90
At3g14900	hypothetical protein	0.13	1.02	7.85
At2g17120	unknown protein	0.34	2.66	7.82

At5g57390	putative protein	0.58	4.51	7.78
At4g27510	hypothetical protein	0.08	0.62	7.75
At3g57440	hypothetical protein	0.11	0.84	7.64
At5g18260	putative protein	0.13	0.99	7.62
At2g04790	hypothetical protein	0.22	1.67	7.59
At4g37000	putative protein	0.12	0.91	7.58
At5g03040	putative protein	0.16	1.21	7.56
At4g22910	putative fizzy-related protein	0.09	0.68	7.56
At5g15510	putative protein	0.12	0.9	7.50
At1g30150	En/Spm-like transposon protein	0.11	0.82	7.45
At3g06020	hypothetical protein	0.09	0.66	7.33
At1g05690	hypothetical protein	0.27	1.98	7.33
At3g17950	hypothetical protein	0.12	0.87	7.25
At4g39030	putative protein	0.12	0.87	7.25
At5g23300	dihydroorotate dehydrogenase precursor	0.2	1.45	7.25
At2g37980	axi 1-like protein	0.04	0.29	7.25
At4g34790	putative protein	0.17	1.22	7.18
At1g27380	hypothetical protein	0.06	0.43	7.17
At4g29490	putative protein	0.07	0.5	7.14
At5g55210	putative protein	0.14	1	7.14
At2g26610	unknown protein	0.15	1.07	7.13
At2g44500	axi 1-like protein	0.27	1.92	7.11
At3g48110	glycine--tRNA ligase precursor	0.25	1.76	7.04
At2g44520	putative heme A: farnesyltransferase	0.12	0.84	7.00
At1g76220	hypothetical protein	0.2	1.4	7.00
At4g02790	hypothetical protein	0.1	0.7	7.00
At4g27250	putative protein	0.27	1.87	6.93
At5g42070	putative protein	0.13	0.89	6.85
At3g62520	putative protein	0.17	1.16	6.82
At5g60750	putative protein	0.11	0.75	6.82
At2g11100	pseudogene	0.32	2.16	6.75
At5g55710	putative protein	0.07	0.47	6.71
At1g47520	polyprotein	0.19	1.27	6.68
At5g43160	putative protein	0.06	0.4	6.67
At1g33780	hypothetical protein	0.21	1.4	6.67
At2g20920	unknown protein	0.14	0.93	6.64
At1g34000	putative protein	0.13	0.86	6.62
At5g65840	unknown protein	0.18	1.19	6.61
At5g50350	unknown protein	0.16	1.05	6.56
At3g12740	unknown protein	0.41	2.69	6.56
At1g59940	response regulator 3	0.27	1.77	6.56
At5g40470	putative protein	0.22	1.44	6.55
At3g58190	putative protein	0.06	0.39	6.50
At2g48090	unknown protein	0.17	1.1	6.47
At3g16310	unknown protein	0.21	1.35	6.43
At5g13820	H-protein promoter binding factor-1	0.14	0.9	6.43
At1g70710	endo-1	0.19	1.22	6.42
At5g13390	putative protein	0.17	1.09	6.41
At4g38610	putative protein	0.19	1.21	6.37
At2g39710	unknown protein	0.22	1.4	6.36
At4g02460	Similar to DNA mismatch repair protein	0.06	0.38	6.33

At1g59840	hypothetical protein	0.19	1.2	6.32
At4g24310	putative protein	0.2	1.26	6.30
At2g14530	hypothetical protein	0.18	1.13	6.28
At2g15760	hypothetical protein	0.11	0.69	6.27
At3g20920	hypothetical protein	0.08	0.5	6.25
At5g20730	putative protein	0.12	0.75	6.25
At1g75460	protease	0.64	3.99	6.23
At2g13870	En/Spm-like transposon protein	0.1	0.62	6.20
At1g75010	hypothetical protein	0.12	0.74	6.17
At5g65780	branched-chain amino acid aminotransferase	0.21	1.29	6.14
At4g36010	thaumatin-like protein	0.16	0.98	6.13
At4g13670	hypothetical protein	0.12	0.73	6.08
At2g33980	hypothetical protein	0.25	1.52	6.08
At4g11050	putative glucanase	0.13	0.79	6.08
At1g48510	cytochrome c oxidase assembly protein Surfeit 1	0.06	0.36	6.00
At5g48370	putative protein	0.16	0.95	5.94
At4g02290	putative endo-1	0.24	1.42	5.92
At4g39980	2-dehydro-3-deoxyphosphoheptonate aldolase	0.11	0.65	5.91
At1g49970	nClpP5	0.1	0.59	5.90
At3g54920	pectate lyase - like protein	1.16	6.84	5.90
At3g02040	hypothetical protein	0.6	3.52	5.87
At5g38190	putative protein	0.16	0.93	5.81
At3g05710	putative syntaxin protein	0.36	2.09	5.81
At4g17280	hypothetical protein	0.24	1.38	5.75
At5g14500	putative protein	0.16	0.92	5.75
At2g34020	unknown protein	0.19	1.09	5.74
At5g05460	putative protein	0.15	0.86	5.73
At4g17330	G2484-1 protein	0.38	2.17	5.71
At5g07900	putative protein	0.23	1.31	5.70
At4g31530	putative protein	11.34	64.15	5.66
At4g33500	putative protein	0.28	1.58	5.64
At1g62180	5\\\'-adenylylphosphosulfate reductase	0.24	1.35	5.63
At2g15820	unknown protein	1.6	8.93	5.58
At2g37000	unknown protein	0.14	0.78	5.57
At5g07540	glycine-rich protein atGRP-6	0.12	0.66	5.50
At5g10910	putative protein	0.18	0.99	5.50
At3g04680	unknown protein	0.11	0.6	5.45
At1g65080	hypothetical protein	0.16	0.87	5.44
At5g56050	unknown protein	0.16	0.87	5.44
At1g66670	ATP-dependent Clp protease (nClpP3)	0.07	0.38	5.43
At1g01550	hypothetical protein	0.25	1.35	5.40
At2g01580	hypothetical protein	0.19	1.02	5.37
At1g35420	unknown protein	0.17	0.91	5.35
At5g61440	thioredoxin-like 3	0.17	0.91	5.35
At5g04980	putative protein	0.12	0.64	5.33
At2g25860	hypothetical protein	0.16	0.85	5.31
At1g32760	unknown protein	0.27	1.43	5.30
At1g70990	hypothetical protein	0.27	1.43	5.30
At1g59590	hypothetical protein	0.18	0.95	5.28
At5g46560	unknown protein	0.18	0.95	5.28
At3g52070	putative protein	0.34	1.79	5.26
At2g33740	putative related to microbial divalent cation tolerance proteins	0.23	1.21	5.26

At2g37040	phenylalanine ammonia lyase (PAL1)	0.14	0.73	5.21
At5g54110	membrane associated protein	0.19	0.99	5.21
At5g56220	putative protein	0.1	0.52	5.20
At1g22110	hypothetical protein	0.1	0.52	5.20
At4g21170	putative protein	0.28	1.45	5.18
At2g39790	hypothetical protein	0.17	0.88	5.18
At2g30100	putative leucine-rich repeat protein	0.24	1.24	5.17
At1g27500	hypothetical protein	0.25	1.29	5.16
At3g12000	hypothetical protein	0.13	0.67	5.15
At1g75310	unknown protein	0.28	1.44	5.14
At5g05730	anthranilate synthase component I-1 precursor	0.08	0.41	5.13
At2g35450	unknown protein	0.2	1.02	5.10
At1g19920	sulfate adenylyltransferase	0.48	2.44	5.08
At2g47590	photolyase/blue-light receptor (PHR2)	0.12	0.61	5.08
At2g19240	hypothetical protein	0.25	1.27	5.08
At2g11380	pseudogene	0.22	1.11	5.05
At4g26220	caffeoyl-CoA O-methyltransferase - like protein	0.19	0.95	5.00
At1g79490	hypothetical protein	0.29	1.45	5.00
At1g12430	hypothetical protein	0.09	0.45	5.00
At2g25180	putative two-component response regulator protein	0.16	0.8	5.00
At2g38070	hypothetical protein	0.11	0.55	5.00
At4g10060	putative protein	0.23	1.15	5.00
At2g37880	hypothetical protein	0.17	0.85	5.00
At2g48140	unknown protein	0.15	0.74	4.93
At2g18820	putative non-LTR retroelement reverse transcriptase	0.14	0.69	4.93
At1g64890	unknown protein	0.12	0.59	4.92
At1g67980	putative S-adenosyl-L-methionine:trans-caffeoyl-Coenzyme A 3-O-methyltransferase	0.11	0.54	4.91
At2g01760	putative two-component response regulator protein	0.17	0.83	4.88
At1g08520	Mg-chelatase	0.19	0.92	4.84
At5g09840	putative protein	0.18	0.87	4.83
At4g00290	hypothetical protein	0.16	0.77	4.81
At1g31230	putative aspartate kinase-homoserine dehydrogenase	0.21	1.01	4.81
At2g35650	putative glucosyltransferase	0.21	1.01	4.81
At4g31590	putative protein	0.22	1.05	4.77
At4g20740	similarity to CRP1	0.13	0.62	4.77
At1g30700	putative reticuline oxidase-like protein	0.25	1.19	4.76
At5g61920	putative protein	0.22	1.04	4.73
At1g20510	hypothetical protein	0.58	2.74	4.72
At2g47670	putative pectinesterase	0.17	0.8	4.71
At5g58990	putative protein	0.17	0.8	4.71
At3g54160	putative protein	0.27	1.27	4.70
At1g72020	unknown protein	0.36	1.69	4.69
At3g17800	unknown protein	0.12	0.56	4.67
At3g50770	calmodulin-like protein	0.16	0.74	4.63
At2g44990	hypothetical protein	0.37	1.71	4.62
At1g65100	hypothetical protein	0.13	0.6	4.62
At2g31170	putative cysteinyl-tRNA synthetase	0.1	0.46	4.60
At1g65370	unknown protein	0.14	0.64	4.57
At4g39570	putative protein	0.27	1.23	4.56
At4g33170	putative protein	0.31	1.41	4.55
At1g34300	hypothetical protein	0.24	1.09	4.54

At1g75400	hypothetical protein	0.17	0.77	4.53
At1g62310	hypothetical protein	0.19	0.86	4.53
At1g43840	hypothetical protein	0.12	0.54	4.50
At3g52540	hypothetical protein	0.5	2.25	4.50
At4g17310	hypothetical protein	0.1	0.45	4.50
At3g21140	unknown protein	0.1	0.45	4.50
At4g12240	hypothetical proteins	0.14	0.63	4.50
At3g21865	unknown protein	0.35	1.57	4.49
At1g67810	putative protein	0.64	2.87	4.48
At1g24350	hypothetical protein	0.27	1.21	4.48
At2g42130	unknown protein	0.13	0.58	4.46
At3g09850	hypothetical protein	7.51	33.43	4.45
At2g24810	putative thaumatin-like pathogenesis-related protein	0.09	0.4	4.44
At4g22180	putative protein	0.25	1.11	4.44
At1g29410	phosphoribosylanthranilate isomerase	0.3	1.33	4.43
At2g47830	unknown protein	0.21	0.93	4.43
At4g39590	putative protein	0.28	1.24	4.43
At5g41380	putative protein	0.32	1.41	4.41
At3g56250	putative protein	0.15	0.66	4.40
At1g05140	unknown protein	0.62	2.72	4.39
At2g38450	unknown protein	0.21	0.92	4.38
At1g22850	unknown protein	0.16	0.7	4.38
At2g21590	putative ADP-glucose pyrophosphorylase large subunit	0.16	0.7	4.38
At3g19490	unknown protein	0.2	0.87	4.35
At4g21020	putative protein	0.29	1.26	4.34
At1g02260	hypothetical protein	0.4	1.73	4.33
At1g15850	mitotic checkpoint protein	0.23	0.99	4.30
At4g34100	putative protein	0.17	0.73	4.29
At2g17540	unknown protein	0.73	3.13	4.29
At4g16110	hypothetical protein	0.14	0.6	4.29
At2g37100	hypothetical protein	0.29	1.24	4.28
At2g23330	putative retroelement pol polyprotein	0.22	0.94	4.27
At4g27030	putative protein	0.22	0.94	4.27
At1g50770	hypothetical protein	0.19	0.81	4.26
At2g26930	putative ripening-associated protein	0.12	0.51	4.25
At4g29540	UDP-N-acetylglucosamine O-acyltransferase - like protein	0.09	0.38	4.22
At3g22700	hypothetical protein	0.14	0.59	4.21
At2g47390	unknown protein	0.19	0.8	4.21
At1g55440	hypothetical protein	0.15	0.63	4.20
At2g36680	unknown protein	0.21	0.88	4.19
At3g01370	unknown protein	0.17	0.71	4.18
At5g35150	putative protein	0.23	0.96	4.17
At3g61870	putative protein	0.24	1	4.17
At1g27510	unknown protein	0.18	0.75	4.17
At1g64150	unknown protein	0.12	0.5	4.17
At4g02040	hypothetical protein	0.13	0.54	4.15
At1g21600	unknown protein	0.13	0.54	4.15
At1g09970	unknown protein	0.2	0.83	4.15
At5g57670	putative protein	0.21	0.87	4.14
At4g09620	putative protein	0.35	1.45	4.14
At2g34790	putative berberine bridge enzyme	0.08	0.33	4.13
At1g07900	unknown protein	0.08	0.33	4.13

At2g41950	hypothetical protein	0.24	0.99	4.13
At4g18570	hypothetical protein	0.27	1.11	4.11
At4g10750	putative aldolase	0.32	1.31	4.09
At3g24810	unknown protein	0.11	0.45	4.09
At3g04650	unknown protein	0.35	1.43	4.09
At4g08330	putative protein	0.13	0.53	4.08
At5g13800	putative protein	0.29	1.18	4.07
At4g30910	leucyl aminopeptidase - like protein (partial)	0.29	1.18	4.07
At1g73150	hypothetical protein	0.15	0.61	4.07
At5g50390	selenium-binding protein-like	0.16	0.65	4.06
At1g48990	hypothetical protein	0.17	0.69	4.06
At2g27290	hypothetical protein	13.04	52.71	4.04
At5g65250	unknown protein	0.24	0.97	4.04
At1g78110	unknown protein	0.74	2.99	4.04
At4g27580	putative protein	0.26	1.05	4.04
At5g07110	putative protein	0.1	0.4	4.00
At5g43780	ATP sulfurylase precursor	0.12	0.48	4.00
At2g38500	hypothetical protein	0.15	0.6	4.00
At5g24000	putative protein	0.12	0.48	4.00
At2g17240	unknown protein	0.14	0.56	4.00
At1g04620	unknown protein	0.08	0.32	4.00
At5g52020	putative protein	0.12	0.48	4.00
At1g44110	mitotic cyclin a2-type	0.16	0.64	4.00
At3g15780	unknown protein	0.23	0.91	3.96
At4g08650	hypothetical protein	0.44	1.74	3.95
At3g06180	unknown protein	0.37	1.46	3.95
At4g02740	hypothetical protein	0.15	0.59	3.93
At1g32080	hypothetical protein	0.15	0.59	3.93
At4g22320	hypothetical protein	0.14	0.55	3.93
At3g49170	putative protein	0.27	1.06	3.93
At3g17550	hypothetical protein	0.12	0.47	3.92
At5g51200	putative protein	0.12	0.47	3.92
At2g41460	DNA-(apurinic or apyrimidinic site) lyase (ARP)	0.11	0.43	3.91
At3g47200	putative protein	0.1	0.39	3.90
At2g31720	hypothetical protein	0.2	0.78	3.90
At2g30490	cinnamate-4-hydroxylase	0.3	1.17	3.90
At1g09830	putative phosphoribosylglycinamide synthetase	0.48	1.87	3.90
At4g16250	phytochrome D	0.36	1.4	3.89
At5g20640	putative protein	0.18	0.7	3.89
At2g32040	unknown protein	0.42	1.63	3.88
At5g57930	putative protein	0.42	1.63	3.88
At2g24630	putative glucosyltransferase	0.57	2.21	3.88
At3g20490	hypothetical protein	0.16	0.62	3.88
At5g28430	putative protein	0.15	0.58	3.87
At3g55800	sedoheptulose-bisphosphatase precursor	0.21	0.81	3.86
At2g34620	hypothetical protein	0.21	0.81	3.86
At1g16160	hypothetical protein	0.07	0.27	3.86
At2g41660	hypothetical protein	0.27	1.04	3.85
At2g27360	putative lipase	0.19	0.73	3.84
At1g52550	hypothetical protein	0.38	1.46	3.84
At1g11470	hypothetical protein	0.17	0.65	3.82

At1g51550	hypothetical protein	0.16	0.61	3.81
At3g30190	hypothetical protein	0.21	0.8	3.81
At1g27210	unknown protein	1.71	6.51	3.81
At4g39620	putative protein	0.15	0.57	3.80
At1g54570	hypothetical protein	0.14	0.53	3.79
At5g15280	putative protein	0.18	0.68	3.78
At2g33100	putative cellulose synthase	0.84	3.17	3.77
At1g79760	hypothetical protein	0.22	0.83	3.77
At2g41040	hypothetical protein	0.35	1.32	3.77
At2g15290	unknown protein	0.21	0.79	3.76
At1g09720	hypothetical protein	0.2	0.75	3.75
At2g43400	putative electron transfer flavoprotein ubiquinone oxidoreductase	0.2	0.75	3.75
At1g69090	hypothetical protein	0.2	0.75	3.75
At1g51080	hypothetical protein	0.26	0.97	3.73
At2g35600	hypothetical protein	0.18	0.67	3.72
At4g17650	putative protein	0.14	0.52	3.71
At4g24910	putative protein	0.24	0.89	3.71
At4g31510	putative protein	0.3	1.11	3.70
At4g18540	hypothetical protein	0.33	1.22	3.70
At4g19490	putative protein	0.19	0.7	3.68
At2g40400	unknown protein	0.28	1.03	3.68
At1g47720	hypothetical protein	0.12	0.44	3.67
At1g12980	hypothetical protein	0.41	1.5	3.66
At4g37420	putative protein	0.26	0.95	3.65
At5g48730	putative protein	0.31	1.13	3.65
At5g42680	putative protein	0.53	1.93	3.64
At4g12060	putative protein	0.25	0.91	3.64
At3g01550	putative phosphate/phosphoenolpyruvate (PPT) translocator	0.13	0.47	3.62
At3g49660	putative WD-40 repeat - protein	0.05	0.18	3.60
At3g19120	hypothetical protein	0.22	0.79	3.59
At3g22550	unknown protein	0.22	0.79	3.59
At1g73470	expressed protein	0.62	2.22	3.58
At5g19000	putative protein	0.47	1.68	3.57
At1g79220	hypothetical protein	0.42	1.5	3.57
At1g18170	unknown protein	0.14	0.5	3.57
At3g47100	hypothetical protein	0.14	0.5	3.57
At2g29630	putative thiamin biosynthesis protein	0.16	0.57	3.56
At5g44780	unknown protein	0.25	0.89	3.56
At1g49380	hypothetical protein	0.34	1.21	3.56
At1g03810	hypothetical protein	0.29	1.03	3.55
At1g06280	hypothetical protein	0.17	0.6	3.53
At4g25060	hypothetical protein	0.38	1.34	3.53
At4g01770	hypothetical protein	0.21	0.74	3.52
At1g22040	hypothetical protein	0.27	0.95	3.52
At3g56010	putative protein	0.16	0.56	3.50
At1g21710	8-oxoguanine DNA glycosylase-like protein	0.26	0.91	3.50
At4g00650	hypothetical protein	0.18	0.63	3.50
At1g75260	unknown protein	0.2	0.7	3.50
At2g34700	putative proline-rich glycoprotein	0.1	0.35	3.50
At3g18770	unknown protein	0.2	0.7	3.50
At3g59300	putative protein	0.1	0.35	3.50

At2g39020	unknown protein	0.28	0.98	3.50
At2g26680	unknown protein	0.2	0.7	3.50
At1g61980	hypothetical protein	0.31	1.08	3.48
At1g61800	glucose-6-phosphate/phosphate-translocator (GPT) precursor-like	0.31	1.08	3.48
At2g20600	hypothetical protein	0.23	0.8	3.48
At2g26580	hypothetical protein	0.15	0.52	3.47
At4g26160	thioredoxin	0.13	0.45	3.46
At4g13200	putative protein	0.24	0.83	3.46
At4g22560	putative protein	0.22	0.76	3.45
At3g01670	unknown protein	0.2	0.69	3.45
At4g11910	putative protein	0.2	0.69	3.45
At1g10470	putative response regulator 3	0.29	1	3.45
At1g61970	hypothetical protein	0.34	1.17	3.44
At1g53000	CMP-KDO synthetase	0.25	0.86	3.44
At1g55630	hypothetical protein	0.21	0.72	3.43
At2g41680	thioredoxin reductase	0.21	0.72	3.43
At5g09570	putative protein	0.14	0.48	3.43
At4g35690	putative protein	0.26	0.89	3.42
At5g52010	putative protein	0.31	1.06	3.42
At2g31480	hypothetical protein	0.24	0.82	3.42
At2g34050	hypothetical protein	0.12	0.41	3.42
At1g62110	hypothetical protein	0.22	0.75	3.41
At3g21580	hypothetical protein	0.2	0.68	3.40
At3g03580	hypothetical protein	0.2	0.68	3.40
At1g75690	unknown protein	0.99	3.36	3.39
At5g56250	unknown protein	0.23	0.78	3.39
At2g07370	unknown protein	0.22	0.74	3.36
At2g32990	putative glucanse	0.11	0.37	3.36
At5g11450	putative protein	0.25	0.84	3.36
At2g42920	hypothetical protein	0.37	1.24	3.35
At2g01140	putative fructose-bisphosphate aldolase	0.35	1.17	3.34
At1g07310	unknown protein	0.39	1.3	3.33
At1g73740	putative UDP-N-acetylglucosamine--N-acetylmuramyl-(pentapeptide)-pyrophosphoryl-undecapren	0.3	1	3.33
At3g18870	hypothetical protein	0.31	1.03	3.32
At5g62840	putative protein	0.28	0.93	3.32
At2g19490	putative recA protein	0.22	0.73	3.32
At4g20090	membrane-associated salt-inducible-like protein	1.42	4.71	3.32
At2g39830	hypothetical protein	0.13	0.43	3.31
At3g02610	putative stearoyl-acyl carrier protein desaturase	0.2	0.66	3.30
At2g36000	hypothetical protein	0.24	0.79	3.29
At3g11960	hypothetical protein	0.07	0.23	3.29
At1g69690	unknown protein	0.35	1.15	3.29
At1g15710	embryo abundance protein (EMB20)	0.07	0.23	3.29
At3g03050	putative cellulose synthase catalytic subunit	0.29	0.95	3.28
At4g02330	hypothetical protein	0.4	1.31	3.28
At5g10160	(3R)-hydroxymyristoyl-[acyl carrier protein] dehydratase -like protein	0.11	0.36	3.27
At1g80560	putative 3-isopropylmalate dehydrogenase	0.15	0.49	3.27
At5g64150	putative protein	0.2	0.65	3.25
At1g32540	zinc-finger protein	0.2	0.65	3.25
At2g22410	hypothetical protein	0.16	0.52	3.25

At3g46050	putative protein	0.45	1.46	3.24
At4g14770	hypothetical protein	0.46	1.49	3.24
At1g77250	hypothetical protein	0.26	0.84	3.23
At4g22760	predicted protein	0.13	0.42	3.23
At1g51100	hypothetical protein	0.18	0.58	3.22
At5g61950	putative protein	0.09	0.29	3.22
At5g39210	hypothetical protein	0.32	1.03	3.22
At4g22430	putative protein	0.14	0.45	3.21
At2g26850	unknown protein	0.29	0.93	3.21
At1g51150	hypothetical protein	0.15	0.48	3.20
At4g36910	putative protein	0.2	0.64	3.20
At5g52110	putative protein	0.2	0.64	3.20
cob	mitochondrial gene; cytochrome b	0.57	1.82	3.19
At3g46880	hypothetical protein	0.22	0.7	3.18
At1g67910	hypothetical protein	0.17	0.54	3.18
At3g23940	dihydroxyacid dehydratase	0.34	1.08	3.18
At5g02830	putative protein	0.17	0.54	3.18
At1g80230	cytochrome c oxidase subunit	0.23	0.73	3.17
At1g65410	hypothetical protein	0.29	0.92	3.17
At1g34590	hypothetical protein	0.06	0.19	3.17
At3g22160	unknown protein	0.12	0.38	3.17
At1g48620	unknown protein	0.12	0.38	3.17
At1g78080	AP2 domain containing protein	0.45	1.42	3.16
At1g48950	hypothetical protein	0.13	0.41	3.15
At5g49020	arginine methyltransferase-like protein	0.46	1.45	3.15
At1g65070	hypothetical protein	0.27	0.85	3.15
At4g25290	hypothetical protein	0.21	0.66	3.14
At3g63170	hypothetical protein	0.14	0.44	3.14
At5g15260	putative protein	0.15	0.47	3.13
At1g65500	unknown protein	0.15	0.47	3.13
At5g12900	putative protein	0.23	0.72	3.13
At3g09070	unknown protein	0.23	0.72	3.13
At3g02930	unknown protein	0.25	0.78	3.12
At5g02050	putative protein	0.17	0.53	3.12
At2g14620	putative endoxyloglucan glycosyltransferase	0.18	0.56	3.11
At5g58210	similar to unknown protein	0.19	0.59	3.11
At1g18680	unknown protein	0.78	2.42	3.10
At3g03880	hypothetical protein	0.59	1.83	3.10
At2g47910	unknown protein	0.2	0.62	3.10
At1g08050	unknown protein	0.1	0.31	3.10
At2g26920	unknown protein	0.21	0.65	3.10
At1g24130	hypothetical protein	0.43	1.33	3.09
At3g21810	unknown protein	0.11	0.34	3.09
At2g26520	hypothetical protein	0.34	1.05	3.09
At1g04360	hypothetical protein	0.13	0.4	3.08
At3g51820	chlorophyll synthetase	0.27	0.83	3.07
At4g00870	expressed protein	0.28	0.86	3.07
At2g30370	hypothetical protein	0.17	0.52	3.06
At2g22230	putative beta-hydroxyacyl-ACP dehydratase	0.17	0.52	3.06
At2g47290	hypothetical protein	0.35	1.07	3.06
At4g17440	hypothetical protein	0.55	1.68	3.05

At2g16460	unknown protein	0.81	2.47	3.05
At5g26850	putative protein	0.22	0.67	3.05
At1g11810	hypothetical protein	0.22	0.67	3.05
At3g50880	putative DNA-3-methyladenine glycosidase	0.22	0.67	3.05
At2g20090	unknown protein	0.23	0.7	3.04
At1g60790	hypothetical protein	0.25	0.76	3.04
At2g02770	unknown protein	0.28	0.85	3.04
At2g17600	unknown protein	0.39	1.18	3.03
At3g21290	unknown protein	0.12	0.36	3.00
At2g01110	TatC-like protein	0.13	0.39	3.00
At1g10522	expressed protein	0.08	0.24	3.00
At5g51110	putative protein	0.25	0.75	3.00
At5g54810	tryptophan synthase beta chain 1 precursor	0.32	0.96	3.00
At5g08010	putative protein	0.25	0.75	3.00
At3g20830	unknown protein	0.17	0.51	3.00
At3g11670	digalactosyldiacylglycerol synthase	0.12	0.36	3.00
At3g27740	carbamoyl phosphate synthetase small subunit	0.16	0.48	3.00
At4g37380	putative protein	0.28	0.84	3.00
At1g10830	unknown protein	0.44	1.31	2.98
At1g76240	hypothetical protein	0.43	1.28	2.98
At3g22430	hypothetical protein	0.3	0.89	2.97
At3g19170	metalloprotease	0.22	0.65	2.95
At3g50530	CDPK-related protein kinase	0.39	1.15	2.95
At5g49120	putative protein	0.36	1.06	2.94
At5g18810	Serine/arginine rich protein - like	0.71	2.09	2.94
At4g08670	putative lipid transfer protein	0.17	0.5	2.94
At1g64880	hypothetical protein	0.33	0.97	2.94
At3g18420	unknown protein	0.31	0.91	2.94
At5g03470	AtB\\\'alpha regulatory subunit of PP2A	0.3	0.88	2.93
At2g32920	putative protein disulfide isomerase	0.44	1.29	2.93
At1g74730	unknown protein	0.14	0.41	2.93
At2g22890	unknown protein	0.48	1.4	2.92
At1g76730	hypothetical protein	0.24	0.7	2.92
At3g52190	putative protein	0.11	0.32	2.91
At1g12760	unknown protein	0.33	0.96	2.91
At3g17700	hypothetical protein	0.09	0.26	2.89
At2g32210	unknown protein	0.44	1.27	2.89
At1g47730	hypothetical protein	0.4	1.15	2.88
At3g52490	putative protein	0.4	1.15	2.88
At1g14840	unknown protein	0.23	0.66	2.87
At2g38970	putative retroelement pol polyprotein	0.15	0.43	2.87
At2g26840	unknown protein	0.22	0.63	2.86
At2g47840	hypothetical protein	0.21	0.6	2.86
At1g67080	unknown protein	0.38	1.08	2.84
At5g18570	GTP-binding protein obg -like	0.55	1.56	2.84
At5g14970	seed maturation -like protein	0.24	0.68	2.83
At1g50420	scarecrow-like 3	0.3	0.85	2.83
At5g16830	syntaxin homologue	0.18	0.51	2.83
At1g73110	rubisco activase	0.41	1.16	2.83
At1g55800	unknown protein	0.23	0.65	2.83
At2g37090	unknown protein	0.23	0.65	2.83

At5g46580	putative protein	0.17	0.48	2.82
At1g04570	hypothetical protein	0.16	0.45	2.81
At4g23450	putative protein	0.21	0.59	2.81
At3g45850	kinesin-related protein - like	0.15	0.42	2.80
At2g21960	putative protein	0.15	0.42	2.80
At3g55250	putative protein	0.24	0.67	2.79
At2g28755	putative dTDP-glucose 4-6-dehydratase	0.19	0.53	2.79
At2g39670	unknown protein	0.19	0.53	2.79
At5g54180	putative protein	0.45	1.25	2.78
At2g31350	putative glyoxalase II	0.44	1.22	2.77
At5g55980	unknown protein	0.26	0.72	2.77
At4g18760	putative protein	0.26	0.72	2.77
At4g24460	hypothetical protein	0.3	0.83	2.77
At2g26550	heme oxygenase 2 (HO2)	0.47	1.3	2.77
At4g28840	putative protein	0.17	0.47	2.76
At2g02500	putative sugar nucleotide phosphorylase	0.17	0.47	2.76
At1g10510	unknown protein	0.12	0.33	2.75
At3g02450	cell division protein FtsH-like protein	0.28	0.77	2.75
At2g44040	unknown protein	0.32	0.88	2.75
At3g10100	hypothetical protein	0.3	0.82	2.73
At2g28790	putative thaumatin	0.15	0.41	2.73
At4g22660	putative protein	0.37	1.01	2.73
At1g68070	putative RING zinc finger protein	0.22	0.6	2.73
At1g74220	hypothetical protein	0.33	0.9	2.73
At3g56410	putative protein	0.33	0.9	2.73
At2g44920	proteomics: thylakoid lumen protein with pentapeptide repeat	0.22	0.6	2.73
At5g61450	putative protein	0.18	0.49	2.72
At3g46790	putative protein	0.32	0.87	2.72
At4g23230	putative protein	0.28	0.76	2.71
At3g02410	hypothetical protein	0.07	0.19	2.71
At5g63390	auxin-independent growth promoter-like protein	0.14	0.38	2.71
At5g14840	putative protein	0.45	1.22	2.71
At4g26310	putative protein	0.38	1.03	2.71
At1g49840	unknown protein	0.24	0.65	2.71
At5g45980	putative protein	0.17	0.46	2.71
At4g34310	hypothetical protein	0.3	0.81	2.70
At5g17840	putative protein	0.1	0.27	2.70
At5g50210	putative protein	0.32	0.86	2.69
At2g28390	hypothetical protein	0.35	0.94	2.69
At4g37200	HCF164; thiol-disulfide interchange like protein	0.35	0.94	2.69
At5g44820	putative protein	0.19	0.51	2.68
At4g22190	hypothetical protein	0.38	1.02	2.68
At5g39410	unknown protein	0.25	0.67	2.68
At4g39970	putative protein	0.37	0.99	2.68
At5g07760	putative protein	0.77	2.06	2.68
At1g51780	hypothetical protein	0.64	1.71	2.67
At4g34830	putative protein	0.15	0.4	2.67
At1g43920	hypothetical protein	0.3	0.8	2.67
At4g19160	putative protein	0.18	0.48	2.67
2827716	predicted protein	0.17	0.45	2.65
At2g14120	dynamin-like protein	0.42	1.11	2.64

At4g16490	hypothetical protein	0.53	1.4	2.64
At3g14940	phosphoenolpyruvate carboxylase (PPC)	0.25	0.66	2.64
At4g00060	hypothetical protein	0.25	0.66	2.64
At3g11490	putative rac GTPase activating protein	0.49	1.29	2.63
At1g50020	tubulin alpha-6 chain	0.19	0.5	2.63
At2g45580	putative cytochrome P450	0.27	0.71	2.63
At5g58560	putative protein	0.08	0.21	2.63
At3g16260	hypothetical protein	0.24	0.63	2.63
At2g45870	hypothetical protein	0.4	1.05	2.63
At5g07890	putative protein	0.32	0.84	2.63
At2g18500	hypothetical protein	0.26	0.68	2.62
At1g70470	hypothetical protein	0.49	1.28	2.61
At5g02850	putative protein	0.28	0.73	2.61
At2g40760	unknown protein	0.35	0.91	2.60
At5g57030	lycopene epsilon cyclase	0.32	0.83	2.59
At2g34470	putative urease accessory protein	0.27	0.7	2.59
At3g44720	putative chloroplast prephenate dehydratase	0.34	0.88	2.59
At3g04550	unknown protein	0.26	0.67	2.58
At4g25720	glutamine cyclotransferase precursor - like protein	0.61	1.57	2.57
At1g27660	hypothetical protein	0.21	0.54	2.57
At1g17210	hypothetical protein	0.14	0.36	2.57
At1g07990	unknown protein	0.14	0.36	2.57
At3g04440	hypothetical protein	0.3	0.77	2.57
At1g65260	HCF155; Similar to chloroplast membrane-associated 30KD protein precursor (IM30)	0.53	1.36	2.57
At1g31790	hypothetical protein	0.62	1.59	2.56
At2g21370	putative xylulose kinase	0.16	0.41	2.56
At4g24930	proteomics: thylakoid lumen protein	0.25	0.64	2.56
At2g22210	pseudogene	0.25	0.64	2.56
At3g06590	unknown protein	0.4	1.02	2.55
At3g44570	putative protein	0.31	0.79	2.55
At3g16290	putative FtsH-like metalloprotease	0.53	1.35	2.55
3249106	unknown protein	0.44	1.12	2.55
At5g56760	serine O-acetyltransferase Sat-52	0.3	0.76	2.53
At5g59400	putative protein	0.15	0.38	2.53
At4g24840	brefeldin A-sensitive Golgi protein - like	0.15	0.38	2.53
At2g38270	unknown protein	0.74	1.87	2.53
At5g23540	26S proteasome	0.25	0.63	2.52
At4g35390	putative protein	0.56	1.41	2.52
At5g04490	putative protein	0.1	0.25	2.50
At4g30710	putative protein	0.18	0.45	2.50
At2g14910	unknown protein	0.24	0.6	2.50
At1g30920	F17F8.21	0.54	1.35	2.50
At1g15390	hypothetical protein	0.18	0.45	2.50
At4g24860	putative protein	0.26	0.65	2.50
At1g27610	hypothetical protein	0.55	1.37	2.49
At5g12150	putative protein	0.23	0.57	2.48
At1g10450	unknown protein	0.21	0.52	2.48
At3g16000	myosin heavy chain-like protein	0.21	0.52	2.48
At3g02875	IAA-amino acid hydrolase (ILR1)	0.72	1.78	2.47
At3g45890	putative protein	0.47	1.16	2.47
At2g28980	putative non-LTR retroelement reverse transcriptase	0.15	0.37	2.47

At1g27540	unknown protein	0.3	0.74	2.47
At3g56110	putative protein	0.26	0.64	2.46
At4g33650	Arabidopsis dynamin-like protein ADL2	0.13	0.32	2.46
At4g13460	putative protein	0.26	0.64	2.46
At3g10420	unknown protein	0.22	0.54	2.45
At2g36480	hypothetical protein	0.97	2.38	2.45
At3g07565	unknown protein	0.18	0.44	2.44
At1g79500	2-dehydro-3-deoxyphosphooctonate aldolase	0.18	0.44	2.44
At4g30210	NADPH-ferrihemoprotein reductase (ATR2)	0.36	0.88	2.44
At1g61960	hypothetical protein	0.43	1.05	2.44
At2g43870	putative polygalacturonase	0.25	0.61	2.44
At1g54710	hypothetical protein	0.16	0.39	2.44
At2g33720	hypothetical protein	0.16	0.39	2.44
At5g57520	CCHH finger protein 2-like protein	0.3	0.73	2.43
At5g38310	hypothetical protein	0.21	0.51	2.43
At2g21990	hypothetical protein	0.42	1.02	2.43
At2g47360	hypothetical protein	0.52	1.26	2.42
At3g43070	putative protein	0.38	0.92	2.42
At2g28620	putative kinesin-like spindle protein	0.24	0.58	2.42
At2g22470	unknown protein	0.48	1.16	2.42
At3g29410	terpene synthase	0.12	0.29	2.42
At3g48870	AtClpC	0.34	0.82	2.41
At2g45290	putative transketolase precursor	0.56	1.35	2.41
At4g03800	hypothetical protein	0.27	0.65	2.41
At5g57970	putative protein	0.15	0.36	2.40
At2g43990	hypothetical protein	0.33	0.79	2.39
At5g01110	putative protein	0.18	0.43	2.39
At1g55580	hypothetical protein	0.39	0.93	2.38
At2g32840	hypothetical protein	0.34	0.81	2.38
At3g52550	hypothetical protein	0.42	1	2.38
At2g22050	hypothetical protein	0.24	0.57	2.38
At5g13340	putative protein	0.19	0.45	2.37
At5g51770	putative protein	0.11	0.26	2.36
At2g02390	putative glutathione S-transferase	0.11	0.26	2.36
At5g03340	transitional endoplasmic reticulum ATPase	0.5	1.18	2.36
At1g72010	unknown protein	0.28	0.66	2.36
At4g19830	putative protein	0.31	0.73	2.35
At3g17470	hypothetical protein	7.01	16.5	2.35
At4g28590	hypothetical protein	0.2	0.47	2.35
At2g29020	unknown protein	0.78	1.83	2.35
At3g45780	nonphototropic hypocotyl 1	0.39	0.91	2.33
At5g14830	putative protein	0.24	0.56	2.33
At4g01650	hypothetical protein	1.41	3.29	2.33
At4g35170	putative protein	0.15	0.35	2.33
At5g57880	unknown protein	0.06	0.14	2.33
At1g74850	hypothetical protein	0.49	1.14	2.33
At5g17280	putative protein	0.34	0.79	2.32
At1g52220	unknown protein	0.56	1.3	2.32
At3g16480	putative mitochondrial processing peptidase alpha subunit	0.25	0.58	2.32
At1g22680	hypothetical protein	0.75	1.74	2.32
At2g41410	calmodulin-like protein	0.66	1.53	2.32
At2g21720	hypothetical protein	0.19	0.44	2.32

At2g25660	unknown protein	0.45	1.04	2.31
At5g48990	putative protein	0.26	0.6	2.31
At5g59080	putative protein	0.49	1.13	2.31
At3g57780	putative protein	0.36	0.83	2.31
At2g29760	hypothetical protein	0.23	0.53	2.30
At5g19150	putative protein	0.23	0.53	2.30
At3g53350	putative protein	0.63	1.45	2.30
At2g03400	unknown protein	0.4	0.92	2.30
At4g35510	putative protein	0.67	1.54	2.30
At5g52530	putative protein	0.47	1.08	2.30
At3g10060	unknown protein	0.24	0.55	2.29
At3g26060	putative peroxiredoxin	0.24	0.55	2.29
At1g02170	unknown protein	0.66	1.51	2.29
At4g35250	putative protein	0.28	0.64	2.29
At3g15690	putative acetyl-CoA carboxylase biotin-containing subunit	0.14	0.32	2.29
At4g08280	putative protein	0.28	0.64	2.29
At5g06410	putative protein	0.07	0.16	2.29
At4g27700	hypothetical protein	0.5	1.14	2.28
At2g05990	enoyl-ACP reductase (enr-A)	0.18	0.41	2.28
At3g24780	hypothetical protein	0.29	0.66	2.28
At1g30610	hypothetical protein	0.29	0.66	2.28
At4g13590	putative protein	0.22	0.5	2.27
At5g27070	putative protein	0.44	1	2.27
At5g44540	putative protein	0.66	1.5	2.27
At4g22650	putative protein	0.26	0.59	2.27
At3g26710	unknown protein	0.41	0.93	2.27
At1g30320	hypothetical protein	0.34	0.77	2.26
At4g23940	cell division protein - like	0.19	0.43	2.26
At3g61540	prolyl aminopeptidase-like protein	0.38	0.86	2.26
At3g09150	hypothetical protein	0.19	0.43	2.26
At3g26840	unknown protein	0.12	0.27	2.25
At2g45450	unknown protein	0.64	1.44	2.25
At1g44920	hypothetical protein	0.16	0.36	2.25
At2g27770	hypothetical protein	0.57	1.28	2.25
At5g46390	carboxy-terminal proteinase D1-like protein	0.29	0.65	2.24
At1g50840	DNA polymerase A family protein	0.29	0.65	2.24
At2g29180	unknown protein	0.25	0.56	2.24
At1g62190	hypothetical protein	0.21	0.47	2.24
At4g10840	putative protein	0.3	0.67	2.23
At5g04440	putative protein	0.13	0.29	2.23
At3g58010	putative protein	0.13	0.29	2.23
At5g07530	glycine-rich protein atGRP-7	0.22	0.49	2.23
At5g26880	putative protein	0.49	1.09	2.22
At2g24850	putative tyrosine aminotransferase	0.09	0.2	2.22
At1g15410	hypothetical protein	0.14	0.31	2.21
At3g02690	unknown protein	0.62	1.37	2.21
At2g30200	putative malonyl-CoA:Acyl carrier protein transacylase	0.39	0.86	2.21
At4g27520	putative protein	0.49	1.08	2.20
At2g14430	putative non-LTR retroelement reverse transcriptase	0.3	0.66	2.20
At3g53130	Cytochrom P450 -like protein	0.1	0.22	2.20
At1g79960	hypothetical protein	0.4	0.88	2.20
At4g08630	hypothetical protein	0.41	0.9	2.20

At3g60860	guanine nucleotide exchange factor - like protein	0.57	1.25	2.19
At1g74600	hypothetical protein	0.32	0.7	2.19
At1g12100	hybrid proline-rich protein	0.27	0.59	2.19
At3g11150	hypothetical protein	0.6	1.31	2.18
At1g54120	hypothetical protein	0.22	0.48	2.18
At1g19480	hypothetical protein	0.33	0.72	2.18
At4g02940	hypothetical protein	0.22	0.48	2.18
At3g52050	putative protein	0.4	0.87	2.18
At3g43640	putative protein	0.12	0.26	2.17
At1g11820	unknown protein	0.3	0.65	2.17
At2g35400	unknown protein	0.19	0.41	2.16
At5g60050	putative protein	0.52	1.12	2.15
At5g51020	putative protein	0.2	0.43	2.15
At5g53930	putative protein	0.4	0.86	2.15
At5g26570	putative protein	0.21	0.45	2.14
At1g05340	unknown protein	0.42	0.9	2.14
At1g44350	putative IAA-amino acid hydrolase	0.14	0.3	2.14
At1g75080	unknown protein	0.29	0.62	2.14
At3g24190	unknown protein	0.52	1.11	2.13
At2g10550	hypothetical protein	0.15	0.32	2.13
At5g58630	putative protein	0.38	0.81	2.13
At2g45310	putative nucleotide sugar epimerase	0.47	1	2.13
At4g29750	putative protein	0.24	0.51	2.13
At3g01170	unknown protein	0.24	0.51	2.13
At2g44550	putative glucanase	0.25	0.53	2.12
At1g67280	unknown protein	0.46	0.97	2.11
At4g14450	hypothetical protein	0.28	0.59	2.11
At4g27990	putative protein	0.38	0.8	2.11
At4g08940	hypothetical protein	0.6	1.26	2.10
At3g22690	hypothetical protein	0.22	0.46	2.09
At1g03260	hypothetical protein	0.11	0.23	2.09
At5g44750	putative protein	0.22	0.46	2.09
At3g04110	putative glutamate receptor (GLR1)	0.22	0.46	2.09
At1g63970	2C-methyl-D-erythritol 2	0.33	0.69	2.09
At1g07850	hypothetical protein	0.22	0.46	2.09
At4g23040	putative protein	0.24	0.5	2.08
At3g15900	unknown protein	0.37	0.77	2.08
At1g52500	hypothetical protein	0.13	0.27	2.08
At3g29185	hypothetical protein	0.41	0.85	2.07
At4g25460	hypothetical protein	0.55	1.14	2.07
At5g51670	putative protein	0.28	0.58	2.07
At5g48130	putative protein	0.28	0.58	2.07
At1g31170	unknown protein	0.31	0.64	2.06
At1g14590	unknown protein	0.31	0.64	2.06
At5g17710	chloroplast GrpE protein	0.31	0.64	2.06
At2g37330	unknown protein	0.36	0.74	2.06
At4g23080	putative protein	0.38	0.78	2.05
At4g25120	putative protein	0.38	0.78	2.05
At4g32590	hypothetical protein	0.39	0.8	2.05
At3g42100	putative protein	0.2	0.41	2.05
At4g09680	putative protein	0.43	0.88	2.05

At1g70200	unknown protein	0.68	1.39	2.04
At3g48000	aldehyde dehydrogenase (NAD+)-like protein	0.5	1.02	2.04
At3g32940	hypothetical protein	0.26	0.53	2.04
At1g24040	unknown protein	0.27	0.55	2.04
At1g23400	unknown protein	0.28	0.57	2.04
At1g73650	unknown protein	0.28	0.57	2.04
At3g24430	mrp protein	0.29	0.59	2.03
At4g39050	kinesin like protein	0.31	0.63	2.03
At5g54140	IAA-amino acid hydrolase homolog ILL3	0.38	0.77	2.03
At4g01360	hypothetical protein	0.38	0.77	2.03
At3g15140	hypothetical protein	0.39	0.79	2.03
At4g00610	hypothetical protein	0.41	0.83	2.02
At2g36920	hypothetical protein	0.49	0.99	2.02
At5g13090	putative protein	0.62	1.25	2.02
At2g31160	unknown protein	0.65	1.31	2.02
At2g32480	unknown protein	0.81	1.63	2.01
At5g48440	putative protein	0.16	0.32	2.00
At3g18270	unknown protein	0.15	0.3	2.00
At1g05750	hypothetical protein	0.17	0.34	2.00
At4g34730	putative protein	0.41	0.82	2.00
At5g66530	apospory-associated protein C-like	0.23	0.46	2.00
At2g39290	putative CDP-diacylglycerol-glycerol-3-phosphate 3-phosphatidyltransferase	0.19	0.38	2.00
At5g54430	putative protein	0.76	1.52	2.00
At1g41670	hypothetical protein	0.27	0.54	2.00
At3g18680	uridylate kinase	0.09	0.18	2.00
At1g63720	hypothetical protein	0.19	0.38	2.00
At2g40300	putative ferritin	0.16	0.32	2.00
At5g17170	unknown protein	0.14	0.28	2.00
At4g08510	hypothetical protein	0.19	0.38	2.00
At5g16110	putative protein	0.17	0.34	2.00
At1g69740	putative aminolevulinate dehydratase	0.14	0.28	2.00
At4g25050	acyl carrier - like protein	0.72	1.43	1.99
At2g44140	unknown protein	0.48	0.95	1.98
At2g43050	putative pectinesterase	0.48	0.95	1.98
At5g43770	unknown protein	0.43	0.85	1.98
At4g36190	putative protein	0.8	1.58	1.98
At3g11690	unknown protein	0.74	1.46	1.97
At1g62290	aspartic protease	0.32	0.63	1.97
At2g05120	unknown protein	0.31	0.61	1.97
At2g35490	putative fibrillin	0.29	0.57	1.97
At5g53490	thylakoid lumenal 17.4 kD protein	0.28	0.55	1.96
At3g24860	unknown protein	0.69	1.35	1.96
At3g04560	unknown protein	0.46	0.9	1.96
At2g27660	hypothetical protein	0.44	0.86	1.95
At4g22520	putative protein	0.43	0.84	1.95
At3g06360	hypothetical protein	0.62	1.21	1.95
At5g61200	putative protein	0.61	1.19	1.95
At2g40980	unknown protein	0.39	0.76	1.95
At4g38400	putative pollen allergen	0.38	0.74	1.95
At4g11090	putative protein	0.36	0.7	1.94
At2g25800	unknown protein	0.62	1.2	1.94

At3g04340	unknown protein	0.44	0.85	1.93
At4g29790	putative protein	0.28	0.54	1.93
At1g18060	unknown protein	0.14	0.27	1.93
At4g18130	phytochrome E	0.28	0.54	1.93
At2g34370	putative selenium-binding protein	0.67	1.29	1.93
At2g35010	thioredoxin	0.13	0.25	1.92
At4g22980	putative protein	0.39	0.75	1.92
At1g51560	unknown protein	0.25	0.48	1.92
At3g09490	hypothetical protein	0.37	0.71	1.92
At1g65010	hypothetical protein	0.24	0.46	1.92
At4g04020	putative fibrillin	0.36	0.69	1.92
At4g25270	putative protein	0.36	0.69	1.92
At3g01360	hypothetical protein	0.46	0.88	1.91
At1g21060	unknown protein	0.23	0.44	1.91
At1g61690	hypothetical protein	0.57	1.09	1.91
At3g59100	putative protein	0.11	0.21	1.91
At3g60000	putative protein	0.21	0.4	1.90
At3g11330	hypothetical protein	0.41	0.78	1.90
At1g32200	glycerol-3-phosphate acyltransferase	0.4	0.76	1.90
At1g01730	unknown protein	0.38	0.72	1.89
At5g52250	putative protein	2.34	4.43	1.89
At4g29920	putative protein	0.37	0.7	1.89
At2g14340	hypothetical protein	0.27	0.51	1.89
At4g38190	putative protein	0.44	0.83	1.89
At5g51070	Erd1 protein precursor	0.52	0.98	1.88
At3g30780	hypothetical protein	0.17	0.32	1.88
At1g67930	putative golgi transport complex protein	0.33	0.62	1.88
At1g47340	hypothetical protein	0.46	0.86	1.87
At4g28210	hypothetical protein	0.53	0.99	1.87
At3g23400	unknown protein	0.3	0.56	1.87
At2g44230	hypothetical protein	0.15	0.28	1.87
At4g18810	putative protein	0.22	0.41	1.86
At2g43890	putative polygalacturonase	0.43	0.8	1.86
At2g35660	putative monooxygenase	0.14	0.26	1.86
At1g72520	putative lipoxygenase	0.27	0.5	1.85
At2g45470	unknown protein	0.67	1.24	1.85
At2g44570	putative glucanase	0.39	0.72	1.85
At2g40800	unknown protein	0.26	0.48	1.85
At3g26900	putative shikimate kinase	0.13	0.24	1.85
At2g32640	hypothetical protein	0.19	0.35	1.84
At2g37380	unknown protein	0.63	1.16	1.84
At2g33430	plastid protein	0.44	0.81	1.84
At5g02020	putative protein	0.43	0.79	1.84
At1g62750	unknown protein	0.97	1.78	1.84
At1g65610	endo-1	0.12	0.22	1.83
At1g11800	unknown protein	0.18	0.33	1.83
At3g25110	acyl-(acyl carrier protein) thioesterase	0.48	0.88	1.83
At2g04540	3-oxoacyl carrier protein synthase	0.18	0.33	1.83
At1g69370	chorismate mutase	0.24	0.44	1.83
At3g27550	hypothetical protein	0.18	0.33	1.83
At3g56140	putative protein	0.47	0.86	1.83

At2g46790	hypothetical protein	0.29	0.53	1.83
At2g27950	unknown protein	0.29	0.53	1.83
At4g07560	putative transposon protein	0.4	0.73	1.83
At5g09760	pectin methylesterase - like protein	0.97	1.77	1.82
At2g19340	unknown protein	0.34	0.62	1.82
At3g57580	putative protein	0.34	0.62	1.82
At3g09050	unknown protein	0.54	0.98	1.81
At1g78790	hypothetical protein	0.32	0.58	1.81
At5g06670	kinesin heavy chain-like protein	0.21	0.38	1.81
At1g05380	hypothetical protein	0.31	0.56	1.81
At4g18420	hypothetical protein	0.41	0.74	1.80
At2g20890	unknown protein	0.46	0.83	1.80
At2g29670	unknown protein	0.51	0.92	1.80
At1g79110	hypothetical protein	0.56	1.01	1.80
At4g32130	hypothetical protein	0.15	0.27	1.80
At5g07770	unknown protein	0.15	0.27	1.80
At4g00180	putative YABBY3 axial regulator	0.35	0.63	1.80
At3g20970	unknown protein	0.5	0.9	1.80
At1g80450	unknown protein	0.45	0.81	1.80
At5g38680	putative protein	0.25	0.45	1.80
At1g62780	unknown protein	0.1	0.18	1.80
At3g10730	hypothetical protein	0.2	0.36	1.80
At3g47970	hypothetical protein	0.2	0.36	1.80
At3g23740	unknown protein	0.49	0.88	1.80
At1g21910	TINY-like protein	0.39	0.7	1.79
At2g20270	putative glutaredoxin	0.29	0.52	1.79
At1g62010	hypothetical protein	0.67	1.2	1.79
At5g54360	unknown protein	0.19	0.34	1.79
At2g48130	unknown protein	0.23	0.41	1.78
At2g20080	unknown protein	0.32	0.57	1.78
At4g30720	putative protein	0.45	0.8	1.78
At1g44030	unknown protein	0.36	0.64	1.78
At5g06990	putative protein	0.27	0.48	1.78
At2g45300	5-enolpyruvylshikimate-3-phosphate (EPSP) synthase	0.35	0.62	1.77
At1g24150	unknown protein	0.61	1.08	1.77
At5g66100	putative protein	0.26	0.46	1.77
At4g03410	hypothetical protein	0.52	0.92	1.77
At4g14930	hypothetical protein	0.26	0.46	1.77
At5g19620	putative protein	0.13	0.23	1.77
At2g18190	putative AAA-type ATPase	0.25	0.44	1.76
At3g04760	hypothetical protein	0.41	0.72	1.76
At2g22880	hypothetical protein	0.49	0.86	1.76
At2g03140	putative LEA (late embryogenesis abundant) protein	0.16	0.28	1.75
At1g07460	lectin	0.16	0.28	1.75
At2g05590	hypothetical protein	0.08	0.14	1.75
At1g50000	hypothetical protein	0.08	0.14	1.75
At3g10620	putative diadenosine 5\\\'	0.36	0.63	1.75
At1g78910	hypothetical protein	0.52	0.91	1.75
At5g66090	unknown protein	0.24	0.42	1.75
At2g21860	unknown protein	0.4	0.7	1.75
At5g09790	putative protein	0.28	0.49	1.75
At3g63190	putative protein	0.34	0.59	1.74

At3g53470	putative protein	0.68	1.18	1.74
At1g52510	hypothetical protein	0.49	0.85	1.73
At5g47890	NADH dehydrogenase 10.5K chain-like protein	0.26	0.45	1.73
At3g15330	hypothetical protein	0.26	0.45	1.73
At3g24440	hypothetical protein	0.48	0.83	1.73
At2g47860	unknown protein	0.22	0.38	1.73
At4g23170	putative protein	12.71	21.9	1.72
At5g11010	putative protein	0.46	0.79	1.72
At3g28460	unknown protein	0.07	0.12	1.71
At3g43520	hypothetical protein	1.04	1.78	1.71
At5g45680	putative protein	0.45	0.77	1.71
At4g31430	predicted protein	0.24	0.41	1.71
At1g52870	unknown protein	0.17	0.29	1.71
At5g30460	putative protein	0.64	1.09	1.70
At5g40850	urophorphyrin III methylase	0.2	0.34	1.70
At3g27180	hypothetical protein	0.2	0.34	1.70
At5g41960	unknown protein	0.1	0.17	1.70
At3g56600	putative protein	0.86	1.46	1.70
At5g05850	putative protein	0.36	0.61	1.69
At1g05650	putative polygalacturonase	0.39	0.66	1.69
At3g57950	putative protein	0.45	0.76	1.69
At2g13710	pseudogene	0.61	1.03	1.69
At4g39610	putative protein	0.48	0.81	1.69
At5g50640	putative protein	0.22	0.37	1.68
At4g35680	putative protein	0.44	0.74	1.68
At1g02070	hypothetical protein	0.47	0.79	1.68
At2g17300	unknown protein	1.02	1.71	1.68
At1g71910	hypothetical protein	0.4	0.67	1.68
At2g37750	unknown protein	0.43	0.72	1.67
At3g13850	hypothetical protein	0.52	0.87	1.67
At1g78310	hypothetical protein	0.61	1.02	1.67
At2g31040	hypothetical protein	0.15	0.25	1.67
At3g14390	putative diaminopimelate decarboxylase	0.36	0.6	1.67
At3g11810	unknown protein	0.48	0.8	1.67
At3g13570	serine/arginine-rich protein	0.15	0.25	1.67
At1g09130	unknown protein	0.71	1.18	1.66
At4g22030	putative protein	0.46	0.76	1.65
At1g56180	hypothetical protein	0.4	0.66	1.65
At1g60670	expressed protein	0.74	1.22	1.65
At2g31250	putative glutamyl tRNA reductase	0.82	1.35	1.65
At1g09780	putative 2	0.69	1.13	1.64
At4g39710	proteomics: thylakloid lumen FKBP-like protein	0.66	1.08	1.64
At4g09700	putative protein	0.22	0.36	1.64
At2g19940	putative N-acetyl-gamma-glutamyl-phosphate reductase	0.57	0.93	1.63
At2g02740	hypothetical protein	0.19	0.31	1.63
At3g02900	unknown protein	0.19	0.31	1.63
At2g30880	unknown protein	0.65	1.06	1.63
At3g44310	nitrilase 1	0.27	0.44	1.63
At1g80480	hypothetical protein	0.27	0.44	1.63
At5g53570	GTPase activator protein of Rab-like small GTPases-like protein	0.16	0.26	1.63
At3g63410	putative chloroplast inner envelope protein	0.42	0.68	1.62

At3g54900	putative protein	0.65	1.05	1.62
At1g56200	unknown protein	0.31	0.5	1.61
At1g61200	hypothetical protein	0.9	1.45	1.61
At5g15980	putative protein	0.28	0.45	1.61
At5g56660	IAA-amino acid hydrolase	0.71	1.14	1.61
At3g55070	putative protein	0.43	0.69	1.60
At2g05180	putative cytochrome P450	0.43	0.69	1.60
At5g66660	At14a protein-like	0.78	1.25	1.60
At2g45440	putative dihydrodipicolinate synthase	0.4	0.64	1.60
At4g39690	putative protein	1.02	1.63	1.60
At5g38060	hypothetical protein	0.47	0.75	1.60
At3g56910	ribosomal protein PSRP5	1.8	2.87	1.59
At5g64580	putative protein	0.32	0.51	1.59
At3g63370	putative protein	0.27	0.43	1.59
At4g00170	putative proline-rich protein	0.22	0.35	1.59
At2g31840	hypothetical protein	0.63	1	1.59
At5g24120	sigma-like factor	0.46	0.73	1.59
At2g21340	unknown protein	0.29	0.46	1.59
At2g18950	hypothetical protein	0.58	0.92	1.59
At5g64860	4-alpha-glucanotransferase	0.29	0.46	1.59
At1g73060	unknown protein	0.24	0.38	1.58
At1g02890	hypothetical protein	0.12	0.19	1.58
At4g20300	putative protein	0.31	0.49	1.58
At4g19460	putative protein	0.38	0.6	1.58
At3g50190	putative protein	1.33	2.1	1.58
At1g03230	unknown protein	0.45	0.71	1.58
At3g51510	putative protein	0.45	0.71	1.58
At5g51100	putative chloroplast Mn SOD	0.61	0.96	1.57
At2g03220	xyloglucan fucosyltransferase AtFT1	0.96	1.51	1.57
At1g10410	unknown protein	0.42	0.66	1.57
At2g43710	stearoyl-ACP desaturase	0.14	0.22	1.57
At4g35710	putative protein	0.28	0.44	1.57
At4g25370	putative protein	0.28	0.44	1.57
3834303	hypothetical protein	0.07	0.11	1.57
At3g42200	putative protein	0.88	1.38	1.57
At5g02250	ribonuclease II-like protein	0.23	0.36	1.57
At3g58660	putative protein	0.39	0.61	1.56
At5g35100	putative protein	0.55	0.86	1.56
At1g10140	unknown protein	0.52	0.81	1.56
At1g69240	putative alpha/beta hydrolase	0.18	0.28	1.56
At2g16650	hypothetical protein	0.36	0.56	1.56
At1g70070	hypothetical protein	0.18	0.28	1.56
At4g40080	putative protein	0.56	0.87	1.55
At3g46950	putative protein	0.73	1.13	1.55
At1g21730	kinesin-like protein	0.22	0.34	1.55
At3g14310	putative pectin methylesterase	0.33	0.51	1.55
At3g50140	putative protein	1.64	2.53	1.54
At1g79350	hypothetical protein	0.94	1.45	1.54
At2g32650	hypothetical protein	0.65	1	1.54
At2g29980	omega-3 fatty acid desaturase	0.39	0.6	1.54
At1g61040	unknown protein	0.56	0.86	1.54

At4g14510	hypothetical protein	0.56	0.86	1.54
At1g80590	hypothetical protein	0.15	0.23	1.53
At4g38080	putative protein	0.77	1.18	1.53
At2g38310	unknown protein	1.09	1.67	1.53
At4g14380	hypothetical protein	0.49	0.75	1.53
At2g44190	hypothetical protein	0.83	1.27	1.53
At5g57990	putative protein	0.17	0.26	1.53
At4g18750	putative protein	0.17	0.26	1.53
At1g01500	hypothetical protein	0.34	0.52	1.53
At5g01080	putative protein	0.76	1.16	1.53
At2g42310	unknown protein	0.21	0.32	1.52
At2g25330	unknown protein	0.44	0.67	1.52
At5g16440	isopentenyl pyrophosphate:dimethyllallyl pyrophosphate isomerase	0.46	0.7	1.52
At4g29400	putative protein	0.23	0.35	1.52
At5g59800	putative protein	0.48	0.73	1.52
At3g56710	SigA binding protein	0.31	0.47	1.52
At2g31980	putative cysteine proteinase inhibitor B (cystatin B)	0.62	0.94	1.52
At2g07710	hypothetical protein	0.7	1.06	1.51
At2g26280	unknown protein	0.37	0.56	1.51
At4g23890	putative protein	2.22	3.36	1.51
At2g22830	putative squalene epoxidase	0.73	1.1	1.51
At4g24090	hypothetical protein	0.42	0.63	1.50
At3g08660	putative non-phototropic hypocotyl	0.16	0.24	1.50
At2g44700	hypothetical protein	0.48	0.72	1.50
At1g19050	response regulator 5	0.24	0.36	1.50
At1g70170	matrix metalloproteinase	0.5	0.75	1.50
At4g10000	putative protein	0.24	0.36	1.50
At2g42940	hypothetical protein	0.14	0.21	1.50
At5g18070	N-acetylglucosamine-phosphate mutase	0.87	1.3	1.49
At1g05150	putative O-GlcNAc transferase	0.69	1.03	1.49
At5g32490	putative protein	0.96	1.43	1.49
At5g08050	putative protein	0.27	0.4	1.48
At1g53140	dynamin-like protein	0.27	0.4	1.48
At1g08640	hypothetical protein	0.48	0.71	1.48
At3g54320	aintegumaenta-like protein	0.23	0.34	1.48
At5g52100	dihydrodipicolinate reductase-like protein	0.23	0.34	1.48
At2g23390	hypothetical protein	0.23	0.34	1.48
At1g54070	unknown protein	0.42	0.62	1.48
At1g12520	unknown protein	0.19	0.28	1.47
At1g74880	unknown protein	1.04	1.53	1.47
At5g03940	signal recognition particle 54CP (SRP54) protein precursor	0.17	0.25	1.47
At2g35840	putative sucrose-6F-phosphate phosphohydrolase	0.94	1.38	1.47
At3g18390	unknown protein	1.39	2.04	1.47
At2g01400	hypothetical protein	0.45	0.66	1.47
At3g26630	unknown protein	1.31	1.92	1.47
At2g42870	unknown protein	0.28	0.41	1.46
At3g06570	unknown protein	0.41	0.6	1.46
At2g37080	putative myosin heavy chain	0.8	1.17	1.46
At2g37240	unknown protein	0.13	0.19	1.46
At4g20120	hypothetical protein	0.26	0.38	1.46

At1g65580	unknown protein	0.13	0.19	1.46
At5g06290	2-Cys peroxiredoxin-like protein	0.89	1.3	1.46
At3g51790	putative transmembrane protein G1p	0.35	0.51	1.46
At1g67710	response regulator	0.35	0.51	1.46
At2g15720	putative non-LTR retroelement reverse transcriptase	0.46	0.67	1.46
At4g31040	hypothetical protein	0.55	0.8	1.45
At1g68430	hypothetical protein	0.64	0.93	1.45
At4g22260	putative protein	0.4	0.58	1.45
At3g14750	unknown protein	0.2	0.29	1.45
At2g02980	hypothetical protein	0.29	0.42	1.45
At1g68660	unknown protein	0.38	0.55	1.45
At4g14620	hypothetical protein	0.18	0.26	1.44
At1g50320	thioredoxin	0.18	0.26	1.44
At4g01220	hypothetical protein	0.09	0.13	1.44
At4g19390	putative protein	0.27	0.39	1.44
At1g62250	unknown protein	0.52	0.75	1.44
At2g22010	unknown protein	0.52	0.75	1.44
At4g21210	putative protein	0.43	0.62	1.44
At4g02070	G/T DNA mismatch repair enzyme	0.34	0.49	1.44
At3g57110	hypothetical protein	0.57	0.82	1.44
At1g11430	DAG protein	0.16	0.23	1.44
At1g72640	hypothetical protein	0.48	0.69	1.44
At1g16880	unknown protein	0.23	0.33	1.43
At4g31060	putative protein	0.53	0.76	1.43
At3g23290	hypothetical protein	0.51	0.73	1.43
At5g08400	putative protein	0.28	0.4	1.43
At3g63320	putative protein	0.63	0.9	1.43
At3g26020	putative B regulatory subunit of protein phosphatase 2A	0.42	0.6	1.43
At1g05385	expressed protein	0.42	0.6	1.43
At4g04430	putative transposon protein	0.35	0.5	1.43
At1g78150	unknown protein	0.26	0.37	1.42
At1g62150	hypothetical protein	0.83	1.18	1.42
At3g50570	proline-rich protein	0.5	0.71	1.42
At1g70180	hypothetical protein	0.31	0.44	1.42
At4g35450	ankyrin repeat-containing protein 2	0.62	0.88	1.42
At4g20690	putative protein	0.31	0.44	1.42
At4g32770	putative protein	0.36	0.51	1.42
At4g02340	expressed protein	0.24	0.34	1.42
At5g22830	putative protein	0.29	0.41	1.41
At1g67440	hypothetical protein	1.26	1.78	1.41
At5g16290	acetolactate synthase-like protein	0.37	0.52	1.41
At4g24860	putative protein	0.72	1.01	1.40
At5g60370	putative protein	0.82	1.15	1.40
At3g43610	putative protein	0.05	0.07	1.40
At1g56020	unknown protein	0.6	0.84	1.40
At1g13280	allene oxide cyclase	0.3	0.42	1.40
At1g73170	putative ATPase	0.68	0.95	1.40
At5g01760	putative protein	0.33	0.46	1.39
At1g33250	unknown protein	0.99	1.38	1.39
At3g02660	putative tyrosyl-tRNA synthetase	0.94	1.31	1.39
At2g44560	putative glucanase	0.69	0.96	1.39

At2g37230	unknown protein	0.69	0.96	1.39
At5g27880	putative protein	2.31	3.21	1.39
At5g19900	putative protein	0.18	0.25	1.39
At1g62390	hypothetical protein	1.08	1.5	1.39
At4g16080	hypothetical protein	0.83	1.15	1.39
At3g05020	acyl carrier protein 1 precursor (ACP)	0.47	0.65	1.38
At5g58260	similar to unknown protein	0.47	0.65	1.38
At2g38550	putative non-green plastid inner envelope membrane protein	0.97	1.34	1.38
At2g34540	hypothetical protein	0.5	0.69	1.38
At1g60550	hypothetical protein	0.37	0.51	1.38
At5g55570	unknown protein	0.77	1.06	1.38
At4g21300	putative protein	0.8	1.1	1.38
At2g28030	putative chloroplast nucleoid DNA-binding protein	0.67	0.92	1.37
At4g14860	hypothetical protein	0.7	0.96	1.37
At1g28150	unknown protein	0.54	0.74	1.37
At3g46780	putative protein	0.46	0.63	1.37
At1g28280	hypothetical protein	0.38	0.52	1.37
At1g35210	hypothetical protein	0.52	0.71	1.37
At1g51660	hypothetical protein	0.74	1.01	1.36
At3g52140	putative protein	0.11	0.15	1.36
At1g30950	putative unusual floral organ (UFO)	1.35	1.84	1.36
At2g01300	unknown protein	0.8	1.09	1.36
At3g57040	responce reactor 4	0.61	0.83	1.36
At5g35710	unknown protein	1.14	1.55	1.36
At5g02190	putative protein	0.39	0.53	1.36
At1g13990	unknown protein	0.39	0.53	1.36
At3g16760	unknown protein	0.9	1.22	1.36
At5g62550	unknown protein	0.93	1.26	1.35
At2g18900	unknown protein	0.93	1.26	1.35
At3g06870	unknown protein	0.68	0.92	1.35
At4g16410	hypothetical protein	0.6	0.81	1.35
At2g24070	unknown protein	0.2	0.27	1.35
At3g54870	kinesin-like protein	0.43	0.58	1.35
At3g12020	hypothetical protein	0.15	0.2	1.33
At5g58410	unknown protein	0.19	0.25	1.32
At1g23640	putative OBP32pep protein	0.13	0.17	1.31
At4g10300	putative protein	0.14	0.18	1.29
At3g57280	hypothetical protein	0.05	0.06	1.20
At5g55220	trigger factor-like protein	0.16	0.12	0.75
3695380	contains similarity to Nicotiana tabacum membrane-associated salt-inducible protein	1.17	0.87	0.74
At1g11750	hypothetical protein	0.42	0.31	0.74
At1g80370	putative cyclin	0.64	0.47	0.73
At2g20460	putative retroelement pol polyprotein	0.41	0.3	0.73
At1g55480	unknown protein	0.78	0.57	0.73
At1g79450	hypothetical protein	0.52	0.38	0.73
At4g12520	pEARLI 1-like protein	1.88	1.37	0.73
At4g19870	putative protein	0.36	0.26	0.72
At2g24020	unknown protein	0.86	0.62	0.72
At1g54520	unknown protein	0.25	0.18	0.72
At1g74790	hypothetical protein	1.03	0.74	0.72
At2g01380	hypothetical protein	1.25	0.89	0.71

At4g32640	putative protein	0.31	0.22	0.71
At4g01050	hypothetical protein	0.92	0.65	0.71
At4g33780	putative protein	4.07	2.87	0.71
At2g39000	unknown protein	0.27	0.19	0.70
At4g23930	putative protein	0.66	0.46	0.70
At4g12500	pEARLI 1-like protein	1.53	1.06	0.69
At5g42380	putative protein	0.26	0.18	0.69
At4g22840	predicted protein	0.54	0.37	0.69
At2g26670	heme oxygenase 1 (HO1)	1.36	0.93	0.68
At1g54580	acyl-carrier protein (ACP)	2.15	1.47	0.68
At3g02030	hypothetical protein	0.63	0.43	0.68
At2g01590	unknown protein	0.22	0.15	0.68
At5g06270	putative protein	1.44	0.98	0.68
At4g23840	putative protein	0.34	0.23	0.68
At2g21170	putative triosephosphate isomerase	0.37	0.25	0.68
At4g21010	putative protein	0.89	0.6	0.67
At2g35370	glycine decarboxylase complex H-protein	1.31	0.88	0.67
At4g03920	putative protein	1.31	0.88	0.67
At4g10810	putative protein	15.61	10.44	0.67
At1g17420	lipoxygenase	0.24	0.16	0.67
At1g30910	hypothetical protein	0.57	0.38	0.67
At1g02730	hypothetical protein	0.15	0.1	0.67
At4g01150	hypothetical protein	3.39	2.26	0.67
At1g32420	hypothetical protein	0.86	0.57	0.66
At3g50180	putative protein	3.42	2.26	0.66
At5g13630	cobalamin biosynthesis protein	2.27	1.5	0.66
At4g34050	caffeoyl-CoA O-methyltransferase - like protein	1.09	0.72	0.66
At5g48920	unknown protein	2.03	1.34	0.66
At5g16620	OuterEnvelopeProtein16	0.55	0.36	0.65
At3g61680	putative protein	0.17	0.11	0.65
At4g22890	putative protein	3.07	1.98	0.64
At5g11550	putative protein	3.01	1.94	0.64
At3g22970	unknown protein	1.18	0.76	0.64
At5g28860	putative protein	1.82	1.17	0.64
At2g25320	unknown protein	0.39	0.25	0.64
At2g22510	unknown protein	2.27	1.44	0.63
At1g80130	unknown protein	0.49	0.31	0.63
At4g22490	RCc3- like protein	1.18	0.74	0.63
At5g47860	putative protein	0.16	0.1	0.63
At1g54630	hypothetical protein	2.18	1.35	0.62
At2g44030	hypothetical protein	1.83	1.13	0.62
At2g30950	putative ftsH chloroplast protease	0.81	0.5	0.62
At2g20020	hypothetical protein	1.53	0.94	0.61
At2g47400	putative chloroplast protein CP12	2.88	1.76	0.61
At2g28760	putative nucleotide-sugar dehydratase	0.72	0.44	0.61
At5g50280	putative protein	0.18	0.11	0.61
At4g03520	m-type thioredoxin	1.81	1.09	0.60
At5g05380	putative protein	0.32	0.19	0.59
At1g58290	glutamyl-tRNA reductase	1.54	0.91	0.59
At4g17600	Lil3 protein (similar to LHC group of proteins)	2.33	1.37	0.59
At2g41180	unknown protein	8.69	5.1	0.59

3695393	contains similarity to retroviral aspartyl proteases	3.43	2.01	0.59
At3g62030	peptidylprolyl isomerase ROC4	0.93	0.54	0.58
At1g79050	replicase	0.85	0.49	0.58
At2g35240	unknown protein	0.56	0.32	0.57
At5g27330	glutamic acid-rich protein	0.93	0.53	0.57
At2g18920	hypothetical protein	0.88	0.5	0.57
At3g18110	hypothetical protein	0.68	0.38	0.56
At2g06030	hypothetical protein	0.18	0.1	0.56
At4g32020	putative protein	0.74	0.41	0.55
At1g74960	putative 3-ketoacyl-ACP synthase	0.31	0.17	0.55
At5g44680	putative protein	0.31	0.17	0.55
At2g28800	chloroplast membrane protein ALBINO3 (ALB3)	0.97	0.53	0.55
At3g43700	putative protein	0.44	0.24	0.55
At4g32340	putative protein	0.83	0.45	0.54
At5g43930	putative protein	0.37	0.2	0.54
At2g45180	putative proline-rich protein	7.52	4.06	0.54
At2g31400	unknown protein	0.56	0.3	0.54
At4g26430	putative protein	0.51	0.27	0.53
At1g74420	putative xyloglucan fucosyltransferase	0.17	0.09	0.53
At4g31990	aspartate aminotransferase	0.34	0.18	0.53
At1g48860	hypothetical protein	0.42	0.22	0.52
At2g34640	unknown protein	0.33	0.17	0.52
At5g35630	glutamate-ammonia ligase (EC 6.3.1.2) precursor	2.06	1.06	0.51
At3g66654	unknown protein	0.7	0.36	0.51
At3g16770	AP2 domain containing protein RAP2.3	1.27	0.65	0.51
At2g39270	putative adenylate kinase	0.83	0.42	0.51
At1g54780	proteomics: thylakloid lumen protein	4.3	2.13	0.50
At1g70350	hypothetical protein	0.89	0.44	0.49
At3g20060	ubiquitin-conjugating enzyme	0.69	0.34	0.49
At4g38440	putative protein	0.27	0.13	0.48
At2g27400	pseudogene	5	2.36	0.47
At3g59400	putative protein	1.65	0.76	0.46
At3g17100	unknown protein	1.59	0.73	0.46
At1g21500	unknown protein	1.7	0.78	0.46
At3g06330	unknown protein	1.33	0.61	0.46
At5g54190	NADPH:protochlorophyllide oxidoreductase A	1.6	0.73	0.46
At3g23670	hypothetical protein	1.04	0.47	0.45
At4g26500	putative protein	0.94	0.42	0.45
At3g07780	unknown protein	0.23	0.1	0.43
At1g29810	hypothetical protein	39.05	16.74	0.43
At5g44230	selenium-binding protein-like	0.07	0.03	0.43
At4g34350	putative protein	3.85	1.6	0.42
At5g47840	putative protein	0.53	0.22	0.42
At4g30620	putative protein	1.67	0.68	0.41
At3g12120	hypothetical protein	5.4	2.15	0.40
At3g09080	hypothetical protein	17.64	6.97	0.40
At1g54500	rubredoxin	0.99	0.39	0.39
At1g12090	hypothetical protein	4.93	1.91	0.39
At3g26580	unknown protein	5.44	2.1	0.39
At1g02560	ATP-dependent Clp protease proteolytic subunit (nClpP1)	1.23	0.47	0.38
At5g05590	phosphoribosylanthranilate isomerase	0.66	0.25	0.38
At1g05860	hypothetical protein	0.48	0.18	0.38

At5g20140	putative protein	0.08	0.03	0.38
At1g24340	hypothetical protein	1.53	0.56	0.37
At5g48300	ADPG pyrophosphorylase small subunit	0.33	0.11	0.33
At5g56290	peroxisomal targeting signal type 1 receptor	3.31	1.04	0.31
At4g02580	predicted NADH dehydrogenase 24 kD subunit	0.3	0.09	0.30
At2g36410	unknown protein	1.01	0.3	0.30
At1g48880	hypothetical protein	2.24	0.65	0.29
At2g14890	putative proline-rich protein	1.42	0.4	0.28
At2g15890	unknown protein	4.34	1.19	0.27
At2g13750	En/Spm-like transposon protein	4.45	1.22	0.27
At1g05130	unknown protein	24.36	5.96	0.24
At3g26740	light regulated protein	24.38	5.73	0.24
At5g52410	unknown protein	4.03	0.88	0.22

DANKSAGUNG

Ich danke Herrn Professor Dr. F. Salamini, daß er mir die Möglichkeit gegeben hat, diese Doktorarbeit am Max-Planck-Institut für Züchtungsforschung anzufertigen.

Ich danke Herrn Dr. D. Leister für die Themenstellung, die Betreuung der Arbeit und die vielen Hilfen, die zum Gelingen dieser Arbeit beigetragen haben.

Ich danke externen Kolaborationspartnern für ihre Hilfe: Herrn Dr. P. Jahns für die HPLC-Analysen und die Anleitung zu den P700-Messungen; Herrn Dr. J. Meurer für die Antikörper gegen die ATPase-a und –b Untereinheit, sowie den Western mit der ATPase-δ Untereinheit und Herrn Prof. Dr. F. A. Wollmann, seinen Mitarbeitern und P. Pesaresi für die Hilfe bei den Messungen der Fluoreszenz-Induktionskinetiken und des Membranpotentials.

Ich danke meinen Kollegen Joachim Kurth, Angela Dietzmann, Claudio Varotto, Martin Weigel, Erik Richly, Alexander Biehl, Paolo Pesaresi und Ania Laskowska.

Besonders danke ich Joachim und Claudio für die vielen Diskussionen, Erik für die Hilfe bei der Bioinformatik und Angela für die vielen kleinen Hilfen im Labor.

Ganz besonderer Dank gilt meinen Eltern, die mich selten zu sehen bekamen und trotzdem auch in diesem Lebensabschnitt immer bei mir waren.

Außerdem danke ich meiner Tante Lotte, die immer sehr viel Anteil an meiner Doktorabeit genommen hat und leider nicht mehr erleben durfte wie sie fertig wurde.

Besonders danke ich auch meinem Bruder Carsten für die stete ärztliche Versorgung meines Computers und den Rückhalt, den er mir immer wieder aufs neue gegeben hat.

Ich danke ganz besonders Tim dafür, daß er immer für mich da war.

As one shepherd said to the other…..

Eidesstattliche Erklärung

Hiermit erkläre ich, daß ich die vorliegende Dissertation selbstständig und mit keinen anderen, als den hier angegebenen Quellen und Hilfmittels angefertigt habe.

Daniela Sabine Maiwald Düsseldorf, den 02.07.03